Molecular Pathological Investigation of the Pathophysiology of Fatal Malaria

Panote Prapansilp

Wolfson College

Nuffield Department of Clinical Medicine

University of Oxford

A thesis submitted for the degree of

Doctor of Philosophy

Trinity 2012

Molecular Pathological Investigation of the Pathophysiology of Fatal Malaria

Panote Prapansilp, Wolfson College, University of Oxford,

D.Phil. thesis, Trinity 2012

Abstract

Malaria remains one of the world's major health problems, especially in developing countries. A better understanding of the pathology and pathophysiology of severe malaria is key to develop new treatments. Different approaches have been used in malaria research including the *in vitro* co-culture models with endothelial cells and both murine and simian animal models. However these are open to controversy due to disagreement on their representativeness of human disease. Using human post-mortem tissue in malaria research is another important approach but is practically challenging, limiting the availability of post mortem samples from malaria patients.

The work in this thesis had two main themes. First I examined the role of the endothelial signalling Angiopoetin-Tie-2 receptor pathway in malaria. Ang-2 has been shown to be a significant biomarker of severe and fatal malaria. I examined the tissue specific expression of proteins from this pathway in post-mortem brain tissues from fatal malaria cases, but found no difference between cerebral malaria and non-cerebral malaria cases. Ang-2 correlated with the severity of malaria in these patients. An attempt to examine the interaction of hypoxia and the Ang-Tie-2 pathway *in vitro* using a co-culture model of human brain endothelial cells was unsuccessful due to contamination of the cell line.

The second part of the thesis aimed to utilise molecular pathology techniques including miRNA and whole-genome microarrays. I have shown for the first time that these can be successfully applied to human post-mortem tissue in malaria. First I used archival tissues to examine the microRNA signature in the kidney of patients with malaria associated renal failure. Second I optimised a protocol to preserve post mortem tissue for molecular pathology, from an autopsy study in Mozambique. Using the subsequent total mRNA transcriptomic data and bioinformatics analysis this work has expanded our knowledge of differential gene expression and the families of genes which are dysregulated in the brain in response to malaria infection.

Acknowledgements

I would like to express my deep gratitude towards my supervisor Professor Nicholas Day, Professor Nicholas White and Professor Pratap Singhasivanon (Dean of the Faculty of Tropical Medicine, Mahidol University) for the inspiration and opportunity to undertake my D.Phil. at Oxford.

I am enormously grateful to Dr Gareth Turner for his brilliant ideas, continued support and advice, and for providing me with such a stimulating project. I am also indebted to his generous effort to improve the quality of this thesis by thorough reviewing, as well as to his moral support during my thesis write up.

I would also like to thank many people in the Nuffield Department of Clinical Laboratory Sciences including Dr Isabelle Medana for helping me with immunohistochemistry and guiding me through my first lab bench work, Professor Charles Lawrie for invaluable comments and suggestions on microRNA-related work, Dr Erica Ballabio for hands-on introduction to molecular biology techniques, Dr Andrew Graham and Dr Kingsley Micklem for their administrative and technical support. Special thanks to all members of Banham group, Boultwood group, Gatter group and Roberts group for being a very pleasant bunch of people to work with, get advice from and go to White Hart with.

I very much appreciate the help of Professor Monique Stins (Johns Hopkins University) who allowed me to work on blood brain barrier model in her laboratory, Dr Josefo Ferro (Beira Central Hospital, Mozambique) who is a local principal investigator of the MEMA autopsy project, Dr Panuwat Chutivongse, Professor Shanop Shoungshoti and Professor Pongsak Wannakrairot (Faculty of Medicine, Chulalongkorn University) who allowed me to do the Bangkok control autopsy project, all members of clinical and laboratory research teams in Bangkok and Beira, and especially the patients who provided their precious tissue for my research.

I would also like to acknowledge generous funding support from the Wellcome Trust, Mahidol-Oxford Tropical Research Unit (MORU), the Faculty of Tropical Medicine, Mahidol University, the Thrasher Research Fund, USA, Wolfson College, Oxford and the Pathological Society, UK.

Beyond those involved in the work itself, I would like to thank all my good friends in Oxford, Baltimore, and Bangkok for keeping me entertained, and particularly Dr Pornthep Tanpowpong (congratulations on your FACPeds from Massachusetts General Hospital!) and Dr Bunpote Siridechadilok for your comments on some parts of the thesis. Critically special thanks also go to Ms Teodora Perea for your patiently support and encouragement during the last period of writing up and for checking spelling in the thesis. I am lucky to be surrounded by so many wonderful people!

Finally I would like to thank my father, mother, sister, uncle, siblings and everyone in my family for their unconditioned love, care, support and inspiration. I hope you are proud of me, both for this work and also of my progress in all other aspects of my life.

Tempus fugit

Declaration

The work included in this thesis is my own. Whenever contributions of others are involved, effort is made to indicate this clearly, with due reference to the literature, and acknowledgement of collaborative research and discussion. The work was done under the supervision of Dr Gareth Turner and Professor Nicholas Day. The thesis has not been submitted for a degree or other qualification to this or any other university.

Table of Contents

List of Figures

List of Tables

Abbreviations

ACT	Artemisinin-based combined therapy
AKI	Acute kidney injury
ALI	Acute lung injury
Ang-1	Angiopoietin 1 (gene = ANGPT1)
Ang-2	Angiopoietin 2 (gene = ANGPT2)
APP	Amyloid precursor protein
AQ_	Aquaporin
ARDS	Acute respiratory distress syndrome
ARF	Acute renal failure
ATCC	American Type Culture Collection
ATN	Acute tubular necrosis
AUROC	Area under the receiver operating characteristic curve
B2M	Beta-2 microglobulin
BBB	Blood-brain barrier
bp	Base pair
BUN	Blood urea nitrogen
cDNA	Complementary DNA
CI	Confidence interval
CK-MB	Creatine kinase muscle-brain
CM	Cerebral malaria
CMV	Cytomegalovirus
CNS	Central nervous system
cRNA	Complementary RNA
CSA	Chondroitin sulphate A receptor
CSF	Cerebrospinal fluid
Ct	Threshold cycle
CX3CL1	Fractalkine
DAB	3,3'-Diaminobenzidine
DAPI	4',6-diamidino-2-phenylindole
DEC-1	deleted in esophageal cancer 1
DEG	Differentially expressed gene
DNA	Deoxyribose nucleic acid
EC	Endothelial cells
ECIS	Electric Cell-Substrate Impedance Sensing
EDTA	Ethylene diamine tetra-acetic acid
ELISA	Enzyme-linked immunosorbent assay
FBS	Fetal bovine serum
FDR	False discovery rate
FFPE method	Formalin-fixed paraffin-embedded method
GCS	Glasgow coma scale
GFAP	Glial fibrillary acidic protein

GFP	Green fluorescent protein
GO	Gene Ontology
GPI	Glycosyl phosphatidyl inositol
GSEA	Gene Set Enrichment Analysis
Hb	Haemoglobin
HBEC	Human brain microvascular endothelial cells
HBSS	Hank's balanced salt solution
HDMEC	Human dermal microvascular endothelial cells
HEK	Human embryonic kidney
HIF-1α	Hypoxia-inducible factor 1 alpha
HIV	Human immunodeficiency virus infection
HMW	High-molecular-weight
HRP-2	Histidine rich protein 2
HUVEC	Human umbilical vein endothelial cells
ICAM-1	Intercellular cell adhesion molecule-1
IF	Immunofluorescence
IgG	Immunoglobulin G
IHC	Immunohistochemical
IL	Interleukin
iNOS	Inducible nitric oxide synthase
IPA	Ingenuity Pathway Analysis
IQR	Interquartile range
IRS	Indoor residual spraying
ITN	Insecticide-treated bed nets
JAK	Janus kinase
KAHRP	knob associated histidine-rich protein
LB	Luria Broth
LMW	Low-molecular-weight
LN	Liquid nitrogen
MAQC	MicroArray Quality Control Consortium
MARF	Malaria associated acute renal failure
MEM	Minimum Essential Medium
MEMA	Moçambique Estúdio Malária Autópsia
miRNA	microRNA
MORU	Mahidol-Oxford Tropical Research Unit
MRI	Magnetic resonance imaging
mRNA	messenger RNA
NARF	Non-acute renal failure
NCBI	National Center for Biotechnology Information (USA)
NCM	Non-cerebral malaria
NF-kB	Nuclear factor kappa-light-chain-enhancer of activated B cells
NO	Nitric oxide
nt	Nucleotide
OR	Odds ratio
OxTREC	Oxford Tropical Research Ethics Committee
panCK	Pancytokeratin
PBS	Phosphate buffered saline

PCR	Polymerase chain reaction
PfEMP-1	*P. falciparum* Erythrocyte Membrane Protein -1
PI3K	Phosphatidyl inositol 3 kinase
PKB/ATK	Protein kinase B
PMI	Posmortem interval
PRBC	Parasitised red blood cells
qRT-PCR	Quantitative reverse-transcription PCR
RBCs	Red blood cells
RDT	Rapid diagnosis tests
RESA	Ring-infected erythrocyte surface antigen
RIN	RNA integrity number
RISC	RNA-induced silencing complex
RNA	Ribonucleic acid
RNase	Ribonuclease
ROC	Receiver operating characteristic
rpm	Round per minute
RPMI	Roswell Park Memorial Institute medium
RT	Reverse transcription
S.O.C.	Super Optimal Broth medium
scaRNAs	Small Cajal body-specific RNAs
SGOT	Serum glutamic aminotransferase
SGPT	Serum pyruvate aminotransferase
SMA	Smooth muscle actin
snoRNA	Small nucleolar RNA
snRNA	Small nuclear RNA
STR	Short tandem repeat
TBS	Tris-buffered saline
TEER	Transendothelial electrical resistance
Tie-2	angiopoietin receptor (gene = TEK)
TNF	Tumor necrosis factor
ULVWF	Ultra-large von Willebrand factor
UTR	Untranslated region
VCAM-1	Vascular cell adhesion molecule-1
VEGF	Vascular endothelial growth factor
VWF	von Willebrand factor (also factor VIIIRA)
WHO	World Health Organization
WPB	Weibel-Palade bodies
WTCHG	Wellcome Trust Centre for Human Genetics

Chapter 1

Introduction

1.1 A historical perspective on malaria

Malaria is an ancient disease known to mankind since the start of human civilisation, and it has tremendously influenced much of human history and population patterns. Actually, the history of malaria predates human history as recent genetic studies have implied that the ancestors of the human malaria parasites were in existence around 500 million years ago, several hundred million years before the first primate ever existed. The oldest evidence of malaria parasites to date has been found in a fossil mosquito preserved in amber, from the Palaeogene period, making it approximately 30 million years old (R. Carter and Mendis 2002). Recent molecular studies have indicated that humans may have contracted *Plasmodium falciparum*, the most common species causing severe malaria in humans, due to cross infection from the gorilla around 12,000 years ago, not from the chimpanzee, bonobo or ancient humans as previously suggested (W. Liu et al. 2010). Human malaria has evolved in concert with its human host, resulting in natural selection of several blood disorders with selective advantage against malaria, such as sickle-cell disease, thalassemias, glucose-6-phosphate dehydrogenase deficiency and the loss of glycophorin C and Duffy antigen (reviewed in R. Carter and Mendis 2002).

Diseases resembling malaria were recognised and recorded in the medical works of ancient civilisations, including the Chinese, Egyptian, Greek and Roman empires; however, the connection between clinical disease, the *Plasmodium* parasite and its mosquito vector was discovered only around the end of the nineteenth century. Before then it had been suggested that malaria was caused by the poisonous vapours emanating from swamps and marshes, hence the two commonly

used name of the disease: “mal’aria” (Italian for bad air) and “paludisme” (from the Latin *palus* for marsh). It was not until 1880 that the causal link between malarial disease and intraerythrocytic parasitic microorganisms, which were later named *Plasmodium*, was established by the French physician Charles Laveran. Not long after that, the Indian-based British surgeon Sir Ronald Ross identified the *Anophelene* mosquito as the vector for malaria parasite transmission (Cox 2010).

1.2 The global burden of malaria

Malaria remains one of the world’s major diseases. More than two billion people, mainly in tropical and subtropical areas, are still at risk (Guerra et al. 2006; Snow et al. 2005) and the economic development of many nations has been hindered by this ancient disease. Statistics during the past 35 years (1965–1990) point out that the yearly gross national product of malaria-endemic countries has risen 2% less than that of non-malaria-endemic countries with an otherwise similar background (Sachs and Malaney 2002). Disproportionately, it costs Africa, the poorest continent in the world, $12 billion dollars each year to battle malaria (Greenwood et al. 2005). In some countries, malaria accounts for as much as 40% of public health expenditure (Roll Back Malaria 2006).

Although exact figures on morbidity and mortality are difficult to obtain, resulting in highly variable results between different studies, it is estimated that during the period 1980–2010 there were approximately 200–500 million new malaria cases and 0.5–2.5 million malaria-related deaths each year globally (systematically reviewed in Murray et al. 2012). Most cases and deaths occur in African children aged below five years old, and malaria is directly responsible for one in five childhood deaths in Africa (Murray et al. 2012; Vogt et al. 2003; World Health Organization [WHO] 2000b). As well as long-term neurological sequelae in a number of survivors (estimated to be up to 10%, but in some studies as high as 25%), evidence has shown that malaria can impair the intellectual and cognitive development of children who survive the severe disease (Fernando et al. 2003), leading to difficulties at school and further economic disadvantages later in life.

Moreover, it contributes to a significant burden of disease in pregnancy. A quarter of severe maternal anaemia and a significant proportion of adverse birth outcomes such as premature delivery, miscarriage, stillbirth and low birth weight can be attributed to malaria (reviewed in Desai et al. 2007).

In developed countries, malaria has been mainly eradicated as a result of spontaneous reduction in contact between malaria vectors and human populations, due to advancement in vector control measures, improved living conditions or climate change. Malaria cases still occur in these countries, mainly in immigrants and travellers returning from malaria-endemic areas, even though rare cases from mosquito transmission or blood transfusion can be seen. There have been approximately 1500 cases each year in both the UK and the USA (Mali et al. 2012). Among industrialised countries, recorded case–fatality ratios range from 1%–3.6%, and commonly involve diagnostic delays (Newman et al. 2004).

According to best estimates (Murray et al. 2012), global mortality had risen to reach a peak of 1.82 million in 2004 due to a growth in the population at risk to malaria, then dropped to 1.24 million in 2010. The World Malaria Report 2011 recognised the reduction in malaria cases and deaths during the last decade, which it attributed to strikingly increased funds for malaria control from a range of international sources through the Global Fund to Fight AIDS, Tuberculosis and Malaria (WHO 2012). These extra funds enabled malaria-endemic countries to substantially increase access to effective control measures including insecticide-treated bed nets (ITN), indoor residual spraying and artemisinin-based combination therapies. However, the WHO's goal of near-zero global deaths by the end of 2015 still seems far fetched.

Experts are still sceptical of this ambitious goal as the present weapons to fight malaria are being challenged by the adaptive ability of malaria parasites and their mosquito vectors. A growing numbers of Southeast Asian countries have been reporting artemisinin resistance in *P. falciparum* malaria since the first reports in 2008 (Dondorp et al. 2009; Noedl et al. 2008). Resistance to

pyrethroids, the common insecticides used in ITN, has been found in 41 countries (WHO 2012). Moreover, research into newer control measures such as new antimalarial drugs and vaccines has been slow to progress. The long-awaited holy grail of an effective malaria vaccine has not materialised, despite implementation of several promising candidate vaccines in clinical trials after decades of intense research.

1.3 The *Plasmodium falciparum* parasite

The intracellular parasitic protozoa genus *Plasmodium*, transmitted by the bite of the female *Anopheles* mosquito, is the causative agent of malaria. There are currently over 200 species of this genus, which can infect many animals including various species of mammal, birds and reptiles. Currently, five species have been recognised as infecting humans in nature, including *P. falciparum*, *P. vivax*, *P. ovale*, *P. malariae* and *P. knowlesi*. Malaria infection due to *P. falciparum* predominates in Africa, and is responsible for the vast majority of severe and fatal disease globally. *P. falciparum* malaria (also called malignant malaria) is the main focus of the work in this thesis.

P. vivax is less virulent but now recognised as the most geographically widespread species, accounting for 50%–95% of malaria episodes outside Africa (R. Carter and Mendis 2002). Rarer cases of severe disease, characterised by severe anaemia, lung disease and renal impairment, and occasional deaths due to severe vivax malaria, are also described (Price et al. 2009). *P. vivax* and *P. ovale* can form a latent stage in hepatocytes; these hypnozoites cause a clinical relapse of malaria long after initial infection and make these parasites difficult to eradicate. *P. malariae* does not form hypnozoites but can persist as an asymptomatic blood stage parasite for several years. *P. knowlesi*, which was primarily a simian malaria parasite, first isolated from long-tailed macaques, has recently been recognised as causing malarial infection in humans in the Pacific and Southeast Asia (Lee et al. 2011). A single report of fatal *P. knowlesi* malaria has been reported by Cox-Singh et al. (2010).

The life cycle of *Plasmodium falciparum*

The complex life cycle of *P. falciparum* occurs in two hosts: vector mosquitos and intermediate human hosts. This is made possible by a complex genome comprising more than 5,000 genes that helps the parasite invade host cells, evade immune responses and pass through multiple phenotypically distinct stages of development (Florens et al. 2002). The life cycle can be summarised in three key stages (Figure 1-1).

1. Pre-erythrocytic stage

The human is an intermediate host for malaria, where the asexual stage of development occurs. When an infected mosquito bites and takes a blood meal, ten to a few hundred slender-shaped sporozoites, from the salivary glands of the mosquito, are injected into the skin. After intradermal inoculation, some invasive sporozoites are destroyed by macrophages while the rest migrate either into a lymphatic channel, where some sporozoites may prime the T cells initiating sporozoite-induced immunity, or into blood vessels (reviewed in Good and Doolan 2007; Vaughan et al. 2008). Within a few minutes, sporozoites in the blood stream reach the liver and invade hepatocytes non-destructively by specific adhesion, inducing invagination of the cell membrane and resulting in the formation of a parasitophorous vacuole within the cytoplasm, where the sporozoite grows and multiplies. Each sporozoite develops into a schizont containing 10,000–30,000 merozoites (or more in case of *P. falciparum*) (Prudêncio et al. 2006). This stage is clinically silent with no symptoms as only a few hepatocytes are affected (Vaughan et al. 2008). After on average of 5–6 days in *P. falciparum* (typically longer in other species), the hepatocytes rupture, releasing merozoites into the bloodstream, which can rapidly invade host red blood cells to initiate the erythrocytic stage of infection.

2. Erythrocytic stage

The merozoites released from ruptured hepatocytes attach and invade red blood cells (RBCs) by multiple receptor-ligand interactions within 60 seconds (reviewed in Cowman and Crabb 2006;

Haldar and Mohandas 2007), minimising the exposure time of parasite antigens to host immune responses. Each merozoite grows and divides within a vacuole into between 8 and 32 new merozoites, successively from ring forms to trophozoites to mature multisegmented schizonts. At the end of the cycle, which last 48 hours in *P. falciparum*, RBCs burst, releasing merozoites to infect more RBCs, This results in a steadily increasing biomass of parasites, released in cyclical surges of parasitaemia, which can rise to levels as high as 10^{13} parasites per host (Greenwood et al. 2008). This replication cycle continues until either the host dies or the immune system can control the infection. Within the RBC, the parasites digest haemoglobin to utilise amino acids for growth, which generates a haemozoin pigment. This is a breakdown product of heme-containing iron, lipids and oxidative side chains, which is toxic to the parasite. Thus, haemozoin is localised within a unit membrane-bound food vacuole in the infected erythrocyte, to protect the developing parasite. Simultaneously, a small proportion of merozoites do not develop to schizonts, but mature into male and female gametocytes which are extracellular, non-pathogenic and crucial for the transmission of the infection to others through further mosquito bites.

3. The sexual stage

Mosquitos are definitive hosts for malaria parasites. When a female mosquito draws a blood meal from an infected human, gametocytes are ingested into the gut of the mosquito, where male and female gametes fuse to form zygotes, then migrate through the mosquito midgut wall and form oocysts. Each oocyst subsequently develops and releases thousands of sporozoites which travel to the mosquito's salivary glands. When the mosquito takes another blood meal, the sporozoites are injected into human skins, causing transmission of malaria parasites to a new human host and thus completing the cycle.

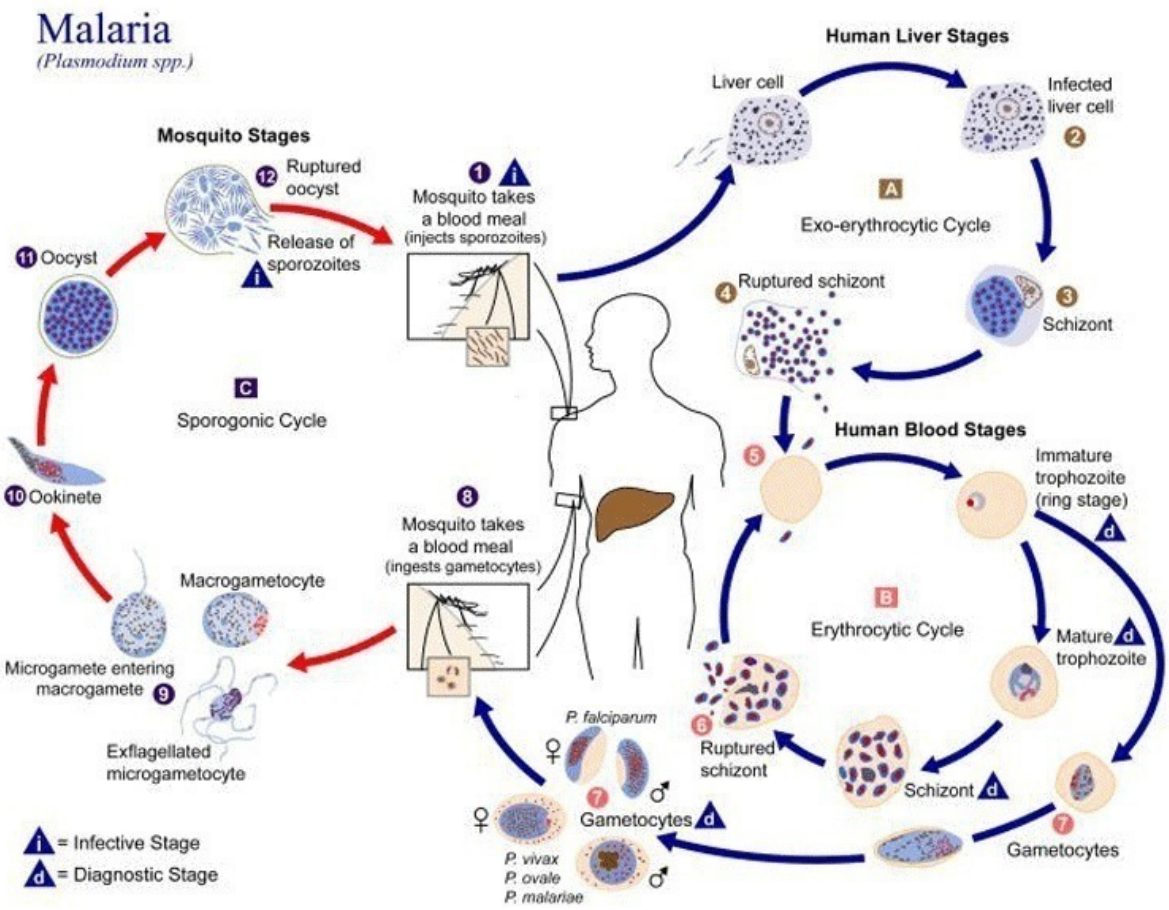

Figure 1-1. The life cycle of *Plasmodium falciparum*

(From: CDC Image Library, Alexander J da Silva and Melanie Moser)

1.4 Clinical presentation of malaria

1.4.1 The clinical spectrum of 'mild' and 'severe' disease

Infection with *P. falciparum* causes a clinical spectrum ranging from asymptomatic infection to life-threatening severe disease or death. Only a minority of *P. falciparum* infections cause severe disease, which is often due to late diagnosis and delayed treatment (WHO 2010). In general, malaria can be categorised into its mild (uncomplicated) and severe (complicated) forms.

The first symptoms of malarial infection are non-specific and similar to viral infection, starting with headache, fatigue, lassitude, muscle and joint pain, and abdominal discomfort, followed by

fever, chills, vomiting and malaise. This is a classic clinical picture of uncomplicated malaria, which people living in endemic areas can usually self-diagnose and, as a result, then seek medical treatment. Thus, malaria is often over-diagnosed based on clinical symptoms alone. The confirmation of malaria diagnosis should be sought using laboratory tests, including light microscopic examination of peripheral blood smears and/or rapid diagnosis tests (RDT). This helps prevent unnecessary use of antimalarial drugs in parasite-negative cases where alternative causes of symptoms need to be excluded.

Well-defined malarial paroxysms, in which fever spikes, chills and rigours occur at regular intervals, can be seen in some patients, more commonly in infection with *P. vivax* and *P. ovale*. At this stage, without other severe complications, the case-fatality rate in *P. falciparum* is very low (approximately 0.1%), if appropriate treatment is given promptly (other human malaria species cause severe complications much more rarely, including *P. knowlesi* and *P. vivax*). However, if treatment is delayed, a patient with *P. falciparum* infection can progress rapidly in hours from having minor symptoms to severe or fatal disease.

1.4.2 Severe malaria

Severe malaria usually manifests with one or more of the following: in adults – coma (cerebral malaria [CM]), anaemia, metabolic disturbance and acidosis, hypoglycaemia, hyperparasitaemia, jaundice, acute renal failure (ARF), acute pulmonary oedema and rarely clotting disturbances; in children – a more limited spectrum of coma, acidosis and severe anaemia predominates. At this stage, the case-fatality increases to 15%–20% in patients receiving treatment, and severe malaria is almost always fatal if it is left untreated. The WHO has developed and defined detailed clinical criteria for the diagnosis of severe malaria, the latest being published in 2000 (WHO 2000a) and, currently being under revision. According to these WHO criteria, severe malaria is diagnosed in a patient who has malaria parasites in the blood with one or more of the complications listed above, where other possible causes have been excluded. Usually, several severe complications exist

together in one patient who develops severe malaria, because the aetiologies of some severe complications are profoundly associated with each other. In hyperendemic areas where the transmission rate of malaria is high, severe malaria predominantly occurs in young children of one month to five years of age, after which a degree of protective immunity to disease develops.

Only CM and malaria-associated ARF (MARF)/acute kidney injury (AKI) are reviewed in further detail here, due to their importance in the work forming this thesis.

CM

CM, which is one of the most common and most severe complications of severe malaria, is a neurological syndrome comprising a potentially reversible diffuse encephalopathy, associated with convulsions and localising neurological signs, which are both poor prognostic features. In order to diagnose CM (WHO 2000a), the following criteria should be fulfilled: 1) detection of asexual form of *P. falciparum* on peripheral blood smear; 2) presence of unrousable coma (Glasgow coma score of 11/15 or less or in children a Blantyre coma score of <2); and 3) exclusion of other possible causes of deteriorating consciousness, such as hypoglycaemia, post-ictal coma or other CNS infections.

Distinguishing CM from other diseases presenting with clinically similar signs is challenging. In malaria-endemic areas, it is difficult to confirm the diagnosis of CM because of the high prevalence of asymptomatic parasitaemia in patients who may have a primary illness due to bacterial sepsis, viral or bacterial encephalopathy (Berkley et al. 1999). Disturbance of consciousness in severe malaria does not only result from CM, but can also be due to the systemic effects of severe malaria such as anaemia, acidosis, hypernatremia and shock. An autopsy study in Malawi reported that approximately 25% of clinically diagnosed CM cases did not have evidence of parasite sequestration in the cerebral microvasculature and had alternative causes for alteration of conscious (T. E. Taylor et al. 2004). Severe malaria is over-diagnosed in endemic areas where the majority of inhabitants are parasitised (Gwer et al. 2007). In African children, true CM is

commonly associated with malarial retinopathy (including orange and white vessels, retinal haemorrhages, and peripheral whitening and papilloedema), which has been proposed as a new diagnostic sign to improve the specificity of the clinical diagnosis of CM (Beare et al. 2006; V. A. White et al. 2009). Malarial retinopathy has also been described in adult Southeast Asian patients (Maude et al. 2009).

Coma, convulsions, brainstem signs and retinal changes are the main neurological features of CM in African children. Coma in children usually develops rapidly after a seizure (Idro et al. 2010). Eighty percent of children with CM are reported to have a history of seizures and 60% have seizures during hospitalisation (Idro et al. 2005). Focal motor and generalised tonic-clonic are the most common types of seizure observed, but subtle or electrographic and status epilepticus are also common (Crawley et al. 1996). Unlike CM in adults, the presence of brainstem signs is common and is associated with increase intracranial pressure.

Coma in adults usually develops more gradually than in children and occurs after drowsiness, disorientation and delirium (Dondorp, Nosten, et al. 2005). Sometime, psychotic behaviours are present as the first symptom of cerebral involvement. Convulsions are less common in adults with less than 15% of cases in large series (Dondorp, Nosten, et al. 2005; Hien et al. 1996). The pattern of seizure is mostly generalised tonic-clonic as seen in children, but status epilepticus is rare. Symmetrical upper-motor-neuron signs are commonly observed but brainstem signs are less common.

Adults and children have similar mortality rates, at about 20%, and the majority of deaths occur in the first 24 hours of admission (WHO 2000a). In surviving cases, adults take longer to recover from coma. The median time of full recovery in adults is 48 hours compared to 24 hours in children (Mohanty et al. 2003). A high incidence of neurological sequelae, of 11%–20% depending on the series, is seen in children. Moreover, 24% of children have some degree of long-term cognitive or developmental impairment, which has been underestimated previously (J. A. Carter

et al. 2005). In contrast, neurological consequences are uncommon in adults recovering from CM; less than 1% is observed in a study in Southeast Asia (Dondorp, Nosten, et al. 2005). These impairments include cranial nerve deficits, cortical blindness, extrapyramidal disorders and neuropathies.

MARF

Renal failure is a relatively common clinical manifestation of severe *falciparum* malaria in South-east Asian adults, but uncommon in paediatric African cases. AKI can present as oliguric or non-oliguric renal failure (Mishra and Das 2008). This has been recognised as having an incidence of approximately 20% in larger clinical series of adult severe malaria (Dondorp, Nosten, et al. 2005). Previous reports of the incidence, severity and prognosis of MARF have provided differing estimates of the prevalence of MARF in malarial infection, which is partly a problem of case definition. For instance, Mehta et al. (2001) reported an incidence of 24/402 cases of smear positive malaria having ARF (6%), all of whom were above 18 years of age. However, this is probably an underestimate of incidence in severe disease, as some of the 402 patients would have been defined as non-severe malaria using the WHO criteria. Nevertheless, of those with MARF over 90% required dialysis and eight died of complications from their malarial infection.

Other severe complications

Severe malarial anaemia (haemoglobin of less than 5 g/dL) is very common in African children, but not in Asian adults. The pathogenesis of severe malarial anaemia is complex and involves several mechanisms, including destruction of RBC, suppression of erythropoiesis and dysreythro-poiesis (reviewed in Perkins et al. 2011). Respiratory distress is a common feature of severe falciparum malaria in both children and adults. Causes of severe respiratory distress include severe anaemia, metabolic acidosis, concomitant pneumonia, aspiration pneumonia, fluid overload, and non-cardiogenic pulmonary oedema caused by acute lung injury (ALI) and acute respiratory distress syndrome (ARDS). Malarial ALI/ARDS is more common in adults than in children and

can develop at the initial presentation of disease or several days after antimalarial treatment when parasitaemia is waning (reviewed in Mohan et al. 2008). Metabolic acidosis is a central feature of severe malaria in both children and adults and has been suggested as the best independent predictor of a fatal outcome. Although metabolic acidosis is largely due to excessive lactic acid, other factors also contribute to acidosis in severe malaria, including unidentified anions, severe anaemia, waste products from parasite metabolism, impaired hepatic blood flow and function, and hypovolaemia (reviewed in Maitland and Newton 2005; Planche and Krishna 2006). Factors contributing to hypolovaemic shock include intravascular fluid leakage, pathological vasodilatation, increased fluid losses and inadequate fluid replacement. However, a recent trial of rapid fluid resuscitation in a large African paediatric cohort, including malaria cases (the FEAST trial), showed no benefit (and in fact an adverse outcome) from rapid fluid bolus therapy (Maitland et al. 2011). Spontaneous bleeding and disseminated intravascular coagulation (DIC) are rare, although thrombocytopenia is common in severe malaria patients, especially children (reviewed in Francischetti et al. 2008).

1.5 Control measures for malaria

Strategies for malaria control measures attempt to prevent transmission of malaria parasites from the mosquito vector to the human host, in order to protect individuals from getting the disease and to reduce the intensity of transmission in the population. Early diagnosis and prompt treatment can reduce morbidity and mortality by preventing the progression of uncomplicated malaria to severe disease, as well as preventing the development of chronic infection which leads to anaemia. Moreover, curing an individual malarial infection reduces the human parasite reservoir, meaning it also curtails malaria transmission.

1.5.1 Mosquito control measures

Of several strategies available for malaria vector control, indoor residual spraying (IRS) and ITN (preferably a long-lasting insecticidal bed net, LLIN) are the most effective and broadly applied interventions (WHO 2012). The ITNs, which include LLINs and conventional treated nets, not only protect the person sleeping under the net but also provide protective effects to the community. The insecticide in ITNs kills the mosquitos that touch it, thus reducing the vector population and intensity of transmission in the surrounding area. IRS, which involves the application of residual insecticides to the inner surface of the household (e.g. walls and roofs), continues to be one of the mainstays for malaria vector control as it has been proven to be responsible for a great reduction in malaria incidence in many countries (Raghavendra et al. 2011). More recently, an exciting alternative to existing control measures, using genetically engineered malaria-resistant mosquitos, has been shown as a proof of principle by several researchers. However, the translation of this approach into routine practice requires consideration of community acceptance, ethics and potential environmental and ecosystem impacts, such as the biology of other mosquito-borne infections (reviewed in Raghavendra et al. 2011).

1.5.2 Drug treatment

Artemisinin derivatives are currently the most potent and most rapidly acting antimalarial drugs. Results from two large clinical trials conducted in Southeast Asia (SEQUAMAT) and Africa (AQUAMAT) have shown that parenteral artesunate (an artemisinin derivative) substantially reduced mortality in Southeast Asian adults and African children with severe malaria, compared to quinine (Dondorp, Nosten, et al. 2005; Dondorp et al. 2010). Thus, the WHO (2012) recommends that all severe malaria cases should be promptly treated with parenteral artesunate, followed by a complete course of oral artemisinin-based combined therapy (ACT). In uncomplicated *P. falciparum* malaria, the ACT should be used instead of using an artemisinin or its

derivatives as a monotherapy to prevent partial parasite clearance, which causes drug resistance (Adjuik et al. 2004).

1.5.3 Vaccine development

Vaccines have eradicated or reduced several infectious diseases of major public health importance, including smallpox, measles and poliomyelitis (André 2003), and there has been an active research effort for decades to develop an effective malaria vaccine. However, this has so far proved unsuccessful, partly due to the lack of clear understanding of effective immune responses to malarial infection, and partly due to practical difficulties in targeting specific antigens in an organism with a complex life cycle. Evidence has suggested that humans can develop long-lasting and protective immunity to malaria disease, although this is different from immunity to infection. More than 40 malaria vaccine projects have reached the clinical trial stage. RTS,S/AS is by far the most advanced candidate vaccine and the only vaccine in a phase 3 clinical trial. It has demonstrated 25%–60% efficacy in different malaria-endemic settings. The ongoing pivotal phase 3 trials, enrolling more than 15,000 children in seven countries in Africa, are expected to finish in 2014. This might be the first malaria vaccine to be used in clinical practice in the next few years, although its efficacy is nowhere near 100% (reviewed in Schwartz et al. 2012). However, because of the scale of mortality and morbidity from malaria, deployment of even this much lower efficacy vaccine might be worthwhile. The development of highly efficacious malaria vaccines is sill of great importance for future malaria eradication.

1.6 The pathology of malaria

All manifestations of malaria disease are caused by the infection of RBC by malaria parasites, which circulate throughout the whole body of the host. This makes malaria a potentially multisystem disease where every organ in the body can show functional and pathological changes. In this

discussion, I have restricted consideration of the pathological changes to those organs which were used for the work included in this thesis, namely the brain and kidney.

1.6.1 The pathology of CM

The most prominent histopathological feature of CM is the presence of PRBC sequestered in the capillaries and post-capillary venules of the brain, reducing the vascular lumen and creating a mechanical obstruction to microvascular circulation. Although sequestration is extensive in most cases of CM, the degree and intensity differs between individuals and within areas of the brain. Sequestration is correlated with increased microvascular congestion and both are independently associated with deeper levels of pre-mortem coma (Pongponratn et al. 2003; Ponsford et al. 2012). Another common neuropathological feature is the presence of microscopic haemorrhages. Several types of haemorrhage are seen, including simple petechial haemorrhages, zonal ring haemorrhages, and Dürck's granulomas, which are most prevalent in white matter and watershed areas. Patients with CM also have malaria pigment (haemozoin), sometimes attached to ruptured erythrocyte membrane ghosts or phagocytosed by host leukocytes. The presence of macroscopic swelling of the brain is common, but is not a universal feature and is more common in African children (S. B. Lucas et al. 1996). Frank brainstem herniation is uncommon in adults, but has been reported in children. Evidence of perivascular oedema together with activation of macrophages in Virchow-Robin space can be seen (Medana and Turner 2006; Medana et al. 2011). Some pathological changes in children differ from those in adults. Studies in Malawian children demonstrated that 75% of cases have intravascular and perivascular pathology (haemorrhages, accumulation of pigmented leukocytes and thrombi) (Dorovini-Zis et al. 2011; T. E. Taylor et al. 2004), whereas leukocytic aggregation, vasculitis or thrombus formation are not consistent in adults (Pongponratn et al. 2003). Acute axonal injury, detected by an accumulation of beta-amyloid precursor protein, was found in post-mortem studies of CM patients. This could represent a reversible but final common pathway to neurological impairment in CM (Medana,

Day, et al. 2002). A recent autopsy study of CM in 50 Malawian children confirms the importance of axonal and myelin damage, blood brain barrier (BBB) breakdown and sequestration of PRBC in the pathology of paediatric CM (Dorovini-Zis et al. 2011).

1.6.2 The pathology of MARF

Pathology studies in Asian patients have reported a number of different findings correlated with the pre-mortem diagnosis of MARF, including acute tubular damage, sequestration of PRBC within glomerular and peritubular blood vessels, accumulation of host leukocytes in peritubular capillaries and a mild endocapillary proliferative glomerulonephritis (Barsoum 2000; Bhamarapravati et al. 1973; Boonpucknavig and Sitprija 1979; Eiam-Ong and Sitprija 1998; Mishra and Das 2008). Contrary to previous reports studying the more chronic and relapsing malarias in African children, a study of a cohort of Southeast Asian adults showed no evidence of established immune complex-mediated glomerulonephritis (Nguansangiam et al. 2007). Possible pathways contributing to renal failure in malaria include PRBC sequestration, leukocyte localisation and activation to release cytokines, and the role of hypoxia.

Previous studies of renal pathology vary in their attribution of glomerulonephritis to the pathophysiology of MARF from *P. falciparum* malaria. Several studies have recorded marked glomerular hypercellularity, mesangial proliferation and both immunofluorescence and electron microscope evidences of immune complex deposition in capillary loops. However, such studies stated that immune complexes were cleared relatively rapidly and the glomerular injury was reversible, in contrast to immune complex nephritis in *P. malariae* (Bhamarapravati et al. 1973). Other studies emphasised that the clinical and biochemical findings in MARF were more in keeping with an ischemic nephropathy or acute tubular necrosis (ATN) (Trang et al. 1992), with little or no proteinuria. The absence of associated hypertension, the rapid resolution without residual renal impairment, together with urinary sediment findings, all suggested that renal failure results from

ATN and not glomerulonephritis. Other authors have also recognised the importance of ATN in contributing to MARF (Eiam-Ong 2003; Zinna et al. 1999).

1.7 The pathogenesis of severe malaria

Despite over a century of active research, it is essentially true to say that the pathophysiology of severe malaria is not well understood. This is important because new strategies to develop methods to fight malaria are still needed. In general, the degree of funding given to research into malaria has lagged behind other rapidly progressing fields such as cancer or chronic inflammatory conditions, which affect patients in richer, more developed countries and result in more income for large pharmaceutical firms. The mechanisms of malaria parasite invasion into host cells, and host immune defences, are key areas to be investigated to understand this complex topic. The interplay of host and parasite interactions, in part illustrated by the complex parasite life cycle, has been discussed in an earlier section (1.3: The *Plasmodium falciparum* parasite). Issues related to the pathogenesis of severe malaria, mainly from *P. falciparum*, will be reviewed in this section.

1.7.1 Malaria is a disease with a wide clinical spectrum

A range of clinical outcomes from asymptomatic to severe complications to death could occur in a person bitten by an infected mosquito. The outcome of an individual infection depends on a number of factors, including prior malaria exposure and resultant immunity, the genetics of host susceptibility and parasite virulence, co-infections such as HIV/AIDS, and socioeconomic factors such as nutrition and access to healthcare.

The clinical presentation of severe malaria is a spectrum of disease with specific complications in different organs. This is partly a question of definition, as other systemic infections such as bacterial sepsis can cause differing presentations depending on the patterns of end organ damage. Initially, therefore, the clinical description of severe malaria tended to focus on the more common clinical presentations which (until recently) were considered more narrow in non- or semi-

immune African paediatric cases, and included CM, anaemia and acidosis. However, adult disease in South or Southeast Asia is associated with a wider spectrum of complications, some of which occur less in African children, such as renal dysfunction or lung involvement. This picture may change over the coming years as more detailed information becomes available from clinical and post-mortem studies and there is broader recognition of the role of co-infections with important pathogens such as HIV/AIDS or bacterial sepsis.

In the past, the predominant presentation of severe falciparum malaria with coma, and the high mortality of the condition, inevitably led to more research concentrating on the mechanisms of disease in the brain during CM, compared to, for instance, the mechanisms of anaemia, lung disease or renal injury.

1.7.2 Genetic diversity of the parasite

Studies from different geographic regions have shown that the genome of *P. falciparum*, comprising of approximately 5000 genes, is much more diverse than the human genome. Certain genes, particularly those under immune selection, have high numbers of single nucleotide pleomorphisms, insertions, deletions and microsatellites (Jiang et al. 2008; Mu et al. 2005; Volkman et al. 2006) .

Genome-wide association studies using pleomorphic markers in the parasite genome have helped to improve understanding of pathogenesis and identify potential therapeutic targets. They have also improved the consistency of malaria research by verifying the phenotypes of parasite cell lines used commonly for laboratory research, which may differ or drift from field-isolated patient strains.

The drug susceptibility of parasites is also influenced by their genetic diversity. Variation in gene copy number in genes known to be associated with metabolic pathways affects drug susceptibility

and resistance (Nair et al. 2008). Thus, identification of genes mediating drug resistance and vaccine failure could advance research into the therapeutics of malaria.

1.7.3 Host factors affecting pathogenesis

Genetic polymorphism and mutation

Advances in molecular genetic technology in recent years have equipped the malaria research community with the ability to search for genetic susceptibility in humans as well as in parasites. Several genetic polymorphisms and mutations in humans affecting the degree of severity of malaria disease are summarised in Table 1-1.

Many RBC disorders are known to have a protective advantage against malaria, including alteration in the structure of β-globin chain (HbS, HbC and HbE), synthesis of globin chains (α- and β- thalassemia), G6PD, Duffy blood group negativity (protective for *P. vivax*), hereditary ovalocytosis and elliptocytosis (reviewed in Boctor and Dorion 2008; R. Carter and Mendis 2002). RBCs in a person with thalassemia are still susceptible to *P. falciparum* invasion but with a much lower parasite multiplication rate (Enevold et al. 2008; O'Donnell et al. 2009). Ovalocytosis is found to have protection against malarial infection in Southeast Asia, in which possible mechanisms include decreased parasite invasion, diminished intraerythrocytic growth and poor cytoadherence of PRBC (Genton et al. 1995).

Polymorphisms in tumour necrosis factor (TNF) genes have been reported to affect the degree of severity of malarial disease (McGuire et al. 1994, 1999). African children with a promoter polymorphism in the TNF gene have a sevenfold increased risk of severe neurological sequelae or death from CM. Severe malaria anaemia is also associated with a different TNF promoter allele.

Table 1-1. Effects of human genetic factors in malaria

Genetic polymorphism	Effect/association	Theoretical mechanism	Reference
LTA + 80	Parasitemia reduction	Lymphotoxin production	(Barbier et al. 2008)
GNAS	Severe malaria	Red cell signaling; invasion inhibition	(Auburn et al. 2008)
INOS	Severe malaria	Decreased iNOS	(Dhangadamajhi et al. 2009)
Pyruvate kinase	Infection	Unknown	(Durand and Coetzer 2008)
ABO glycosyltransferase	Severe malaria anemia	Decreased resetting of red blood cells	(Fry et al. 2008)
Toll-like Receptors (TLR-1, -6, and -9)	Malaria and high parasitemia	Innate immunity	(Leoratti et al. 2008)
FLT1	Placental malaria	Unknown	(Muehlenbachs et al. 2008)
TIM1	Cerebral malaria	Induction of Th2 anti-inflammatory responses	(Nuchnoi et al. 2008)
IL-10	Severe malaria anemia	Anti-inflammatory activity of enhanced IL-10 production	(Ouma et al. 2008)
CR-1 (promoter)	Cerebral malaria	Increased clearance of infected cells	(Cockburn et al. 2004; Teeranaipong et al. 2008)
TNF	Neurological sequelae, cerebral malaria and anemia	Induced cytokine storm	(McGuire et al. 1994, 1999)
RBC disorder/ Blood group	**Effect/association**	**Theoretical mechanism**	**Reference**
α- and β- thalassemia	Partial protection against severe complications	Unclear	(reviewed in Hedrick 2011 and Weatherall 2008)
HbS	Partial protection against severe complications	Impaired parasite growth, accerated removal of PRBCs, enhanced immunity	(reviewed in Hedrick 2011 and Weatherall 2008)
HbC	Protective advantage against malaria	Decreased PfEMP-1 expression	(Fairhurst et al. 2005)
HbE	Protective advantage against malaria	Impaired parasite invasion	(Chotivanich et al. 2002)
G6PD	Partial protection against severe complications	Accelerated oxidative membrane damage, enhanced phagocytosis	(Cappadoro et al. 1998; Williams 2006)
Hereditary ovalocytosis	Resistance to high levels of parasitemia	Impaired parasite invasion and growth	(Genton et al. 1995)
Hereditary elliptocytosis	Protective advantage against malaria	Impaired parasite invasion and growth	(Chishti et al. 1996)
Duffy-negative blood group	Protective advantage against malaria	Impaired parasite invasion	(reviewed in Weatherall 2008)

Immunity

One of the main contributing factors to the diversity of immune responses to malaria is the transmission intensity. Individuals living in high transmission areas such as Sub-Saharan Africa develop nearly complete protective immunity in early adulthood following repeated infection. These individuals are still susceptible to parasitaemia and malarial fever but rarely develop severe disease or a fatal outcome. In contrast, individuals living in low transmission areas (e.g. Southeast Asia) are at risk of severe complications and death, although they do acquire "semi-immune" status which is not enough to be protective from severe or fatal disease. Individuals not living in endemic areas can develop a detectable antibody response but the response is not protective against initial infection (Doolan et al. 2009). There is evidence that infant susceptibility to malaria is affected by maternal malaria and gravidity. The risk of having malaria in the first year of life is higher in children of multigravid women compared to primigravid women (Mutabingwa et al. 2005; Schwarz et al. 2008).

1.7.4 Pathophysiological mechanisms

Ultimately, all disease and therefore clinical manifestations of malaria are caused by PRBCs circulating within erythrocytes in the vasculature, which supplies every organ in the host. Thus, the involvement of RBCs makes malaria a multi-organ system disease. The infection of RBCs by malaria parasites results in progressive alterations to the erythrocyte's structure, biochemistry and function, leading to severe complications and death if host immune response or drug therapy fails. Numerous potential mechanisms have been proposed to contribute to the development of severe malaria, some of which are summarised as follows.

Sequestration and cytoadherence

Sequestration is a process whereby PRBCs infected with the late trophozoite and schizont parasite stages adhere to vascular endothelium and disappear from the peripheral circulation. It is an important component of the pathogenesis of malaria caused by *P. falciparum*, which is the only

human malaria parasite that can induce cytoadherence of infected erythrocytes to human endothelial cells (ECs), via formation of sticky knobs on the surface of PRBCs (Newbold et al. 1999; S. S. Oh et al. 1997). The knobs are composed of a combination of parasite proteins including PfEMP-1, KAHRP, PfEMP-2 and RESA, and human proteins including spectrin, actin and band 4.1 (Aikawa 1988; Sharma 1991, 1997).

The most important of these parasite proteins is termed *P. falciparum* Erythrocyte Membrane Protein-1 (PfEMP-1). PfEMP-1 is encoded by a family of approximately 60 *var* genes in each parasite genome and undergoes rapid antigenic variations though an incompletely understood process (Bull and Marsh 2002; Chookajorn et al. 2008). A new variant PfEMP-1 that has a different antigenic phenotype occurs at a rate of approximately 2% in every parasite cycle (D. J. Roberts et al. 1992). This rapid appearance of antigenic heterogeneity contributes to the parasite's escape from the human immune system (reviewed in Kyes et al. 2007). Data from Bull et al. (1998) indicated that, in semi-immune individuals who have been infected with malaria previously, the parasite which causes severe disease tends to be one which the immune system has not encountered before, hence infection with a new PfEMP-1-expressing parasite is associated with severe disease.

The knob proteins on the PRBC surface bind to receptors on a variety of cell types, including platelets, leukocytes and ECs. Important human receptors, to which malaria-induced knobs can bind, include CD36 (on endothelium, leukocytes and platelets), ICAM-1 (on endothelium and leukocytes) and CSA (in the placenta). Cytoadherence begins at approximately 12 hours of parasite development and is prominent in the second half of the asexual life cycle, leading to the disappearance of parasites from peripheral circulation (Silamut and N. J. White 1993). Sequestration also leads to partial blood flow obstruction, inflammation and endothelial barrier breakdown (Newbold et al. 1999).

A variety of host receptors mediating cytoadherence have been elucidated. These are summarised in Table 1-2 in order of their discovery. One important caveat regarding these results is that, whilst some receptors have been proven to be clinically important, others may be less so, particularly those identified *in vitro* by panning and selection but not found to be a major binding phenotype when clinical parasite isolates are examined. Recent studies of the genetic selection pressure on the cognate parasite-binding molecule PfEMP-1 have indicated that only two of these, CD36 and ICAM-1, exert strong evolutionary pressure on PfEMP-1, making them probably the most relevant *in vivo* (Janes et al. 2011). CSA binding is the most important interaction in the causation of placental (maternal) malaria, which is a success story in terms of trying to link a binding phenotype to the causation of an organ-specific disease (Maubert et al. 2000).

Sequestration is not distributed homogeneously throughout the body; it is greatest in the brain and prominent in the heart, eyes, intestine and adipose tissue. In the brain, the distribution of sequestration also differs between vessels. This phenomenon could be explained by differences in the expression of endothelial receptors. As mentioned above, PfEMP-1 is able to bind to various endothelial ligands. These ligands are distributed differently in various organs. CD36 is expressed on the endothelium in almost every organ but is absent on the brain endothelium, where ICAM-1 is the most predominant potential receptor. ICAM-1 is up-regulated by pro-inflammatory cytokines, therefore potentially increasing sequestration. ICAM-1 levels are increased in the brain of patients with CM and co-localise with vessels showing PRBC sequestration (Turner et al. 1994).

Although CD36 is not expressed in the brain endothelium, it may still contribute to sequestration in the brain microvessels through CD36 expressed on the platelets, which serve as a bridge between PRBCs and brain ECs (Wassmer et al. 2004). Early in the blood stage of *P. falciparum* infection, the endothelium is activated and rapidly releases a number of molecules from Weibel-

Palade bodies (WPB), especially including ultra-large von Willebrand factor (ULVWF). After the release, ULVWF strands, many of which remain attached to the endothelial surface, rapidly bind numerous platelets and become platelet-decorated ULVWF. Circulating PRBCs then adhere to the platelet-decorated ULVWF through CD36 on the platelets, contributing to the PRBC sequestration in the brain microvessels in a CD36-dependent manner (Bridges et al. 2010). These findings correlate with the results from autopsy studies on Malawian children with CM, which found significant platelet accumulation in microvessels (Grau et al. 2003; T. E. Taylor et al. 2004).

Table 1-2. Human host molecules which support cytoadhesion of *Plasmodium falciparum*-infected erythrocytes

Molecule	Comment	Ref.
Thrombospondin	First receptor identified, but appears to mediate binding to altered red cell surface Band-3 protein rather than a specific parasite encoded molecule	(J.Z. Lucas and Sherman 1998; D. D. Roberts et al. 1985)
CD36	Commonest receptor for clinical isolate binding, widely expressed on endothelium apart from the brain. Also a rceptor for rosetting and monocyte/platlete binding	(Handunnetti et al. 1992; Ockenhouse et al. 1989)
ICAM-1 / CD54	An inducible receptor on all endothelial beds, common binding phenotype in field isolates. Some evidence to link expression to cerebral malaria	(Berendt et al. 1989, 1992; Ockenhouse, Betageri, et al. 1992)
Chondroitin-sulphate A (CSA)	Major receptor in placenta during maternal/placental malaria,	(Fried and Duffy 1996)
E-selectin	Inducible endothelial cell molecule. Discovered by panning on recombinant protein	(Ockenhouse, Tegoshi, et al. 1992)
VCAM-1	Inducible endothelial cell molecule Discovered by panning on recombinant protein	(Ockenhouse, Tegoshi, et al. 1992)
CD31 / PECAM	Constitutively expressed on all endothelial cells	(Treutiger et al. 1997)
Integrin α(v)β3	Identified by selectve panning of binding to cerebral endothelial cells *in vitro*	(Siano et al. 1998)
Hyaluronic acid	Also a placental malaria receptor	(Beeson et al. 2000)
Heparan sulphate	Some controversy as to whether CSA moieties expressed on the background of heparan sulphate actually mediate binding to this molecule	(Vogt et al. 2003)
Fractalkine (CX3CL1)	Chemokine receptor expressed on endothelial cells, *in vivo* relevence unclear	(Hatabu et al. 2003)

In addition, recent studies have found that high circulating levels of ULVWF are associated with cerebral and severe forms of *P. falciparum* malaria (de Mast et al. 2007; Larkin et al. 2009). The accumulation of ULVWF has been reported to result from a deficiency of ADAMTS13 (a von Willebrand factor cleaving protease) in severe malaria (de Mast et al. 2009; Larkin et al. 2009). This mechanism has also been described in other conditions, including sepsis, diffuse inter-vascular coagulation and thrombotic thrombocytopenic purpura (de Mast et al. 2009).

Reduction in microvascular flow and hypoxia

In addition to sequestration of PRBCs, reduction in microvascular flow also results from markedly decreased deformability of both PRBCs and non-infected RBCs, which is strongly associated with fatal outcome (Dondorp et al. 2000). Reduction in blood flow causes hypoxia, lactic acid production, reduction in the supply of metabolic substrates, and leads to organ dysfunction. Moreover, the phenomena of rosetting (the adherence of PRBCs to non-infected RBCs), auto-agglutination (the adherence of PRBCs to PRBCs) and platelet-mediated clumping could theoretically further impair flow in microvessels. Whether impedance of flow by sequestration of PRBC or other host cells such as leukocytes and platelets leads directly to hypoxia is as yet unclear.

Studies of hypoxia in human brain tissues with CM have not demonstrated a definitive relation-ship between expression of acute markers of hypoxia such as hypoxia-inducible factor 1 alpha (HIF-1∝ or DEC-1 (Medana et al. 2010) or longer-term 'footprints' of a hypoxic response such as vascular endothelial growth factor (VEGF) and its receptors (VEGF-Rs) (Deininger et al. 2003; Medana et al. 2010). Interestingly, the relationship between hypoxia and susceptibility to experimental CM in the murine model has recently been shown to be highly significant (Hempel et al. 2011), despite the fact that this model is characterised by a lack of cerebral sequestration of PRBCs.

RBC membrane rigidity and deformability

Decreased deformability of the entire population of RBC in *P. Falciparum* infection also leads to increased splenic clearance and loss of RBC, contributing in part to anaemia. Several mechanisms may be responsible for the increase in rigidity and reduction in deformability of the RBC. These include the inhibition of Na+/K+ pump on the red cell membrane, heme-induced oxidative damage of the red cell membrane, and alteration in the phospholipid bilayer (Clark et al. 2006; Nuchsongsin et al. 2007; Park et al. 2008). Anaemia in *P. falciparum* infection is also caused by other mechanisms, including the suppression of erythropoiesis by cytokines and haemozoin-induced apoptosis in erythroid cells in the bone marrow (Clark et al. 2006; Lamikanra et al. 2009), as well as possibly haemolysis from the shearing effect on RBCs by the platelet-decorated ULVWF strings (Lopez 2010).

Parasite biomass

The parasite load in *P. falciparum* infection can be very high, even exceeding 30%, while in *P. vivax* it rarely exceeds 2%, even in the severe cases (Anstey et al. 2009; Miller et al. 2002). This is due to the fact that *P. vivax* preferentially infects only young RBC, limiting its reproductive capacity. In contrast, due to its wide array of parasite-encoded molecules and highly redundant, alternate invasion pathways, *P. falciparum* can invade RBC of all ages and exponentially expand to a very high parasite burden (Weatherall et al. 2002).

Sequestration of mature parasites in vascular beds allows the accumulation of very high parasite biomass despite low (or absent) circulating levels in peripheral blood. Thus, it is clinically difficult to estimate the exact parasite burden in a host by examination of peripheral blood smear alone. The circulating level of histidine rich protein 2 (HRP-2), a *P. falciparum*-derived protein released at schizogony, has been observed to correlate with the severity of clinical disease and has been proposed to be used as an indirect measure of parasite burden in living patients (Dondorp, Desakorn, et al. 2005).

Cytokines and host immune response

The interaction between malaria parasites and the host immune response is complex and poorly understood. Studies have suggested that a cytokine storm – a potentially fatal immune reaction with elevated level of various cytokines – occurs in the setting of severe malaria, leading to a systemic inflammatory response syndrome (SIRS)-like state with a high circulating level of nitric oxide (NO) and TNF. However, evidence is still limited (Maitland and Marsh 2004). Almost all cytokines examined are either raised or decreased in severe and fatal malaria, but none are specific for malarial disease.

At the completion of the *P. falciparum* erythrocytic life cycle every 48 hours, the PRBC bursts, releasing newly developed merozoites into the bloodstream along with numerous other components which may be immunologically active. These include red cell membrane debris, haemozoin pigment, membrane-bound parasite food vacuoles and glycosylphosphatidylinositol (GPI) anchors. These toxic products activate ECs and macrophage to release cytokines and inflammatory mediators such as TNF, interferon-γ, interleukin (IL)-1, IL-6, IL-8, macrophage colony-stimulating factor, and lymphotoxin, as well as superoxide and NO. The systemic manifestations of malarial infection have been largely attributed to release of a repertoire of cytokines in response to toxic products at schizogony (Clark et al. 2006). In addition to these cytokines, plasmodial DNA, which is a constituent of and presented by haemozoin, can also induce fever by up-regulating COX-2 prostaglandin and other inflammatory cytokines via interaction between plasmodial DNA and Toll-like receptor-9 (Parroche et al. 2007; Schumann 2007). Haemozoin has also been observed to cause apoptosis in erythroid cells in the bone marrow, leading to anaemia (Awandare et al. 2007).

Some cytokines can also promote sequestration of PRBC, contributing to the severity of the disease. *P. falciparum*-derived GPI, a special class of glycolipid that can anchor proteins to the outer surface of the cell membrane, plays an important role in inducing the production of TNF,

NO, and pro-inflammatory cytokines such as IL-1, IL-6 and IL-12 from macrophages (Krishnegowda et al. 2005; Vijaykumar et al. 2001; Zhu et al. 2005). These cytokines are known to induce surface-adhesion molecules on the endothelium such as ICAM-1, VCAM-1 and E-selectin. Moreover, GPI also directly up-regulate the expression of ICAM-1, VCAM-1 and E-selectin via tyrosine kinase-dependent signal transduction (Schofield et al. 1996). Therefore, GPI-linked parasite proteins and host cytokine release could theoretically promote sequestration. However, it has been established that systemic endothelial activation, leading to up-regulation of potential sequestration receptors such as ICAM-1, occurs in uncomplicated as well as severe malaria (Turner et al. 1998).

Recent studies have suggested molecular evidence for endothelial and tissue damage in severe malaria. This includes elevated circulating levels of tissue-injury indicators such as lactate, creatine kinase muscle-brain (CK-MB), myoglobin and angiopoietin-2 (Ang-2) as well as increased soluble endothelial receptors such as E-selectin, ICAM-1, TNF-R1, TNF-R2 and VCAM-1 (Day et al. 2000; Ehrhardt et al. 2005; Molyneux et al. 1993; Peyron et al. 1994; Turner et al. 1998; Yeo et al. 2008).

Coagulation system

Activation of the blood coagulation cascade has been proposed to play an important role in the pathogenesis of severe malaria in recent studies (Francischetti 2008; Haldar et al. 2007; W. R. J. Taylor et al. 2008; Wassmer et al. 2008). Several tissue factors including D-dimer and thrombin-antithrombin complexes are elevated in severe malaria, but the coagulation cascade is usually activated in the absence of overt bleeding (normal prothrombin time and thromboplastin time). Both the activation of a coagulation cascade and the consumption of platelets by the binding to ULVWF as described previously could be the cause of thrombocytopenia, which is a common feature of severe malaria and can also be observed in uncomplicated malaria. However, frank DIC is only a rare complication of severe malaria.

1.8 The Angiopoietin–Tie 2 receptor signalling pathway in malaria

Angiopoietins are soluble proteins, which are classified as growth factors that promote angiogenesis from pre-existing blood vessels. There are now 4 identified angiopoietins: Ang-1, Ang-2, Ang-3 and Ang-4. These angiopoietins are ligands for Tie-2 receptors, which were originally discovered in 1993 as an endothelial specific receptor (Schnürch and Risau 1993). Subsequently, Tie-2 receptors have also been found to be expressed on a range of non-endothelial cells including carcinoma cells, fibroblasts, keratinocytes, smooth muscle cells, lymphocytes, haematopoietic stem cells, neurons and glial cells (reviewed in Makinde and Agrawal 2008). Ang-1 and Ang-2 are the best-characterised ligands for Tie-2, and were the first to be identified (Davis et al.1996; Maisonpierre et al. 1997). Ang-1 is constitutively expressed in many cell types including pericytes, smooth muscle cells, fibroblasts and some tumor cells, whereas Ang-2 is almost exclusively expressed by endothelial cells (reviewed in Fiedler and Augustin 2006). Angiopoietins and Tie-2 are vital to the formation of mature blood vessels. Gene deletion or mutation of Ang-1, Ang-2 or Tie-2 resulted in severe defects in vascular development, leading to embryonic lethality in mouse knock out studies (Gale et al. 2002; Maisonpierre et al. 1997; Sato et al. 1995; Suri et al. 1996).

Beside its role in angiogenesis, the Ang-Tie-2 receptor system plays an important role in the regulation of vascular maintenance and homeostasis, via a signalling pathway where Ang-1 and Ang-2 competitively bind to their receptor Tie-2 (Figure 1-2). This competition determines the level of endothelial cell activation and responsiveness to other exogenous stimuli, thus facilitating both inflammation (via TNF and IL-1) and angiogenesis (via VEGF). This system is therefore a permissive gateway for the action of other molecules on endothelial cell function and activation (Fiedler and Augustin 2006).

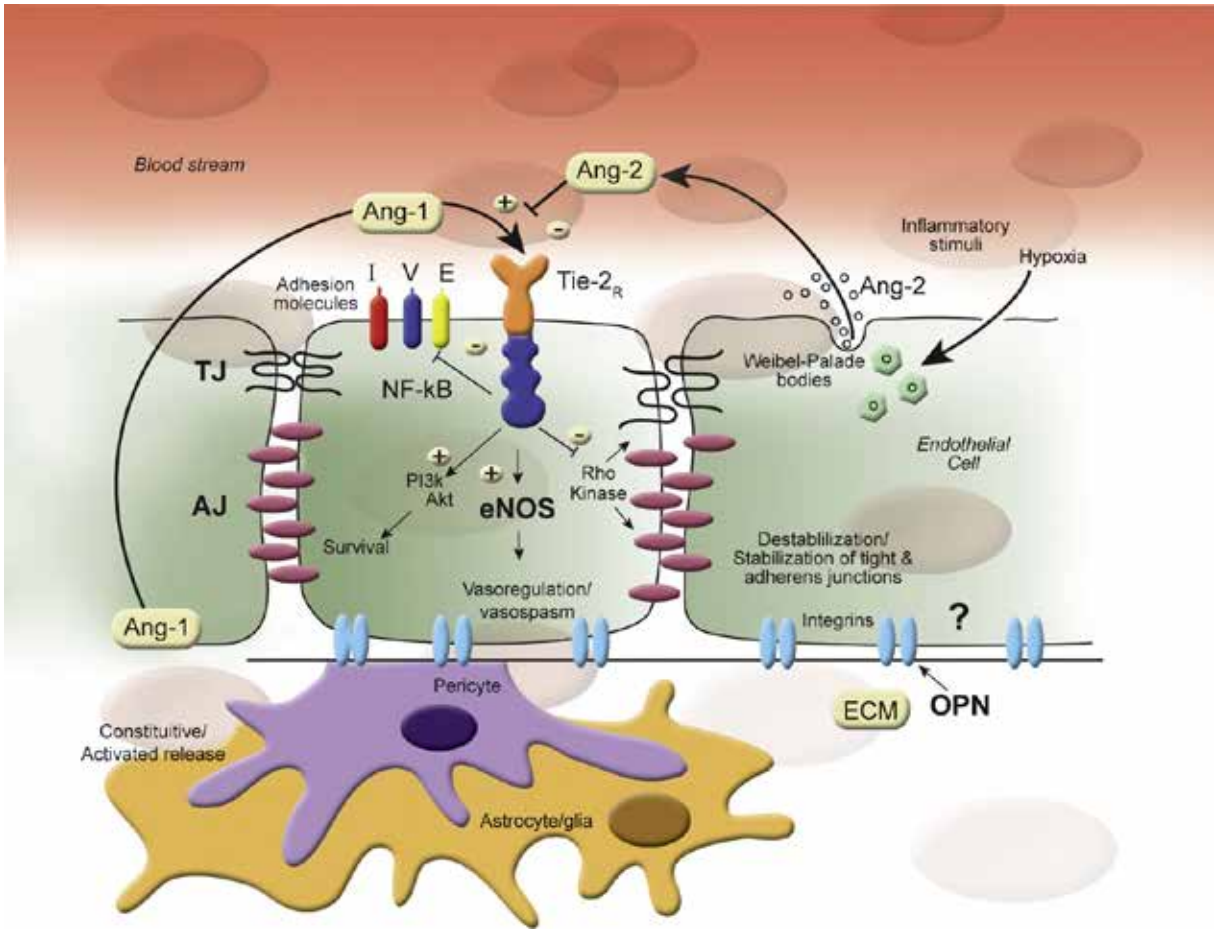

Figure 1-2. Effects of angiopoietins and Tie-2 receptor on the BBB

This figure shows Ang-1 and Ang-2 signalling in regulating the quiescent and activated endothelium phenotypes at the BBB. The constitutive Ang-1-mediated Tie-2 signalling maintains quiescent state of the endothelium through several downstream signalling pathways including activating PI3K/ATK pathway (resulting in cell survival), inhibiting both Rho Kinase (resulting in stabilisation of intercellular junctional molecules) and NF-κB (resulting in anti-inflammatory effects). Ang-2 is released from WPB in response to exogenous stimuli such as hypoxia and inflammation, where it competitively binds to the Tie-2 receptor. Ang-2 mediated Tie-2 signalling results in destabilised endothelium, enhanced responsiveness to other cytokines and inflammatory cell recruitment. Tie-2 also regulates eNOS activity, which is involved in vascular tone control. (Reprinted from *Pathophysiology*, in press, Chittiboina et al., Angiopoietins as promising biomarkers and potential therapeutic targets in brain injury, Copyright (2012), with permission from Elsevier)

1.8.1 Endothelial activation in malaria

The interface between the circulation and endothelium appears a critical boundary in severe disease and as central to the pathogenesis of CM. During severe malarial infection, there is

systemic activation of ECs including the cerebral ECs of the BBB (Turner et al. 1994; Turner et al. 1998). Activated endothelium has increased permeability through the disruption of endothelial transmembrane proteins, and shows up-regulation of a variety of surface-adhesion molecules including intercellular cell adhesion molecule-1 (ICAM-1), vascular cell adhesion molecule-1 (VCAM-1), P- and E-selectin (Dejana 2004; Fiedler and Augustin 2006; Hawkins and Davis 2005; Nag et al. 2009; Turner et al. 1994). Moreover, activated ECs rapidly exocytose pre-synthesised and stored molecules from WPB in response to changes in the vascular microenvironment. Although the main constituent of WPB is VWF and its propeptide, other molecules including P-selectin, CD63, IL-8, endothelin-1, tissue plasminogen activator and Ang-2 are also released. The release of WPB is the initial step in the transition from a resting endothelial phenotype to activated responsive endothelium (Fiedler 2004; Pfaff et al. 2006; Pober and Sessa 2007; Rondaij et al. 2006).

1.8.2 Balance of Ang-1 and Ang-2 and integrity of endothelium

The Ang–Tie-2 ligand-receptor system is a key regulator of the maintenance of functional integrity in both quiescent and activated endothelium (Fiedler et al. 2006). In most contexts, Ang-1-mediated Tie-2 signalling maintains endothelium in a quiescent state, but Ang-2, which functions as an antagonist ligand of Tie-2, can destabilise this and sensitise endothelial response to inflammatory and angiogenic cytokines such as TNF, IL-1 and VEGF (Fiedler and Augustin 2006). In order to maintain the quiescent phenotype of endothelium, ECs need constitutive Tie-2 signalling mediated by Ang-1 binding, which is mainly released from pericytes, fibroblast and smooth muscle cells and incorporated into extracellular matrix after secretion (Xu 2001). Activation of Tie-2 signalling requires phosphorylation, and is involved in several downstream signalling pathways including both activating phosphatidylinositol 3 kinase (PI3K) and protein kinase B (PKB-ATK) pathways and inhibiting nuclear factor (NF)-κB (Makinde and Agrawal 2008). These pathways protect cells from apoptosis and loss of intercellular junctional complexes and

inhibit inflammatory responses. Exogenous stimuli such as physical damage, hypoxia or impaired endothelial NO production cause rapid exocytosis of Ang-2 stored in WPB from the ECs, which competitively binds to the Tie-2 receptor, negatively regulating constitutive Ang-1-mediated Tie-2 signalling (Fiedler 2004; Y. Q. Huang 2002; H. Oh et al. 1999; Yeo et al. 2008). Consequently, Ang-2-Tie-2 binding results in destabilisation of endothelium and enhances EC responsiveness to other cytokines. Continued exposure of ECs to Ang-2 in the presence of other cytokines such as TNF, IL-1 and VEGF results in the induction of an inflammatory response (TNF and IL-1) and angiogenesis (VEGF), and additionally induces Ang-2 overexpression in ECs. However Ang-2 up-regulation in the absence of other stimuli results in EC apoptosis and subsequent vascular regression. Ang-2 can therefore act as an autocrine dynamic regulator of the rapid adaptive response of endothelium (Fiedler and Augustin 2006).

1.8.3 Angiopoietins in malaria

Recent *in vivo* studies have implicated the dysregulation of angiopoietins in the pathogenesis of severe and fatal malaria. In adults with CM and non-cerebral severe malaria (NCM), plasma Ang-2 has been associated with reduced endothelial NO bioavailability (Yeo et al. 2008) and mortality (Jain et al. 2011; Yeo et al. 2008), with Ang-2 a better predictor of death than venous lactate (Yeo et al. 2008). In children, increased plasma Ang-2 and the Ang-2/1 ratio, and reduced Ang-1, have been associated with disease severity and risk of death in CM (Conroy et al. 2009, 2010; Lovegrove et al. 2009). Nevertheless, the mechanisms by which the Ang-Tie-2 pathway contributes to CM and NCM, and fatal outcome, remain unclear.

The value of such biomarkers in diagnosis in a developing world context is questionable as it depends on clinical and laboratory facilities which are often lacking, and once a diagnosis of malaria is established using established methods such as blood film microscopy or RDTs then it is clear from recent large multicentre trials that the most effective treatment is prompt ACTs. Having a bedside Ang-2 test would not help this process, and raised Ang-2 levels may not be

specific to malaria, as they increased in other conditions (including critically ill patients (Lukasz et al. 2008), severe sepsis (Mankhambo et al. 2010), congestive heart failure (Chong et al. 2004) and chronic kidney disease (David et al. 2010)), so are not disease specific. Therefore, an association of the Ang-Tie-2 pathway with malaria is mainly helpful in establishing pathogenesis and suggesting routes for adjunctive therapy.

The therapeutic use of angiopoietins has been investigated in experimental murine models of brain ischemia, where Ang-1 inhibits BBB breakdown, stimulates the recruitment of neuroblasts and promotes behavioural recovery (Ohab et al. 2006). The Ang-Tie2 signalling pathway could potentially be a target for neuroprotective adjunctive therapy in CM. However their tissue-specific expression and specificity in target organs such as the brain or kidney had not been studied in human fatal malaria cases.

1.9 Research strategies to study the pathophysiology of severe malaria

1.9.1. Animal models

Extensive investigations into the pathogenesis of malaria have been conducted using various strategies in humans, animal models and *ex vivo* tissue cultures. The murine model of CM, which was first published 35 years ago, has been widely used as an experimental model of human severe malaria, in particular using strains which are susceptible and resistant to neurological illness as a model of CM. However, there has been some controversy about conclusions based on this model (for instance, those used to propose adjunct clinical trials in humans) due to the differences in the histopathology and clinical manifestations between the mouse and human. The concerns were reflected in a string of publications in 2010 discussing the relevance of murine models for the study of human CM, started by White et al. (2010), which resulted in the polarisation of the malaria research community on this topic (Craig et al. 2012).

The murine model of CM is a specific model almost exclusively using *P. berghei* (ANKA strain) as the pathogen on the C57BL/6 or CBA mice, because *P. falciparum*, the causative agent of human CM, does not cause an infection in mice, and the infections of most of other strains of *P. berghei* in most of other strains of mice do not cause lethal encephalopathy.

The main pathological difference between murine 'experimental' CM and human CM is that there is an extensive accumulation of inflammatory cells and platelets in the microvasculature of the brain in mice infected with *P. berghei* ANKA, instead of the sequestration of PRBC, which is one pathological hallmark of human CM, whilst there is no or very little degree of parasite sequestration in the mouse brain. In addition, there is good evidence for the clinical neurological illness underlying murine CM being an immune-mediated encephalitis (Lovegrove et al. 2008), whereas the level of leukocyte accumulation observed in human CM is low and variable. Although there is some degree of sequestration of PRBC in the mice infected with *P. berghei* ANKA via CD36 adhesion, this sequestration occurs mainly in the lungs and adipose tissue, rather than in the brain. In CD36-/- mice infected with *P. berghei* ANKA, no sequestration is observed but the infected mice still develop cerebral syndrome (Franke-Fayard et al. 2005). This finding dissociates the cerebral sequestration of PRBC from the occurrence of CM in the murine model and indicates a discrepancy in the fundamental cause of cerebral syndrome between murine and human CM.

Moreover, murine models provide different clinical pictures of neurological impairment to human ones. In one murine CM study, researchers developed a model wherein the mice had neurological impairment and developed coma, but all of the mice subsequently died (Medana et al. 2001), compared to about a 20%–30% fatality rate in human CM. In another study, mice developed a reversible neurological symptom but not coma, which is the clinical diagnostic hallmark of human CM (Neill and Hunt 1992). In addition to the differences in the pathological features and clinical pictures mentioned above, there has been no convincing evidence of benefits from transferring a

number of adjuvant therapies which were successful in the murine model to effective interventions in human CM. Most of the adjuvant treatments studied in murine models have shown a dramatic effect in preventing or reducing the genesis of cerebral syndrome (44 out of 48 different potential therapeutic measures so far); however, these interventions have failed to show benefits in human clinical trials and in some cases have been harmful (N. J. White et al. 2010).

Despite these differences, murine models remain one of the main approaches to the understanding of the pathogenesis of human CM. A number of immunological mechanisms determined by host response which contribute to the pathogenesis of CM were first described in murine models and then later confirmed as occurring in human CM. These include release of anti- and pro-inflammatory cytokines, BBB dysfunction and endothelial activation.

The other main animal model used to study CM and severe malaria is non-human primates (NHP), which have greater genetic and phenotypic similarity to humans. Several host/parasite combinations in NHP models such as *P. coatneyi* in Japanese macaques (*Macaca fuscata*) and rhesus macaques (*Macaca mulatta*) can exhibit PRCB sequestration, rosetting and severe clinical manifestation, mimicking *P. falciparum* infection in humans (Aikawa et al. 1992; Kawai et al. 1995). Although *P. knowlesi* infection in rhesus macaques can produce a severe clinical syndrome that is almost always fatal, whether it is useful as a model for human CM is questionable, as neither PRBC sequestration in the brain microvessels nor any clinical signs of CM are seen (Craig et al. 2012; N. J. White 2008). However, its relevance has increased with the recent discovery of *P. knowlesi* as a human pathogen and the description of fatal disease (Cox-Singh et al. 2008). NHP models have been used to model PRBC sequestration in the brain vasculature, as well as to investigate its effects (Aikawa et al. 1992). In addition, their use in neuroimaging studies has begun to give us clues as to the metabolic processes occurring in the brain during severe malarial infection (Kawai and Sugiyama 2010).

1.9.2 *In vitro* EC models

Although animal models allow mechanistic studies of the genesis of malaria disease, primarily in regard to the immunological responses of the host to malarial infection, they lack the ability to investigate some other key underlying mechanisms, and their use in screening for potential therapies is controversial (Craig et al. 2012). Thus, *in vitro* models are essential to pathophysiological studies of malarial disease and the development of effective treatments and vaccines. The use of *in vitro* models in malaria research started from the successful *ex vivo* continuous cultivation of *P. falciparum* in RBCs, which was firstly reported in 1976 by Trager and Jenson. Since then co-culture experiments with isolated primary or immortalised human EC lines, including human umbilical vein ECs (HUVEC), dermal microvascular ECs and brain or lung ECs, has allowed the delineation of the host receptors which allow PRBC adhesion and studies of the post-adhesive events and their functional effect on endothelial monolayers.

Several key elements of the pathophysiology of severe malaria have been delineated using an *ex vivo* cell culture approach. These include the identification of sequestration receptors on EC-mediating static or rolling cytoadherence of PRBC, such as CD36, ICAM-1 and CSA. Tripathi et al. (2007) successfully used an *in vitro* human BBB model to show that PRBC but not uninfected-RBC significantly decreased BBB integrity by measuring transendothelial electrical resistance (TEER) in real time. Their model demonstrated ICAM-1-mediated signalling following PRBC binding causes significant up-regulation of the mRNA transcripts associated with immune response and apoptosis, stimulating signalling via a NF κB cascade using microarray technology (Tripathi et al. 2009). In addition, EC-free systems can be used to examine the rheological factors contributing to microvascular obstruction. Shelby et al. (2003) demonstrated in real time the effect of RBC deformability on the capillary blockage using microfluidic devices.

1.9.3 The developing applications of molecular pathology in malaria research

What is molecular pathology?

Broadly speaking, pathology is the study of disease, with a focus on aetiology and pathogenesis, through the examination of morphological and molecular modifications of cells and tissues. Molecular pathology is an emerging discipline within the field of pathology. Both share the same conceptual foundation, which is to investigate the linkage of manifestations of diseases and the underlying mechanisms causing disease in tissues, cells and body fluids. Since the discovery of DNA by Watson and Crick more than 50 years ago, the pace of scientific discovery in biomedical sciences has strikingly increased due to significant innovations in techniques and methodologies used in molecular biology research, particularly the new high-throughput methods of proteomics and genomics. These have helped increase understanding of the molecular basis of normal and disease states in human and other organisms. Today, molecular pathology uses various techniques in molecular biology and other disciplines (including genomics, proteomics, and system biology) to complement the information on disease morphology and aetiology gained from conventional histopathological, ultrastructural or immunohistochemical examination.

Because of this revolution in theoretical biology, the concept of pathology is changing as scientists and physicians search for a deeper understanding of the precise genetic and molecular mechanisms of human diseases, in order to provide better diagnosis and prognosis and individualise treatment to take account of host responses (for instance to chemotherapy of a particular cancer), as well as to develop newer prevention and treatment measures for diseases. Molecular pathology can be seen as a crossover discipline sharing some aspects of diagnostic clinical pathology, molecular biology, biochemistry, genomics, proteomics and genetics. It utilises techniques in molecular biology, where nucleic acids and proteins are analysed after their extraction from organs, tissues, cells or bodily fluids using polymerase chain reaction (PCR)-based amplification of particular genes, or rapid throughput screening of whole genomes by microarray techniques or

next-generation sequencing. In addition, chromosomal or molecular morphology can be analysed *in situ* using methods such as immunohistochemistry (IHC) or fluorescence in situ hybridisation (FISH).

Molecular pathology in human malaria

Pathological studies in human malaria have been performed for over a century, since the seminal studies in the late nineteenth century by Italian malariologists and pathologists Camillo Glogi, Ettore Marchiafava and colleagues (reviewed in Cox 2010). However, they are relatively sparse, considering the burden of the disease worldwide, mainly because of the difficulty of obtaining human tissue for use in research. Tissues from malaria-infected individuals can only be collected at post-mortem after the disease progresses to death, despite any treatment. Biopsy of tissues in living malaria patients, which is a common practice in cancer and the main source of human tissue for cancer research, is ethically questionable because it is too invasive and does not provide clinical information for diagnosis or treatment of malaria. Some studies have examined muscle biopsies or skin biopsies taken during life (Turner et al. 1998), but examination of the brain in living patients is clearly impossible, although newer radiological methods such as functional MRI offer some hope of gaining functional insight into disease processes during life. Most malarial deaths also occur in Africa, where facilities to conduct research may be limited and cultural acceptance of post-mortem examination for research projects may be low. Thus, relatively few large-scale autopsy studies of human malaria have been conducted, leading to limited opportunities for prospective molecular pathological studies.

A key concern in conducting molecular-based research is tissue quality, particularly when these are collected at post-mortem. Unlike animal models, where conditions prior to and at death can be strictly controlled and manipulated, human autopsy tissues are subjected to numerous uncontrollable factors such as various courses of disease progression and appropriate treatments received in each patient. These are confounding factors that can affect the quality of the tissue. Some of the

traditionally recognised confounders are related to pre-mortem events, including agonal factors (e.g. hypoxia, pyrexia, coma, seizures, acidosis, dehydration, or treatment) and the duration of the agonal state (reviewed in Hynd et al. 2003). Others are related to post-mortem events such as the interval between death and tissue fixation, temperature of the corpse and the environment, bacterial contamination, optimisation of tissue fixation, processing and storage conditions (Hynd et al. 2003; Stan et al. 2006; Tomita et al. 2004; Weis et al. 2007). In addition, some confounders are still incompletely understood and unpredictable. There are also unexplainable variations in the quality of the tissue from different areas of the same brain or from different cases with similar pre- and post- mortem conditions (Ferrer et al. 2008).

Post-mortem tissue is routinely and conveniently preserved by formalin fixation, processing in graded solutions of alcohols to dehydrate a tissue, and embedding in paraffin blocks (i.e. the formalin-fixed paraffin-embedded (FFPE) method). This provides good morphological preservation for histopathological examination but is harmful to nucleic acids and protein, due to extensive crosslinks of protein–protein and protein–nucleic acid, which subsequently leads to nucleic acid fragmentation. This affects the results of sensitive molecular techniques examining labile mRNAs such as qRT-PCR and gene expression microarrays, although it should be noted that DNA is more stable and often yields adequate results from fixed material (reviewed in Kretzschmar 2009). Preservation of tissue intended for RNA analysis requires other fixative methods, the most common of which is snap freezing, either in the liquid or vapour phase of liquid nitrogen (LN). This has proved to be the gold standard of tissue-preservation methods for sensitive molecular-based studies. However, conducting such methods is not easy or even not possible in some circumstances because it requires trained technicians with necessary specialised equipment and access to LN. These are often difficult to obtain in areas where autopsy studies on malaria are conducted.

To date, there have been no studies that successfully use malaria-infected human organs for highly sensitive molecular techniques such as gene expression microarray or whole-genome sequencing. However, this does not mean that various molecular biology techniques and genomic analysis have not been successfully applied in genomic studies of the human host and the malaria parasite. In this type of research, the human DNA is usually extracted from the blood, which is much more easily obtained than human organs. Although the sequencing of the human genome from blood has provided an opportunity to understand the genetic pleomorphisms associated with susceptibility and resistance to malarial infection, it is not able to reveal the mechanistic responses of the host or host–parasite interactions during the course of malarial infection at tissue or cellular level.

1.9.4 Genomic approaches in malaria

Most pathophysiological studies in CM to date have been restricted to the assessment of a small number of individual factors that have been predefined and hypothesised as potentially important effectors in the disease. Such studies may use a murine model to examine the effects of a gene knockout, such as interferon gamma (Amani et al. 2000), or examine human tissues with clinicopathological correlation and IHC, as was used to identify the potential role of axonal injury with β-APP (Medana, Day, et al. 2002). These studies can verify the significance of a small number of particular predefined factors but lack the power to evaluate all possible potential factors and their interactions in the complex pathways of CM pathogenesis. An alternative approach is to use various technologies in genomic research such as high-throughput sequencing and whole-genome microarrays, which allow the evaluation of the whole human genome at a single time point. In other words, rather than examining the expression of a single gene product or a small group of genes in a particular signalling cascade, every gene in a tissue can be analysed simultaneously. This approach depicts the whole picture of what happens in a particular tissue at the transcriptome level. Complemented with bioinformatics, genomic data may give clues as to which

pathways are physiologically relevant, and allow comparison with data generated by similar techniques in other human diseases.

This approach has now been used in *P. berghei* ANKA-infected murine models and *in vitro* endothelial co-culture models to study the pathogenesis of CM (Chakravorty et al. 2007; Delahaye et al. 2007; Lovegrove et al. 2007; Miu et al. 2008; Oakley et al. 2008; Schaecher et al. 2005; Sexton et al. 2004; Tripathi et al. 2009). These results have revealed several novel potential factors contributing to CM in the murine model, such as neuronal apoptosis, suppressed erythropoiesis, changes in glycolytic pathways, and interferon-regulating processes. As yet, no such studies have been carried out using human cases of fatal malaria. This approach offers the possibility of analysing the expression of the whole set of genes simultaneously in humans with fatal severe malaria, as well as identifying novel pathways associated with the pathogenesis of human CM and other severe complications. It also allows the examination of tissue-specific events linked to particular clinical syndromes of the disease, such as coma or lung/kidney injury.

1.10 MicroRNA

1.10.1 What is microRNA?

MicroRNAs (miRNA) are small non-coding RNAs that have been recognised as important post-transcriptional regulators of gene expression in a wide range of species. The miRNA is initially transcribed in the nucleus as a much longer transcript (pri-miRNA) from a non-protein-coding genomic region before being processed by type III RNA endonuclease Drosha into pre-miRNA with 60–70 nucleotides and a hairpin loop structure. It is then transported by exportin-5 into the cytoplasm, where it is further processed by type III endonuclease Dicer into a mature miRNA duplex of usually 21–23 nucleotides in length (Peters and Meister 2007). The sense strand of the mature miRNA duplex then forms an RNA–protein complex with Argonaut proteins. This RNA–protein complex, which is known as RNA silencing complex (RISC), regulates gene

expression by binding its "seed region", 2–8 nucleotides, of the miRNA to the 3' untranslated region (UTR) of the target gene based on sequence complementarily; this results in either the inhibition of RNA translation or the degradation of the target messenger RNA (mRNA) (Bartel 2009). The biology of miRNA is illustrated in Figure 1-3. Since the discoveries of the first two members of the miRNA family in 1993 (lin-4) and 2000 (let-7), 1,898 unique mature miRNAs have now been identified to date in the human and a total of 18,226 hairpin precursor miRNAs expressing 21,643 mature miRNAs in 168 species (http://www.mirbase.org; release 18, November 2011). Although there is a relatively small number of miRNAs compared to the number of mRNA transcripts in the human genome, one single miRNA can regulate up to 200 mRNAs and one mRNA can be controlled by several miRNA (Lim et al. 2005). It is estimated that 30% of human genes are regulated by miRNAs (Lewis et al. 2005).

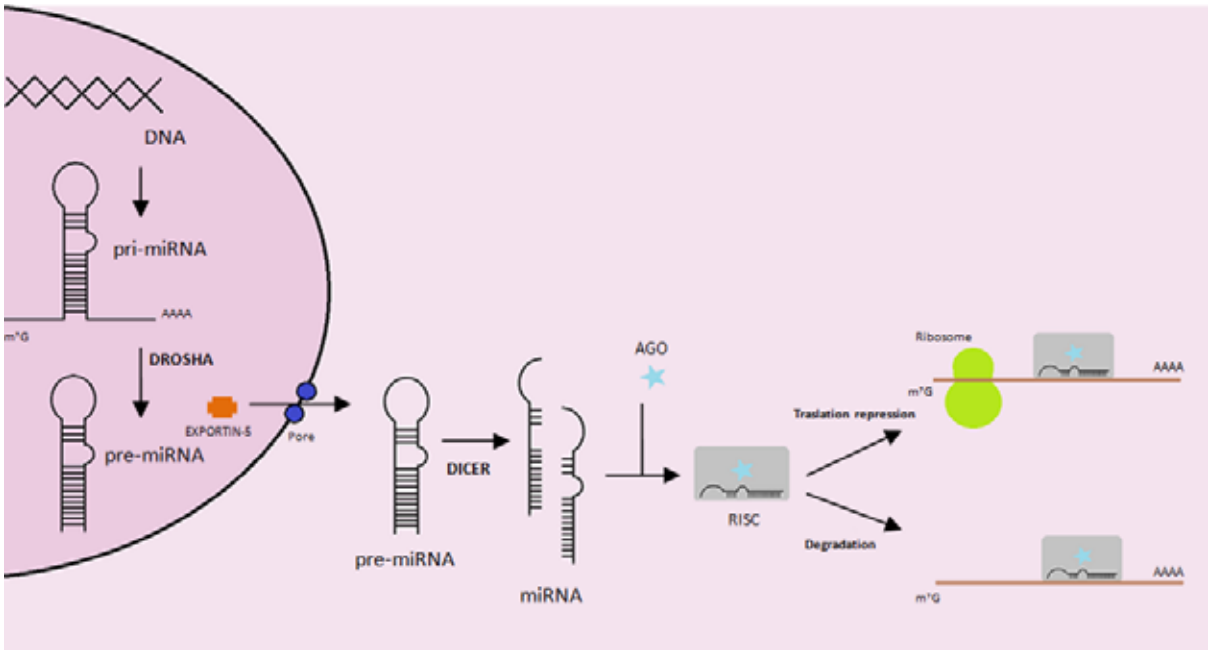

Figure 1-3. The biology of miRNAs

The figure shows the mechanisms by which small non-coding miRNA can be transcribed, exit the nucleus and influence translation of mRNA transcripts in the cytoplasm.

1.10.2 miRNA is well preserved in formalin-fixed, paraffin-embedded tissues

FFPE tissues are the most common type of samples in clinical histological practice and they are normally archived with extensive documented clinicopathological histories. However, despite excellent RNA isolation methods, RNAs from FFPE samples are usually fragmented to a broad size distribution and chemically modified to a degree that is incompatible with molecular applications; one study indicated that only 3% of extracted mRNA from FFPE samples was suitable for subsequent qRT-PCR analysis (Godfrey et al. 2000). This problem almost certainly rules out the possibility of using routine FFPE tissue for mRNA expression analysis by microarray technology, which requires high-quality RNA samples.

In contrast to mRNA, miRNAs are much less susceptible to the deleterious effect of tissue fixation and embedding processes. This might be in part due to their smaller size, which represents a difficult target for enzymatic or chemical cleavage. Furthermore, it is postulated that miRNA might be protected from the modification effect of formalin fixation because most mature miRNAs are tightly incorporated into RISC; although, no concrete evidence has been reported (Jung et al. 2010; A. Liu et al. 2009). Due to the uniformity in structure and limited size range of miRNAs, proportional degradation occurs in most miRNA transcripts (Klopfleisch and Weiss 2011). In addition, several studies have shown that the miRNA expression profiles from FFPE tissues correlate well with those from fresh frozen tissues (Dijkstra et al. 2012; Li et al. 2007; A. Liu et al. 2009; Szafranska et al. 2008).

1.10.3 miRNA and human disease

A growing body of evidence has implicated the roles of miRNA in various molecular pathways regarding the developmental, physiological and pathological responses of cells and tissues, including cellular metabolism, proliferation, differentiation, apoptosis, infection and tumorigenesis (Bushati and Cohen 2007). In cancer research, where miRNA has been extensively studied, the

miRNA expression profile is now being considered as a potentially diagnostic and prognostic marker, as well as a starting point in the development of therapeutic interventions (Waldman and Terzic 2008). Evidence also suggests a role for miRNA in the central nervous system homeostasis and the host response to external stimuli such as infection. Malaria infection disturbs cerebral function by complex mechanisms involving both local effects of PRBC sequestration and systemic immunological responses of the host, leading to BBB leakage and dysfunction of astroglial cells and neurons. Studies in other diseases and experimental tissue culture have identified a number of miRNAs in the response and/or the regulation of such mechanisms that may be involved in CM pathogenesis, such as tissue hypoxia (X. Huang et al. 2010), and host response to other pathogens (Xu Wang et al. 2009). Moreover, miRNA dysregulation has been found in the brain in relation to several different conditions, such as neurodegeneration, schizophrenia, cancer and HIV infection.

1.10.4 miRNA and malaria

Few studies of miRNA expression have been done on malaria. Two papers have reported that there is no miRNA in *P. falciparum*, although there is abundant accumulation of miR-451 in PRBC, which could be a residue of erythroid differentiation (Rathjen et al. 2006; Xue et al. 2008). A single study of miRNA expression in the murine model of CM recently identified that three miRNAs (let-7i, mir-27s and mir-150) were overexpressed in the brain of CBA mice infected with *P. berghei* ANKA (model of CM), in comparison with *P. berghei* K173 (model of NCM) (El-Assaad et al. 2011). However, miRNA expression profiling in human tissue infected with malaria has not as yet been reported.

1.11 Summary of aims

The aims of the work included in this thesis are twofold. The first theme is an examination of the role of the Ang-Tie-2 system in the pathogenesis of complications of human malaria, in particular coma in CM and renal injury in MARF. My group had been interested in the role of hypoxia and endothelial activation in the genesis of coma in CM and tubular injury in MARF, but previous studies of hypoxic-regulated molecules such as HIF-1α and VEGF as "fingerprints" of hypoxia in human tissues had been unsuccessful (Medana et al. 2010). Therefore, this study:

1. Investigates the expression of the Ang-Tie-2 pathways in the brain in CM and NCM patients. This is designed to see whether the association of raised Ang-2 and Ang-2/Ang-1 ratios seen in clinical cases of severe and CM is due to any tissue-specific expression of these proteins in the brain, such as endothelial expression (Chapter 3).

2. Model the effects of the Ang-Tie pathway, in combination with hypoxia and cytokine activation on human cerebral EC phenotype, function, signalling and transcriptome using an *in vitro* co-culture model of human brain ECs with *P. falciparum*-infected erythrocytes (Chapter 4).

The second major theme is to investigate the application of molecular pathology in malaria research using post-mortem human tissues from fatal malaria, to examine specific pathophysiological mechanisms suggested from previous histopathological, animal and *in vitro* studies:

3. To develop and optimise techniques to successfully extract high-quality miRNA from FFPE tissue for use in miRNA expression study by microarray and qRT-PCR techniques (Chapter 5).

4. To use archival FFPE tissue to examine the miRNA expression profile in the kidney of patients with and without MARF, to identify human miRNA transcripts that could be a signature of malarial infection, and new biological pathways potentially contrib-

uting to the pathogenesis of kidney injury. This included examining whether any specific miRNAs influenced the expression of mRNA transcripts for members of the Ang-Tie-2 signalling pathway in MARF (Chapter 5).

5. To collect tissues from a new autopsy study of fatal malaria in African children from Mozambique, to develop a biobank of human malaria tissue samples for comparison with adult non-immune Southeast Asian adults, and for use in gene expression analysis (Chapter 6).

6. To optimise techniques of tissue preservation for highly sensitive molecular biology techniques (instead of preservation by LN storage) by a systemic comparison of factors affecting RNA quality from tissue preserved in RNAlater and in LN (Chapter 6).

7. To conduct the first systematic analysis of human post-mortem tissues from fatal malaria using gene trancriptome analysis (for mRNA) and miRNA array analysis on multiple tissues, and examining pathways of gene transcription in the brain in severe malaria using bioinformatics analysis (Chapter 7).

Chapter 2

Material and Methods

General chemicals were purchased from Sigma-Aldrich® (UK and USA) unless otherwise specified. Recipes of buffers and cell culture media are presented in Appendix A.

2.1 Patients and autopsy studies

This thesis used clinical data and autopsy tissue samples taken from studies of the pathology of fatal malaria based in Vietnam and Mozambique, as well as control autopsy samples from the UK and Thailand. Human tissue and clinical data collected from these studies were used in various chapters in this thesis. Clinical, biochemical and pathological details of the patients from Vietnam and UK were published in previous studies (e.g. in Day et al. 1999, 2000; Medana et al. 2011; Nguansangiam et al. 2007; Pongponratn et al. 2003; Ponsford et al. 2012).

2.1.1 Vietnam malaria autopsy series (from AQ trial)

This series of 50 fatal cases of severe falciparum malaria in Vietnamese adults was conducted as part of a double-blinded trial of artemether versus quinine for the treatment of severe malaria in Vietnam (AQ trial) (Hien et al. 1996) at the centre for Tropical Diseases, Cho Quan Hospital, Ho Chi Minh City, Viet Nam, during 1991–1995. Within the trial, clinical data, blood and cerebrospinal fluid (CSF) specimens were collected as indicated for appropriate diagnosis and treatment. Patients were diagnosed with malaria using serial blood films and subsequent blood PCR. All were classified according to the WHO (1990) criteria for severe falciparum malaria. Relatives gave written informed consent for entering the study. This was the source of FFPE malaria brain and kidney specimens used in this thesis (chapters 3 and 5, respectively). Protocols

for tissue sampling, storage and use for research were approved by the Ethical and Scientific Committee of the Centre for Tropical Diseases in Ho Chi Min City, OXTREC 029-02, COREC (C01.002) and Human Tissue Authority license number 12217.

2.1.2 UK control autopsy series

The non-malaria cases used for normal control FFPE tissue blocks were from a collection of routine autopsy cases performed at the John Radcliffe Hospital, Oxford, UK, where specific written consent for retention of brain tissue for research purposes had been given. These autopsies were performed by Dr Gareth Turner during 1998–2000.

2.1.3 Bangkok control autopsy series

As part of this thesis, autopsies were conducted on routine hospital and forensic cases (n = 10) at the Pathology and Forensic Department of King Chulalongkorn Memorial Hospital, Bangkok, Thailand in June 2009. Specific written consent for entering the study was given by relatives and fit recruitment criteria. This study aimed to systematically compare different tissue-preservation techniques and design protocols for performing autopsy and specimen collection to maximise the quality of RNA extraction from human post-mortem tissue for high-throughput genomic analysis (discussed in Chapter 6). The kidney tissues from this study were also used as controls in miRNA expression analysis of MARF in Chapter 5. The ethical permission for autopsy and the use of tissue collection for research purposes was approved by the Institutional Review Board of the Faculty of Medicine, Chulalongkorn University.

2.1.4 Mozambique: Beira Moçambique Estúdio Malária Autópsia (MEMA) autopsy study

Our group has been conducting an autopsy study of fatal malaria in the Beira Central Hospital, Mozambique since December 2008, in collaboration with Dr Josepho Ferro (Department of

Anatomical Pathology, Hospital Central de Beira and University Catholique de Mozambique). I helped to set up and conduct the MEMA study, details of which will be discussed in Chapter 6. The tissues collected from this study were used in microarray experiments in Chapter 7.

2.2 Post-mortem specimen preservation

2.2.1 Archival specimens

FFPE tissue

In AQ trial autopsies, tissues from various organs including the brain, lung, kidney, liver, bowel and heart were collected at autopsy within 24 hours of death (median 7 hours), fixed in 10% buffered formalin, then transported to the John Radcliffe Hospital, Oxford to be embedded in paraffin and processed using standard histological methods in the Neuropathology and Histopathology laboratories. The brain specimens of the UK normal controls were collected and preserved in the same way at the John Radcliffe Hospital. All paraffin blocks were stored at room temperature in the Nuffield Department of Clinical Laboratory Science, Oxford, until use.

Plasma samples

As part of the AQ trial, plasma samples were generated by centrifugation of EDTA-preserved venous blood samples at 5000 rpm for three minutes, then aliquoted and stored at –80˚C until use.

CSF samples

CSF samples from the AQ trial were collected when the procedure was clinically indicated (for instance, to exclude another infectious cause of coma such as meningitis or encephalitis). These were aliquoted neat without any additives, spun and frozen at –80 ˚C until use.

2.2.2 New specimens

FFPE tissue

Tissues of various organs from autopsy studies in Thailand were collected at autopsy within 24 hours of death, fixed in 10% buffered formalin for three days, then processed and embedded in paraffin at the Department of Pathology, Chulalongkorn University, Thailand. Tissues from the autopsy study in Mozambique were fixed in 10% buffered formalin, then transported to the Department of Pathology, Chulalongkorn University for tissue processing and paraffin embedding.

LN preservation

Fresh post-mortem specimens to be preserved by snap freezing in LN were cut into a small piece, approximately 5x5x5 mm, in order to ensure the immediate freezing process to avoid ice crystal artefacts. Then, the cut tissue was wrapped in aluminium foil and inserted into a pre-labelled 2.0 ml cryovial. The cap was screwed securely and the cryovial was immediately submerged in LN. This technique allowed the tissue not to be exposed directly to LN, which helps prevent drying and fragility of the frozen tissue.

RNAlater-fixed tissue

Fresh post-mortem specimens to be preserved for molecular pathology methods (extraction of DNA, miRNA or mRNA) were fixed in RNAlater® solution (Ambion, UK). They were cut on a sterile petri dish with a sterile disposable scalpel into 5 mm squares, in order to ensure rapid fixation. Three to four tissue squares were put in 4.0 ml of RNAlater solution, refrigerated at 4°C for 24 hours and then transferred to a -20°C freezer for long-term storage. RNAlater-fixed tissue was shown to have similar RNA quality to tissue preserved by LN (Chapter 6). Therefore, only RNAlater-fixed tissue collected from MEMA, not LN fixed tissue, was used in the integrated analysis of miRNA and mRNA expression profiling by microarray experiments in Chapter 7.

2.3 Detection and quantification of Ang-1, Ang-2 and Tie-2 proteins in post-mortem brain tissue by IHC

2.3.1 IHC

IHC was performed using monoclonal antibodies against three different protein markers of the Ang-Tie pathway, including the Ang-1, Ang-2 and the Tie-2 receptor. Details of the primary antibodies used are summarised in Table 2-1. Staining was performed on 4 μm sections of FFPE brain tissues cut using a rotatory microtome onto coated immunoslides (SupaFrost, Thermo Fisher Scientific, UK), from all malaria and control cases. The slides were heat fixed for 10 minutes at 60°C, de-waxed in xylene, rehydrated in graded alcohol series and then underwent microwave antigen retrieval in Tris-EDTA pH 8 for 10 minutes. Detection of bound antibody was visualised using the high-sensitivity Novolink™ Polymer detection system (Leica Biosystems, UK), according to the manufacturer's instructions. In brief, sections were sequentially incubated with the following reagents provided in the kit (except primary antibodies, which were purchased separately): peroxidase block (10 minutes), protein block (5 minutes), primary antibody (2 hours), post-primary block (30 minutes) and Novolink Polymer (30 minutes), with two five-minute washes in TBS in between each step. The peroxidase activity was developed with prepared DAB working solution (mixture of 50 μl of DAB chromogen and 1 ml of Novolink DAB substrate buffer). The slides were then washed in double-distilled water and sections counterstained with haematoxylin for 30 seconds before a repeat washing and being coverslipped using Aquamount medium (Thermo Fisher Scientific, UK). Negative controls, included in each run, comprised sections immunostained as above with omission of the primary or secondary antibodies. Staining was examined using an Olympus BX-40 (Olympus, UK) microscope at various magnifications.

Several different commercially available antibodies with different antigen-retrieval methods were tested. Optimal staining could only be obtained using quite low dilutions of primary antibody

with high-sensitivity polymer-mediated secondary antibody visualisation, which has up to 50-fold greater sensitivity compared with traditional streptavidin–biotin complexes. Using a high-sensitivity detection system gave higher non-specific background staining in some cases.

Table 2-1. Primary antibodies used in this thesis

Antibody	Clone	Dilution	Host species	Supplier (Cat. No.)
Primary antibodies for the immunostaining of Ang-Tie-2 pathway in the brain				
Ang-1	171718	1:20	mouse, monoclonal	Sigma (A0604)
Ang-2	N/A	1:50	rabbit, polyclonal	Abcam (ab65835-100)
Tie-2	N/A	1:100	rabbit, polyclonal	Santa Cruz (SC-9026)
Primary antibodies for the immunochemical characterisation of HBEC				
panCK	AE1/AE3	1:50	mouse, monoclonal	Abcam (ab80826)
CD31/PECAM	WM59	1:200	mouse, monoclonal	Sigma (P8590)
SMA	1A4	1:400	mouse, monoclonal	Sigma (A2547)
GFAP	N/A	1:400	rabbit, polyclonal	Dako (Z0334)
VWF	N/A	1:200	rabbit, polyclonal	Dako (A0082)

2.3.2 Quantitation of vascular immunostaining

Vessels were considered positive for Ang-1, Ang-2 and Tie-2 when any part of the vessel including ECs, basement membrane, pericytes or smooth muscle were stained. Vessels positive for Ang-1, Ang-2 and Tie-2 were counted and the number of positive vessels in 150–300 fields in each slide at x200 magnification was used to calculate the number of positive vessels per cm^2. This was converted to a Vascular Expression Score (VasExp) as follows: Ang-1; low = 0–20 vessels/cm^2, moderate = 20–40 vessels/cm^2, high = > 40 vessels/cm^2: Ang-2; low = 0–200 vessels/cm^2, moderate = 200–400 vessels/cm^2, high => 400 vessels/cm^2: Tie-2; low = 0–10 vessels/cm^2, moderate = 10–20 vessels/cm2, high = > 20 vessels/cm^2. Both the number of positive vessels per cm^2 and the VasExp were used in histopathological and clinicopathological correlations where appropriate.

2.3.3 Semiquantitation of neuronal and astroglial immunostaining

Ang-1 and Ang-2 expression in neurons and astroglial cells was classified in a semi-quantitative scoring system of both the number of cells staining and the intensity of expression. Cell numbers were classified according to a percentage score as follows: score 0 = percentage of stained cells 1% or less, score 1 = 1–10%, score 2 = 10–50% score 3 = > 50%. The intensity score was defined as: score 0 = no staining, score 1 = weak staining (+/–), score 2 = moderate staining (+), score 3 = strong staining (++). The neuronal expression (NeuExp) of Ang-1 and Ang-2 was represented as the sum of the percentage score and intensity score (NeuScore) and also divided into two groups of "low" (low NeuExp, NeuScore ≤ 3) and "high" neuronal expression (high NeuExp, NeuScore ≥ 4). The astroglial expression (GliExp) of Ang-1 and Ang-2 was classified based on a similar system combining the percentage score with the intensity score into "low" (low GliExp, GliScore ≤ 3) and "high" astroglial expression (high GliExp, GliScore ≥ 4). However, due to much lower expression of Tie-2 on neurons and astroglia cells, it could not be quantitated using the same scoring system as Ang-1 and Ang-2. Rather than using both the number of cells and the intensity of staining, the semi-quantitative scoring system for Tie-2 expression on neurons and astroglial cells was based on the number of cells staining as follows: "low" neuronal or astroglial expression (low NeuExp or GliExp) = percentage of stained cells 1% or less and "high" neuronal or astroglial expression (high NeuExp or GliExp) = percentage of stained cells > 1%.

2.4 Quantification of Ang-1, Ang–2 and Tie-2 proteins in the plasma and CSF

Plasma and CSF concentrations of Ang-1, Ang-2 and Tie-2 were measured by quantitative sandwich ELISA (Quantikine ELISA kits, DANG10, DANG20 and DTE200 respectively, R&D Systems, UK), according to the manufacturer's instructions. In brief, a monoclonal antibody specific for Ang-1, Ang-2 or Tie-2 was pre-coated onto a microplate (96-well plate).

Plasma and CSF samples were diluted in reagent diluent (provided in the kit) and standard curves were generated using the kit's recombinant human proteins. Each sample was plated in duplicate and incubated for 2 hours at room temperature on a horizontal orbital microplate shaker set at 500 rpm, then washed four times with the wash buffer provided. Secondary monospecific antibodies were added according to manufacturer's recommended dilutions and incubated for 2 hours at room temperature on the shaker. Following a further four washes, the substrate solution was added to the wells and incubated for 30 minutes, during which colour developed in proportion to the amount of test proteins bound in the initial step. The reaction was stopped and the microplate was read at 450 nm with wavelength correction set to 540 nm (Infinite® Pro 200 plate reader, Magellan software, Tecan). Concentrations were interpolated from 5-PL parameter-logistic (5-PL) standard curve fitting.

A total of 62 plasma samples and 12 CSF samples from patients with severe malaria were examined, all in duplicate. 22/62 plasma samples and 12 CSF samples were from fatal malaria cases included in the immunohistochemical analysis. The other 40 plasma samples were randomly selected from severe malaria patients in the same AQ trial, including fatal cases (n = 10/40) and survivors (n = 30/40).

2.5 Extraction of miRNA from FFPE tissue for Affymetrix miRNA Microarray (Chapter 5)

A commercially available RNA isolation kit for FFPE tissue, RecoverAll (Ambion, UK), was used. This kit was designed to extract total nucleic acids including DNA, RNA and miRNA from FFPE tissue. Some adjustments to the manufacturer's protocol were made to optimise the RNA yield and purity from the archival FFPE blocks of malaria cases. These adjustments included increased de-paraffinisation time from one x three minutes to two x five minutes at 55°C heating, increased digestion time with proteinase K at high temperature (20 hours at 50°C followed by 20

minutes at 70˚C), eluting RNA by 95˚C water and adding RNA cleanup steps (RNeasy MinEluet® Cleanup Kit, Qiagen, UK). Sections from the FFPE block were cut at 14 μm thickness using a rotatory microtome, using sections from the interior of the paraffin block to avoid tissue exposed to the atmosphere during storage, which may damage nucleic acids by oxidation. Four to eight sections from each paraffin block, depending on the size of tissue surface in each block, were used as starting material. After a series of de-paraffinisation, ethanol washes and protease digestion, nucleic acids were purified using a glass-fibre filter cartridge on a kit column. DNase was then added on the filter to digest genomic DNA. Total RNA including miRNA was eluted by high temperature nuclease-free water. Using this optimised protocol, RNA yield and sample purity increased dramatically compared to the manufacturer's protocol. The total RNA extracts were stored at −80˚C until used.

2.6 Extraction of high and low molecular weight RNA from fresh frozen tissue and RNAlater-fixed tissue

2.6.1 To compare RNA quality between RNAlater-fixed tissue and fresh frozen tissue (Chapter 6)

High molecular weight RNA (defined as total RNA excluding small RNA species smaller than ~200 nucleotides) from the brain samples fixed in either RNAlater reagent or fresh frozen in LN in this project were isolated at MORU, Bangkok using commercially available kit (RNeasy Lipid Tissue Mini Kit, Qiagen, UK). Approximately 80–100 mg of brain tissue was homogenised by a handheld rotor-stator homogeniser (PRO200, PRO Scientific, USA) in 1 ml of QIAzol Lysis Reagent (phenol and guanidine thiocyanate) provided in the kit. Total RNA was isolated according to the manufacturer's instructions. The quantity and quality of RNA extracts were tested on Nanodrop 1000 (Thermo Scientific, USA) and Agilent 2100 Bioanalyzer (Agilent Technologies, USA). Purified RNA samples were stored at −80˚C until used.

2.6.2 In the gene expression and miRNA expression profile (Chapter 7)

Total RNA including miRNA, snRNA and other small RNA species from the brain, lung, liver and kidney specimens, fixed in RNAlater reagent from the MEMA autopsy study, were isolated using a commercially available kit (miRNeasy Mini Kit, Qiagen, UK). Small RNA species including miRNA were then enriched in a separate fraction by RNeasy MinElute® Cleanup Kit, Qiagen, UK). Approximately 80–100 mg of the brain, 70–80 mg of the lung , 40–50 mg of kidney and 30–40 mg of liver were homogenised by the gentleMACS Dissociator with M tube (Miltenyi Biotec, Germany), programme RNA_01, in 700 µl of QIAzol Lysis Reagent provided in the miRNeasy Mini Kit. After addition of 140 µl of chloroform, the homogenate was separated into aqueous and organic phases by centrifugation for 15 minutes at 12,000x g at 4°C. The upper, aqueous phase (containing RNA) was extracted, then one volume of 70% ethanol was added to provide appropriate binding conditions for HMW RNA molecules (larger than ~200 nt) on a silica-membrane filter. The sample was then transferred into an RNeasy Mini spin column (silica-membrane cartridge). The flow-through contained small RNA species while larger RNA molecules bound with the filter cartridge. Both fractions were then separately extracted. The flow-through was then mixed with 0.65 volumes of 100% ethanol and transferred to an RNeasy minElute spin column. The small RNA species now bound with the filter cartridge. After a series of washes by buffer RWT, RPE (supplied in the kits) and ethanol, according to the instructions in Appendix A of the miRNeasy Mini Kit manual, larger RNA was twice eluted by 60 µl of nuclease-free water and small RNA species were twice eluted by 14 µl of nuclease-free water. The quantity and quality of RNA extracts were tested on Nanodrop 1000 (thermo Scientific, USA, and Agilent 2100 Bioanalyzer (Agilent Technologies, USA). Purified RNA samples were stored at -80°C until used.

2.7 Evaluation of RNA quality: Purity and integrity

2.7.1 RNA purity

The purity of RNA extracts was assessed by Nanodrop 1000 Spectrophotometer (Thermo scientific, USA) using an A260/A280 ratio and A260/A230 ratio (A260 = absorbance at 260 nm, A280 = absorbance at 280 nm, A230 = absorbance at 230 nm). Nucleotides absorb at 260 nm. The A260/A280 ratio of ~2.0 and A260/A230 of 2.0-2.2 are considered as "pure" for RNA samples. If the ratios are lower than expected, this indicates the presence of contaminants which absorb at 230 or 280 nm, including carbohydrate, phenol and protein.

2.7.2 RNA integrity

The integrity of RNA in RNA extracts was evaluated using an Agilent 2100 Bioanalyzer in conjunction with RNA 6000 Nano-LabChip kit (Agilent Technologies, USA), in accordance with the manufacturer's instructions. This chip-based system is an automated microcapillary electrophoresis device using microfluidic technology to provide electrophoretic separations of fluorescent-labelled RNA fragments according to their molecular weight. RNA fragments were subsequently detected by laser-induced fluorescent detection. Results were presented as digital electropherograms and digital gel-like images. The RNA Integrity Number (RIN), which is a measurement of the degree of degradation in a total RNA sample, was generated using the manufacturer's algorithm and software. The RIN values range from 10, which represents fully intact RNA, down to one, which represents totally degraded RNA. RIN values greater than six have generally been regarded as acceptable for gene expression analysis in previously published studies (Hatzis et al. 2011; Schroeder et al. 2006).

2.8 miRNA microarray

2.8.1 Determining miRNA profiles in the kidneys of adult malaria and control patients (FFPE kidney blocks)

Affymetrix GeneChip miRNA Array version 1 was used for miRNA expression profiling in this study, examining tissue from FFPE kidney blocks from Vietnamese and Thai patients. The array contained the miRNA of 71 species, including complete coverage of the human miRNA listed in the Sanger miRBase database release 11.0, April 2008 (Griffiths-Jones et al. 2008). Prior to array hybridisation, total RNA was labelled with proprietary biotin-labelled 3DNA® dendrimer signal amplification molecules, which is a branched structure of DNA conjugated with numerous labels (Stears et al. 2000) using a FlashTag™ Biotin HSR kit (Genisphere, USA). With this labelling technique, no PCR amplification or reverse transcription was needed.

FlashTaq Biotin HSR RNA Labelling (Poly A Tailing)

Approximately 500 ng of total RNA containing LMW RNA (isolated from FFPE kidney blocks) in 8 µl was added with 2 µl RNA spike control oligos, 1.5 µl 10X reaction buffer, 1.5 µl 25mM $MnCl_2$, 1.0 µl diluted ATP mix (1:500) and 1 µl PAP enzyme and was incubated for 15 minutes at 37°C.

FlashTaq Biotin HSR RNA Labelling (Ligation)

The sample was put on ice and 4 µl 5X FlashTaq Biotin HSR ligation mix was added, then 2 µl T4 DNA ligase, then incubation for 30 minutes at room temperature. The ligation reaction was stopped by adding 2.5 µl HSR stop solution.

Array hybridisation

The array hybridisation cocktail was prepared by adding the following reagents to 21.5 µl biotin-labelled sample in order:

- 50 µl 2X hybridisation mix (GeneChip Hybridisation, Wash and Stain Kit, Affymetrix)
- 15 µl 27.5% formamide
- 10 µl DMSO
- 5 µl 20X heat-activated eukaryotic hybridisation controls (GeneChip Eukaryotic Hybridisation Control Kit, Affymetrix)
- 1.7 µl Control Oligonucleotide B2, 3nM (GeneChip Eukaryotic Hybridisation Control Kit, Affymetrix)

The hybridisation cocktail was incubated at 99°C and 45°C, each for five minutes sequentially. 100 µl of this hybridisation cocktail was then injected into the array cartridge. The array was incubated in Affymetrix Hybridisation Oven 640 set at 60 RPM and 48°C for 16 hours.

Array washing and staining

After 16 hours of hybridisation, the GeneChip array underwent a series of washes to remove the non-hybridised miRNA and staining by incubation with a streptavidine-phycoerythrin conjugate, using GeneChip Hybridisation Wash and Stain Kit on an Affymetrix fluidics station 450 (fluidics script FS_0003), according to the manufacturer's protocols.

Array scanning and data processing

Fluorescence signals were detected using an Affymetrix G3000 GeneArray Scanner and image analysis was done by Affymetrix GeneChip Command Console 3.0 (AGCC) software. Raw image data were imported into the Affymetrix miRNA QC Tool Software, version 1.0.33.0 for RMA global background correction, quantile normalisation, and median Polish summarisation. The probe set normalised log ratios (average of four identical probes) were used for subsequent analysis in GeneSpring GX 11 software (Agilent Technologies).

2.8.2 Determining miRNA profiles in the brains of paediatric malaria and control patients from the MEMA series (RNAlater-fixed brain)

The Affymetrix GeneChip miRNA Array version 2, which provides complete coverage of the 131 organisms (including human miRNA) listed on the Sanger miRBase database release 15 (April 2010), was used for miRNA expression profiling in this project. During this study, Affymetrix updated the GeneChip miRNA Array to version 2 and discontinued the array version 1 used above for FFPE tissues.

Approximately 200–300 ng of enriched LWM RNA was labelled, hybridised, washed, stained and scanned using the same protocols as above. Raw image data generated from AGCC was then processed with a new version of Affymetrix miRNA QC Tool Software (version 1.1.1.0), which contains annotation data on the updated probe sets in GeneChip miRNA Array version 2. The same data processing steps as the above project were applied. The normalised log ratios were used for subsequent analysis in GeneSpring GX 11 software.

2.9 Messenger RNA microarray (whole-genome expression profiling)

2.9.1 Overview

The whole-genome gene expression profiling of post-mortem tissue from the MEMA study was generated using Illumina HumanHT-12 V4 BeadChip microarray with Illumina Whole-Genome Gene Expression Direct Hybridisation Assay. The laboratory procedures associated with the Illumina microarray platform (including sample labelling, microarray hybridisation, washing and scanning) were performed in collaboration with the High-Throughput Genomics group at the Wellcome Trust Centre for Human Genetics (WTCHG), Oxford University. Briefly, the total RNA was extracted from fresh tissues (brain, kidney, lung, spleen, liver and heart) taken from three malaria-infected and three control patients from the MEMA study and stored in RNAlater

as described above. The quality of the extracted RNA samples was assessed by Nanodrop and Bioanalyzer 2100 as described earlier, before each sample was sent to the WTCHG for the microarray-associated laboratory procedures. After microarray scanning, the raw expression values of each probe set for genes on each array were sent back to the author for data processing and analysis.

2.9.2 Illumina HumanHT-12 V4 BeadChip

The HumanHT-12 V4 BeadChip is a microarray from Illumina Inc, CA, USA. It was designed specifically for the study of whole-genome expression profiling in humans. It provides genome-wide transcriptional coverage of 47,231 transcripts in National Center for Biotechnology Information (NCBI) Human RefSeq Release 38 (November 2009) and the legacy UniGene database, including well-characterised genes, gene candidates, splice variants and well-established sequences. The Illumina BeadChip microarray is fabricated using Illumina's proprietary BeadArray technology (Figure 2-1). In brief, approximately 300,000 copies of the same 50-mer oligonucleotide probe sequence are covalently attached to a silica microbead (3 microns in diameter), which is then immobilised in a well on the surface of the microarray by a random self-assembly mechanism (Gunderson et al. 2004). An average of 15 copies of each bead type is present on every HumanHT-12 V4 BearChip array, resulting in a high level of bead-type redundancy, which provides a high level of data reproducibility and array robustness. Each microbead also has a 29-mer oligonucleotide address sequence attached, which is used for a hybridisation-based procedure to decode the array and map the location of each bead (Gunderson et al. 2004). This step also validates the hybridisation performance of every bead on the manufactured arrays. The HumanHT-12 V4 BeadChip arrays are arranged in a multi-sample format (12 samples per chip) for high throughput and reduced sample-to-sample variability.

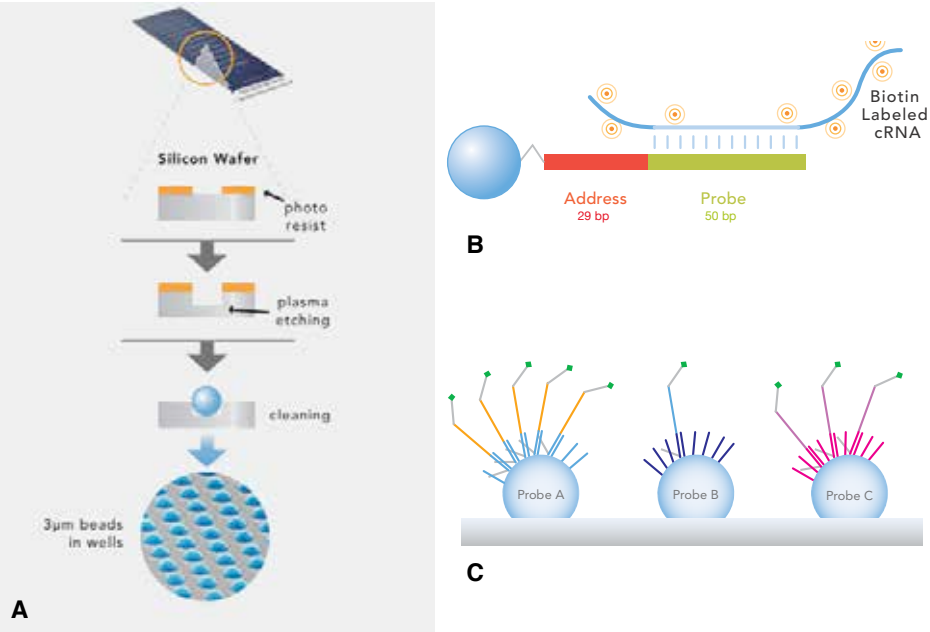

Figure 2-1. Illumina BeadArray Technology

(A) Microbeads are randomly assembled and held in microwells on the surface of Illumina BeadChip array by Van der Waals forces. (B) Each sequence-specific oligonucleotide attaching on the microbead is composed of a 50-bp oligonucleotide probe sequence and a 29-bp oligonucleotide address sequence. The probe sequence acts as the capture sequence in which a biotin-labelled cRNA strand complementary to the probe sequence is hybridised. The address sequence is used for decoding the array and mapping the location of each bead. (C) Each bead is covered with hundreds of thousands of copies of a specific oligonucleotide probe sequence. (All adapted from Illumina's documents)

2.9.3 Illumina Whole-Genome Gene Expression Direct Hybridisation Assay

The following sections describe the Direct Hybridisation Assay workflow for processing the twelve-sample BeadChips. The Illumina Direct Hybridisation Assay uses a standard Eberwine protocol assay (Van Gelder et al. 1990), in which gene-specific probes are used to detect labelled cRNAs.

Sample labelling

The first step in the direct hybridisation assay is generating an amplified pool of biotin-labelled cRNA using the Illumina TotalPrep™ RNA amplification kit (Ambion, UK). According to the manufacturer's protocol, in brief, approximately 500 ng of total RNA (isolated from the

RNAlater-preserved tissue as described earlier) in 11 µl had 9 µl of Reverse Transcription Master Mix added and was incubated for two hours at 42 °C to reverse transcribe mRNA fractions to single-stranded cDNAs. Then, 80 µl of Second Strand Master Mix was added to each sample and incubated for two hours at 16 °C to produce a double-stranded DNA template for transcription. After that, the cDNA was purified by adding 250 µl cDNA Binding Buffer to the sample, then passed through a cDNA Filter Cartridge which was then washed with 500 µl Wash Buffer. The cDNA was eluted with a total of 19 µl 55 °C water. The *in vitro* transcription (IVT) step was performed to amplify and label multiple copies of biotinylated cRNA from the double-stranded cDNA templates by adding 7.5 µl of IVT Master Mix to each purified cDNA sample and incubated for four hours at 37 °C. The labelled cRNA was purified by mixing it with 350 µl of cDNA Binding Buffer and 250 µl of 100% ethanol, then passed through a cRNA Filter Cartridge, followed by washing with 650 µl Wash Buffer. The cRNA was then eluted with 100 µl 55 °C water.

BeadChip array hybridisation

The total mass of cRNA in each sample was normalised to 750 ng in 5 µl, then mixed with 10µlHyb Mix, before dispensing it to a BeadChip array. Each BeadChip array had 12 sample-inlet ports. The RNA-loaded BeadChips were then placed into a Hybridisation Chamber insert, which was then inserted into a Hybridisation Chamber. Each Hybridisation Chamber, which accommodated four BeadChip arrays, was placed into Illumina Hybridisation Oven and incubated for 16 hours at 58 °C with rocking set at speed 5.

BeadChip array washing and staining

After 16 hours of hybridisation, the BeadChip array underwent a series of washes to remove the non-hybridised cRNA, following by staining with Cy3-Streptavidin to detect analytical probes that had been hybridised to the BeadChip, according to the manufacturer's protocols.

BeadChip array scanning

Fluorescence signals on the beads of the BeadChip array were detected and recorded in high-resolution images using the Illumina iScan Reader. The images were then analysed using the Illumina GenomeStudio version 1.6.0 to generate raw expression values for each sequence-specific probe. The raw data were then exported to other software packages for subsequent data processing and analysis.

2.9.4 Data processing and statistical analysis

Normalisation of microarray data is required to minimise variations between different arrays in a single experiment caused by systemic errors that are not due to factors under investigation (e.g. disease, treatment, time, etc.). However, the data should be normalised without reducing real variations (Schmid et al. 2010). Studies comparing different normalisation methods on Affymetrix and Illumina microarray platforms have shown that normalisation methods must be selected carefully because they can greatly influence outcomes in downstream analyses. (Allison et al. 2006).

In this whole-genome microarray experiment, raw expression values of each sequence-specific probe on the Illumina BeadChip microarray were generated from image analysis of the scanned-array images, using Illumina GenomeStudio version 1.6.0. Then, the raw probe-level expression values were exported to other software packages for subsequent data processing and gene expression analysis. The data processing pipeline utilises the R statistical programming language in combination with software packages in the Bioconductor project (Gentleman et al. 2004), including lumi (for normalisation) (Du et al. 2008), arrayQualityMetrics (for quality control) (Kauffmann et al. 2009) and limma (for differential expression analysis) (Smyth 2004). The pipeline for gene expression analysis is summarised in Figure 2-2.

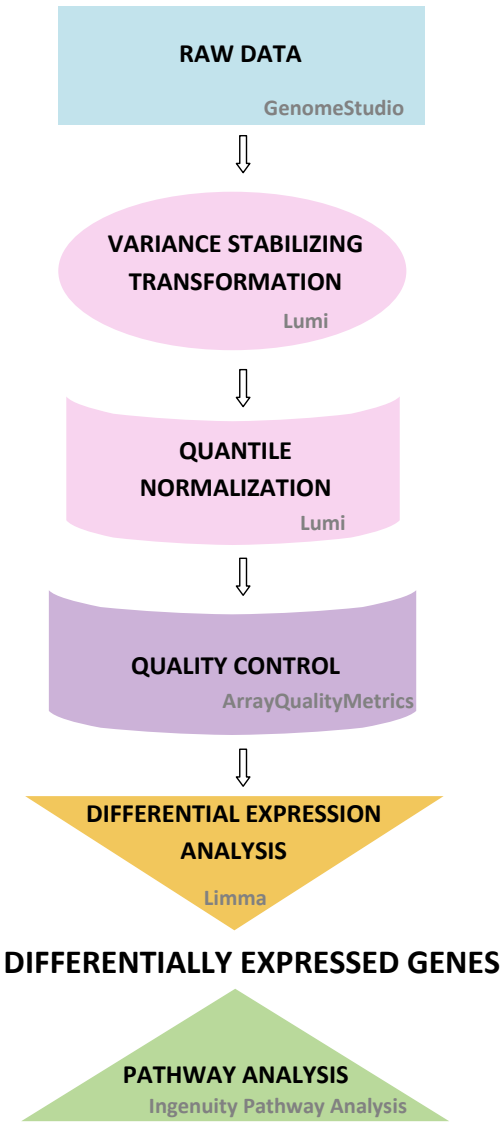

Figure 2-2. Data processing pipeline of the whole-genome expression from Illumina HumanHT-12 V4 BeadChip microarray

Normalisation

The first step in processing Illumina data employs Variance Stabilising Transformation (VST) in combination with quantile normalisation as suggested by Lin et al. (2008). The raw probe-level expression values without background subtraction exported from GenomeStudio were imported into the Bioconductor package lumi for data normalisation. Lin applied VST before quantile normalisation to improve the detection power of differential expression compared to using either a log2 transformation followed by quantile normalisation or a Variance Stabilising Normalisation,

as previously proposed by Rocke et al. (2001) and Huber et al. (2002). This is because the VST algorithm takes advantage of a large number of within-array replicates in the Illumina BeadChip microarray (9–30 copies of each sequence-specific probe) to reduce the heteroskedasticity (non-uniformity of variance) of the dataset, which allows the data to fit more precisely the assumptions of statistical techniques that are subsequently applied to detect differentially expressed genes.

Although a recent study comparing 25 different ways of pre-processing Illumina HumanHT-12 V3 BeadChip array data (Schmid et al. 2010) has suggested that the best normalisation methods for their dataset are log2 transformation in combination with either quantile normalisation or robust spline normalisation, using this option on this dataset gave similar results to that suggested by Lin et al. Thus, the normalisation method employing VST with quantile normalisation was used in analysing the Illumina BeadChip microarray data in this thesis. Background subtraction was not performed because it had a negative impact on data quality in my pilot analyses, in accordance with results from other published papers (Schmid et al. 2010).

Quality control

Quality control, which is a crucial step to identify outliers, batch effects, overly noisy experiments and experimental design problem, was performed in the Bioconductor software package arrayQualityMetrics. This computed a number of quality-control plots, including signal density, box plots, an array similarity heatmap, variance and mean plot, MA plot (M = intensity ratio, A = average intensity) and principal components analysis plot. In general, an array that has a minor problem, which typically receives one or two quality test failures, is correctable by normalisation. If the results from an individual array do not pass three or more quality tests, that array should be removed from the experiment in order to prevent a negative influence on subsequent differential expression analysis. Figure 2-3 shows examples of quality-control plots of the dataset from this experiment. Due to space limitations, details of how to interpret the quality-control plots are omitted but they can be found in arrayQualityMetrics's documentation (Kauffmann et al. 2009).

In this Illumina array experiment, three out of 18 samples failed on three quality-control tests and were removed from the data analysis pipeline (two malaria samples and one control sample).

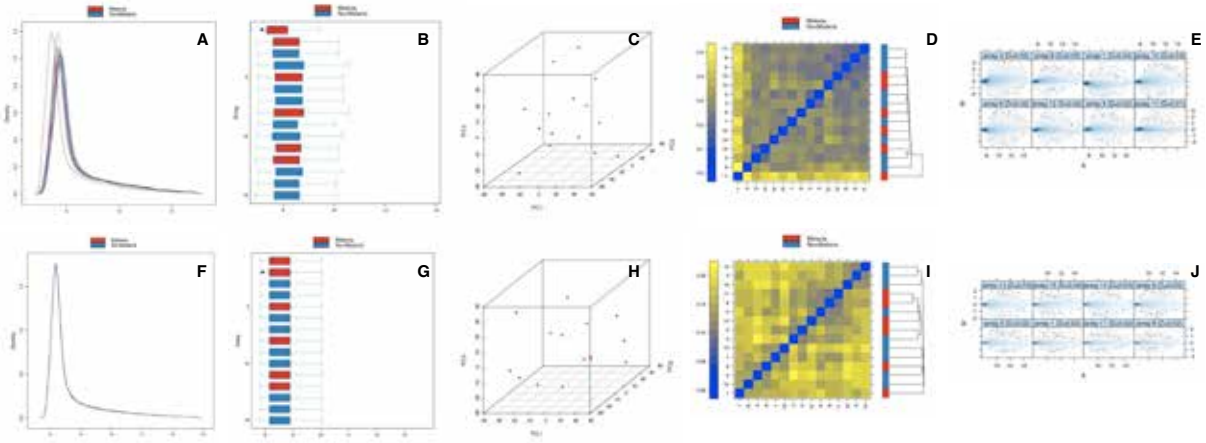

Figure 2-3. Examples of quality-control plots of the dataset from this microarray experiment, generated from Bioconductor package arrayQualityMetrics

(A-E) generated from raw expression values. (F-J) generated from batch-corrected normalised expression values. A and F are signal density plots. (B) and (G) are signal box plots. (C) and (H) are 3D principal components analysis plots. G and I are between-sample heatmap plots. (E) and (J) are MA plots (M = intensity ratio, A = average intensity).

Differential expression analysis

The Bioconductor package limma, utilising linear models for the analysis of differential gene expression, was used because it is highly robust to various data distributions and experiments with small number of arrays. Its robustness is due to its algorithm, which allows for "borrowing information from the ensemble of genes which can assist in inference about each gene individually" (Smyth 2004). It has also been proved to be much more reliable than other statistical methods in differential expression analysis, such as ANOVA, t-test, Significance Analysis for Microarray, VarMixt and RankProt (Dondrup et al. 2009). A list of differentially expressed genes (DEGs) in malaria cases compared to non-malaria cases was generated ($P < 0.05$ and fold-change cutoff = 1.5) and then was used for pathway analysis.

2.10 Real-time qRT-PCR for miRNA

2.10.1 Reverse Transcription of mature miRNA

Complementary DNA from mature miRNA was synthesised using the miRNA reverse transcription kit and the stem-loop Megaplex™ reverse transcription primer pool (Human Pool A, Applied Biosystems, UK), which allowed simultaneous reverse transcription of up to 380 miRNAs and endogenous controls, according to the manufacturer's instructions. Briefly, 3 µl of total RNA, including HMW and LMW RNA (approximately 400–600 ng), had reverse transcription primer mix (10X), reverse transcription buffer (10X), MultiScribe™ Reverse Transcriptase (50 U/µl), dNTPs with dTTP (100 mM), MgCl2 (25 mM) and RNase inhibitor (20 U/µl) added to it in a total reaction volume of 7.5 µl. The reaction was incubated on ice for five minutes, followed by pulsed reverse transcription of 40 cycles at 16°C for two minutes, 42°C for one minute and 50°C for one second using a PCR machine (Applied Biosystems GeneAmp® 9700 PCR System). The reverse transcriptase was inactivated by incubation at 85°C for five minutes. All reverse transcriptase reactions included no-template and minus-reverse transcription controls. No pre-amplification reaction was conducted.

2.10.2 Real-time PCR amplification

The reverse transcription product was diluted 30-fold, then had TaqMan® MicroRNA Assay (20X), as listed below, and SensiMix™ Probe (2X) master mix (Bioline, UK) added in a total reaction volume of 20 µl. Cycling conditions were as follows: 95°C for 10 minutes followed by 45 cycles of 95°C for 15 seconds and 60°C for one minute. All TaqMan reactions were performed in triplicate on the Roche LightCycler 480 real-time PCR machine (Roche Diagnostics, UK) in 96-well plate setup. Negative control reactions, omitting the reverse transcription product template, were also included in every run. Data were produced as fluorescent signal amplifications plotted against number of cycles. The Ct value (threshold cycle), the first cycle at which a fluorescent

signal was detected above a defined threshold, was generated by LightCycler 480 software and exported for subsequent analysis with Microsoft Excel. The list of TaqMan MicroRNA Assay and endogenous controls Assay used in the experiments in Chapter 5 includes let-7g, miR-16, miR-19b, miR-26b, miR-99a, miR-214, miR-500, miR624, miR-744, miR-886-5p, RNU6B, RNU44, and RNU48.

2.11 Real-time qRT-PCR for mRNA

2.11.1 Reverse transcription of mRNA

Reverse transcription of total RNA was performed with the RETROscript® kit (Ambion, UK), according to the manufacturer's instructions. Briefly, approximately 1500 ng of total RNA (isolated from transfected cells by Trizol Reagent, Life Technologies), had random decamers (5 μM) and RNase-free water added to it to make a reaction volume of 12 μl, followed by incubation for three minutes at 85°C to denature the RNA. The mixture was then made up with the reverse transcription buffer (10X), dNTP mix (0.5 mM), RNase inhibitor (0.5 U/μl) and MMLV Reverse Transcriptase (5 U/μl) in a reaction volume of 20 μl, followed by incubation for one hour at 43°C for cDNA synthesis and for 10 minutes at 92°C to inactivate the Reverse Transcriptase.

2.11.2 Real-time PCR amplification

Real-time qRT-PCR was performed using TaqMan Gene Expression Assays on the Roche LightCycler 480 real-time PCR system. The reverse transcription product (cDNA) was diluted 30-fold, then 4 μl of the reverse transcription product had TaqMan Gene Expression Assay (20X) (which consists of two sequence-specific PCR primers and a TaqMan Assay-FAM labelled minor groove binder probe) and Roche LightCycler® 480 SYBR Green I Master Mix (2X) added to it, in a reaction volume of 20 μl. Each TaqMan Assay was run in triplicate on 96-well plate using cycling conditions as follows: 50°C for two minutes, then 95°C for 10 minutes, followed by 40

cycles of 95°C for 15 seconds and 60°C for one minute. Data was produced as fluorescent signal amplifications plotted against number of cycles. The Ct value (threshold cycle), the first cycle at which a fluorescent signal was detected above a defined threshold, was generated by LightCycler 480 software and exported for subsequent analysis with Microsoft Excel. The list of TaqMan Gene Expression Assay and endogenous controls Assay used in experiments in Chapter 5 includes ANGPT1, ANGPT2, TEK and B2M.

2.12 Validation of miRNAs predicted targets

2.12.1 ANGPT1, ANGPT2 and TEK 3'UTR luciferase reporter constructs

miTarget™ miRNA Target Sequence 3' UTR Expression Clones for human ANGPT1, ANGPT2 and TEK were purchased from GeneCopoeia, USA. These expression clones contain 3' UTR sequences of either ANGPT1 (Accession: NM_001146.3), ANGPT2 (Accession: NM_001147.1) or TEK (Accession: 000459.2) inserted in the pEZX-MT01 vector downstream of a firefly luciferase gene, under control of an SV40 promoter for expression in mammalian cells. This generates a chimeric transcript containing both firefly luciferase coding and target genes 3'UTR sequences (Figure 2-4). The pEZX-MT01 also has a kanamycin resistance gene for selection of bacterial transformation and a *Renilla* luciferase gene under control of a CMV promoter to normalise firefly luciferase signal intensities across samples, which is necessary for eliminating differences in transfection efficiencies and cell viability. A miRNA 3' UTR target control vector (GeneCopoeia, CmiT000001-MT01), containing pEZX-MT01 vector without target gene insertion, was used as a control for luciferase assay and to assess the specificity of the interaction of miRNA constructs and the vectors.

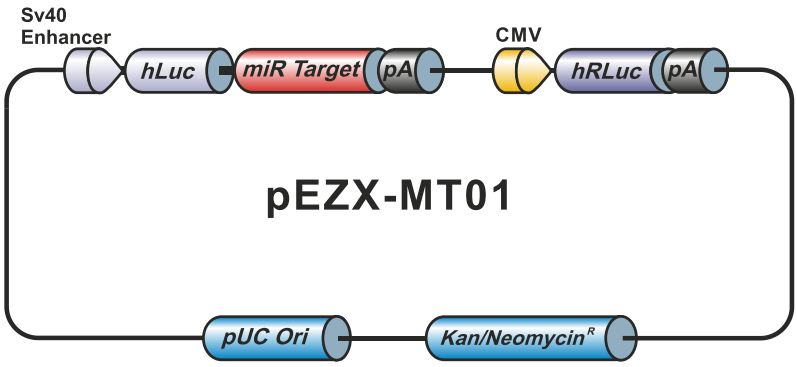

Figure 2-4. GeneCopoeia miTarget vector with dual luciferase reporters
(from GeneCopoeia's documents)

2.12.2 Expansion of the luciferase reporter constructs

Each luciferase reporter construct was transformed into One Shot® TOP10 Chemically Competent *E. coli* (Invitrogen) according to the manufacturer's instructions. 3 µg of the DNA construct was added into a vial of One Shot® *E. coli*. The mixture was incubated on ice for 30 minutes, heat shocked for 30 seconds at 42°C in a water bath and placed on ice for two minutes. Then, 250 µl of SOC medium (supplied in the One Shot® *E. coli* kit) was added to each vial and this was incubated at 37°C for one hour at 225 rpm on a horizontal shaker. The culture was then diluted fivefold in LB medium and then spread on an LB agar plate containing kanamycin (100 µg/ml). The selective plate was incubated at 37°C overnight before a single isolated colony of transfected *E. coli* cells was selected and propagated in 100 ml LB liquid medium containing kanamycin (100 µg/ml) in a conical flask by incubation at 37°C for 14 hours on a rotating shaker at 300 rpm.

2.12.3 Purification of luciferase reporter constructs

The plasmids inside transformed bacteria cells were extracted using EndoFree® Plasmid Maxi kit (Qiagen, UK) according to the manufacturer's protocol. The kit is based on the modified alkaline lysis method, followed by binding of the plasmid DNA to a Qiagen Anion-Exchange Resin filter under appropriate pH conditions. The bacteria cells were spun down at 4500 x *g* for 20 minutes at

4°C. The bacterial pellet was lysed completely by 10 ml Buffer P1 with vortexing, followed by adding 10 ml Buffer P2, mixing thoroughly by vigorously inverting the sealed tube 4–6 times and incubating at room temperature for five minutes. Then, 10 ml of chilled Buffer P3 was added to the lysate and mixed immediately and thoroughly. The lysate was poured into the QIAfilter cartridge and incubated at room temperature for 10 minutes to allow a flotation of precipitate containing proteins, genomic DNA and detergent. The cap of the QIAfilter cartridge outlet was removed and the plunger was inserted into the QIAfilter cartridge to filter the lysate into a 50 ml tube. Endotoxin removal buffer (Buffer ER) was then added to the lysate and incubated for 30 minutes, followed by pouring the endotoxin-free lysate into a QIAGEN-tip 500. This consists of a resin filter which binds the purified plasmid DNA, and allows the lysate to pass through the filter by gravity. The tip was then washed twice with Buffer QC. The plasmid DNA was eluted with 15 ml of Buffer QN, followed by precipitating the DNA with 10.5 ml room temperature isopropanol and being centrifuged at 5000 x *g* for 60 minutes at 4°C. The DNA pellet was then washed with 5 ml endotoxin-free room temperature 70% ethanol and centrifuged at 5000 x *g* for 60 minutes at 4°C. The supernatant was carefully decanted and the pellet was completely air dried. The DNA was then re-dissolved in endotoxin-free Buffer TE, and 2 µl analysed on a Nanodrop-1000 for concentration and purity. The purified luciferase reporter constructs were stored at –80°C until use.

2.12.4 Sequencing

All extracted pEZX-MT01 3'UTR expression plasmids (ANGPT1, ANGPT, TEK and control) were sequenced to verify the accuracy of the plasmid sequences. The primers for all plasmids were used as follows: Forward primer: 5'-GATCCGCGAGATCCTGAT-3'; Reverse primer: 5'-TTGGCGTTACTATGGGAACAT-3'. The DNA sequencing reactions were prepared using the BigDye® Terminator V1.1 Cycle Sequencing Kit (Applied Biosystems). Briefly, the extracted plasmid (100 µg) had BigDye Terminator V1.1/3.1 Sequencing Buffer (5X), Ready Reaction Mix

(4 µl), either forward or reverse primer (3.2 µl), and RNase-free water (7.8 µl) added to it, in a total reaction volume of 20 µl. Cycling conditions were as follows: 96˚C for one minute, followed by 25 cycles of 96˚C for 10 seconds, 50˚C for five seconds and 60 ˚C for four minutes. The sequencing reactions were then purified using ethanol/sodium acetate precipitation in 96-well reaction plate as follows. The sequencing reaction had 1 µl of 3 M sodium acetate and 25 µl of 95% ethanol added, which was followed by the sealing of the plate and brief vortexing. The plate was incubated at room temperature for 15 minutes before spinning down at 3000 x *g* for 30 minutes at 4˚C. The supernatant was discarded and 100 µl of 70% ethanol was added. The plate was centrifuged at 3000 x *g* for 30 minutes at 4˚C. The supernatant was discarded and the pellet was air dried. The sample was re-suspended in injection buffer (HiDi) and kept on ice. The electrophoresis was performed using a 48 capillary ABI-3730 DNA analyser (Applied Biosystems) by the Weatherall Institute of Molecular Medicine DNA Sequencing Service, Oxford University.

The returned sequencing data were analysed using 4Peaks software 1.7.2 (Mekentosj Inc., UK). The nucleotide sequences of the plasmids (containing ANGPT1, ANGPT2 or TEK) were compared with the library of human sequences in the NCBI database (http://www.ncbi.nlm.nih.gov) using Basic Local Alignment Search Tool (BLAST) bioinformatics querying (http://blast.ncbi.nlm.nih.gov). This confirmed the accuracy of the expanded plasmid sequences.

2.12.5 Cell culture

Human Embryonic Kidney 293 cells (HEK 293, ATCC CRL-1573™), obtained from American Type Culture Collection (ATCC), USA, were used in transfection procedures for the luciferase assay experiment. All cell culture was carried out in a class II safety cabinet using aseptic techniques. The adherent cells were grown in 25cm^2 sterile canted-neck screw-top plastic tissue-culture flasks in supplemented culture media, incubated in a humidified 37˚C incubator with 95% air and 5% carbon dioxide. Media were replaced every two days and the cells were subcultured

when reaching 80%–90% confluency at a seeding condition of $5x10^3$ cells per cm^2 (approximately 1:6 to 1:10 weekly). The cells were passaged at least three days to reach 80%–90% confluency prior to being used for transfection. Non-supplemented culture media were used to wash the anchorage cells before performing cell detachment using Trypsin-Vernase® EDTA (1X) (Lonza, UK). Alliqouts of cells were frozen down in Recovery™ Cell Culture Freezing Medium (Gibco, UK) at -80˚C, then transferred to LN vapour for long-term storage.

2.12.6 Transfection

HEK 293 cells were transfected with a combination of miTarget™ miRNA target Sequence 3' UTR Expression Clones in mammalian expression vectors with dual luciferase reporter gene (GeneCopoeia, USA) and miRNA constructs. Control reactions included transfection with plasmid plus scramble miRNA (acaguagucugcacauugguua), plasmid alone, and mock transfection (no sequence). Cells were transfected by electroporation using the Amaxa® Cell Line Nucleofector® kit (V) (Lonza, UK) according to Amaxa's optimised protocol. Transfection efficiency was measured using a GFP-containing plasmid and by qRT-PCR. Briefly, the cells were trypsinised to detach from the culture flask, washed by supplemented culture media to quench trypsin activity, counted and aliquoted to $1x10^6$ per sample. The sample was centrifuged to remove supernatant. The cell pellets were then re-suspended in 100 µl Nucleofector® Solution V at room temperature, followed by adding a combination of a plasmid (4 µg) with a miRNA construct (30 pmol), plasmid alone (4 µg) or pmaxGFP® plasmid (4 µg). The mixture was transferred to a cuvette and underwent electorporation using the Nucleofector™ II device with the Q-001 program. The transfected cells was then immediately gently transferred to pre-equilibrated supplemented culture media in a 6-well plate at a final volume of 1.5 ml per well. This was incubated in a humidified sterile 37˚C with 5% carbon dioxide incubator for 48 hours, prior to luciferase assay. The miRNA constructs used in luciferase experiments includes miR-19b, miR-181a, miR-204, miR- 211, miR-486-5p and scramble-miR.

2.12.7 Luciferase assay

Using Luc-Pair™ miRNA Luciferase Assay from GeneCopoeia, the activities of firefly luciferase and *Renilla* luciferase were sequentially measured from a single sample on GloMax® 20/20 Luminometer (Promega, UK). Briefly, the 6-well plate of transfected cells was removed from the incubator, the growth media were aspirated and 1.2 ml of the solution I was added directly to cultured cells in each well. After waiting for three minutes, 80 µl of the cell lysate was transferred into a 1.5 ml tube, placed in the sample holder of the luminometer. 20 µl of 5X working solution I (mixture of substrate I and Solution I, 1:40) was then injected into the reaction tube, eliciting firefly luciferase luminescence which was then cumulatively measured for two seconds by the luminometer. Next, 100 µl of working solution II (mixture of substrate II and solution II, 1:200) was added, which simultaneously quenched the firefly luciferase and elicited *Renilla* luciferase luminescence, and was again cumulatively measured for two seconds. The ratio of luminescence from firefly luciferase and *Renilla* luciferase was calculated.

2.14 Preparation of primary cultures of human brain microvascular ECs (HBEC) for use in an *in vitro* co-culture model (Chapter 4)

2.14.1 Isolation of HBEC from brain tissue

HBEC were isolated from temporal lobe brain tissue removed from patients with intractable epilepsy at the Department of Neurology, School of Medicine, Johns Hopkins University, USA. Specific written informed consent was given by the patients and all procedures were approved by Johns Hopkins' institutional review board. The cell isolation and culture procedures were carried out using the aseptic technique in a class II safety cabinet, incubated in a humidified 37°C incubator with 95% air and 5% carbon dioxide. Upon receipt of the fresh brain tissue from a neurosurgical operation, the brain was placed on a sterile petri dish (on ice), and the meninges

with large vessels were removed using sterilised surgical forceps. Each separated piece was transferred into isolation media (IM), in 15 ml Falcon tubes. The brain was homogenised by repeatedly pipetting until the brain pieces could be passed back and forth effortlessly through a 10 ml pipette, followed by 10 gentle strokes in a Dounce Homogeniser. The homogenised brain tissue was filtered through a 40 μm nylon-mesh cell strainer (placed over 50 ml Falcon tubes), where microvessel fragments were retained by the mesh. The vessel fraction was collected by washing the mesh with IM until it was clear. The sample was centrifuged at 4°C for 10 minutes at 200 *g*, followed by re-suspending the pellet with 5 ml of enzymatic digestion media and incubated with rotation for 30 minutes to one hour at 37°C. The sample was then centrifuged at 4°C for 10 minutes at 200 *g* and washed with IM repeatedly several times to remove residual enzymes. The pellet was then re-suspended in 2–4 ml of HBEC + E/H culture media, depending on the size of the pellet, and gently transferred to a collagen-coated T-25 tissue-culture flask. The culture was examined daily on an inverted microscope with phase contrast, and (usually about 2–4 days later), the culture media were carefully changed when ECs began to migrate from hump-like microvessel fragments and proliferate on the bottom of the flask as a monolayer. The media were changed every week and cultures monitored carefully for bacterial or fungal contamination. Small endothelial clusters were usually visible after 8–10 days and cell confluency was achieved in one month.

2.14.2 Culture of the pre-isolated HBEC line HB56

HB56 was a HBEC line characterised by Prof. Monique Stins' group in 2007 as described in previous publications (Stins et al. 1997; Tripathi et al. 2007; Tripathi et al. 2009). To start a cell culture, an aliquot of cells was quickly thawed from nitrogen freezing and washed in HBEC + E/H media, then re-suspended in 4–5 ml in a T-25 culture flask. The media were changed every two days and the cells were subcultured in T-25 or T-75 flasks when reaching 80%–90% confluency, at a seeding density of $1x10^4$ cells per cm^2. HBSS was used to wash the anchored cells before

performing cell detachment using Trypsin-Vernase® EDTA (1X). The cells were used between passage 6 and passage 11 throughout the experiment.

2.14.3 Characterisation of the HB56 primary brain EC line

Due to ambiguous results from the Electric Cell-Substrate Impedance Sensing (ECIS) experiments using the HB56 cell line, further characterisation was performed to confirm the authenticity of the HB56 and exclude cell line cross-contamination prior to further experiments. This included using IHC and immunofluorescence (IF) to confirm the surface phenotype and for preparation of DNA for short tandem repeat (STR) analysis. Before immunostaining, the HB56 cells were subcultured into collagen-coated Nunc Lab-Tek® 8-well chamber slides (Thermo Scientific, USA) and incubated for two days until 70%–80% confluent.

IHC

IHC was performed to examine the expression of endothelial-specific markers, including factor VIIIRA (von Willebrand factor, VWF) and CD31, and non-endothelial markers, including pancytokeratin (panCK), glial fibrillary acidic protein (GFAP) and smooth muscle actin (SMA), using a VECTASTAIN® Elite ABC Systems kit (Vector, USA). Details of the primary antibodies used are summarised in Table 2-1. In brief, the cells were fixed in situ on the 8-well chamber slide with freshly made acetone-methanol (1:1, Sigma) at –20˚C for 10 minutes, followed by three five-minute washes in PBST. The cells were then incubated with blocking solution for 15 minutes, followed by addition and incubation of 1˚ antibodies for two hours at room temperature (200–300 µl per well). After three washes of PBST, 2˚ antibodies (biotinylated anti-mouse IgG, BA-2000 and biotinylated anti-rabbit IgG, BA-1000 - Vector, USA) were applied to the cells for 30 minutes at room temperature. The cells were washed three times with PBST and incubated with VECTASTAIN ABC Reagent for 5–10 minutes until the colour developed. The slide was detached from the media chamber and mounted with a cover slip for light microscope examination.

IF

IF staining for the same markers (panCK, CD31, SMA, GFAP, VWF) was carried out using an indirect two-layer IF staining method. Double immunolabelling of panCK with GFAP and panCK with VWF was also conducted. Cells were fixed with 4% paraformaldehyde at room temperature for five minutes, followed by three five-minute washes in PBS, incubated with blocking solution for 30 minutes, then incubated with 1° antibodies for two hours at room temperature. After three five-minute washes in PBS, the cells were incubated in 2° antibodies for two hours at room temperature (1:250 Alexa Fluor® 555 donkey anti-mouse IgG, and 1:250 Alexa Fluor® 488 donkey anti-rabbit IgG, Invitrogen). The cells were washed twice with PBS and incubated for five minutes with DAPI (1:5000 DAPI, Invitrogen) for nuclear counterstaining. The slide was then detached from the media chamber and mounted with a coverslip for fluorescent microscope examination using the Axio Observer Z1 inverted fluorescent microscope with AxioVision imaging software (Carl Zeiss Microscopy GmbH, Germany).

STR analysis

The DNA of the HB56 cell line and other five cell lines in Prof. Stins' laboratory was extracted using Trizol Reagent (Life Technologies, USA), according to the manufacturer's instructions, and the purified DNA of each cell line was sent to the Fragment Analysis Facility, Johns Hopkins University, for STR analysis. The DNA purification was performed by Ms Mary Motari, a research assistant in Prof. Stins' laboratory.

2.15 *In vitro* culture of *P. falciparum*-infected Erythrocytes

2.15.1 Parasite culture

Malaria parasite culture was performed according to methods originally described by Trager and Jenson (1978). Blood group O erythrocytes from healthy blood donors were infected with *P. Falciparum* parasites, clone 3D7, obtained from Johns Hopkins Malaria Research Institute, and

maintained at 1–2% haematocrit with 5–10% parasitaemia in complete malaria media in a 37°C incubator with malaria gas mixture (5% CO2, 5% O2 and 90% nitrogen). The assessment of the parasitaemia and parasitic stage was carried out on a daily basis by microscopic examination of thin blood smears stained with Giemsa. The growth media were changed regularly and fresh, uninfected RBCs were added every 48 hours.

2.15.2 Synchronisation of parasite culture

Because co-culture experiments examining binding of PRBCs to EC cultures require parasites in the trophozoite stage, trophozoites were enriched to around 90% prior to use by the sorbital lysis method and Percoll density gradient centrifugation. In this method, one day before the experiments, the sorbital lysis method was carried out. PRBCs were concentrated by centrifugation, washed, and incubated in warm 5% sorbital for 20 minutes, resulting in the survival of only ring-stage parasites. These young parasites were re-cultured for 24 hours to mature to the trophozoite stage. The next day, synchronised trophozoites were then enriched using Percoll density gradient centrifugation. Three gradients were prepared with 40%, 60% and 80% Percoll™ (GE Healthcare, USA) in complete malaria media. Three layers of Percoll gradients were made in a 15 ml Falcon tube by carefully filling the tube with 3 ml of 40% Percoll gradient, then 3 ml of 60% Percoll gradient and 4 ml of 80% Percoll gradient, sequentially. 1 ml of PRBC pellet was then carefully added on top of the gradient column, followed by centrifugation at 3000 *g* for 30 minutes at 4°C with soft acceleration and without breaking at the end of the spin. Highly synchronised mature parasites floating in between 60%–80% gradients were collected and washed in complete malaria media before use in EC co-culture experiments.

2.16 Assessment of barrier integrity of HBEC monolayers

2.16.1 Principles of measuring barrier integrity using the ECIS system

One of the unique characteristics of BBB endothelium is the tight and adherens junctions between cerebral ECs, the function of which can be directly assessed by monitoring TEER. The tight junctions set up a barrier to passage of cells and solutes across the BBB, which can alter in pathological states. Several methods have been developed to measure the breakdown in barrier function, such as measuring the partition of labeled tracer molecules, which are normally excluded by a healthy BBB. This can be done *in vivo* using techniques such as examining the ratio of partition of albumin between the serum and CSF, or *in vitro* using transwell insert systems. Another system that measures overall barrier function is the measurement of TEER, which examines the overall gradient of electrical charge across the EC barrier, a product of the exclusion or leakage of all solute molecules. Breakdown allows increased passage of charged molecules either between or through EC, and therefore reduces the resistance of the monolayer. Measuring TEER has been used widely to study pathology and pharmacology at the BBB (Deli et al. 2005). The BBB possess high TEER and the TEER values *in vivo* were estimated to be between 1500 and 2000 Ω cm^2 (Hatherell et al. 2011). The ECIS system from Applied Biophysics, USA, were used to non-invasively monitor the TEER of cell monolayers in real time. The cells grown on the electrodes at the bottom of the ECIS arrays act as insulators which decrease an electric current across the electrodes, resulting in increased impedance. The impedance measured by the ECIS system is related to the number of cells covering the electrodes, the morphology of cells, the tightness of cell junctions, and the nature of cell attachments. Figure 2-5 shows a diagrammatical representation of the ECIS principle.

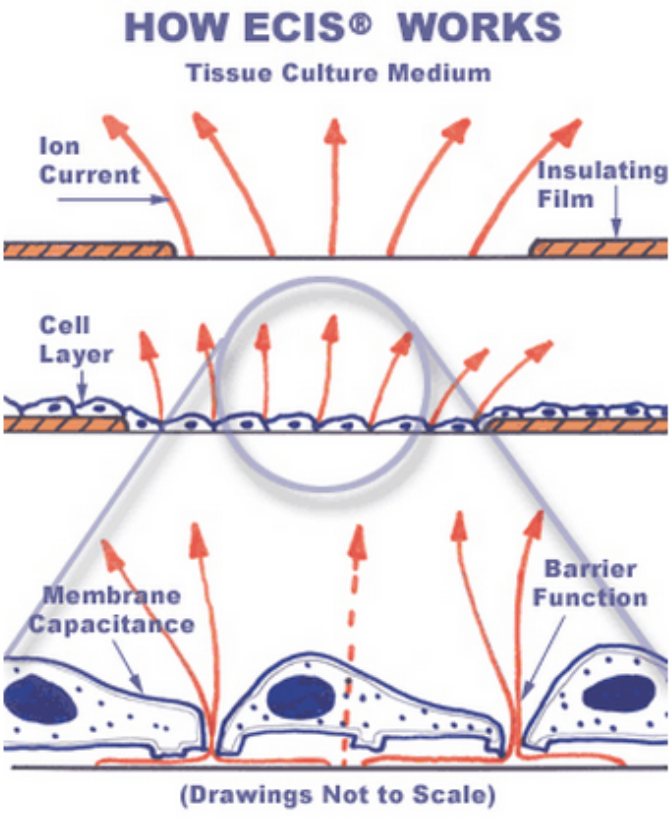

Figure 2-5. The principle of the ECIS system
(from Applied Biophysics' documents)

2.16.2 Preparation of HBEC for ECIS arrays

The barrier function and integrity of HBEC monolayers were non-invasively monitored in real time by measuring the electrical impedance of cell monolayers on small electrodes using ECIS Zθ system (Figure 2-6A). All experiments used 8W10E+ type ECIS electrode arrays (Figure 2-6B), consisting of 40 regularly spaced gold-plate electrodes over 0.9 cm^2 surface of culture area in each well. The array was coated with rat tail collagen type I (BD Biosciences, USA) before 4 x 10^4 cells of HBEC in 400 µl HBEC media were seeded to each well (8-well per array). The cells were grown for 4–5 days to form confluent monolayers, which demonstrated TEER values of 1400–1600 Ω cm^2 on the ECIS system with an AC frequency setting of 4,000 Hz. This system has a capability to monitor up to 16 different conditioned cultures simultaneously. On the evening

before experiments, the media were changed to 400 µl of 5% FBS in RPMI (serum starved media) to enhance the expression of surface-adhesion molecules on the ECs.

2.16.3 Construction of a hypoxic chamber for HBEC culture

For assessing the effect of hypoxia on the HBEC monolayers during PRBC exposure, ECIS electrode arrays were cultured in a self-made hypoxic chamber. The hypoxic chamber was made from a plastic box (Figure 2-6 C and D). Four small holes were made in the walls of the box, with two holes for leads connecting the ECIS Array Station to the ECIS Zθ System Controller and two for gas entry and exit valves. The lid of the chamber could be opened widely for convenient manipulations of the ECIS electrode array, such as addition of cytokines or PRBCs. When the lid was closed, it created an airtight chamber. The hypoxic condition inside the chamber was created by passing a special gas mixture containing 1% oxygen, 4% carbon dioxide and 95% nitrogen through one valve for two minutes. The special gas mixture replaced the normal air (containing approximately 20% oxygen), which was pushed to exit the chamber through the other valve during the gassing process. This chamber maintained a very low oxygen state throughout the hypoxic experiments to mimic the hypoxic condition *in vivo* during PRBC sequestration.

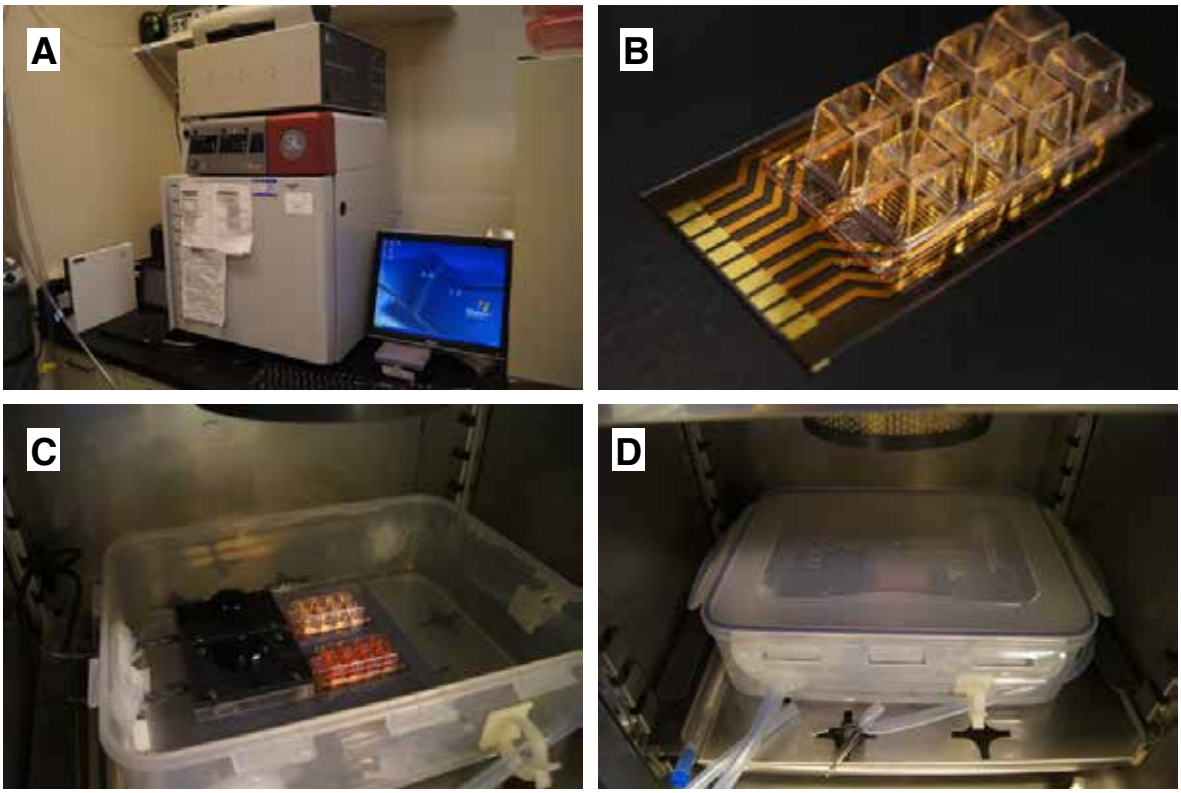

Figure 2-6. Actual photographs of ECIS system used for monitoring transendothelial electrical resistance (TEER) of HB56 monolayer

(A) An ECIS Zθ System Controller, a humidified incubator dedicated to ECIS experiments and a computer with Windows operating system. (B) A 8W10E+ type ECIS electrode array. (C) Two ECIS electrode arrays (8W10E+) on a 16-well ECIS Array Station in the hypoxic chamber (lid open). (D) The hypoxic chamber (lid closed) inside the humidified incubator.

Chapter 3

A Clinicopathological Correlation of the Expression of the Ang-Tie-2 Ligand-Receptor Pathway in the Brain in *P. falciparum* Malaria

3.1 Introduction

3.1.1 Aims and background

Recent *in vivo* studies have implicated the dysregulation of angiopoietins in the pathogenesis of severe and fatal malaria. Plasma concentrations of Ang-2 and the Ang-2/Ang-1 ratio were associated with disease severity and mortality in adults and children with falciparum malaria (Conroy et al. 2009, 2010; Jain et al. 2011; Lovegrove et al. 2009; Yeo et al. 2008;). As these markers reflect systemic endothelial activation, which is known to occur in severe malaria, the finding that these levels are specifically higher in CM than NCM patients raised the possibility that release of Ang-2 in the brain may reflect specific endothelial dysfunction in the brain in CM. The Ang-Tie2 signalling pathway could potentially be a target for neuroprotective adjunctive therapy in CM.

The role of tissue expression of the angiopoietins in malaria had not previously been studied. This part of my thesis therefore aimed to use IHC on brain tissues from fatal malaria cases to examine the expression patterns of Ang-1, Ang-2 and their receptor Tie-2 on cerebral ECs or parenchymal cells in the brain of human CM and NCM cases. Using semi-quantitative and quantitative assessment, the pattern and degree of staining was examined to determine whether this specifical-

ly increased in CM, or correlated with clinical data on coma or other severe clinical features. In a limited number of the available cases from adult Vietnamese patients, plasma and CSF were also available, so the levels of these markers were measured using quantitative ELISA and correlated with the clinical, neuropathological and immunohistochemical features of severe and fatal malaria using multivariate statistical analysis.

3.2 Materials and methods

3.2.1 Malaria and non-malaria cases

A total of 81 adults were included in this clinicopathological study. 63 were severe malaria cases selected from the AQ trial (Hien et al. 1996), admitted at the centre for Tropical Diseases in Ho Chi Min City, Vietnam between 1991 and 1995. These were diagnosed with malaria using serial blood films and subsequent blood PCR. All were classified according to the WHO (1990) criteria for severe falciparum malaria. 18 were normal controls from routine autopsy at John Radcliffe Hospital (Oxford, UK). These normal controls had clinically confirmed multi-organ dysfunction and a variety of different causes of death, with normal appearances on subsequent neuropathological examination.

3.2.2 Malaria brain specimens

Of the 63 severe malaria cases, 33 died and 30 survived. The brains of 23 of the 33 fatal malaria cases were included in the IHC study along with the brains of 18 normal controls from the UK. The brain specimens were collected at autopsy within 24 hours (median 7 hours), fixed in 10% formalin, then embedded in paraffin and processed using standard methods as previously described (Medana, Day, et al. 2002).

3.2.3 Plasma and CSF specimens.

Plasma samples from 62 out of the 63 severe malaria cases were used for the quantitation of the angiogenic proteins by ELISA. CSF samples were available from only 12 severe malaria cases. Venous blood samples were taken immediately after admission into EDTA anticoagulant. Plasma samples were generated by centrifugation at 5000g for three minutes, then aliquoted and stored at −80 °C until use. CSF was taken when the procedure was clinically indicated, aliquoted neat without any additives, spun and frozen at −80 °C until use (Medana, Hien, et al. 2002).

3.2.4 Detection of Ang-1, Ang-2 and Tie-2 proteins in the brain

Tissue expressions of Ang-1, Ang-2 and Tie-2 were detected using the IHC technique. Details of the immunostaining procedure and IHC assessment score were presented in section 2.3. Three areas of the brain from each case were examined, including the cortex, diencephalon and brain stem, to determine any site-specific variations in the patterns of immunoreactivity. With each brain area, the pattern and intensity of staining were examined in three different cellular components, including vessels, neurons and astroglial cells. In total, 41 cases (23 fatal malaria patients, 18 fatal non-malaria patients) were evaluated. Of the 23 fatal malaria patients, 13 were defined as dying from CM and 10 from NCM.

3.2.5 Detection of Ang-1, Ang-2 and Tie-2 in the plasma and CSF

Plasma and CSF concentration of Ang-1, Ang-2 and Tie-2 were measured by quantitative sandwich ELISA (Quantikine ELISA kits, DANG10, DANG20 and DTE200 respectively, R&D Systems, UK), according to the manufacturer's instructions (details in section 2.4). A total 62 plasma samples and 12 CSF samples from patients with severe malaria were examined, all in duplicate. 22 of the 62 plasma samples and 12 CSF samples were from fatal malaria cases included in the immunohistochemical analysis. The other 40 plasma samples were from severe malaria patients in the same AQ trial, including fatal cases (n = 10/40) and survivors (n = 30/40).

3.2.6 Statistical analysis

Analyses were performed using Stata/SE 9.2 (StataCorp LP, Texas, USA), with a *P*-value less than 0.05 taken as being statistically significant. Continuous variables were tested for normal distribution with the Kolmogorov-Smirnov test. This showed that the distribution of all continuous variables measured was not normal. Thus, data were summarised with median and interquartile values, and non-parametric tests including Kruskal-Wallis, Mann-Whitney U test, and Wilcoxon matched-paired signed-ranks test were used to compare between groups where appropriate. Correlations between continuous variables were tested by Spearman's rank correlation.

For IHC expression score data, due to the correlated nature of data obtained from different areas of the brain within the same patient (three areas of the brain from one patient), intra-class correlations, which affected the standard errors of the estimates, were taken into account by using clustered robust standard errors (one patient as one cluster) with univariate logistic or ordered logistic regressions where appropriate.

The prognostic value of plasma angiopoietins, Tie-2 and other biomarkers was assessed by calculating the area under the receiver operating characteristic curve (AUROC). The AUROCs were compared non-parametrically using DeLong's method.

Multivariate analyses were conducted by either linear regression or logistic regression, depending on the nature of the dependent variable. Stepwise techniques were used manually in the light of clinical judgments where appropriate.

3.3 Results

3.3.1 Patterns of Ang-1, Ang-2 and Tie-2 immunostaining in the brain

Ang-1, Ang-2 and Tie-2 staining could be found in the cytoplasm and/or nucleus of a range of cells, including neurons, astroglial cells, ECs, pericytes, and perivascular smooth muscle cells, in the brain sections of malaria and non-malaria patients (Figure 3-1). No specific staining pattern for each angiogenic marker is observed in brain sections from CM, non-CM or normal controls. There was considerable heterogeneity in the expression of Ang-1, Ang-2 and Tie-2 between patients and in the different brain areas of each patient. The expression of Ang-1 and Ang-2 was more commonly seen on larger neurons or astroglial cells than smaller neuron or astroglial cells. All three proteins could be seen on different cellular components of small- and medium-sized vessels, including ECs, pericytes and perivascular smooth muscles, but Ang-1 was almost always not seen on ECs. All these three angiogenic markers were also observed in axonal fibres, intravascular serum and RBCs either with or without parasites. However, Tie-2 staining on astroglial cells was exclusively found in malaria cases and not constitutive in controls.

3.3.2 Comparative quantitation of Ang-1, Ang-2 and Tie-2 expression between three different areas of the brain

The statistical tests used in this section were either logistic regression (for categorical variables - NeuExp and GliExp) or linear regression (for continuous variables - the number of positive vessels per cm^2). The hypothesis of the test was that there was a statistically significant relationship between the response variable (IHC expression score) and the predictor variable (the brain area). The *P*-value represented the overall *P*-value for each regression equation. This means that whenever the *P*-value is lower than 0.05, the brain area statistically and significantly affects the IHC expression score. In other words, whenever the *P*-value is lower than 0.05, there is a significantly difference in the IHC expression score among the 3 brain areas used in the analysis.

Vascular component: The number of positive vessels per cm^2 varied between each marker: (median, IQR) Ang-1 (22, 8 – 44); Ang-2 (160, 80 – 316); Tie-2 (9, 1.44 – 21.79). These variables were highly negatively skewed and could not be successfully transformed toward normality. When considering all cases in all clinical groups (Table 3-1), Tie-2 showed significantly higher expression in vessels in the cortex (cortex > diencephalon = brain stem) (overall *P* =0.048, linear regression), but the expression levels of Ang-1 and Ang-2 did not vary between the brain areas. In malaria cases (Table 3-2), the expression of Tie-2 on vessels in different areas of the brain remained unchanged, with a lower *P*-value (cortex > diencephalon = brain stem) (overall *P* = 0.023, linear regression). Ang-2 expression did not vary in different areas of the brain in malaria cases, but Ang-1 expression was significantly higher in the brain stem (brain stem>cortex=diencephalon) (overall *P* = 0.028, linear regression).

Neuronal component: Across all clinical groups (Table 3-1), the brain stem was associated with the higher expression of Ang-1 on neurons (brain stem [OR 3.59, 95%CI 1.615 – 7.98] > cortex = diencephalon) (overall *P* = 0.003, logistic regression), and the higher expression of Tie-2 on neurons [brain stem (OR 2.04, 95%CI 1.2 – 6.6) > cortex = diencephalon] (overall *P* = 0.030, logistic regression). No differences were seen in Ang-2 neuronal expression between brain areas. However, within the malaria cases (Table 3-2), the neuronal expression of Ang-1, Ang-2 and Tie-2 showed no significant variation either between different areas of the brain or the clinical categories of CM or NCM.

Astroglial component: Across all clinical groups (Table 3-1), the cortex was associated with the higher astroglial expression of Ang-1 (cortex [OR 2.3, 95%CI 1.24 – 4.27] >brain stem = diencephalon) (overall P =0.001, logistic regression). Astroglial expression of Ang-2 and Tie-2 did not differ between the areas of the brain. When considering malaria cases only (Table 3-2), the pattern of Ang-1 remained unchanged, with a slightly increased *P*-value (cortex > brain stem =

diencephalon) (overall P = 0.023, logistic regression). Ang-2 and Tie-2 did not show any differences in different areas of the brain.

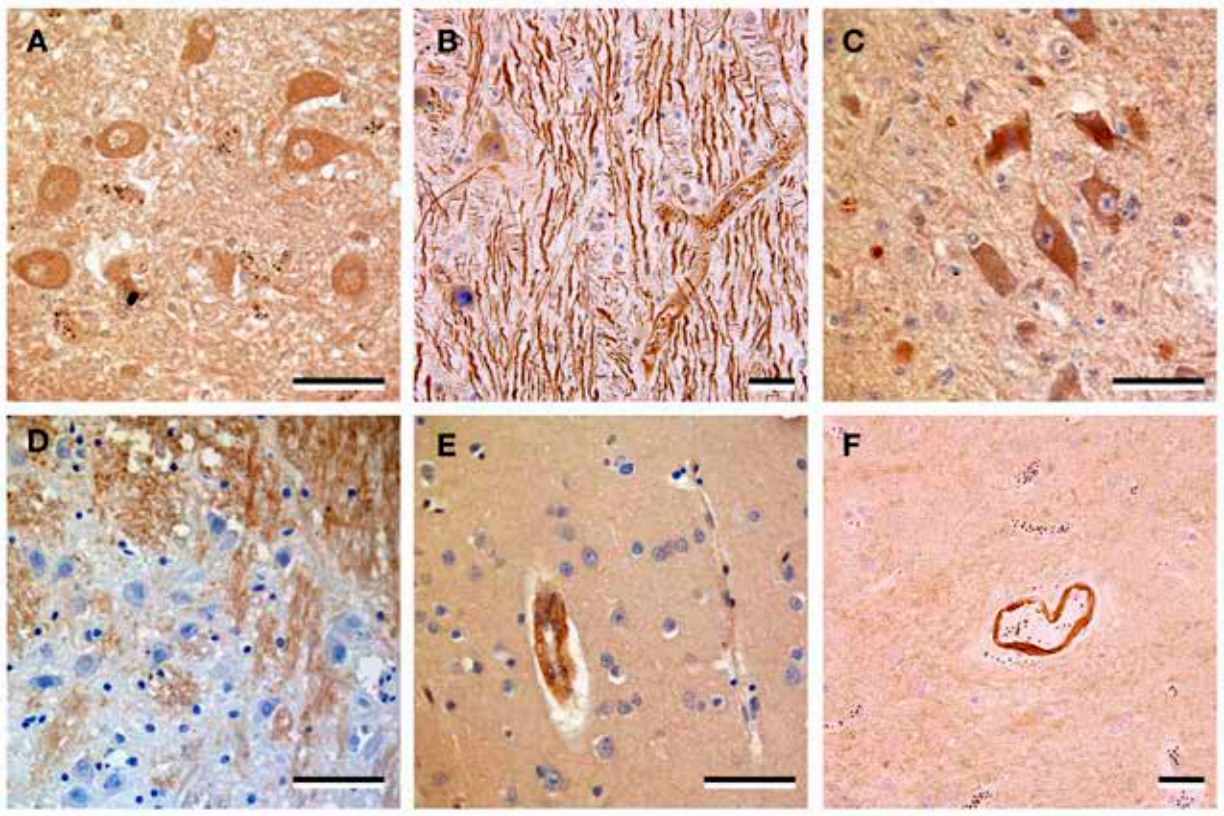

Figure 3-1. The immunostaining of Ang-1, Ang-2 and Tie-2 in brain sections from fatal malaria cases (A, B, C, F) and fatal non-malaria cases (D, E)

There was substantial heterogeneity in the expression patterns of Ang-1, Ang-2 and Tie-2 between patients and within different brain regions in each patient. This figure demonstrates examples of immunostaining patterns that are observed but do not necessarily occur in all patients or exclusively occur only in malaria or non-malaria cases. (A, D) Ang-1 was more commonly seen on larger neurons or astroglial cells than smaller neurons or astroglial cells. Ang-1 was seen on perivascular smooth muscles and pericytes, but not usually on ECs. Strong staining was occasionally observed on neuropil and axonal bundles. (B, E) Strong Ang-2 labelling was found on axonal bundles, large neurons, astroglial cells, perivascular smooth muscles, pericytes, ECs and some parasitised RBCs. (C, F) Strong Tie-2 labelling was seen on large and small neurons, astroglial cells, perivascular smooth muscles, pericytes and ECs. (F) Only one vessel showed Tie-2 staining. All sections were counterstained using Haematoxylin. Scale bars = 60 μm.

Table 3-1. Angiogenic marker expression in different cellular components across brain areas of all cases (n = 41)

Angiogenic marker	Tissue component	Expression score	Brain area			
			Brain stem	Cortex	Diencephalon	*P-v*alue
Ang-1	NeuExp	Low	10 (24.39%)	21 (51.22%)	22 (53.66%)	0.003*
		High	31 (75.61%)	20 (48.78%)	19 (46.34%)	
	GliExp	Low	23 (56.1%)	12 (29.27%)	20 (48.78%)	0.001*
		High	18 (43.9%)	29 (70.73%)	21 (51.22%)	
	Positive vessels/cm^2 (median, range)		26 (15-54)	20 (8-34)	21 (5.3-40)	0.070$
Ang-2	NeuExp	Low	15 (36.59%)	21 (51.22%)	24 (58.54%)	0.113*
		High	26 (63.41%)	20 (48.78%)	17 (41.46%)	
	GliExp	Low	37 (90.24%)	30 (73.17%)	31 (75.61%)	0.115*
		High	4 (9.76%)	11 (26.83%)	10 (24.39%)	
	Positive vessels/cm^2 (median, range)		212 (144-354)	153 (64-298)	149 (98-306)	0.170$
Tie-2	NeuExp	Low	24 (58.54%)	26 (63.41%)	33 (80.49%)	0.030*
		High	17 (41.46%)	15 (36.59%)	8 (19.51%)	
	GliExp	Low	36 (87.8%)	36 (87.8%)	39 (95.12%)	0.232*
		High	5 (12.2%)	5 (12.2%)	2 (4.88%)	
	Positive vessels/cm^2 (median, range)		8 (1-18)	10 (3.4-27)	8 (1-20)	0.048$

*Logistic Regressioin with clustered robust standard errors, $Linear Regression with clustered robust standard errors

Table 3-2. Angiogenic marker expression in different cellular components across brain areas of malaria cases only (n = 23)

Angiogenic marker	Tissue component	Expression score	Brain area			
			Brain stem	Cortex	Diencephalon	*P-v*alue
Ang-1	NeuExp	Low	3 (13.04%)	7 (30.43%)	8 (34.78%)	0.091*
		High	20 (86.96%)	16 (69.57%)	15 (56.22%)	
	GliExp	Low	8 (34.78%)	2 (8.7%)	4 (17.39%)	0.023*
		High	15 (65.22%)	21 (91.30%)	19 (82.61%)	
	Positive vessels/cm^2 (median, range)		34 (18-76)	20 (8-44)	21.67 (7-40)	0.028$
Ang-2	NeuExp	Low	7 (30.43%)	9 (39.13%)	8 (34.78%)	0.820*
		High	16 (69.57%)	14 (60.87%)	15 (65.22%)	
	GliExp	Low	23 (100%)	20 (86.96%)	16 (69.57%)	0.167*
		High	0 (0%)	3 (13.04%)	7 (30.43%)	
	Positive vessels/cm^2 (median, range)		220 (114-348)	153 (48-298)	149 (80-254)	0.271$
Tie-2	NeuExp	Low	11 (47.83%)	15 (65.22%)	15 (65.22%)	0.324*
		High	12 (52.17%)	8 (34.78%)	8 (34.78%)	
	GliExp	Low	23 (100%)	23 (100%)	23 (100%)	can't be calculated
		High	0 (0%)	0 (0%)	0 (0%)	
	Positive vessels/cm^2 (median, range)		8 (0-23)	21 (3.4-44)	12 (5-22)	0.023$

*Logistic Regressioin with clustered robust standard errors, $Linear Regression with clustered robust standard errors

3.3.3 Immunostaining of Ang-1, Ang-2 and Tie-2 differentiates malaria cases from controls but not CM from NCM

No significant differences were found between the immunostaining patterns of Ang-1, Ang-2 and Tie-2 on all three cellular components (neurons, astroglial cells and vessels) in CM cases compared to NCM (Fig 3-2). However, there were significant differences in the patterns of immunostaining of Ang-1, Ang-2 and Tie-2 in malaria cases compared to non-malaria cases, especially in neurons and astroglial cells (Figure 3-2). Summaries of the staining patterns and odds ratios are shown in Figure 3-3.

Ang-1: The incidence of high Ang-1 expression in neurons and astroglial cells was greater in malaria cases (73.91%, 79.71%, respectively), compared to non-malaria cases (35.19%, 24.07%, respectively) ($P < 0.001$). Ang-1 expression in vessels did not differ between malaria and non-malaria cases.

Ang-2: The incidence of high Ang-2 expression in neurons was greater in the brain sections of malaria cases (65.22%), compared to non-malaria cases (33.33%) ($P = 0.002$). Ang-2 astroglial expression was lower in malaria compared to non-malaria ($P = 0.078$), a finding which became statistically significant after adjusting for age and sex ($P = 0.038$).

Tie-2: Reduced expression of Tie-2 was observed in astroglial cells in malaria cases. All malaria cases (100%) expressed low Tie-2 on astroglial cells (low GliExp), compared to 77.78% of non-malaria cases ($P < 0.001$, Fisher's exact). The vascular expression of Tie-2 was significantly higher in malaria cases (high VasExp 40.58%), compared to non-malaria cases (low VasExp 11.1%) ($P = 0.049$). There was a non-significant trend for increased incidence of Tie-2 neuronal expression in malaria compared to non-malaria ($P = 0.059$).

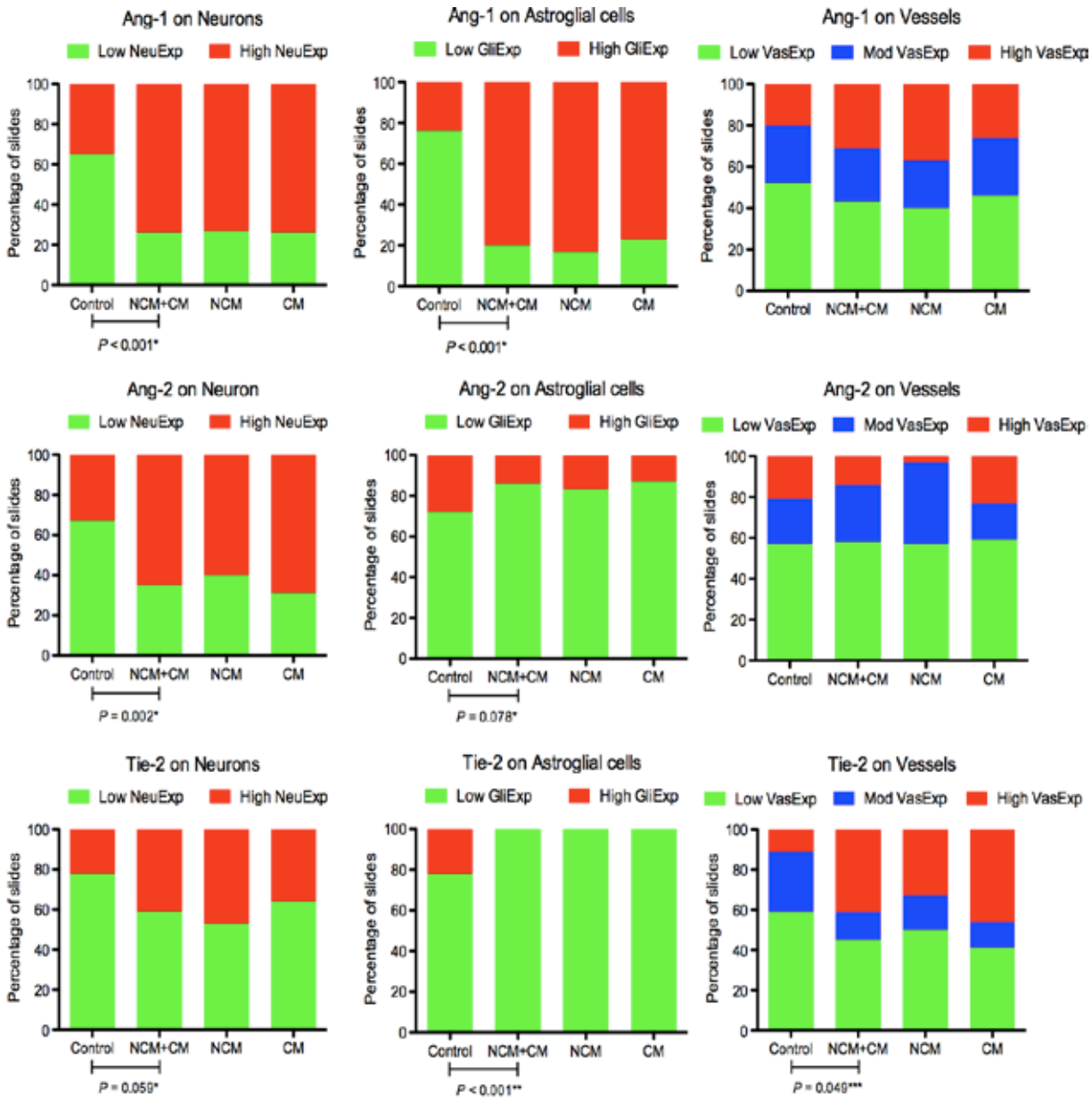

Figure 3-2. Proteins Ang-1, Ang-2 and Tie-2 were differentially expressed in the brain of fatal malaria patients compared to fatal non-malaria patients.

Graphs show percentages of slides according to proteins, cellular components and expression scores. The immunostaining patterns of Ang-1, Ang-2 and Tie-2 in malaria cases were significantly different to those in non-malaria cases, especially the staining for neuronal and astroglial components. However, these proteins were not differentially expressed in CM compared to NCM. (*Logistic Regression with clustered robust standard errors, **Fisher's Exact Test, ***Ordered Logistic Regression with clustered robust standard errors)

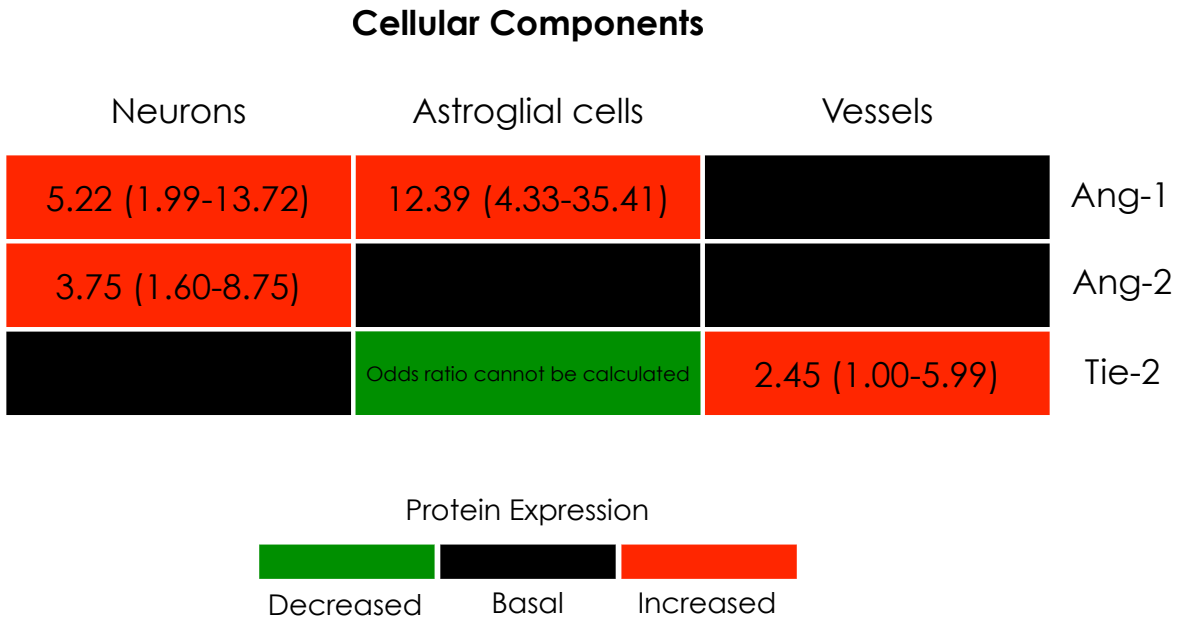

Figure 3-3. Summary of expression pattern of angiogenic proteins and odds ratios of having high expression scores of these proteins in the brain of fatal malaria patients compared with fatal non-malaria patients.
Using IHC, increased expression of Ang-1 in neurons and astroglial cells, increased expression of Ang-2 in neurons, and increased expression Tie-2 in vessels were observed in the brain of fatal malaria patients compared to fatal non-malaria patients. Decreased expression of Tie-2 in astroglial cells was observed in fatal malaria cases. Values are odds ratios of having high expression scores (high NeuExp, GliExp or VasExp) of angiogenic proteins in the brain of fatal malaria patients compared to fatal non-malaria patients. In brackets = 95%CI.

3.3.4 Increased expression of Ang-1 and Ang-2 in neurons is associated with microscopic haemorrhages

Microscopic cerebral haemorrhages are a common but non-specific neuropathological finding in CM. Two main types of haemorrhage are seen: simple petechial haemorrhage and organised ring haemorrhages. Both types of haemorrhage are not exclusively specific to CM, but also present in NCM and other forms of disease such as bacterial infections and thrombotic phenomena such as bone marrow embolism and barotrauma. They represent focal damage to the microvasculature and hence to the regulation of ECs' barrier function. Therefore, I examined the correlation between

the immunostaining patterns of Ang-1, Ang-2 and Tie-2 and microscopic haemorrhage in the brain.

Within the brain sections of malaria cases in this study, 40.6% showed haemorrhages. Petechial haemorrhages (88.9%) were more common than ring haemorrhages (11.1%). No significant difference in the incidence of haemorrhages was found between CM and NCM in this series. There was no correlation between the vascular or astroglial expression of Ang-1, Ang-2 or Tie-2 and the incidence or number of haemorrhages per cm^2. However, a high NeuExp of Ang-1 (OR = 7.11, 95%CI = 1.50 – 33.64) was associated with the presence of microscopic haemorrhages (P = 0.013).

Taking all clinical groups (malaria and non-malaria) into account, high neuronal expressions of Ang-1 (OR = 13.30, 95%CI = 3.27 – 54.09) and Ang-2 (OR = 5.5, 95%CI = 1.77 – 17.01) were significantly associated with the presence of haemorrhage (P = 0.003, P < 0.0001).

3.3.5 Immunostaining of Ang-1, Ang-2 and Tie-2 is not associated with parasite sequestration in the brain

No correlation was found between the degree of PRBC sequestration in cerebral microvessels (as measured by the percentage of vessels showing sequestered PRBC in a section) and the expression of any of the angiogenic proteins in vessels, astroglial cells or neurones.

3.3.6 CSF levels of circulating Ang-1, Ang-2 and Tie-2 are much lower than those in plasma

Sixty-two plasma samples of malaria patients were available and used for quantitative ELISA. Only a limited number of CSF samples were available from cases where IHC had been performed on the corresponding case (n = 12). The median and interquartile ranges of CSF and plasma levels of Ang-1, Ang-2 and Tie-2 are shown in Table 3-3.

Table 3-3. Circulating angiogenic marker concentrations and clinical complications of severe malaria patients

		Ang-1 (pg/ml)	Ang-2 (pg/ml)	Tie-2 (pg/ml)	Ang-2/Ang1 Ratio
CSF (n=12)		10.27 (8.1-11.1)	609 (388-1059)	247.6 (119-343)	-
Plasma (n=62)		543.15 (401-837)	21126 (11590-33595)	28232 (22425-33418)	39.25 (23.14-62.56)
Fatal outcome	**No (n=30)**	591.36 (377.8-862.7)	14883 (9369-24849)	28232 (17288-33106)	30.55 (18.00-48.28)
	Yes (n=32)	495.33 (401.0-825.2)	28215 (17040-42921)	28213 (22684-34395)	42.54 (30.57-70.07)
	P-Value*	0.95	0.002	0.68	0.029
Hyperpara-sitemia	**No (n=41)**	688.94 (412-976)	18706 (11590-33565)	26013 (22684-34277)	31.26 (18.39-53.22)
	Yes (n=21)	495.33 (377-615)	23863 (16110-34426)	28709 (22425-32990)	55.63 (41.60-69.26)
	P-Value*	0.08	0.36	0.88	0.01
Jaundice	**No (n=19)**	459.77 (263-787)	9692 (7064-12949)	22907 (15334-29245)	21.94 (8.18-60.95)
	Yes (n=43)	591.36 (401-963)	25041 (18288-41865)	28824 (22981-37659)	41.60 (30.17-63.16)
	P-Value*	0.13	<0.000	0.016	0.031
Anaemia	**No (n=23)**	495.33 (401-787)	12848 (9369-24519)	29245 (24960-33418)	28.10 (18.00-44.05)
	Yes (n=39)	555.18 (377-988)	26565 (13657-41865)	23800 (19090-35373)	41.70 (30.55-71.30)
	P-Value*	0.92	0.004	0.19	0.009
ARF	**No (n=23)**	495.33 (377-713)	11615 (8376-18706)	27908 (22684-32990)	30.10 (18.00-43.75)
	Yes (n=39)	664.38 (401-988)	26788 (18288-43978)	28709 (21318-37659)	41.60 (30.17-69.26)
	P-Value*	0.06	<0.000	0.58	0.06
Hypo-glycemia	**No (n=44)**	567.21 (401-812)	18497 (9829-26217)	28805 (22907-34825)	31.60 (18.78-48.28)
	Yes (n=18)	519.24 (377-963)	32948 (13657-45867)	23241 (19853-32679)	57.99 (37.34-85.16)
	P-Value*	0.98	0.007	0.29	0.019
Shocked	**No (n=38)**	173.50 (401-988)	19932 (11590-31282)	28767 (22684-37659)	33.94 (18.78-56-24)
	Yes (n=24)	459.77 (389-591)	24191 (11841-34918)	27699 (21817-31751)	43.62 (29.77-76.06)
	P-Value*	0.053	0.36	0.48	0.13
Hyper-lactataemia	**No (n=39)**	688.94 (401-988)	18706 (10415-33565)	27718 (21171-37659)	32.66 (22.77-59.84)
	Yes (n=23)	495.33 (377-713)	24601 (12444-35352)	28786 (23501-32990)	43.48 (23.14-70.88)
	P-Value*	0.14	0.36	0.69	0.2
CM	**No (n=29)**	495.33 (308-812)	21540 (13657-31021)	24960 (19090-37818)	41.60 (29.66-62.56)
	Yes (n=33)	579.28 (436-850)	18706 (9692-34426)	28709 (22918-32990)	37.55 (20.65-63.61)
	P-Value*	0.41	0.75	0.49	0.59
Pure CM	**No (n=54)**	519.24 (377-837)	24191 (12848-34485)	28633 (22425-35373)	41.35 (29.66-66.28)
	Yes (n=8)	713.50 (471-862)	7237 (5178-11321)	25407 (19415-29744)	8.18 (5.65-20.55)
	P-Value	0.31	<0.000	0.27	0.002

Values are presented as median (IQR), *Mann-Whitney U test

The CSF concentrations of all three were significantly lower than the plasma concentration of themselves in the same cases (ranging from three to 800 times) (P = 0.0005, Wilcoxon matched-paired signed-ranks test) (Figure 3-4).

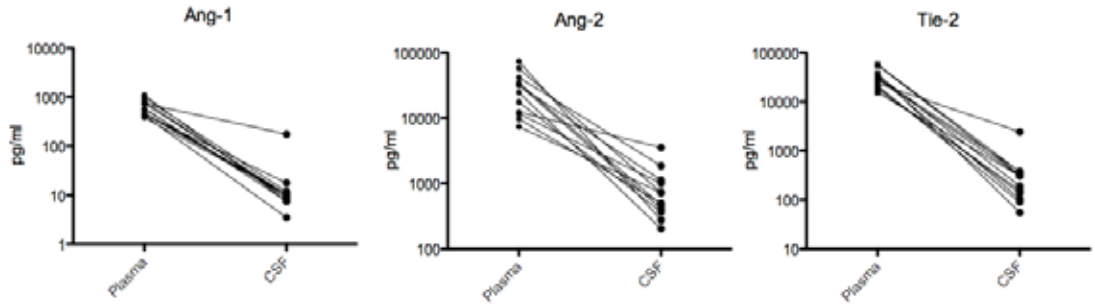

Figure 3-4. Biomarker levels in CSF and plasma.
The levels of circulating Ang-1, Ang-2 and Tie-2 in CSF were significantly lower than in plasma in all cases available for the study (n = 12) (P = 0.0005, Wilcoxon matched-paired signed-ranks test).

3.3.7 Plasma levels of Ang-2 and Ang-2/Ang-1 ratio are significant predictors of fatal outcome, and Ang-2 levels are predictive independent of plasma lactate concentration

The level of Ang-2 and the ratio of Ang-2/Ang-1 (plasma samples collected at time of admission) were significantly higher in patients with fatal outcome than survivors (P = 0.002 and P = 0.029, respectively). Ang-1 and Tie-2 concentrations were not associated with a fatal outcome (Table 3-3).

In order to assess the prognostic value of the Ang-2 and Ang-2/Ang-1 ratio, receiver operating characteristic (ROC) curves were plotted. Ang-2 has an area under curve (AUROC) of 0.727 (95%CI = 0.6 – 0.85), and Ang-2/Ang-1 ratio has an AUROC of 0.662 (0.522-0.802). The prognostic values of these two plasma markers were not significantly different from each other and the prognostic values of both were not significantly different from other laboratory measures,

which have been described previously as important prognostic markers in severe malaria, including plasma lactate, or other markers such as creatinine or TNF (Table 3-4).

Table 3-4. Comparison of prognostic value of plasma marker concentrations for fatal outcome

Marker	AUC (95%CI)	Compared to Ang-2	Compared to Ang-2/ Ang-1 Ratio
Ang2	0.727 (0.600-0.854)		
Ang2/Ang1 Ratio	0.662 (0.522-0.802)	0.82, 0.36	
Creatinine	0.708 (0.575-0.840)	0.09, 0.77	0.22, 0.64
Lactate	0.666 (0.528-0.804)	0.4, 0.52	0.01, 0.93
TNF (n=32)	0.696 (0.528-0.863)	0, 1	0.57, 0.75

AUC = area under ROC curve, Data are x^2, *P*-value unless otherwise indicated. All X^2 and *P*-value are calculated from pariwise nonparametric comparison of areas under ROC curve.

A multivariable logistic regression model was constructed to assess whether these angiogenic proteins were independently associated with death, using fatal outcome as the dependent variable and the angiogenic proteins as well as creatinine, lactate and TNF as the independent variables. In this model, none of the markers were independently significantly associated with death. Then, a backward stepwise approach was used which showed that Ang-2 (OR = 1.000036 per pg/ml, 95%CI = 1.000004 – 1.000068) and lactate (OR = 1.21 per mmol/L, 95%CI = 1.032 – 1.435) were independently associated with fatal outcome. Ang-2 and lactate remain significant prognostic markers after adding into the model other clinical and biochemical parameters, including age, sex, presence of shock, presence of hypoglycaemia, admission Glasgow coma score, admission haematocrit and parasite count.

3.3.8 Plasma levels of Ang-2 and Ang-2/Ang-1 ratio are associated with multiple clinical complications of severe malaria

High plasma levels of Ang-2 were significantly associated with the presence of several complications of severe malaria, including fatal outcome, jaundice, anaemia, ARF and hypoglycaemia (Table 3-3). High Ang-2/Ang-1 ratios were also associated with the same clinical complications

as Ang-2, but with slightly lower magnitude. Hyperparasitaemia was associated with a high Ang-2/Ang-1 ratio and low Ang-1 but not independently associated with raised Ang-2. High plasma levels in Tie-2 were associated with the presence of jaundice but not the other complications.

3.3.9 Plasma level of Ang-2 is not a biomarker for CM but a prognostic marker for progressive multi-organ dysfunction in severe malaria

The presence of CM was not related to the plasma concentrations of Ang-1, Ang-2 and Tie-2 in this series of patients; however, patients with "pure" CM (CM patients with coma only and without other complications of severe malaria) had significantly lower Ang-2 concentration and Ang-2/Ang-1 ratio than the other patients (Table 3-3).

This led to an assessment of the relationship between plasma Ang-2 concentration and the number of criteria of severe malaria according to the WHO's classification of severe disease (2000a). Ang-2 levels were significantly associated with the number of severe complications of severe malaria occurring in a patient ($P < 0.001$, Kruskal-Wallis) (Table 3-5). This indicated that Ang-2 could be a prognostic marker of progressive multiple organ dysfunction in severe malaria. Conversely, there were no correlations between Ang-1 or Tie-2 concentrations and the number of severity criteria.

Table 3-5. Baseline Ang-2 plasma concentration stratified by the number of severe criteria

No. of severe criteria	N	Ang-2 (pg/ml)	Ang-2/Ang1
1	16 (25.8%)	9730 (7237-15240)	20.55 (8.18-55.63)
2	28 (45.2%)	22616 (14883-34889)	38.53 (28.74-61.15)
3	8 (12.9%)	23532 (15977-28215)	51.66 (17.19-67.77)
4	9 (14.5%)	34485 (31282-43978)	41.60 (37.34-70.88)
5	1 (1.6%)	58192	94
Kruskall-Wallis		P <0.000	$P = 0.10$

3.3.10 Correlation of clinical and laboratory parameters with plasma levels of Ang-1, Ang-2 and Tie-2 proteins

Spearman's rank correlations were calculated between plasma concentrations of Ang-1, Ang-2 or Tie-2 and a number of various clinical and biochemical markers at admission, including GCS, respiratory rate, haematocrit, white blood cell count, platelets, parasite count, liver function tests, creatinine, glucose, electrolytes, lactate, TNF, and arterial blood gas measures. The summary of the correlations of some important markers of malaria severity is presented in Table 3-6.

Plasma Ang-1 concentration was positively correlated with the admission levels of platelets. This finding may reflect platelet production and release of circulating Ang-1 (Li et al. 2001). However, the Ang-2 and Ang-2/Ang-1 ratio were negatively correlated with platelet counts. There were positive correlations between body temperature and concentrations of Ang-1 and Tie-2, raising the possibility that these proteins might play a role in body temperature regulation in response to the disease. Plasma Ang-2 was correlated with several indicators of disease activity/severity, including increased white cell counts, increased liver enzymes (SGOT and SGPT), decreased renal function (elevated BUN, creatinine and potassium) and metabolic acidosis (low pH, high pCO2). Moreover, plasma Ang-2 concentration was strongly positively correlated with CSF concentrations of quinolinic acid and picolinic acid, which have been previously measured in the CFS of these patients, and shown to be strongly associated with ARF in this group (Medana, Hien, et al. 2002). There were no correlations between admission parasite count and the plasma levels of Ang-1 Ang-2 or Tie-2, but admission parasite count was significantly correlated with the ratio of Ang-2/Ang-1.

Lactate and pyruvate levels, which could also contribute to metabolic acidosis, were not correlated with Ang-1, Ang-2 and Tie-2. This finding suggests that Ang-2 levels were correlated with metabolic acidosis in a manner independent of lactate levels (Spearman's rho = 0.09, $P = 0.47$).

Table 3-6. Summary of correlations between plasma angiogenic markers and laboratory parameters

		Ang-1	Ang-2	Tie-2	Ang-2/Ang1 Ratio
Body temperature	**rho, P-value***	0.2788, 0.029	ns	0.441, <0.000	
	n	61		62	
Haematocrit	**rho, P-value***	ns	-0.368, 0.003	ns	ns
	n		62		
Parasite count	**rho, P-value***	ns	ns	ns	0.3, 0.018
	n				61
Platelets	**rho, P-value***	0.305, 0.018	-0.294, 0.022	ns	-0.442, <0.000
	n		60		59
White blood cells	**rho, P-value***	ns	0.471, <0.000	ns	ns
	n		59		
BUN	**rho, P-value***	ns	0.733, <0.000	ns	0.554, 0.002
	n		27		27
Creatinine	**rho, P-value***	ns	0.619, <0.000	ns	0.293, 0.02
	n		62		61
Potassium (K)	**rho, P-value***	ns	0.311, 0.027	ns	ns
	n		50		
SGOT	**rho, P-value***	0.317, 0.014	0.415, 0.001	ns	ns
	n	59	60		
SGPT	**rho, P-value***	ns	0.283, 0.028	ns	ns
	n		50		
TNF	**rho, P-value***	0.416, 0.017	ns	ns	ns
	n	32			
Lactate	**rho, P-value***	ns	ns	ns	ns
	n				
Pyruvate	**rho, P-value***	ns	ns	ns	ns
	n				
PH	**rho, P-value***	ns	-0.42, 0.004	ns	ns
	n		44		
pCO2	**rho, P-value***	ns	-0.4832, <0.000	ns	-0.438, 0.003
	n		44		43
CSF Kynurenic	**rho, P-value***	ns	ns	ns	ns
	n				
CSF Quinolinic	**rho, P-value***	ns	0.711, <0.000	ns	0.625, <0.000
	n		31		30
CSF Picolinic	**rho, P-value***	ns	0.753, <0.000	ns	0.708, <0.000
	n		31		

*Spearman's rank correlation. No adjustments for multiple comparison have been made. All parameters were measured from plasma samples (except indicated as CSF) at time of admission, ns = not significant.

3.3.11 Plasma levels of Ang-2 and lactate were independently associated with metabolic acidosis

As described above, plasma Ang-2 levels were closely correlated with several established prognostic indices of malaria disease severity and several factors indicating disease activity. As the various clinical manifestations and laboratory parameters of severe malaria are interlinked, I constructed a backward stepwise multivariable linear regression model to determine the factors contributing to plasma Ang-2 level, with the plasma level of Ang-2 as the dependent variable and haematocrit, parasite count, platelets, white cell counts, creatinine, SGOT, and lactate as possible explanatory factors. All of these parameters were independently and significantly associated with the level of Ang-2 in this model and together they accounted for 67% (R^2 = 0.677) of the variance in Ang-2 (Model A, Table 3-7).

As described earlier, there were no correlation between lactate and Ang-2 in the univariate analysis, and the multivariable logistic regression model predicting death as an outcome showed that Ang-2 and lactate were independent factors contributing to death. However, in this linear regression model (Model A, Table 3-7), lactate was a significant independent contributing factor to Ang-2. This suggests that there were other confounding factors related to the levels of Ang-2 and lactate. This could be metabolic acidosis, which is closely related as a complication of severe malaria to renal failure and hyperlactatemia, as reported elsewhere (Day et al. 2000). Therefore, admission arterial blood pH, representing one measure of metabolic acidosis, was added into the model. Adding pH removed the independent significance of lactate, creatinine, and platelets, so these were removed from the model; thus, only haematocrit, parasite count, white cell count and SGOT remained significant factors associated with levels of Ang-2 (Model B, Table 3-7). This supported the hypothesis that Ang-2 was not directly correlated with lactate but that both of them (together with renal dysfunction) were correlated with one common manifestation of severe disease – metabolic acidosis.

Table 3-7. Summary of multivariate regression models

Model	Dependent variable	Regression type	Independent variables	Coefficients (95%CI)	Standardised Coefficients	*P* - value
A	Plasma Ang-2	Linear regression	Haematocrit	-506.65 (-933 to -80)	-0.2294042	0.021
			Parasite count	0.0116 (0.004 to 0.019)	0.2893166	0.003
		R^2=0.677	Platelet	-0.200 (0.333 to -0.067)	-0.27261	0.004
			White cell	1.260 (0.746 to 1.774)	0.4790173	<0.000
			Creatinine	1965 (20.2 to 3911)	0.2087163	0.048
			SGOT	44.60 (19.61-69.58)	0.3070279	0.001
			Lactate	-1539 (-2416 to -661.7)	-0.3230233	0.001
			Constant	23369 (3808 to 42930)	-	0.02
B	Plasma Ang-2	Linear regression	Haematocrit	-591.39 (-1111 to -71)	-0.275	0.027
			Parasite count	0.0111 (0.002 to 0.020)	0.280	0.017
		R^2=0.623	White cell	1.44 (0.832 to 2.057)	0.352	<0.000
			SGOT	71.96 (23.07 to 120.85)	0.530	0.005
			Constant	9200 (-12672 to 31072)	-	0.399

3.4 Discussion

IHC for Ang-1, Ang-2 and Tie-2 on post-mortem brain tissue in fatal malaria cases revealed significant differences in the expression in ECs and parenchymal cells compared to controls. However, there was no significant difference in the expression of any of these markers in ECs, glia or neurons in brain tissue between the CM and NCM cases. Immunostaining of Ang-1, Ang-2 and Tie-2 was also not associated with *P. falciparum*-infected erythrocyte sequestration in the brain. However, Ang-1 and Ang-2 expression in neurons was significantly correlated with the incidence of microscopic haemorrhages.

The finding of angiopoietins in neurons was surprising because we expected the staining to be predominantly in ECs. This raised the possibility that the staining was non-specific, perhaps due to leakage of plasma protein across the BBB and uptake by neurons. However several features argue that this is specific neuronal staining. Several studies have shown that Ang-1 and Ang-2 can be expressed by neurons and the up-regulation of these angiogenic proteins in neurons is

associated with neuronal differentiation and development, via Tie-2 and beta integrin receptors on neurons (Bai, Cui, et al. 2009; Bai, Meng, et al. 2009; Chen et al. 2009; X. S. Liu et al. 2009). Control cases in this project showed much lower levels of staining compared to malaria cases. Moreover, in each individual case, whether control or malaria cases, only a subset of neurons stained, not every neuron, which might be expected if the staining were truly non-specific. However, this result should be confirmed using techniques such as in situ hybridisation for Ang-1 and Ang-2 mRNA on neurons, or in situ PCR on tissue sections, which might confirm the presence of these mRNA transcripts in neuronal cells.

Analysis of the staining patterns of other cells such as ECs and glial cells was independent of the presence or absence of neuronal staining. If considering only vascular staining, it can be concluded that there was a significant increase in Tie-2 expression on vessels in the brain of malaria cases compared to non-malaria controls, but no significant difference in the expression of Ang-1 and Ang-2 was seen between both clinical groups.

Plasma and CSF levels of Ang-1, Ang-2 and Tie-2, measured by ELISA, compared fatal cases with surviving patients from the same study. Plasma levels of Ang-2 and Ang-2/Ang-1 ratio were associated with the number of severe malaria complications and were significant and independent predictors of metabolic acidosis and fatal outcome. Activation of the Ang-Tie-2 pathway in severe malaria is therefore related to acidosis, a number of severity criteria and outcome, but is not a specific event in the brain during CM.

Plasma concentrations of Ang-2 and the Ang-2/Ang-1 ratio were confirmed as independent predictors of death in severe falciparum malaria in this study, as seen in all other severe malaria series to date. These include series of adult severe malaria from Indonesia (Yeo et al. 2008), adult CM from India (Jain et al. 2011), and paediatric CM series from Uganda (Erdman et al. 2011; Lovegrove et al. 2009) and Malawi (Conroy et al. 2009). The number of cases examined in this

study is lower than these other studies but the results imply that this still leant adequate statistical power to delineate the significant association of Ang-2 levels with poor prognosis.

Previous pathological studies of CM have demonstrated the presence of endothelial activation in the cerebral microvasculature (Turner et al. 1994), which occurs as part of a wider systemic endothelial activation in severe malaria, and which is not specific to cases who develop coma (Turner et al. 1998). The pathophysiology of endothelial activation in CM has been hypothesised to occur in response to both systemic factors (such as the release of cytokines or a soluble malaria toxin) or local vasoactive substances such as NO, VEGF or WPB products such as Ang-2. My group has previously examined the expression of NOS subtypes in the brain in CM (Maneerat et al. 2000) and activation of the VEGF signalling pathway (Medana et al. 2010). The expression of the angiopoietins and their ligand Tie-2 in the brain in CM and NCM cases was examined to determine the extent to which they were specific to CM, as well as whether this pathway showed a direct link to the clinical features of coma before death.

However, the significant staining patterns of Ang-1, Ang-2 and Tie-2 on neurons and astroglial cells in the brain of malaria cases compared to controls, as well as the association of increased Ang-1 and Ang-2 staining on neurons with the incidence of microhaemorrhages, may imply that in cases with BBB breakdown the influence of this pathway may extend to the parenchymal cells of the brain. Examination of other tissues which represent end organs showing specific injury in severe malaria patients may help determine whether the Ang-Tie-2 pathway also mediates tissue-specific damage in other sites, such as the lung or kidney.

Chapter 4

Examining the Roles of the Ang-Tie-2 Pathway and Hypoxia in the Interaction between Malaria-Parasitised Erythrocyte Binding and Cultured Brain ECs *in vitro*

4.1 Introduction

4.1.1 Background

Pathological examination of tissues from patients dying of CM demonstrates sequestration of parasitised erythrocytes due to specific cytoadherence to cerebral ECs through adhesion molecules such as ICAM-1. Given the association between malarial infection, PRBC localisation in the cerebral microvasculature and the clinical syndrome of CM, the BBB is clearly a critical interface in the disease (Medana and Turner 2006). The malaria parasite is able to induce coma whilst remaining within the brain vasculature without entering the parenchyma. Pathological and molecular studies show PRBC binding to the cerebral vasculature causes widespread EC and astroglial activation and changes to EC junctional protein expression (Brown et al. 2001; H. Kim et al. 2011; Medana and Turner 2006;).

In vitro models of the BBB utilising primary HBEC cultures by Tripathi et al. (2006, 2009) have demonstrated that PRBC binding to ECs causes specific receptor-mediated and adhesion-independent signalling events, including the increased expression of ICAM-1, translocation of NF-κB and activation of pro-inflammatory molecules including CCL20, CXCL1, CXCL2 and

TNF through the NF-κB signalling pathway. Their model has also shown that the PRBC but not normal RBC can dramatically decrease BBB integrity in a dose-dependent manner (Tripathi et al. 2007). A recent study has discovered that the adhesion of PRBC to HBEC causes a transfer of malarial antigens from PRBC to the HBEC by a trogocytosis[a]-like process, leading to the activation of the immune system and the opening of inter-EC junctions (Jambou et al. 2010).

These intravascular events are hypothesised to lead to secondary neuropathological changes in CM, including widespread astroglial activation, axonal injury, and oedema. Some of these responses may be transduced across the BBB due to direct, parasite-adhesion-mediated signalling, whilst another possible mechanism may be soluble parasite or RBC-derived products (such as haemozoin or parasite GPI-linked 'toxins') acting at a distance. The other critical determinant of microvascular function during CM will be the effects of systemic complications of severe malarial disease, such as hypoxia, acidosis or hypoglycaemia, acting locally on the BBB. The role of hypoxic responses in the pathogenesis of CM is not clear, but markers of hypoxic injury such as HIF-1α, VEGF and VEGF-R are up-regulated in the brain in CM (Medana et al. 2010). Moreover, increased HIF-1α expression has been linked in the murine model of CM to the development of coma (Hempel et al. 2011), despite the fact that this model is characterised by a lack of cerebral sequestration of PRBCs.

4.1.2 Aims

The work in the previous chapter studied the expression of the Ang-Tie-2 pathway of EC activation in the post-mortem human brain, because these molecules had been implicated as prognostic indicators in severe malaria and CM. To investigate the interrelationship between

[a] Trogocytosis is the intercellular exchange of membrane material, which can lead to transfer of proteins from one cell surface (such as an EC) to another (such as a lymphocyte). This was originally identified in the immune system where antigen-presenting cells transfer membrane to lymphocytes allowing better presentation of non-self antigen in association with MHC molecules. This differs from emperipolesis, which is the wholesale transfer of one cell to within the cytoplasm of another, most often with reference to phagocytosis of whole red cells into lymphocytes.

hypoxia, PRBC binding and EC activation caused by the Ang-Tie-2 pathway, I therefore designed a study using an *in vitro* model of the BBB to examine the effects of hypoxia, TNF and Ang-2 on the TEER of HBEC monolayers co-cultured with PRBCs in real time. Subsequent genome-wide transcriptional profiling of the HBECs from the co-cultures experiments was also planned in order to investigate novel genes and pathways associated with the experimental conditions mimicking the PRBC sequestration *in vivo*. This project was performed at Prof. Monique Stins' laboratory at Johns Hopkins University, Baltimore, USA, using an *in vitro* model of HBEC developed in her laboratory, where I spent 3-month time learning techniques of HBEC isolation and culture, and TEER-related experimental techniques.

4.2 Material and methods

4.2.1 HBEC cell lines

As described in section 2.14, HBEC were initially isolated from a temporal lobe brain specimen acquired from an epilepsy patient at the Department of Neurology, School of Medicine, Johns Hopkins University, Baltimore, USA. However, due to the slow growth rate of the newly isolated HBEC and time limitations restricting my visit, experiments were subsequently conducted using HB56, which was a previously isolated HBEC line characterised in Prof. Stins' laboratory.

4.2.2 Assessment of barrier integrity of HBEC monolayers using ECIS

The barrier function and integrity of HBEC monolayers was non-invasively monitored in real time by measuring the electrical impedance of cell monolayers on small electrodes using ECIS Zθ system, Applied Biophysics, USA). The principle and protocol related to the ECIS system was described in section 2.16.

Different permutations of experimental conditions were investigated to examine the effects of exogenous addition of TNF, Ang-2 and exposure to hypoxia on the barrier integrity of HBEC

monolayers, both as a baseline and also followed by PRBC co-culture experiments. The permutations consisted of the addition of TNF (0.5 and 1 ng/ml, human recombinant, Promega, USA), Ang-2 (50 and 100 and 1,000 ng/ml, human recombinant, R&D, USA), PRBC or control uninfected RBC, and hypoxic incubation. These were added as appropriate (as detailed in the following result sections) and TEER was continuously recorded every five minutes for up to 24 hours. Each experimental condition was performed in duplicate and all experiments were repeated twice. Data are shown as average normalised values (subsequent TEER values were divided by the starting values, meaning the starting normalised values = 1).

4.2.3 *P. Falciparum*-infected RBC preparation

Methods for continuous cultivation of *P. Falciparum*-infected RBC, and synchronisation of parasite culture by the sorbital lysis method and Percoll density gradient centrifugation, were detailed in section 2.15.

4.2.4 Phenotyping of HB56

After ambiguous behaviour on the part of the HB56 cell cultures was noticed during experiments using the ECIS system, the HB56 was re-characterised to confirm the surface phenotype using IHC and IF techniques as detailed in section 2.14.

4.2.5 STR profiling

Total DNA was extracted from HB56 cell line and the other five cell lines used in Prof. Stins' laboratory using Trizol Reagent (Life Technologies, USA), according to the manufacturer's instructions. For each cell line, 200 ng of DNA in 10 µl of purified water was analysed by STR profiling at the Fragment Analysis Facility at Johns Hopkins University. STR profiles were generated by simultaneously amplifying multiple STR loci and amelogenin (for sex determination) using the Promega PowerPlex® kit (Promega, USA). Amplified STR fragments labelled

with fluorescent dyes were then separated by capillary electrophoresis and the number of repeats of each STR locus was determined using the GeneMapper® software (Applied Biosystems, USA). The selected markers included eight STR loci from 13 Combined DNA Index System (CODIS) core STR loci: CSF1PO: 5q33.3–34; D13S317: 13q22–q31; D16S539: 16q24-qter; D5S818: 5q21–q31; D7S820: 7q; TH01: 11p15.5; TPOX: 2p23-2pter; and vWA: 12p12-pter. A sex chromosome locus, amelogenin (Xp22.10-22.3 and Y), was also used for gender identification. This panel was identical to the panel used in the ATCC STR database in order to enable easy database search and comparison.

4.3 Results

4.3.1 Newly isolated primary HBEC

Initially, the isolation of primary HBECs was successfully carried out from a temporal lobe brain tissue removed from a patient with intractable epilepsy according to procedures described in section 2.14.1. The isolation procedure was completed in approximately four hours, giving numerous microvessel fragments floating in culture media in a T25 flask. As seen by phase-contrast microscopy (Figure 4-1), ECs started to migrate from the microvessel fragments two to four days post-isolation and slowly proliferated and formed islands of cells with varying phenotypes on the bottom of the flask. The small endothelial islands were seen after around eight to ten days but a confluent monolayer was not formed until after approximately one month, showing the typical cobblestone appearance of EC cultures. The slow growth rate of this newly isolated HBEC primary line unfortunately precluded its use in characterisation and subsequent co-culture experiments.

Therefore, experiments to study the effects of angiopoietin and hypoxic conditioning on BBB integrity, and changes subsequent to co-culture with PRBCs, were switched to use a previously

isolated HBEC cell line (HB56). The HB56 was used throughout the experiments described in this chapter.

4.3.2 The *in vivo* model to assess the effects of TNF and Ang-2 on the TEER of HB56 monolayers during the exposure to exogenous stimuli including PRBC and hypoxia

Effects of TNF and Ang-2 on TEER

To assess the effects of TNF and Ang-2 on the HB56 monolayer's integrity, the HB56 cells were plated at $4x10^4$ cells per well on type I collagen-coated ECIS electrode arrays (8W10E+ Culture-ware array, Applied Biophysics). The cells were allowed to grow to achieve the cell confluency for 4–5 days, which usually resulted in TEER values of 1,400–1,600 Ω cm^2, on the ECIS system with an AC frequency setting of 4,000 Hz. On the evening prior to the experiments, the media were changed to 5% FBS in RMPI (serum starved media, SM) to enhance the expression of surface-adhesion molecules on the ECs. On the day of the experiment, the SM in each well was changed to newly prepared SM supplemented with either TNF (0.5 or 1 ng/ml), Ang-2 (50, 100 or 1000 ng/ml) or a mixture of 0.5 nl/ml TNF with 50 ng/ml Ang-2. The negative control was normal SM culture media without supplements. The TEER in each culture was simultaneously and continuously recorded every five minutes for 24 hours.

All HB56 cultures with supplemented TNF had marked increases in TEER compared to cultures without TNF. Cultures with supplemented Ang-2 had a similar TEER pattern over time to the negative control, regardless of their various Ang-2 concentrations. This showed no effect from Ang-2 on the HB56 cultures (Figure 4-2).

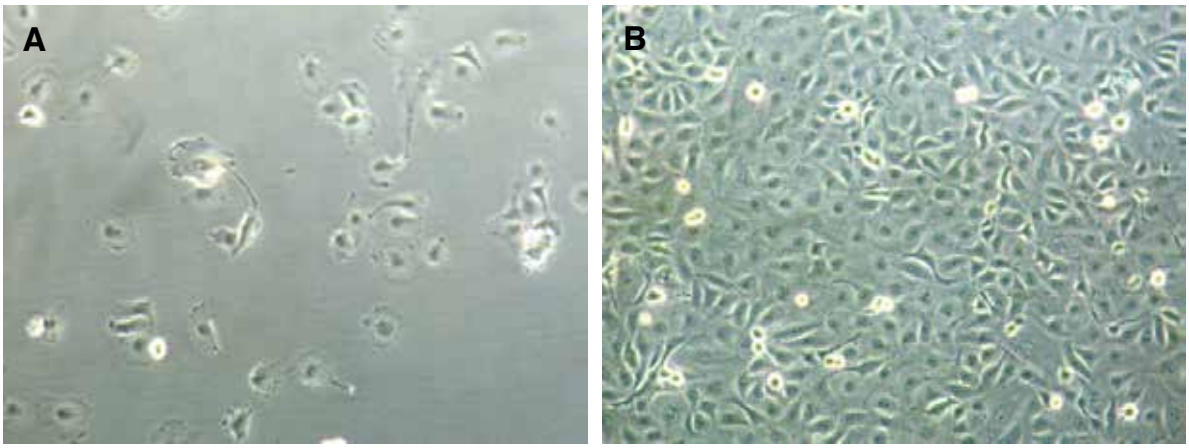

Figure 4-1. Phase-contrast microscopy of newly-isolated primary HBEC

(A) The endothelial cells emerged from the end of the micro-vessel fragments around two to four days after isolation. (B) Cell confluence was achieved approximately one month after the isolation, showing the typical cobblestone appearance of endothelial cell cultures (all 200x original magnification).

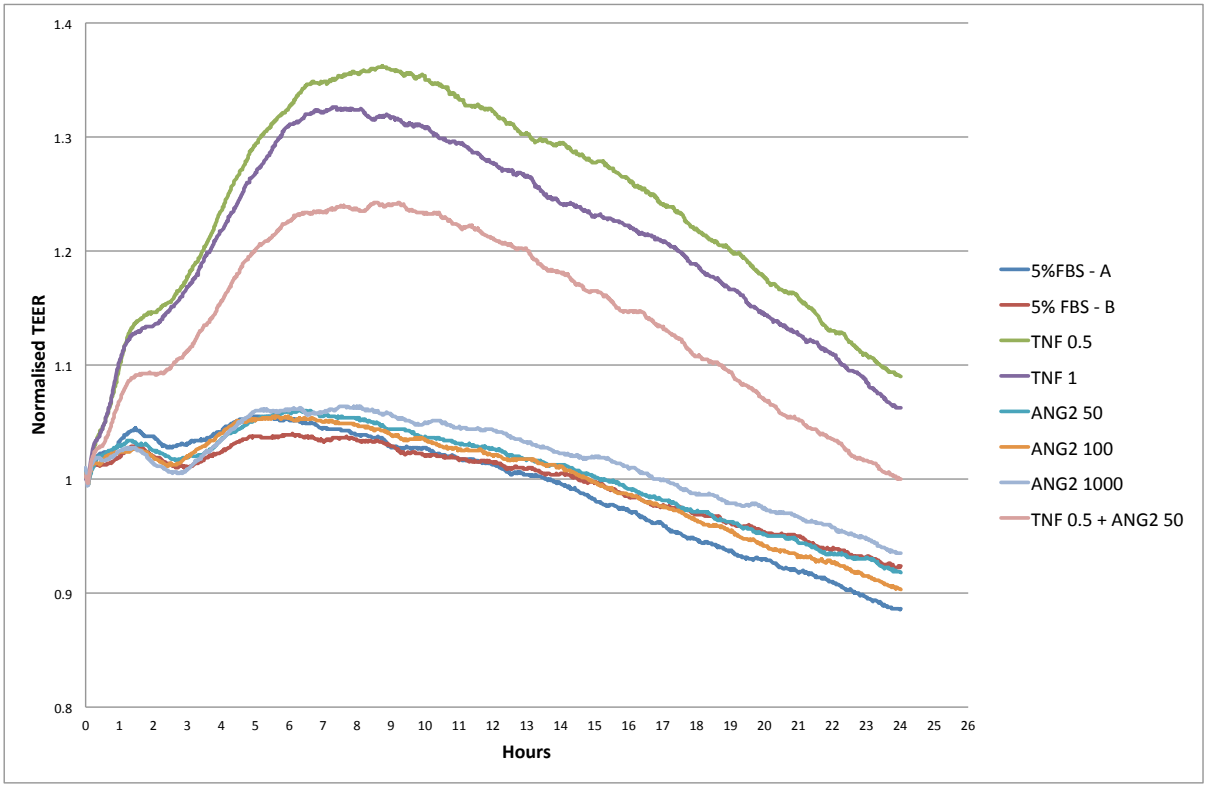

Figure 4-2. TEER of HB56 cultures exposed to different concentrations of TNF and Ang-2 measured with the ECIS

TEER values are shown as normalised resistance (subsequent values divided by initial values). There is a slow decrease in all curves over 24 hours which reflects a gradual decrease in monolayer integrity (and falling TEER). Addition of TNF dramatically increases the TEER of HB56 cell cultures, whereas Ang-2 had no effect on TEER.

Effects of PRBC on TEER

To assess the effects of PRBC on the TEER of the HB56 and the roles of TNF and Ang-2 in regard to the barrier integrity during PRBC exposure, the HB56 cultures were prepared on ECIS electrode arrays as described above. Eight different experimental permutations were performed, including four conditions with exposure to PRBC (SM, SM supplemented with 0.5 ng/ml TNF, or 50 ng/ml Ang-2 or 0.5 ng/ml TNF mixed with 50 ng/ml Ang-2) and four conditions with exposure to uninfected RBC as controls (same culture media conditions as the PRBC exposure).

As shown in Figure 4-3, prior to the addition of RBC or PRBC, the TEER of HB56 responded to TNF and Ang-2 in the same way as was seen in the previous experiment. All the cultures exposed to TNF had continuous increases in TEER, while the TEER in the cultures without TNF supplemented continuously decreased during the five-hour period of TEER monitoring. After the addition of RBC or PRBC, different TEER patterns were seen between the cultures with RBC exposure and PRBC exposure. The TEER of cultures exposed to PRBC dramatically decreased during the first one to two hours, then started to gradually increase and level off around 10 hours later. On the contrary, the TEER of cultures exposed to RBC steadily decreased from the beginning of RBC exposure to the end of the monitoring period.

It seemed that TNF had a protective effect on the change to TEER of HB56 because all the cultures with TNF had a higher TEER than cultures without TNF at the end of the experiment. However, this effect occurred prior to the addition of PRBC or RBC. When looking at the slopes of the TEER curves after the addition of RBC or PRBC, it was clear that TNF and Ang-2 actually did not have a differential effect on the TEER of HB56 culture during either PRBC or RBC co-culture. This was because the slopes of the TEER curves, which reflected the degree of changes in leakiness, were affected by RBC or PRBC addition alone, independently of TNF or Ang-2 exposure.

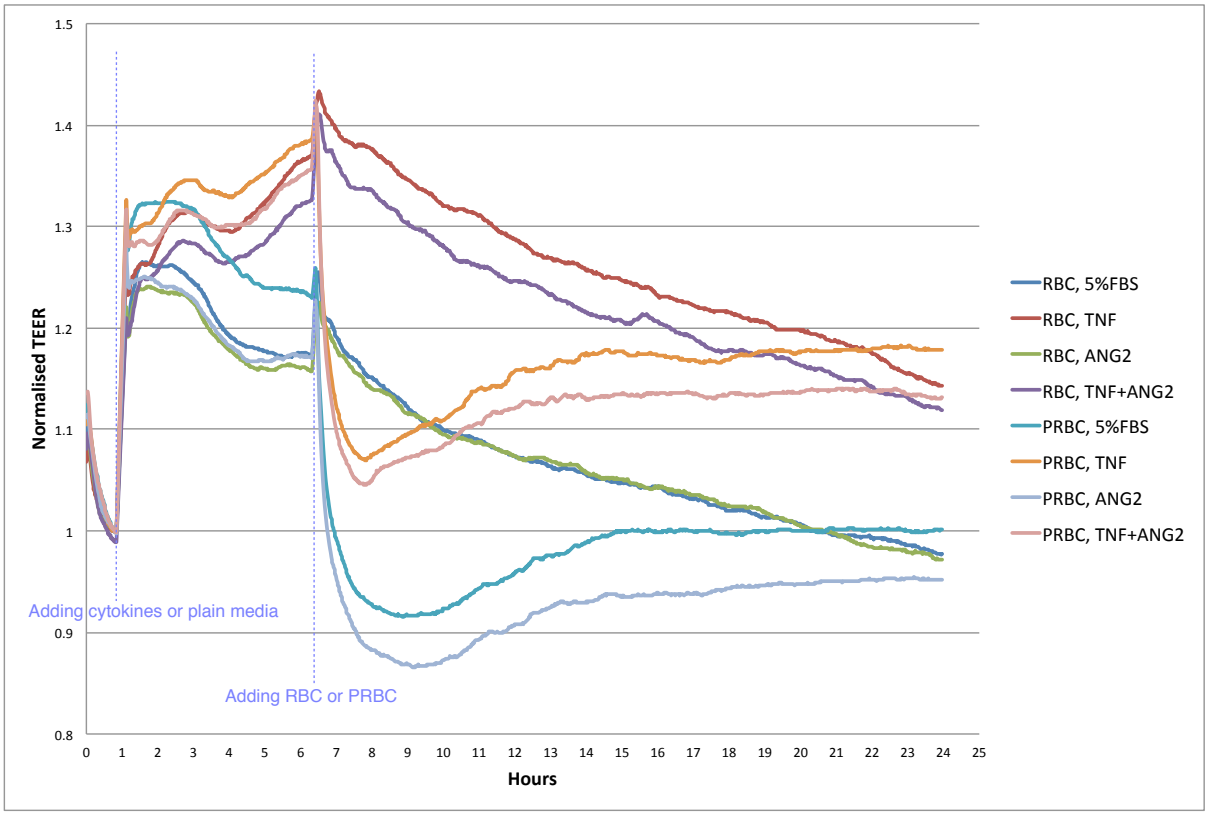

Figure 4-3. TEER of HB56 cultures measured with ECIS, following pre-treatment with TNF or Ang-2, and subsequent co-culture with PRBC or control uninfected RBCs

TEER values are shown as normalised resistance (subsequent values divided by initial values at the time of adding cytokines or plain media). PRBC, but not uninfected RBC, dramatically decreases the TEER of HB56 cultures during the first one to two hours after PRBC exposure, followed by gradually increased TEER. Both TNF and Ang-2 did not affect the TEER patterns of HB56 cultures after PRBC or RBC exposure.

Effects of hypoxia on TEER

The effects of hypoxic conditioning on the integrity of HB56 during PRBC exposure were studied using ECIS electrode arrays cultured in a hypoxic chamber. HB56 monolayers were prepared in the same manner as the previous experiment until the step in which the addition of PRBC or RBC takes place, when the ECIS electrode arrays were placed in the hypoxic chamber. The chamber was then gassed by the special gas mixture containing 1% oxygen, 4% carbon dioxide and 95% nitrogen for two minutes and remained airtight throughout the experiment. The special gas mixture went into the chamber through a valve to replace the normal air (containing approximately 20% oxygen), which was pushed to exit the chamber through the other valve. This meant the

chamber had a very low oxygen state, so as to mimic the hypoxic condition occurring during malaria parasite sequestration *in vivo*. The TEERs of all eight different experimental permutations (the same combinations as in the previous experiment under normoxia) were recorded simultaneously and continuously for 24 hours, as shown in Figure 4-4.

Under continuous hypoxic culture, all HB56 cultures with RBC showed gradually decreasing TEERs similar to TEERs in the normoxic state but declining more rapidly. This resulted in TEERs at the end of 24 hours being lower than the starting TEERs (starting with a normalised TEER of 1). However, the HB56 cultures with PRBC had dramatically and continuously decreased in TEERs for 10 hours before started to slowly decrease. This was in contrast to the same conditions without hypoxia, where TEER in response to PRBC co-culture dramatically decreased transiently for two hours and then began to return to normal. The TEERs of these cultures with PRBC did not recover over time, as seen in the normoxic state (compared with Figure 4-3). This implies that the co-culture of PRBC with HB56 under hypoxic conditions could exacerbate the leakiness in endothelial monolayers caused by PRBC co-culture alone.

Summary

In the normoxic state, before HB56 exposure to either RBC or PRBC, TNF but not Ang-2 increased the TEER of the HB56 monolayers. After exposure to either RBC or PRBC, both TNF and Ang-2 did not have a synergistic effect on the TEER of HB56. PRBC dramatically decreased TEER in the first two hours after exposure, followed by a gradual recovery to similar TEER values as RBC exposure after 10 hours. The main cause of differences in TEER at the end of the experiment was the addition of TNF, which dramatically increased the TEER of HB56 before the addition of RBC or PRBC.

Hypoxia caused the TEER of the HB56 monolayer in every experimental permutation to drop in the more extensive degree compared to the same experimental permutation in the normoxic state. Hypoxia also eliminated the ability of HB56 to regain TEER after a few hours of PRBC

exposure, as was seen in normoxic conditions. This could be seen as implying an important role for hypoxia in the reduction in BBB integrity during malarial infection.

These results were puzzling, because Ang-2 is a potent stimulator of EC activation and was expected to decrease TEER (e.g. increase monolayer 'leakiness'), as was exogenous TNF. The increase in TEER induced by TNF could reflect an adaptive response to activation, but due to the counterintuitive results I then decided to re-characterise the cell line to check its endothelial phenotype.

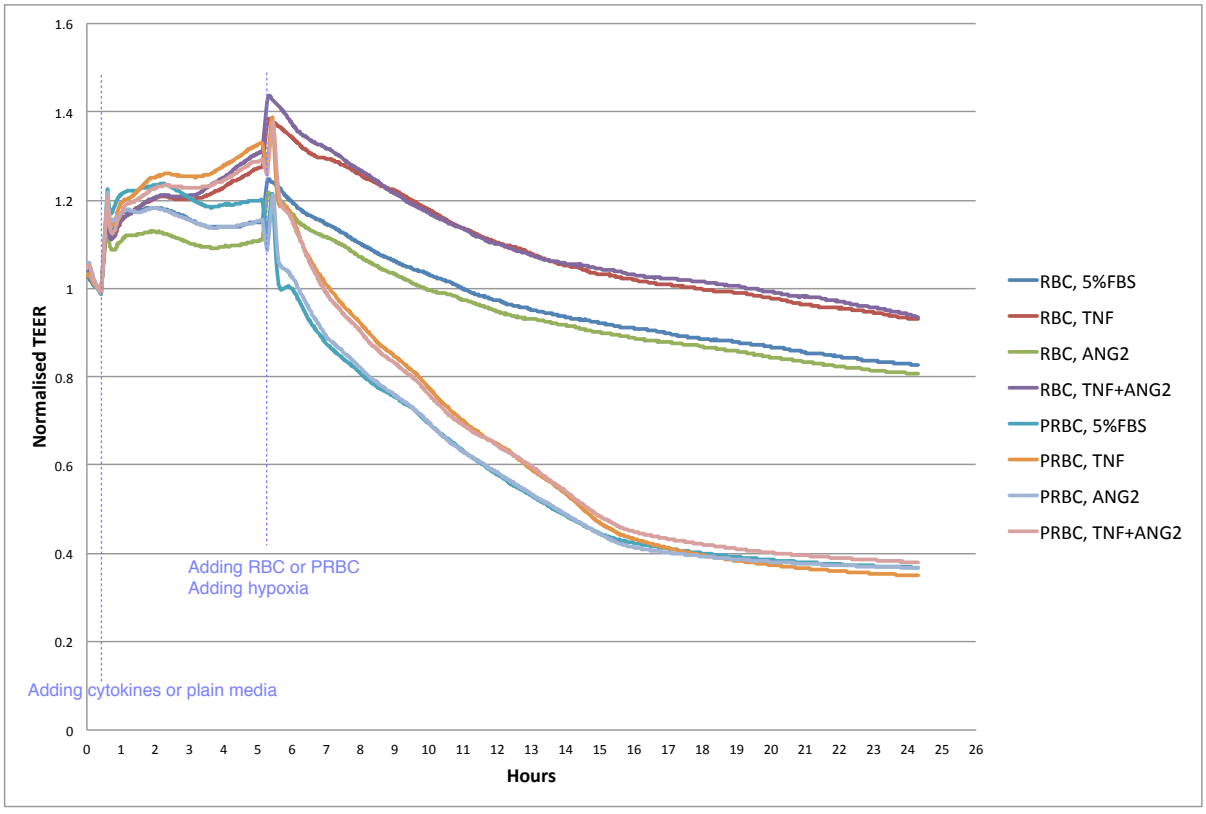

Figure 4-4. TEER of HB56 cultures measured with ECIS, following cytokine exposure and co-culture with PRBC or RBC under hypoxic conditions

TEER values are shown as normalised resistance (subsequent values divided by initial values at the time of adding cytokines or plain media). Under hypoxic conditions, HB56 exposed to PRBC loses the ability to regain TEER as seen in the normoxic condition in Figure 4-3. Overall loss of TEER is greater over 24 hours in all co-cultures with PRBC.

4.3.3 Repeat characterisation of HB56

The finding that the HBEC cultures using the HB56 cell line did not respond as expected to exogenous Ang-2 (from physiologic to severely pathologic concentrations) raised concerns over the endothelial phenotype or purity of HB56. Thus, repeat characterisation of the HB56 cell line was performed using various techniques including IHC and IF to confirm the surface phenotype of the HB56 cell line. STR analysis was also performed on HB56 and five other cell lines used in Prof. Stins' laboratory in order to investigate the likelihood that the HB56 had been misidentified or there were cross-contaminations between the different cell lines.

Surface phenotype of HB56 cell line using IHC and IF

To confirm the endothelial phenotype and rule out other possible phenotypes including epithelial, smooth muscle and astroglial derivation, IHC and IF staining were performed on 70%–80% confluent HB56 cells grown on 8-well chamber slides using a panel of endothelial-specific markers, including VWF and CD31, and non-endothelial markers, including panCK, GFAP and SMA. The procedures related to IHC and IF staining and visualisation were described in section 2.14.3. The results showed that HB56 cells did not express an EC marker (VWF and CD31), but did express the epithelial cell marker (panCK) by both IHC and IF. It was also weakly positive for GFAP staining by IF but not by IHC. The cells were negative for SMA and VWF using both IHC and IF. The IHC and IF results revealed that the HB56 cell line was not endothelial but more likely to be epithelial or astroglial in origin (Figure 4-5).

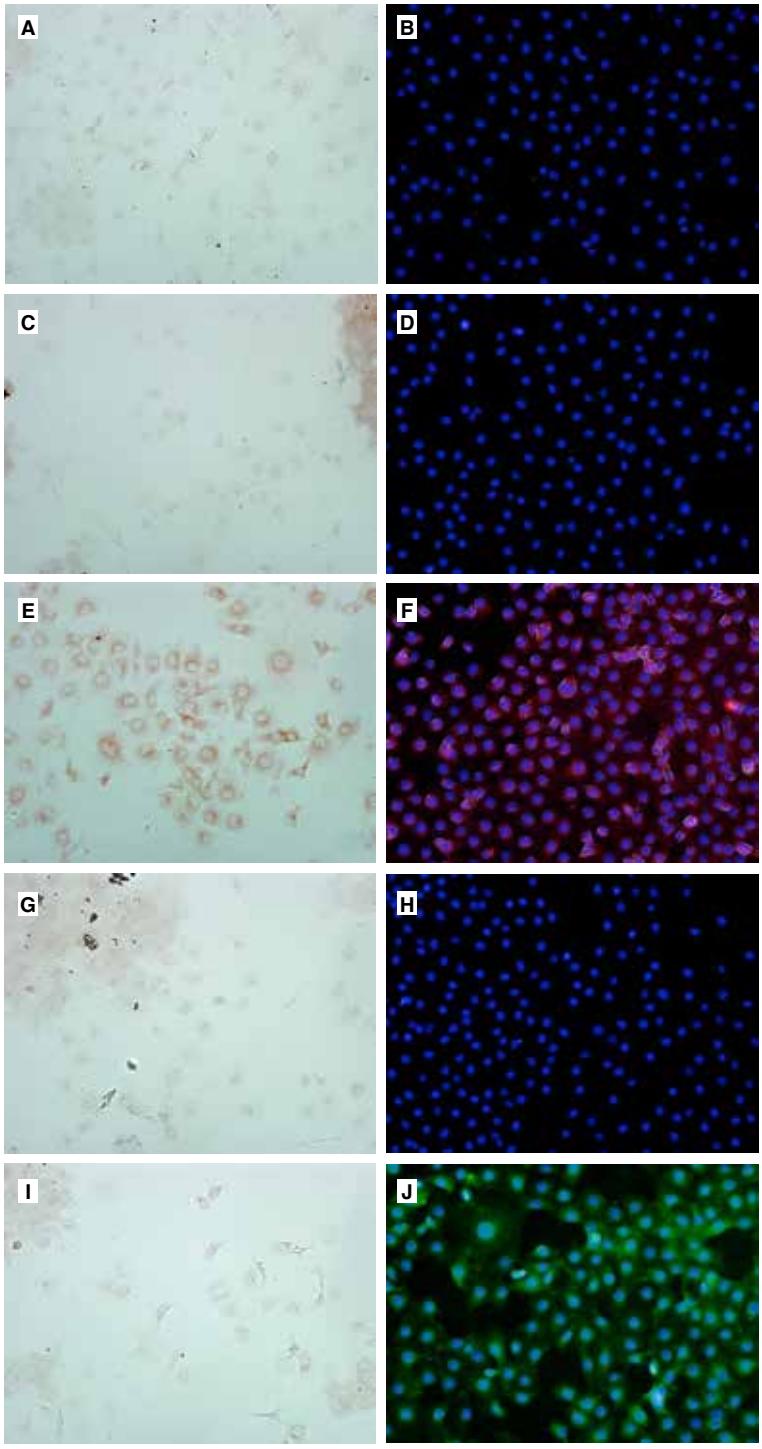

Figure 4-5. Characterisation of the HB56 cell line by immunohistochemistry (A,C,E,G,I) and IF microscopy (B,D,F,H,J)

The HB56 cells labelled with antibodies against CD31 (A and B), VWF (C and D) are negative, whereas pancytokeratin (panCK) (E and F) is strongly positive. SMA (G and H) is negative. GFAP, although negative on IHC (I), showed some staining on IF (J). Primary antibodies for CD31, panCK and SMA were labelled with Alexa Flour® 555 donkey anti-mouse IgG which emits visible orange staining. Primary antibodies for GFAP and VWF were labelled with Alexa Flour® 488 donkey anti-rabbit IgG which emits visible green staining. Nuclei were counterstained with DAPI for IF (all 200x original magnification).

STR analysis

STR loci are repetitive DNA sequences that have varying number of repeats, scattered mostly in the non-coding region of the human genome. The pleomorphism of STR can be used as a DNA fingerprint of an individual genome. A panel of primers to specific pleomorphic STR loci is used to amplify these loci by PCR. Then, the number of repeats of each STR locus is determined. In normal human DNA, STR loci generally have two alleles but there may be more than two alleles in cancer cells. STR profiling in this chapter used a panel of eight different core STR markers and a sex chromosome locus, which was identical to the panel used in the ATCC STR database to enable comparison of our data with cell lines data published in the ATCC STR database. This panel gives a one in 10^8 discrimination rate for the unique genetic fingerprint of individuals (Lins et al. 1998).

A total of six cell lines previously characterised as HBEC (i.e. HB56, HB13, HB1X, HB51, tHBEC, and HBXV) were documented to originate from the brain tissue of different donors and should therefore have different unique genotypes. However, the STR profiles of these six cell lines were identical to each other (in all nine loci examined), but different from HeLa (immortalised cervical cancer) and K562 (human immortalised myelogenous leukemia), which were used as technical controls for STR profiling (Table 4-1). This finding indicated that the six cell lines must have been cross-contaminated with the same unknown cell line in the past.

In order to identify the origin of the contaminating cell line, the STR profile generated from these cell lines was compared to STR profiles of human cell lines in ATCC STR database (http://www.atcc.org/CulturesandProducts/CellBiology/STRProfileDatabase/tabid/174/Default.aspx). The STR profile of these lines was identical to that of a cell line called ECV-304 and almost identical to the STR profile of T24 (Table 4-1). Historically, Takahasi and Sawasaki (1992) reported in 1990 that ECV304 cells originated from umbilical vein ECs by spontaneous transformation. Since then, it had been widely used as an alternative to primary HUVEC. However,

about a decade later, scientists reported that ECV304 was a derivative of T24, which was one of the best-growing bladder carcinoma cell lines developed in 1970s (Dirks et al. 1999; Drexler et al. 2002). Presumably, Takahashi's original discovery of a spontaneous transformation was therefore actually a contamination event with an immortalised carcinoma cell line. Combined, these results indicated that HB56 were not a brain EC line but had been cross-contaminated with ECV304 at some previous stage.

Table 4-1. STR profiles of six putative primary brain endothelial cell lines

Cell line	Source	AMELX	CSF1PO	D13S317	D16S539	D5S818	D7S820	TH01	TPOX	vWA
HB56	Dr. Stins	X X	12 12	12 12	9 9	10 10	10 11	6 6	8 11	17 17
HB13	Dr. Stins	X X	12 12	12 12	9 9	10 10	10 11	6 6	8 11	17 17
HB1X	Dr. Stins	X X	12 12	12 12	9 9	10 10	10 11	6 6	8 11	17 17
HB51	Dr. Stins	X X	12 12	12 12	9 9	10 10	10 11	6 6	8 11	17 17
tHBEC	Dr. Stins	X X	12 12	12 12	9 9	10 10	10 11	6 6	8 11	17 17
HBXV	Dr. Stins	X X	12 12	12 12	9 9	10 10	10 11	6 6	8 11	17 17
Hela	FAF	X X	9 10	12 13.3	9 10	11 12	8 12	7 7	8 12	16 18
K562	FAF	X X	9 10	8 8	11 12	11 12	9 11	9.3 9.3	8 9	16 16
ECV304	ATCC	X X	12 12	12 12	9 9	10 10	10 11	6 6	8 11	17 17
T24	ATCC	X X	10 12	12 12	9 9	10 12	10 11	6 6	8 11	17 17

Note: Every single number correlates to the number of nucleotide repeats for any given marker. 2 numbers in each cell represent 2 alleles for each marker. Abbreviation: FAF = Fragment Analysis Facility at Johns Hopkins University; ATCC = American Type Culture Collection, USA.

STR analysis of the cell lines HB56, HB13, HB1X, HB51, tHBEC and HBXV and two cell lines used as technical controls (Hela and K562). STR profiles of ECV304 and T24 were obtained from the ATCC STR database.

4.4 Discussion

In this chapter, I initially isolated primary HBECs from a temporal lobe brain specimen. I planned to use the newly isolated HBECs in the subsequent study of the effects of hypoxia, TNF and Ang-2 on the TEER of HBECs during PRBC exposure. However, due to their slow growth rate, the cells used in subsequent experiments on the ECIS system were switched to HB56, which was isolated and documented as HBEC by Prof. Stins' laboratory in 2007 (Tripathi et al. 2007; Tripathi et al. 2009).

The ECIS system from Applied Biophysics is one of several technologies used to measure TEER non-invasively in real time. Confluent monolayers of HBECs present a high TEER, which is a characteristic of brain-specific ECs due to their specialised tight and adherence junctions causing a high resistance in brain EC monolayers, compared to other types of cultured endothelium (Bernas et al. 2010; Hatherell et al. 2011). Monitoring the TEER of the HBECs using the ECIS system enables simultaneously direct evaluation of several different experimental conditions that may affect the tightness or leakiness of the barrier. Applying PRBCs and hypoxic conditions at the same time on HBEC cultures in the ECIS system, as conducted in this chapter, was a novel approach to examining BBB integrity during malarial infection and had not been attempted before. However, this *in vitro* model is still far from a perfect imitation of the *in vivo* situation because the BBB is much more complex than single brain endothelium monolayers. Recent publications have emphasised the complex interactions between brain endothelium, astrocytes, neurons and extracellular matrix in the establishment, maintenance and regulation of BBB function (reviewed in Abbott et al. 2006).

A growing number of *in vitro* models of the BBB have been investigated, most of which use murine or porcine brain ECs and rat astrocytes in co-cultivation conditions across a physical matrix or Transwell insert system (Balbuena et al. 2010). In consequence, although the co-cultivation of brain ECs with astrocytes comes closer to mimicking the *in vivo* situation, it is difficult to extrapolate results from these non-human-cell-based experiments to the human *in vivo* situation. Multi-cultivation models for BBB using purely human cells have been investigated by a few researchers but are expensive to establish and difficult to maintain. Hatherell et al. (2011) constructed an *in vitro* human BBB model using tri-cultivation of human-derived brain ECs, astrocytes and pericytes in a three-dimensional configuration based on the use of artificial porous membranes. This model, so far the most advanced human-derived BBB model, could be explored to examine the application in CM research.

As detailed in section 1.6, Ang-2, which acts as an autocrine dynamic regulator of the rapid adaptive response of endothelium, can destabilise a quiescent endothelium and sensitise endothelial response to inflammatory and angiogenic cytokines such as IL-1, VEGF and TNF (Fiedler and Augustin 2006). The work in this chapter was designed to investigate the effects of TNF and Ang-2 on the resistance of HBECs under exogenous stimuli, including PRBC and hypoxia. I hypothesised that TNF and Ang-2 would individually decrease the TEER of HBECs and that TNF and Ang-2 would synergistically affect the HBECs. I also hypothesised that, during the *in vivo* CM situation when PRBC sequestration in the microvasculature of the brain causes some degree of hypoxia in the surrounding brain tissue, TNF and Ang-2 were contributing factors to further brain tissue damage as a result of decreasing BBB integrity.

Different concentrations of exogenous recombinant TNF and Ang-2 were investigated, ranging from physiologic to pathologic levels (based on previous studies) in order to ensure the complete coverage of possible TEER responses. I also collected supernatant and purified total mRNA from the ECs, planning further investigations of soluble markers for endothelial activation by ELISA and gene expression profile by microarray. However, because HB56 was subsequently shown not to be an EC line HBEC, in the end these experiments were not carried out.

The misidentification and cross-contamination of cell lines has been a widespread problem in the research community for over 50 years. It is estimated that 15%–36% of research papers reported the use of cell lines that had been misidentified or cross-contaminated (Drexler et al. 2003; M. Zhao et al. 2011). There were several classic examples of the use of misidentified cell lines which were cross-contaminated and overtaken by faster-growing cell lines. For example, widely used cell lines cross-contaminated with HeLa cervical cancer cells included Int-407 (described as "non-transformed intestinal epithelial cells"), WISH (described as "non-transformed amniotic epithelial cells") and Chang liver (described as "normal liver cells"). ECV304 is another classic example. It was initially described as a "spontaneously transformed human umbilical vein endothelial cell

line", but later confirmed as a derivative of the T24 bladder cancer cell. It is intriguing that ECV304 has continued to be used as a model of ECs in peer-reviewed journals despite the demonstration that ECV304 did not originate from EC by groups of scientists more than 10 years ago (Dirks et al. 1999; Drexler et al. 2002) (Figure 4-6).

One way to avoid this problem would have been to validate the authenticity of the cell lines by performing more careful IHC and STR characterisation initially, as recommended by ATCC Standards Development Organization Workgroup ASN-0002 (2010). Despite the failure of the work, the experimental methods and development of a 'home-made' hypoxic chamber will be applied in a repeat of this study to a commercially sourced HBEC line following the completion of my thesis. The question of whether hypoxia synergistically alters BBB function in addition to exogenous factors such as the Ang-Tie-2 pathway certainly remains an interesting potential pathophysiological factor in CM.

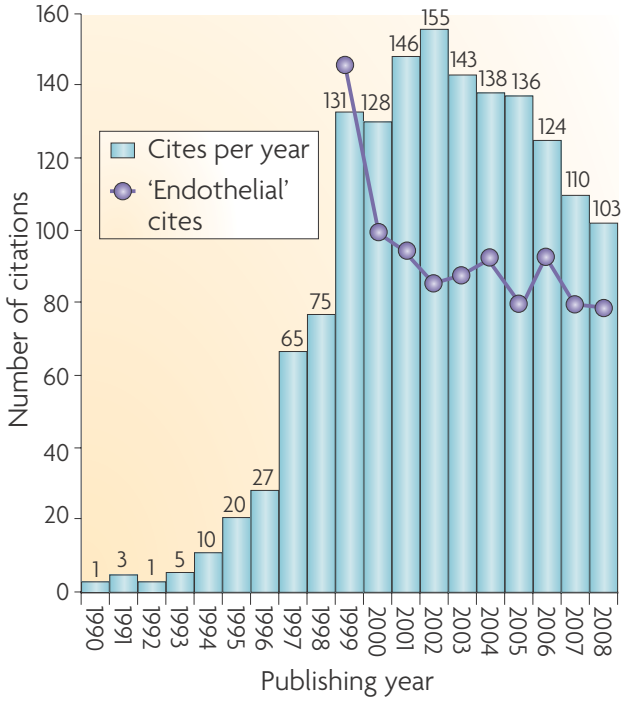

Figure 4-6. Number of citations of T24 bladder cancer cells in publications from 1990 to 2008 and number of citations of T24 referred to as normal endothelial cells

(From: ATCC Standards Development Organization Workgroup ASN-002, *Nature Reviews Cancer*. p 441. Vol. 10. June 2005)

Chapter 5

A Study of miRNA Expression in the Kidney in Patients with MARF

5.1 Introduction

5.1.1 Aims

The aims of the work in this chapter are: 1) to examine the miRNA expression profile in the kidney of adult patients with MARF; 2) to validate the approach of extracting miRNA from FFPE tissues; and 3) to identify new biological pathways that could potentially be involved in the pathophysiology of ARF/AKI in severe malaria.

Because access to fresh human tissue from cases of malarial infection is limited, my initial aim was to develop a protocol to isolate high-quality miRNAs from archival FFPE tissue (some of which was almost 20 years old) in the brain and kidney. This was successful in archival FFPE kidney tissue and subsequently used in microarray experiments. Target prediction and pathway analysis were done and the findings represent the first miRNA study in human malaria, which should contribute to our understanding of the pathophysiology of renal failure in severe malaria at post-transcriptional regulation level.

Because the previous work on Ang-Tie-2 expression in the brain had shown no specific association with coma in CM cases, but some relationship with acidosis, I also looked specifically at miRNAs which might target genes of the Ang-Tie-2 pathway in the kidney. Novel miRNAs targeting Ang-1 (ANGPT1) and Tie-2 (TEK) genes were also identified for the first time. I then

validated the results of miRNA extraction from tissues of MARF patients by luciferase reporter assays, to prove that the putative miRNAs identified in patients bound to and altered expression of the Ang genes *in vitro*.

5.2 Materials and methods

5.2.1 Malaria and non-malaria cases

A total of 25 cases were included in this study, with 16 of the 25 being fatal severe malaria cases from the AQ trial (see section 2.1.1 for details of the AQ trial). These cases were defined as suffering from MARF or non-ARF (NARF) on the basis of clinical, biochemical and histological features, as detailed in previous studies (Day et al. 2000; Nguansangiam et al. 2007). Nine out of 25 were normal controls selected from the Bangkok autopsy series as detailed section 6.2.2. This was a heterogeneous group, but on the basis of medical history and autopsy histology they had no malarial infection and had other definitive causes of death, including acute myocardial infarction, hypovolemic shock and electrocution. Their clinical and pathological details are summarised in Table 6-2. Control and malaria cases were matched as far as possible for variables including post-mortem interval, age, sex and ethnic, in order to eliminate confounding factors affecting gene expression patterns, so that observed differences in miRNA expression were due to malarial infection.

5.2.2 Kidney specimens

miRNA was isolated from 25 archival FFPE blocks of kidneys (16 malaria patients and nine controls). These kidneys were collected at autopsy within 24 hours, fixed in 10% buffered formalin, and processed using standard methods.

5.2.3 Optimisation of miRNA isolation from FFPE tissue

Tissue quality concerns

The blocks of malaria cases used were archival FFPE human kidney from the AQ trial, conducted during 1991 to 1995 (Hien et al. 1996). This presented a technical challenge in terms of the determining the quality of miRNA extracted from these aged tissues. However, compared to mRNA, miRNAs are more robust and well preserved in FFPE tissue, as previously discussed in section 1.10.2. Moreover, in an experimental study of the correlation of RIN value and miRNA degradation, the levels of miRNA expression remain virtually unchanged from samples with the highest RIN (near 10) to the lowest RIN (lower than one) (Jung et al. 2010). Thus, various changes to standard protocols were attempted to optimise miRNA isolation procedures for FFPE tissue and then validated using qRT-PCR and miRNA array protocols for RNA samples extracted from archival autopsy samples.

miRNA extraction

A commercially available RNA isolation kit for FFPE tissue, RecoverAll (Ambion), was used as a starting point for the optimisation of RNA isolation. This kit was designed to extract the total nucleic acids from FFPE tissue, including DNA, RNA and miRNA. Attempts to isolate miRNAs from the brain FFPE blocks were unsuccessful despite extensive protocol adjustments. The quality and the yield from this set of brain tissues were not high enough to be used in a microarray platform (data not shown). In contrast, the kidney FFPE blocks from the same AQ trial gave much higher miRNA quality; although both the brain and kidney blocks were collected, processed and stored in the same conditions. This is possibly because of the higher cellular content of the kidney tissue compared to the brain, or the longer period in formalin fixation of the brain (up to six weeks before whole brain cutting), which might be harmful to the RNA in the tissue. The optimised protocol for RNA isolation from FFPE tissue was detailed in section 2.5.

Validation of the presence of miRNA transcripts by quantitative real-time PCR

In order to initially verify the presence of miRNA in the isolated RNA samples, approximately 500 ng of total RNA from two samples (the kidney from two malaria patients) were reverse-transcribed using the TaqMan MicroRNA Reverse Transcription kit (Applied Biosystems, UK) and cDNA amplified using specific primers provided in the TaqMan MicroRNA Assay kit, according to the manufacturer's instructions. Then, the qRT-PCR measurements were carried out on the LightCycler 480 real-time PCR machine (Roche Diagnostics, UK) in a 96-well plate with runs up to 45 cycles. TaqMan MicroRNA Assays (Applied Biosystems, UK) were used to measure the following miRNAs: hsa-miR-210 and has-miR-16, and a small nuclear RNA (snRNA) RNU6B. Each sample was run in triplicate and mean values for the cycle threshold (Ct) were used for calculations. The data indicated that miR-16, miR-210 and RNU6B were detectable in both samples. Thus, the miRNA isolated from the archival FFPE kidney blocks using the optimised RNA isolation protocol as previously described should be good enough for subsequent microarray experiments.

Table 5-1. Quantitative RT-PCR data obtained for miRNAs in two archival FFPE kidney samples.

Sample	MicroRNA	Average Ct	Std Dev
Kidney 1	RNU6B	37.37	0.24
	miR-16	34.01	0.08
	miR-210	35.94	0.14
Kidney 2	RNU6B	38.89	0.96
	miR-16	32.71	0.14
	miR-210	34.71	0.14

This validation experiment used qRT-PCR to examine the presence of miRNA in two archival FFPE kidney samples. Results show average Ct values and standard deviation (Std Dev) of the Ct from three technical replicates for RNU6B, miR-16 and miR-210.

5.2.4 miRNA expression profiling

The miRNA profiles of the kidney specimens from malaria (n = 16) and non-malaria (control, n = 9) were generated using Affymetrix GeneChip miRNA Array version 1, which provides complete coverage of the human miRNA listed on the Sanger miRBase database release 11.0 (April 2008). The microarray hybridisation, scanning and data processing were done as described in section 2.8.

5.2.5 Validation and quality control of Affymetrix GeneChip miRNA Array

To ensure the quality and integrity of the microarray expression results, several quality-control procedures were performed. RNA spike control oligos, consisting of five different oligos, were added into the purified RNA sample prior to FlashTag labelling (poly A tailing). Signal intensity plots of these oligos were then generated and inspected in Affymetrix miRNA QC Tool software v.1.0.33.0 to confirm poly A tailing and ligations steps and to detect the presence of RNases or reaction inhibitors within the isolated RNA samples (Figure 5-1). Samples demonstrating a low detectable signal of one of the spike control oligos (mean intensity of less than 1000) would be excluded from the microarray experiment; however, all 25 samples used in the GeneChip microarrays (16 malaria and nine control kidneys) did not have this problem and all were included in the experiment for further data analysis.

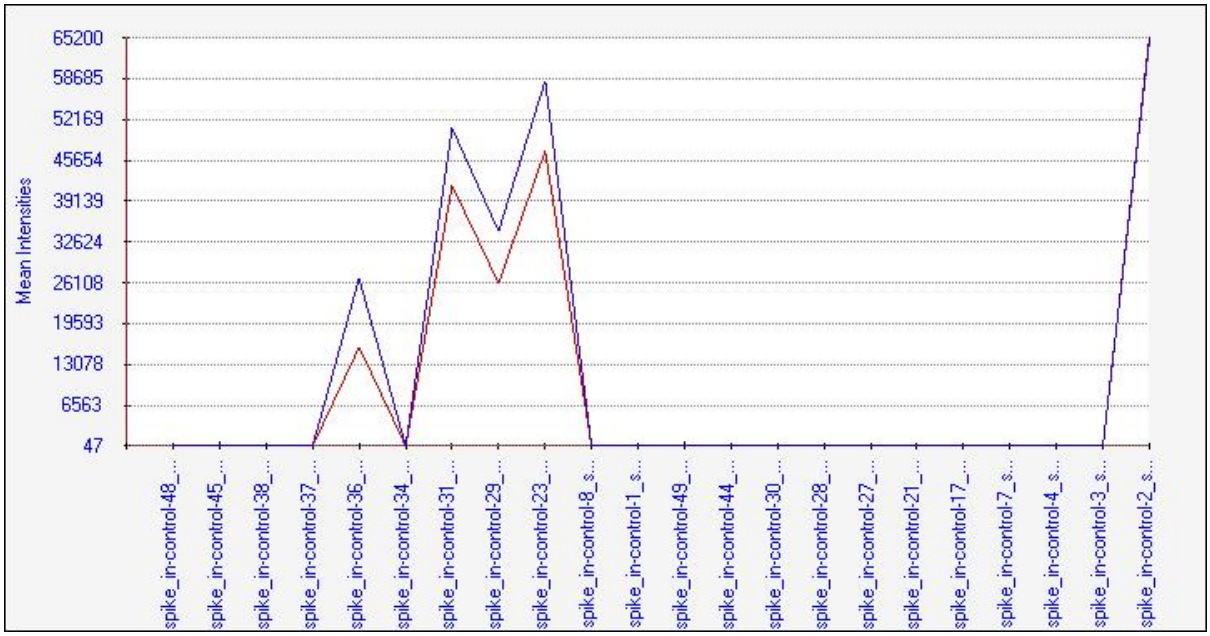

Figure 5-1. Quality-control panel from Affymetrix GeneChip miRNA microarray

Examples of good-quality spike control oligo panels of two microarray chips using miRNA isolated from two different FFPE kidneys with high signal-background ratio in all five internal control probe sets (spike control oligos 36, 31, 29, 23 and 2), which was added into the RNA samples prior to microarray hybridisation. The vertical axis represents mean intensities of sequence-specific probe sets for each transcript (average of four probes per one transcript).

5.3 Results

5.3.1 Overview of the miRNA expression data

The complete human miRNA profile (miRBase release 11.0, April 2008, n = 847) of kidneys from malaria samples (n = 16) and non-malaria samples (control, n = 9) was generated using Affymetrix GeneChip miRNA Array version 1. The expression of 842 human miRNAs was determined to be detectable in at least one sample, either in malarial or non-malarial kidney, by our analysis pipeline (on the basis of "detected above background" in Affymetrix miRNA QC Tool software).

A total of 840 miRNAs were present in at least one malaria sample and 801 miRNAs were present in at least one control sample. The Venn diagram in Figure 5-2A shows that 41 miRNAs were present only in the malaria group but not in Control and that two miRNAs were present

only in Control but absent in malaria cases. Most of the miRNAs were detectable in both malaria and Control.

A total of 235 miRNAs were present in all 16 malaria samples and 311 miRNAs were present in all nine control samples. The Venn diagram generated from these lists (Figure 5-2B) shows that 40 miRNAs were present in the malaria group only but absent in the control group, and that 116 miRNAs were present in the control group only but absent in malaria.

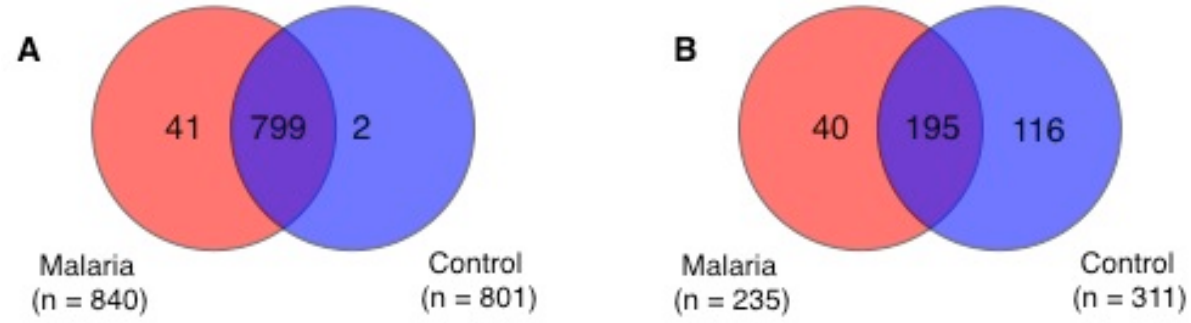

Figure 5-2. Venn diagram of miRNAs present in (A) at least one sample in either clinical group, (B) in 100% of the samples in either clinical group.

Unsupervised cluster analysis

In order to interpret these results, an unsupervised cluster analysis of the miRNA expression data was performed, using a hierarchical clustering algorithm with a Euclidean distance measure and the average linkage rule in GeneSpring GX version 11.5. Unsupervised clustering is an exploratory technique that allows the data to organise itself without prior knowledge of clinical information or sample labelling. This approach is used to understand the whole dataset and help with visualisation, without making assumptions about the underlying clinical groups. Similar genes and similar conditions in the dataset are reordered next to each other. This analysis revealed that malaria samples showed a miRNA expression profile significantly distinct from controls. However, the cluster analysis could not find any distinct miRNA expression pattern associated with MARF (Figure 5-3) compared to NARF cases.

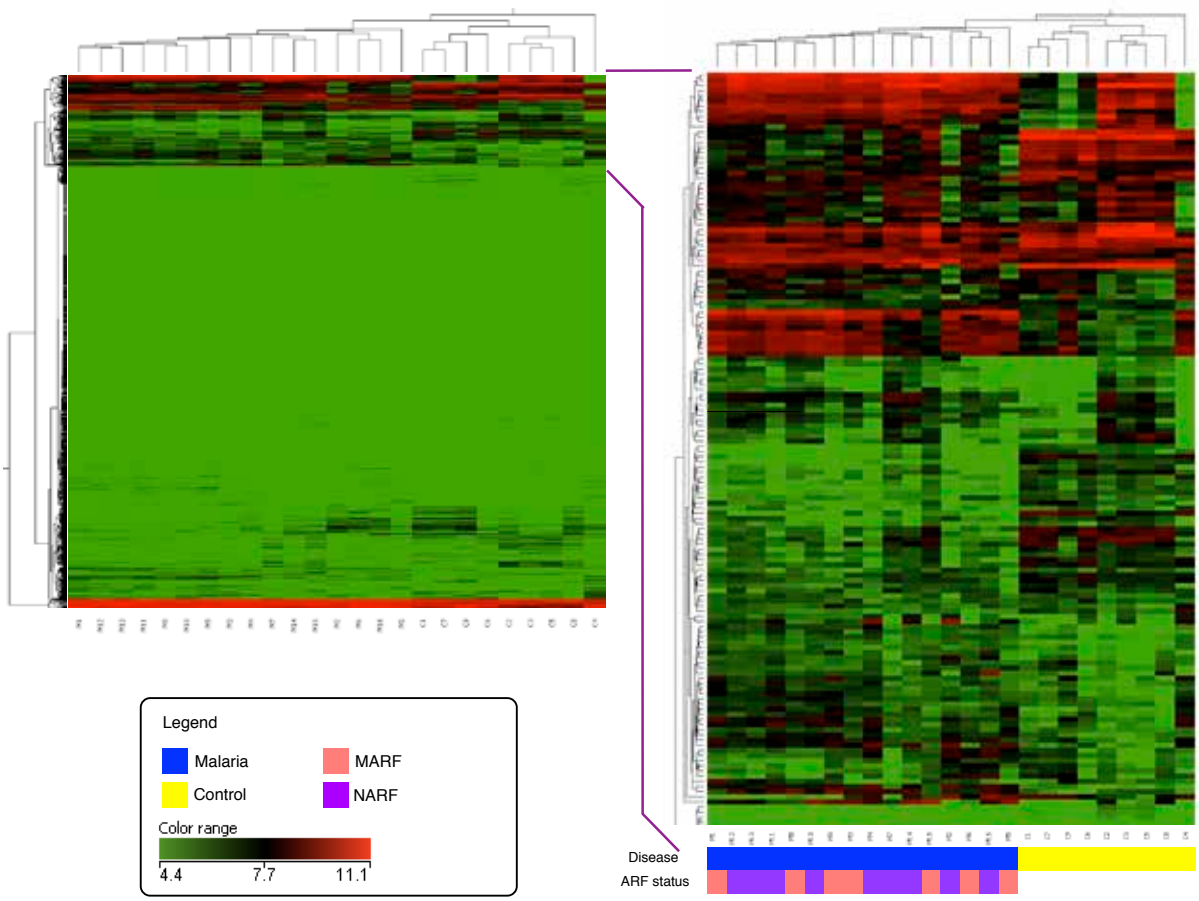

Figure 5-3. Unsupervised hierarchical cluster analysis of total miRNA transcript expression data from the kidney of malaria (n = 16) and control (n = 9) samples

This heatmap shows that malaria samples distinctly clustered from control samples but MARF cases did not cluster distinctly from malaria with non-ARF.

Differential expression analysis of malaria vs. control

A total of 200 distinct miRNAs were differentially expressed in malaria samples compared to controls - adjusted $P < 0.05$, T-test with Benjamini-Hochberg's control for false discovery rate (FDR) (Benjamini and Hochberg 1995). 157 of these miRNAs were dysregulated more than twofold. Of these, 75 were up- and 82 were down-regulated in malaria compared to controls (a full list of these miRNAs is shown in Appendix B, Table B-1 and B-2.

MiRNAs that were significantly up- and down- regulated more than fourfold (Table 5-2) were selected and used for cluster analysis (Euclidian distance measure and complete linkage rule),

distinguishing malaria and control samples. These highest deregulated miRNAs were also used for the class-prediction model by the leave-one-out cross-validation Support Vector Machine algorithm, which provided 100% accuracy in predicting control samples and 93.75% accuracy in predicting malaria samples (overall accuracy = 96%).

Table 5-2. List of the 24 most up- and 23 most down- regulated miRNAs differentially expressed in malaria cases compared to controls (adjusted *P*-value cutoff of 0.05 and fold-change cutoff of 4)

Up-regulated miRNA	Fold change	Adjusted *P*-value
hsa-let-7a-2 // hsa-let-7a-3 // hsa-let-7a-1	8.362	0.000925
hsa-let-7d	4.609	0.000105
hsa-let-7e	5.752	0.002466
hsa-let-7g	4.133	0.014879
hsa-let-7i	5.564	0.000775
hsa-let-7f-1 // hsa-let-7f-2	4.823	0.021928
hsa-miR-16-1 // hsa-miR-16-2	4.194	0.032156
hsa-miR-17	4.894	0.016456
hsa-miR-20a	5.336	0.019494
hsa-miR-106a	4.763	0.010701
hsa-miR-103-2 // hsa-miR-103-1	4.336	0.022438
hsa-miR-296-3p	4.824	0.000006
hsa-miR-371	7.817	0.000005
hsa-miR-509-2 // hsa-miR-509-3 // hsa-miR-509-1	15.331	0.001214
hsa-miR-572	8.713	0.000003
hsa-miR-659	4.046	0.000046
hsa-miR-886	5.660	0.000065
hsa-miR-760	4.270	0.000377
hsa-miR-939	4.523	0.000242
hsa-miR-940	4.389	0.002349
hsa-miR-1268	4.904	0.000005
hsa-miR-1281	4.454	0.000925
hsa-miR-1308	9.761	0.000002
hsa-miR-373*	4.459	0.001050

Down-regulated miRNA	Fold change	Adjusted *P*-value
hsa-miR-19b-1 // hsa-miR-19b-2	-6.015	0.000022
hsa-miR-22	-6.239	0.000046
hsa-miR-28-3p	-6.141	0.000274
hsa-miR-100	-4.928	0.000056
hsa-miR-99b	-5.705	0.000011
hsa-miR-30d	-5.408	0.000081
hsa-miR-10a	-4.699	0.002099
hsa-miR-10b	-5.446	0.000438
hsa-miR-125b-1 // hsa-miR-125b-2	-12.077	0.000000
hsa-miR-145	-5.767	0.000588
hsa-miR-125a	-4.668	0.000017
hsa-miR-127-3p	-5.829	0.000180
hsa-miR-151-3p	-12.817	0.000002
hsa-miR-339	-4.288	0.000173
hsa-miR-422a	-4.063	0.000062
hsa-miR-486	-13.071	0.000005
hsa-miR-494	-4.028	0.016752
hsa-miR-193b	-9.167	0.000000
hsa-miR-500	-5.670	0.000765
hsa-miR-501	-9.653	0.000004
hsa-miR-576-3p	-4.653	0.030753
hsa-miR-606	-4.441	0.006846
hsa-miR-1826	-11.248	0.000006

5.3.2 Overview of the miRNA expression data generated in malaria samples (8 MARF vs. 8 NARF)

In order to examine whether there were miRNAs associated with ARF/AKI within the malaria group (n= 16), a separate analysis was performed comparing MARF samples (n = 8) with NARF samples (n = 8). Filtering the expression signals showed that a total of 304 miRNAs were present in all MARF cases and 284 miRNAs were present in all NARF cases. A Venn diagram (Figure 5-4) generated from these two lists revealed that 69 miRNAs were present in MARF but absent in NARF and that 49 miRNAs were present in non-MARF but absent in MARF. Most miRNAs (n = 235) were present in both clinical groups.

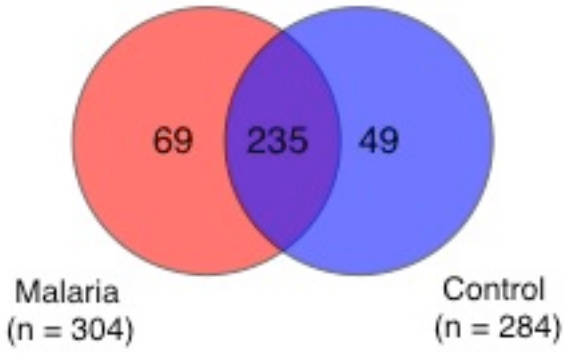

Figure 5-4. Venn diagram of miRNAs present in 100% of the samples in either clinical group, showing their segregation between MARF and NARF groups

Differential expression analysis of MARF vs. NARF

Despite the different profiles of miRNA, statistical comparison showed no overall differential expression between MARF and NARF cases (using a cutoff of adjusted $P < 0.05$, T-test with Benjamini-Hochberg's control for FDR). However, there were five miRNAs that had at least a twofold difference in the expression value, two of which were up-regulated (miR-923 and miR-1826) and three of which were down-regulated (miR-31, miR-296-5p and miR-1249) in MARF compared to NARF cases (Figure 5-5). These five miRNAs represent a novel miRNA profile associated with renal diseases in human malaria.

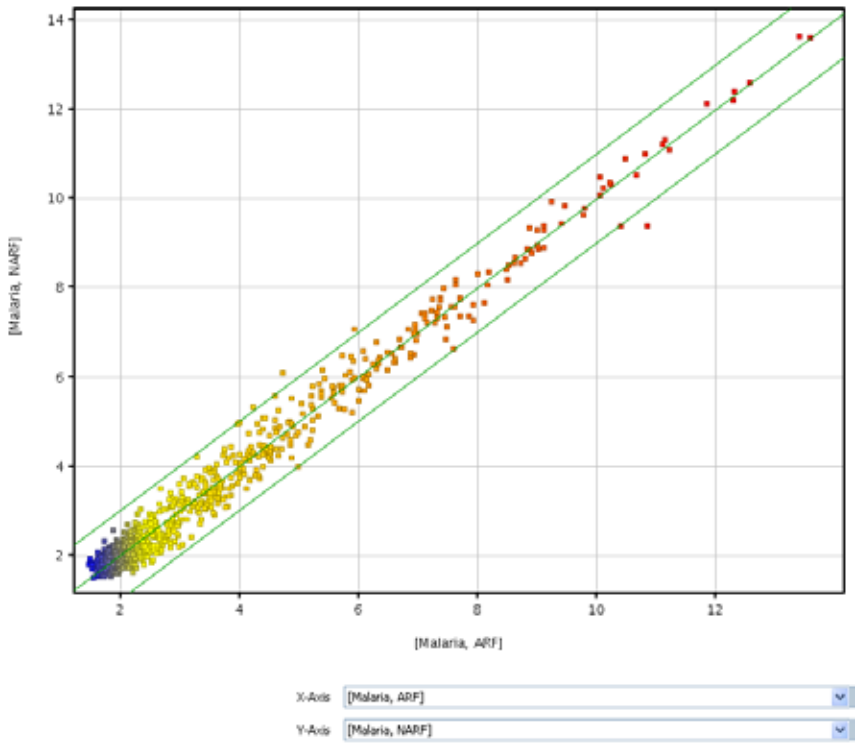

Figure 5-5. Scatter plot of averaged normalised expression values between MARF (x-axis) and NARF (y-axis) The parallel green lines represent the twofold threshold. Each dot represents the level of a single miRNA. Five miRNAs were located outside this threshold, indicating they were more than twofold dysregulated in expression. No overall statistically significant differential expression was shown over the whole miRNA sample between MARF and NARF groups.

5.3.3 Validation of the miRNA expression analysis results using qRT-PCR

Gene expression profiling using microarrays has become the method of choice for translational research because it allows the study of a large number of genomic transcripts in parallel on one chip. However, many factors, from specimen-collection procedure to microarray technique, can influence the quality of the results. Fastidious microarray protocols often lead to false positive discoveries. Thus, the validation of expression differences is usually achieved using an independent technique such as a Northern blot, or qRT-PCR is the more widely used technique for microarray validation because the other techniques require a considerably larger amount of RNA and are time consuming and labour intensive (Rajeevan et al. 2001). Put simply, if the miRNA extracted from the tissue can be amplified using PCR, and the array result (up- or down-regulation and the

amount of change) is independently confirmed by PCR, then the result from the array is more likely to be real.

Selection of miRNA transcripts for validation

Because of the large number of individual miRNA levels generated in an array approach, it is usual to select a subpopulation of these to validate the microarray results. Various ways exist to decide which transcripts should be chosen for validation, either non-randomly selection (e.g. the greatest fold changes) or random selection. It has been suggested in previous studies that random or stratified-random sampling is a better gene selection method because it provides richer generalisation about the microarray experiment and can provide a quality index for subsequent cross-study analysis (Miron et al. 2006). Thus, to validate the miRNA expression profile generated from this microarray experiment, a random sampling approach was chosen for microarray result validation. Nine randomly selected miRNAs (let-7g, miR-16, miR-19b, miR-99a, miR-214, miR-500, miR-624, miR-744, miR-886-5p) were measured by qRT-PCR in all malaria and control samples.

Selection of endogenous gene controls for qRT-PCR normalisation

The selection of an endogenous control that is highly abundant and stably expressed across the test sample set is extremely important to ensure accurate qRT-PCR results. It is known that the quantification error in qRT-PCR is caused by several factors, including sample-to-sample variation, RNA integrity variation, differences in amount of starting material and reverse transcription efficiency. Currently, the most accurate method to eliminate these biases is the relative gene expression technique which utilises the normalisation of target gene expression levels to endogenous control genes. However, in miRNA experiments, there is no universal endogenous control that is suitable for every tissue type or disease. Thus, it is crucial to test for the most suitable endogenous control genes in each individual experiment.

The most suitable endogenous control genes were identified from microarray data through statistical analysis using GeneSpring GX v11.5 and Normfinder algorithms (Vandesompele et al. 2002). In brief, microarray data from all malaria and control samples were analysed in GeneSpring GX. The data were filtered in every sample on a normalised expression level (upper limit = 95 percentile, lower limit = 75 percentile) to obtain a stably expressed gene list across all 25 samples (Figure 5-6). This procedure generated 34 normalisation gene candidates, including 29 snRNAs and five miRNAs, which were further analysed using Normfinder (Microsoft Excel applets).

Normfinder showed that snRNA U104 was the most stable transcript (stability value = 0.024, the lower the more stable) and that a combination of U26 and snRNA ACA7 gave the highest stability (stability value = 0.019). Table 5-3 shows 20 most stable endogenous gene candidates, according to Normfinder. However, these candidates could not be used in the qRT-PCR testing because Megaplex™ primer pool and TaqMan Assay did not support these transcripts. So, I selected other endogenous gene candidates including RNU6B, RNU44, RNU48, miR-16 and miR-26b, which have been widely used as endogenous controls in previously published publications and supported by the laboratory system I was using.

Validation results from qRT-PCR were consistent with the microarray results

The result from the microarray was validated by measuring the expression values of the nine randomly selected miRNAs by qRT-PCR. The comparison of the results from both microarray and qRT-PCR revealed that data from both platforms were in agreement, confirming that the data generated from the microarray experiment were reliable and reproducible (Figure 5-7).

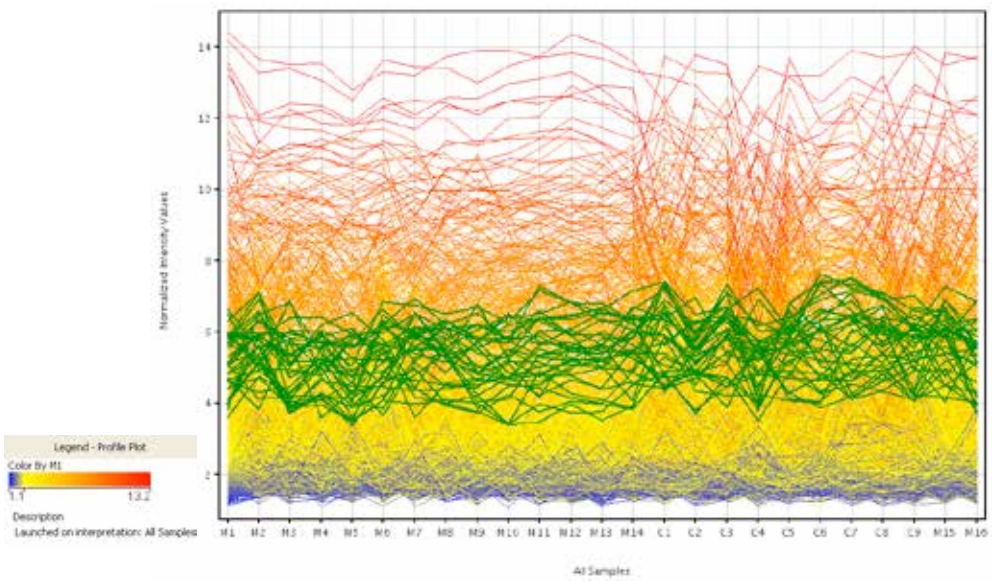

Figure 5-6. Expression intensity of all human 1769 transcripts, including miRNAs, snRNAs and scaRNAs, across all 25 samples (15 malaria and nine controls)

The highlighted green lines are 34 transcripts (normalisation gene candidates) that were filtered on normalised expression values between the 75th and 95th percentile in order to find endogenous control gene candidates that were stably expressed in all samples. The list of 34 normalisation gene candidates generated at this step was then analysed in NormFinder.

Table 5-3. List of the 20 most stable endogenous control gene candidates from the microarray data, analysed using Normfinder

Rank	Gene Symbol	Stability Value
1	U104	0.024
2	U17a	0.037
3	U8	0.039
4	ACA57	0.039
5	ACA31	0.048
6	ACA61	0.053
7	hsa-miR-1180	0.054
8	U59A	0.055
9	U26	0.058
10	ACA21	0.059
11	ACA7	0.060
12	hsa-miR-130a	0.061
13	U75	0.069
14	ACA54	0.069
15	ENSG00000207516	0.079
16	E3	0.084
17	HBII-419	0.085
18	hsa-miR-30c-2-Star	0.085
19	U63	0.086
20	HBII-210	0.086

Best gene	U104
Stability value	0.024
Best combination of two genes	U26 and ACA7
Stability value for best combination of two genes	0.019

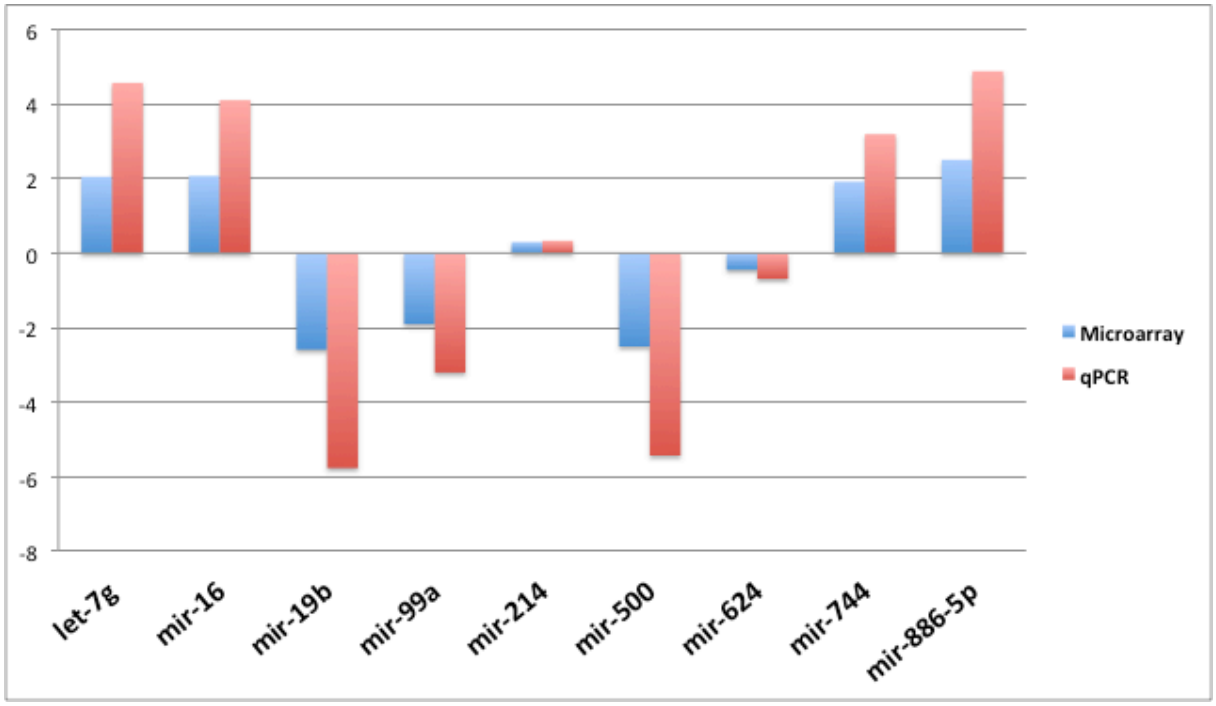

Figure 5-7. A comparison of the microarray data and qRT-PCR results, for the validation of the miRNA microarray results using qRT-PCR

Nine miRNAs were randomly selected and amplified using qRT-PCR. The height of the columns in the chart represents the log2 ratio of averaged fold-change (malaria/control) in expression across 16 malaria and nine control patients. The result indicates that the results of the microarray were in agreement with the qRT-PCR results, in terms of up- or down-regulation and approximate fold changes in expression.

5.3.4 Pathway analysis of differentially expressed miRNAs targets

Following the identification of a list of miRNAs from differential expression analysis, a further pathway analysis was performed. This is the process that maps a list of genes to known pathways and determine which pathways are over-represented in the given gene list. This approach transcribes massive amounts of gene expression data into more biologically meaningful results – into sets of known biological pathways. In this study, pathway analysis was done using experimentally observed target mRNAs (retrieved from public databases) of differentially expressed miRNAs from the microarray results. Therefore, the only miRNA transcripts used were those which had already been described in other studies as having a biologically known mRNA target gene.

Pathway analysis by Gene Set Enrichment Analysis (GSEA)

GSEA (www.broadinstitute.org/gsea) (Subramanian et al. 2005) is a computational method that ranks genes in the given dataset according to their relative expression and class distinction, and then compares this list of ranked genes against a large archival collection of gene sets (know biological pathways in multiple databases) in order to determine whether the members of the ranked genes are statistically enriched in one of the known biologically pathways. GSEA calculates an enrichment score (ES) that reflects the degree of overrepresentation of a gene set (known biological pathway) at the extremes (top or bottom) of a ranked gene list. The algorithm compares these two set of genes by walking down the ranked gene list, and whenever a gene belonging to a gene set (known biological pathway) is found in the ranked list, the ES is increased by the amount of significance of that gene in the ranked list. Whenever a gene not in the ranked gene list is found, the ES is decreased. GSEA then calculates the statistical significance (nominal *P*-value) of the ES by permuting the class labels and recalculating the ES of the gene set, generating a null distribution of ES. This empirical phenotype-based permutation method is repeated 1000 times (the default setting in this experiment). Next, GSEA generates a normalised enrichment score (NES) by taking into account the size of the gene set and then uses the NES to calculate the FDR (q-value), which is the probability that a given gene set (with a given NES) represents a false positive finding. GSEA suggests using a FDR of 0.25, meaning that the result is likely to be invalid one out of four times, which is reasonable in testing for pathway candidate discovery. Too stringent a FDR threshold may result in potentially significant results being missed.

Currently, there is no publicly available database for pathway analysis that contains miRNA identifiers. A number of web-based databases exist which are used for understanding of biological system and molecular networks, including KEGG (www.genome.jp/kegg), Gene Ontology (www.geneontology.org), GenMAPP (www.genmapp.org) and GSEA, but they have not yet

integrated miRNA knowledge into their pathway database. In other words, miRNA cannot directly be used in pathway analysis using currently and publicly available databases. Only mRNAs, not miRNAs, can be used in pathway analysis. Therefore, a list of mRNAs that were proven by other publications to be regulated (targeted) by individual miRNA identified as significantly dysregulated in malaria in this study were identified, then used in the pathway analysis by GSEA.

In order to do this, the experimentally observed mRNA targets of the differentially expressed miRNAs between malaria and control patients (n = 157), were retrieved from the four databases TarBase (Sethupathy et al. 2006), miRecords (Xiao et al. 2009), TargetScan (Lewis et al. 2005) and Ingenuity Expert Findings (www.ingenuity.com) for subsequent pathway analysis in GSEA. Not all miRNAs had experimentally observed mRNA targets and some miRNAs had multiple mRNA targets. Some miRNAs were observed to be clustered together and had the same mRNA targets (e.g. let-7a/ let-7f/ let-7c) (see Appendix B, Table B-3).

GSEA using ranked gene lists of experimentally observed mRNA targets (n = 360) of the up-regulated miRNA list in our malaria cases, with pathway definitions from the Gene Ontology (GO) database, revealed seven significant gene sets specific to the malaria phenotype at FDR < 0.25 (Table 5-4). Table 5-5 shows a complete list of enriched genes in each significant gene set (pathway) and the miRNAs that regulate individual gene.

Table 5-4. Results of Pathway Analysis using experimentally proven gene targets of miRNAs that were found to be up-regulated in malarial kidneys

Gene set	No. genes in set	NES	NOM *P*-val	FDR q-val
Regulation of Apoptosis	25	1.7409	0.0000	0.0957
Regulation of Programmmed Cell Death	25	1.6683	0.0183	0.0738
Programmed Cell Death	29	1.5598	0.0488	0.0877
Negatve Regulation of Developmental Process	15	1.5241	0.0523	0.0809
Apoptosis	29	1.5226	0.0357	0.0650
Regulation of Molecular Fundtion	16	1.3056	0.1608	0.1526
Regulation of Catalytic Activity	15	1.2753	0.1552	0.1514

Abbreviations: FDR, false discovery rate; NES, normalized enrichment score; NOM *P*-val, nominal *P*-value.

The same procedure was conducted on the ranked gene list of experimentally observed mRNA targets (n = 312) of the down-regulated miRNA list with pathway definitions from GO, KEGG, GenMAPP and Biocarta (www.biocarta.com). No gene set enrichment was observed.

Table 5-5. Gene targets of miRNA significantly up-regulated in malarial kidneys, grouped in biological functions (seven significant pathways) as identified by GSEA

Core enrichment of gene in 7 significant pathways								MicroRNA regulating core gene	
Core gene	Apoptosis	Program cell death	Regulation of program cell death	Regulation of Apoptosis	Negative regulation of develop-mental process	Regulation of molecular function	Regulation of catalytic activity	MicroRNA dysregulated in malaria	Database used for experimentally observed mRNA target (become core gene in GSEA)
ARHGDIA	Yes	Yes	Yes	Yes	Yes	No	No	miR-16/miR-497/miR-195 (i.o.)	TB,TSH
BCL2L2	Yes	Yes	Yes	Yes	Yes	No	No	miR-16/miR-497/miR-195 (i.o.)	IEF,TSH,MR
CADM1	Yes	Yes	Yes	Yes	No	No	No	miR-16/miR-497/miR-195 (i.o.)	TSH,MR
CARD8	Yes	Yes	Yes	Yes	No	Yes	Yes	miR-16/miR-497/miR-195 (i.o.)	MR
CCND3	No	No	No	No	No	Yes	Yes	miR-16/miR-497/miR-195 (i.o.)	TSH,MR
CDK5RAP1	No	No	No	No	No	Yes	Yes	miR-16/miR-497/miR-195 (i.o.)	TB,TSH
EGFR	No	No	No	No	No	Yes	Yes	miR-16/miR-497/miR-195 (i.o.)	TB
FGF2	No	No	No	No	No	Yes	Yes	miR-16/miR-497/miR-195 (i.o.)	TB
GTF2H1	No	No	No	No	No	Yes	Yes	miR-16/miR-497/miR-195 (i.o.)	MR
HBXIP	Yes	Yes	Yes	Yes	Yes	Yes	Yes	miR-16/miR-497/miR-195 (i.o.)	TB
PDCD4	No	No	No	No	No	No	Yes	miR-16/miR-497/miR-195 (i.o.)	TSH,MR
HSP90B1	Yes	Yes	Yes	Yes	Yes	No	No	miR-16/miR-497/miR-195 (i.o.)	MR
MCL1	Yes	Yes	Yes	Yes	Yes	No	No	miR-16/miR-497/miR-195 (i.o.)	MR
NOTCH2	Yes	Yes	Yes	Yes	Yes	No	No	miR-16/miR-497/miR-195 (i.o.)	TB,TSH
RHOT1	Yes	Yes	No	No	No	No	No	miR-16/miR-497/miR-195 (i.o.)	MR
RTN4	Yes	Yes	Yes	Yes	Yes	No	No	miR-16/miR-497/miR-195 (i.o.)	TB,TSH
TIA1	Yes	Yes	Yes	Yes	No	No	No	miR-16/miR-497/miR-195 (i.o.)	MR
TNFSF9	Yes	Yes	No	No	No	No	No	miR-16/miR-497/miR-195 (i.o.)	TB
BTG1	Yes	Yes	Yes	Yes	No	No	No	miR-371b-5p/miR-616*/miR-373* (i.o.)	IEF
BCL2	Yes	Yes	Yes	Yes	Yes	No	No	miR-16/miR-497/miR-195 (i.o.)	IEF,TB,TSH,MR
BNIP2	Yes	Yes	Yes	Yes	Yes	No	No	miR-20a/miR-106b/miR-17-5p (i.o.)	IEF,TSH
CDKN1A	Yes	Yes	Yes	Yes	No	No	No	miR-20a/miR-106b/miR-17-5p (i.o.)	IEF,TB,TSH,MR
E2F1	Yes	Yes	No	No	No	No	No	miR-20a/miR-106b/miR-17-5p (i.o.)	IEF,TB,TSH,MR
PDCD4	No	No	No	No	No	Yes	No	miR-16/miR-497/miR-195 (i.o.)	TSH,MR
BCL2	No	No	No	No	No	Yes	No	miR-20a/miR-106b/miR-17-5p (i.o.)	TSH,MR
HIPK3	Yes	Yes	Yes	Yes	Yes	Yes	Yes	miR-20a/miR-106b/miR-17-5p (i.o.)	TB,MR
PTEN	Yes	Yes	Yes	Yes	No	Yes	Yes	miR-20a/miR-106b/miR-17-5p (i.o.)	IEF,TSH
TP63	Yes	Yes	Yes	Yes	No	No	No	miR-20a/miR-106b/miR-17-5p (i.o.)	IEF
VEGFA	Yes	Yes	Yes	Yes	Yes	No	No	miR-20a/miR-106b/miR-17-5p (i.o.)	TSH,MR
RB1	No	No	No	No	No	Yes	Yes	miR-20a/miR-106b/miR-17-5p (i.o.)	IEF,TB,TSH,MR
ADORA1	Yes	Yes	Yes	Yes	No	No	No	miR-292-5p/miR-290/miR-293* (i.o.)	MR
MADD	Yes	Yes	Yes	Yes	No	Yes	Yes	miR-292-5p/miR-290/miR-293* (i.o.)	MR
MAPK1	Yes	Yes	Yes	Yes	No	Yes	No	miR-292-5p/miR-290/miR-293* (i.o.)	MR
CNTN4	No	No	No	No	Yes	No	No	miR-292-5p/miR-290/miR-293* (i.o.)	MR
BCL2L1	Yes	Yes	Yes	Yes	Yes	No	No	let-7a/let-7f/let-7c (i.o.)	IEF,TSH
BCL2L11	Yes	Yes	Yes	Yes	Yes	No	No	let-7a/let-7f/let-7c (i.o.)	IEF
CASP3	Yes	Yes	Yes	Yes	No	No	No	let-7a/let-7f/let-7c (i.o.)	TSH,MR
CDC25A	No	No	No	No	No	Yes	Yes	let-7a/let-7f/let-7c (i.o.)	TSH,MR
F2	No	No	No	Yes	No	Yes	Yes	miR-16/miR-497/miR-195 (i.o.)	TB
CDK6	No	No	No	No	Yes	No	No	let-7a/let-7f/let-7c (i.o.)	MR
CCND1	No	No	No	No	No	No	Yes	miR-20a/miR-106b/miR-17-5p (i.o.)	TSH,MR

Abbreviations: i.o. = includes others in the same cluster; TB = TarBase; TSH = TargetScan Human; MR = miRecords; IEF = Ingenuity Expert Findings; miR-16/miR-497/miR-195 (i.o.) = hsa-miR-15, hsa-miR-15a, hsa-miR-15b, hsa-miR-15b MM1, hsa-miR-16, hsa-miR-195, hsa-miR-424, hsa-miR-497; miR-371b-5p/miR-616*/miR-373* (i.o.) =; hsa-miR-371b-5p, hsa-miR-373*, hsa-miR-616, hsa-miR-616*; miR-20a/miR-106b/miR-17-5p (i.o.)= hsa-miR-106a, hsa-miR-106b, hsa-miR-17, hsa-miR-17-5p, hsa-miR-20, hsa-miR-20a, hsa-miR-20b, hsa-miR-519d, hsa-miR-526b*, hsa-miR-93; miR-292-5p/miR-290/miR-293* (i.o.) = hsa-miR-371-5p, miR-290, miR-290-5p, miR-292-5p, miR-293*; let-7a/let-7f/let-7c (i.o.) = hsa-let-7a, hsa-let-7a MM1, hsa-let-7b, hsa-let-7c, hsa-let-7d, hsa-let-7e, hsa-let-7f, hsa-let-7g, hsa-let-7i, hsa-miR-4458, hsa-miR-4500, hsa-miR-98;

The complete list of enriched genes in each of seven significant gene sets (pathways) from GSEA and the miRNAs regulating the individual genes, using four separate databases to identify target mRNAs on the basis of previously validated studies.

5.3.5 miRNAs associated with the Ang-Tie-2 pathway.

Because previous work, and the study done in Chapter 3, showed that Ang-1, Ang-2 and Tie-2 molecules may be linked to the pathogenesis of severe malaria, I then specifically examined the miRNA data to determine whether any transcripts were identified in malarial kidneys that could regulate the expression of these important molecules. Currently, there is no published information on the relationship between these three molecules and any human miRNA. Therefore, I investigated whether any of the malaria-associated miRNAs (from microarray results) potentially target the three angiogenic genes.

Target-prediction approach

Initially, four different publicly available miRNA target-prediction algorithms (Target Scan (Lewis et al. 2005), Pictar (Krek et al. 2005), DIANA-microT (Maragkakis et al. 2009) and miRDB (Xiaowei Wang 2008)) were used to identify miRNAs that have a high possibility of binding to 3'UTR of either ANGPT1, ANGPT2 or TEK (gene symbols of Ang-1, Ang-2 and Tie-2, respectively). This generated a large list of miRNAs which was subsequently narrowed down to focus on transcripts dysregulated in malarial kidneys (within the list of 157 miRNAs differentially expressed more than twofold in malaria vs. control). With this approach, only four candidate miRNAs were found to be potential post-transcriptional regulators of the three angiogenic molecules (Table 5-6), and all of them were down-regulated in malaria (mir-19b, mir 181a, mir-204 and mir 486-5p). This is in keeping with increased expression of the mRNA molecules in the Ang-Tie-2 pathway, as miRNAs are negative regulators of gene expression.

Table 5-6. The list of four miRNAs deregulated in malaria that are predicted to have target in ANGPT1, ANGPT2 or TEK by four different target-prediction algorithms

	ANGPT1	ANGPT2	TEK
miR-19b	-	MD	-
miR-181a	-	PT	-
miR-204	TS,PT,DN,MD	-	-
miR-486-5p	-	-	MD

MD = miRDB, PT = Pictar, TS = TargetScan, DN = DIANA

Confirmation of target prediction by luciferase reporter assay

To confirm the results from the target-prediction algorithms, I used an *in vitro* luciferase reporter assay to examine the effect of miR-19b, miR-181a, miR-204 and miR-486-5p on ANGPT1, ANGPT2 and TEK expression via targeting the 3' UTR of these genes. Luciferase bioluminescence was measured in HEK293 cells co-transfected with pEZX-MT01 3'UTR expression vectors for human ANGPT1, ANGPT2 or TEK (dual luciferase reporter vectors) and miRNA constructs for miR-19b, miR-181a, miR-204 or miR-486-5p. 3'UTR is the area where the potential binding sites of candidate miRNAs are, and 3'UTR is tagged downstream of a firefly luciferase gene. This means that when the miRNA of interest binds to the 3'UTR in the vector, inhibiting RNA transcription, the firefly luciferase luminescent signal will decrease. For accurate comparisons between different luciferase assay reactions, the firefly luciferase luminescence was then normalised with *Renilla* luciferase luminescence in the same sample to eliminate confounding factors that can affect the firefly luciferase luminescence, such as variability in the starting cell number, differences in transfection efficiencies and cell viability.

To control for non-specific interaction between miRNA constructs and the luciferase reporter in the vector, parallel experiments were conducted on the same batch of HEK293 co-transfected with these luciferase reporter vectors and scrambled miRNA, which did not have any binding sites on the vectors. Other control reactions included HEK293 transfected with vectors alone and mock transfection (no sequence). All mock transfection gave no luminescent activity and

transfections with vector alone gave similar luminescent activity to co-transfection with vector and scrambled miRNA. All experiments were repeated three times.

In HEK293 cells transfected with ANGPT1 3' UTR expression vector, the sample co-transfected with miR-204 produced a significant decrease in luciferase luminescent activity by about 45% compared to the sample co-transfected with scrambled miRNA (P = 0.0151, Friedman test with Dunn's correction for multiple comparison). Sample co-transfected with other miRNAs showed some degrees of reduction in luminescent activity but nothing statistically significant was observed. In HEK293 cells transfected with ANGPT2 3'UTR expression vector, there was no statistically significant difference in luciferase luminescence between groups (Figure 5-8).

In HEK293 cells transfected with TEK 3'UTR expression vector, co-transfection with miR-486-5p significantly repressed TEK 3'UTR-mediated luciferase luminescence by about 38%, in comparison with cells co-transfected with scramble miRNA *(*P = 0.0012, Friedman test with Dunn's correction for multiple comparison). Samples co-transfected with other miRNA constructs showed some degree of reduction in luminescence but without statistical significance (Figure 5-8).

In summary, these luciferase experiments showed that two miRNAs, including miR-204 and miR-486-5p, identified as down-regulated in malaria kidney, bound to and suppressed mRNA expression of Ang-1 and Tie-2 genes *in vitro*, respectively.

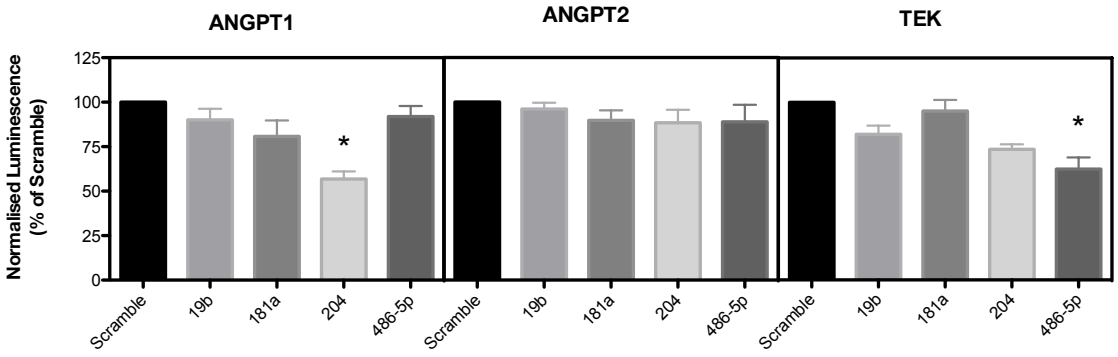

Figure 5-8. miRNA can Suppress expression of Ang-1 and Tie-2 genes *in vitro*
Effects of miRNA transcripts included miR-19, miR-181a, miR-204, miR-486-5p and scrambled miRNA (negative control) on the bioluminescence activity of dual luciferase vectors containing 3'UTR of ANGPT1, ANGPT2 or TEK in HEK293 cells. Bars denote the mean determinations of luciferase bioluminescent activity for at least three separate co-transfection experiments (error bars = SEM). The plotted values are the ratios of firefly luciferase signal normalised to *Renilla* luciferase signal in the same sample and are presented as a percentage of the average signal for the transfection with scrambled miRNA (compared within experiments that use the same 3'UTR dual luciferase vector). Asterisks denote comparisons in which normalised luminescent signal of a transfection with a miRNA was significantly different ($P < 0.05$) from a transfection with the scrambled miRNA.

5.4 Discussion

In this chapter, a protocol for isolated high-quality miRNA retrieval from archival FFPE blocks of kidney was optimised and successfully used to study miRNA expression profile in in malaria cases with and without ARF using microarray experiments. The results were validated using qRT-PCR and represent the first study of miRNA expression in human tissues with malaria.

The kidney is a vital organ responsible for the regulation of fluid, water, electrolyte and blood pressure, as well as the excretion of waste products. It also produces important hormones such as erythropoietin. miRNAs have been proven to play an important role in several aspects of renal development, renal function, and maintenance and progression of several kidney diseases. Data from such studies have shown that there are some miRNAs that tend to be renal specific. These include miR-146a, miR-886, miR-192, miR-194, mir-204, miR-215 and miR-216 (reviewed in Chandrasekaran et al. 2012). Hundreds of miRNAs have been predicted to control the expression

of aquaporins (AQs), which are important water channels on the renal tubular epithelial cells. However, so far only one miRNA (mir-320a) has been experimentally validated as having a direct interaction with AQ1 and AQ4 gene expression (Sepramaniam et al. 2010).

Although the renal expression profiles of miRNAs have been examined in other diseases including diabetic nephropathy, polycystic and fibrotic kidney disease, hypertension-related renal diseases, lupus nephritis, and cancer (reviewed in Chandrasekaran et al. 2012), the miRNA expression in malaria-associated kidney injury has not been previously examined. This makes it more difficult to interpret the significance of individual dysregulated miRNAs, and more studies are needed to build knowledge on malaria-associated kidney injury.

The results presented here show that the miRNA expression profile of malaria patients is distinct from controls in unsupervised cluster analysis. The heatmap showed the similarity of the miRNA changes in malaria patients, and indicates that specific miRNA changes are occurring in the kidney of malaria cases which are different from control. Although no specific differences could be seen between malaria cases with ARF/AKI, this may be because of the small sample sizes used.

One recent study published since this work was begun has documented miRNA levels in the murine model of experimental CM (El-Assaad et al. 2011). The study identified three miRNAs (let-7i, miR-27a and miR-150) that were differentially expressed in the brain of murine CM mice compared to controls. It showed no changes in miRNA transcripts in the heart, but did not examine other organs such as the kidney.

Target-prediction and pathway analysis using mRNA targets of up-regulated miRNAs in malaria-infected kidneys identified seven enriched gene sets: *Regulation of Apoptosis, Regulation of Programmed Cell Death, Programmed Cell Death, Negative Regulation of Development Process, Apoptosis, Regulation of Molecular Function* and *Regulation of Catalytic Activity*. Because miRNAs are repressors of mRNA transcription or protein translation and this pathway analysis reflects only

up-regulated miRNAs in malaria, the seven enriched gene sets are predicted to be under-represented in malaria-infected kidneys. This implies that malarial infection altered the expression of miRNAs in the kidney involved in the repression of apoptosis/programmed cell death and catalytic activity. Various pathological changes occur in the kidney after malarial infection, more marked in adult than paediatric cases, and this leads to a number of clinical manifestations ranging from mild renal dysfunction (reversible on rehydration) through AKI and potentially fatal anuric renal failure. The challenge of interpreting our dataset is to relate gene expression and control mechanisms by miRNA with phenotypic changes in the kidney, such as tubular epithelial cell injury. The main host response mechanisms identified here related to repression of apoptosis and catalytic activity, which could represent a protective response, either to parasite sequestration, host immune cell functions or systemic complications of malaria such as shock.

Novel miRNAs targeting ANGPT1 and TEK genes were also identified for the first time. The role of the angiopoietin pathway in the genesis of ARF/AKI is unknown, although clinical studies have indicated that Ang-1 (Conroy et al. 2009) and Ang-2 (as shown in Chapter 3 and Yeo et al. 2008) levels are significantly associated with the incidence of renal failure in adult malaria patients. One way of examining the role of the Ang-Tie pathway would be to replicate the immunohistochemical study performed on the brain to examine staining of these angiogenic molecules in the kidney. However, an attempt to validate the results by using Western blotting to detect Ang-1 and Ang-2 expression in these kidney tissues was not successful (data not shown). Importantly, this validation experiment showed some of the problems with using *in silico* prediction of mRNA targets of miRNA transcripts. A large number of potential miRNAs were predicted to target the Ang-1, Ang-2 or Tie-2 genes. However, *in vitro* only two out of 12 combinations of miRNA to mRNA target showed significant biological activity. Hence, the wider use of predictive algorithms such as in the pathway analysis should therefore be treated with some caution until further validation experiments are done.

Other studies have examined the role of miRNA changes in AKI due to ischaemic reperfusion injury (IRI) (Shapiro et al. 2011; Godwin et al. 2010). These showed that nine miRNAs (miR-21, miR-20a, miR-146a, miR-199a-3p, miR-214, miR-192, miR-187, miR-805 and miR-194) are differentially expressed following IRI and suggested that miR-21 may play a role in protecting tubular epithelial cells from ischemia via TGF-beta signalling. Although the pathophysiology of IRI could be quite similar to one aspect of renal injury in malaria (reduced blood flow to the kidney tissue due to microvascular blockage), the miRNA signatures from the IRI study were quite different to those in the present study. MiR-21, which was the most important miRNA in IRI pathophysiology from the murine model, was not differentially expressed in our study of malaria-infected human kidneys. Only three miRNAs were differentially expressed in both studies. One miRNA (miR-20a) was up-regulated in both malaria and IRI but miR-214 and miR-187 showed opposite changes in expression. This could be in part due to differences in the host response mechanisms to malarial infection between humans and mice.

Although more work needs to be carried out to further validate these results, this is the first ever large-scale study of miRNA expression profile in human tissue from malaria patients. The lack of fresh frozen tissues from the kidney in these patients meant that extraction of mRNA and mapping miRNA changes onto respective changes in mRNA transcription was not possible in this group. This would be the next important step in understanding the importance and role of the specific changes observed in malaria patients compared to controls.

Chapter 6

An Autopsy Study of Fatal *P. falciparum* Malaria in Mozambique and Optimisation of Tissue Collection for Molecular Pathology Methods

6.1 Introduction

6.1.1 Background

As discussed in section 1.10, one of the challenges in malaria pathophysiology research is access to human tissue. For instance, in cancer research, where dissecting tumour out of the living patient is part of diagnosis or surgical treatment, access to fresh tissue is relatively straightforward, allowing rapid and optimal handling and fixation for specific molecular techniques. Obtaining human tissue (except blood and urine) from living malaria patients is ethically questionable as in most cases this does not provide any benefit to the patient. Perhaps one exception would be a renal biopsy, where the diagnosis of AKI is in doubt, but other examples of studies on biopsy tissues such as skin or muscle biopsies from living patients (García et al. 1999; Turner et al. 1998) have been purely research based. Access to brain tissue in living CM patients is clearly impossible. Human tissue used in malaria research worldwide is therefore usually only available at autopsy. Autopsy studies are challenging to organise for ethical and logistic reasons, as well as the issues of preservation and transportation of the collected specimens. Perhaps most importantly, the value of autopsy studies depends on the quality of the clinical data available on the patient. Most deaths from malaria occur in less well-developed countries where clinicopathological correlation can be difficult, laboratory investigations such as blood chemistry or microbiology may be unavailable,

and conducting a proper basic autopsy is challenging. Thus, over the last 120 years there have only been a limited number of large-scale autopsy studies of human malaria, leading to limited access to human tissue for recently developed molecular pathological studies.

As part of this thesis I had access to FFPE histology tissues collected from an autopsy series of severe malaria in Vietnam. This set of tissues has been used in a number of pathological and immunohistochemical studies during the past 15 years. Although miRNA expression profiling of the kidneys was successfully generated from FFPE tissues from the AQ_trial (Chapter 5), an attempt to extract miRNA from brain tissues of this series was unsuccessful probably due to age, fixation and lower cellularity in the brain sections.

To conduct molecular pathological studies using a transcriptome approach, a new set of human tissues with high-quality RNA preservation was required. Moreover, it has been reported that some pathological findings in fatal paediatric cases differ from those in adults, as discussed in section 1.7.1. Thus, my group decided to conduct a new autopsy study of paediatric malaria cases in Mozambique. My contribution to this study, the MEMA, included writing and implementing autopsy and specimen-collection protocols, and performing autopsies.

Before MEMA started to recruit, a study to validate autopsy procedure and specimen-collection techniques that would yield the best tissue quality for use in molecular studies was conducted in Bangkok, Thailand. This study allowed me to perform a feasibility study of mRNA extraction and gene expression analysis on samples of post-mortem human organs, examining the effects of pre- and post-mortem factors, tissue collection, storage and RNA isolation techniques. This study also formed a tissue bank of control patients for use in histological, immunohistochemical studies and the comparison of gene expression profiles between malaria and non-malaria individuals together with the baseline difference of gene expression in different genetic backgrounds.

6.1.2 Concerns about the quality of human post-mortem tissue

Human post-mortem tissue is valuable for the study of many different diseases. A key concern in conducting molecular research based on post-mortem tissue is the quality of the tissue. Unlike for humans, collection of animal post-mortem tissue can be optimised by controlling and manipulating agonal conditions, and fixation can be optimised by perfusion techniques. As discussed in section 1.10.2, this limitation introduces numerous potential confounding factors that may affect the quality of the tissue and results generated from downstream molecular-based techniques, including qRT-PCR, gene expression microarray and whole-genome sequencing.

Recent studies have focused on identifying measures of tissue quality for human post-mortem tissue. Several studies have proved that the 28S/18S ratio, the historical and commonly used measure of RNA quality, is not suitable as a marker of quality for mRNA (Weis et al. 2007). The brain pH has been proposed as a different marker, as it correlates with other quality markers and it affects the gene expression profile; however, pH alone lacks the ability to be applied as a screening tool (Mexal et al. 2006). Most studies agree that the RIN, which is generated from an Agilent 2100 Bioanalyzer, is by far the most accurate screening measure to evaluate the quality of RNA samples prior to their use in ultra-sensitive platforms such as microarray analysis (Ferrer et al. 2008; Stan et al. 2006; Weis et al. 2007). The Bioanalyzer generates digital electropherograms and calculates RIN using the manufacturer's algorithm, which takes more components of the electropherogram into account than previously possible with standard agarose gels (algorithm described in Schroeder et al. 2006). This creates a more robust and reliable prediction of the integrity of RNA, compared to other traditional methods.

Measuring of the RIN is now accepted as a common practice for screening RNA samples to be used in whole-genome microarray or next-generation sequencing. Samples with RIN values higher than seven are generally accepted as of high quality and suitable for mRNA expression profiling by microarray. However, not all mRNA transcripts have the same vulnerability to

degradation. Thus, an RIN value of seven is not a magic number to reject or accept the use of that sample for molecular studies. To generate robust and reproducible microarray results, various quality-control measures as suggested by microarrays' manufacturers and MicroArray Quality Control Consortium (MAQC) are still crucial for the quality evaluation of microarray experiments (MAQC Consortium et al. 2006).

6.1.3 Aims and work carried out in this chapter

The major aim of this project was to collect human tissues for use in further molecular-based studies by conducting an autopsy study of paediatric fatal malaria in Mozambique, complemented with high-quality clinical and laboratory data. A feasibility study conducted in Bangkok allowed selection of a method to optimise autopsy tissue specimen collection and preservation protocols for subsequent mRNA and miRNA extraction. In the feasibility study, I conducted a systematic comparison between different specimen preservation techniques to preserve labile mRNAs in post-mortem tissue, including snap freezing in LN, and two different protocols of a commercially available RNA preservation reagent, RNAlater®.

6.2 Material and methods

6.2.1 MEMA series

Case selection

The MEMA study has been funded by the Thrasher Foundation, USA since the start of the project in December 2008. Ethical approvals for this study were granted from the Mozambique Ministry of Health and the Oxford Tropical Research Ethics Committee (OxTREC). The first year of the project was spent on administrative work to form an operational team, develop standard operating procedures and set up a collaboration with the Pathology Department and Paediatric Department at the Hospital Central de Beira. The hospital is a university-based

hospital and a main referral hospital for Beira and surrounding regions, where high rates of HIV infection of up to 30% are reported in the adult population but unknown in paediatrics. Two malaria admission seasonal peaks are seen in January to April and in September.

All paediatric deaths related to a clinical diagnosis of severe malaria in the hospital, based on clinical diagnosis and screening with blood film and a malaria RDT, using rapid immunochromoatographic strip assay for PfHRP-2 (Paracheck-Pf®, Orchid Biomedical Systems, India). Cases were notified to local research nurses and doctors who were responsible for obtaining informed consent for entering the autopsy study from the next-of-kin if the patient died, and collecting all clinical information on a standardised form. Where written permission was given for autopsy by the parent/legal guardian, the cadaver was transported to the mortuary to be refrigerated at 4°C as soon as possible. Time of death, refrigeration and autopsy were recorded. All subjects were tested for hepatitis B, hepatitis C and HIV infections using post-mortem serum through commercial rapid tests (SD Bioline Rapid Test for HBsAg, anti-HCV and anti-HIV 1&2, Standard Diagnostic Inc., Korea). Only cases with negative results from all the three markers were accepted. The autopsies were performed using a standard protocol by pathologists on a rota including Dr Josepho Ferro, Dr Gareth Turner, Dr Robert Marshall and myself. All organs were removed, dissected, weighed, sliced and examined macroscopically. Microscopic examination of histology slides was done later in Bangkok after tissue processing took place. All findings were recorded in a standardised autopsy information form.

Tissue collection, handling and storage

At autopsies, tissues from the predefined-areas of the brain, heart, lung, liver, pancreas, spleen, bowel, kidney, adrenal glands, thyroid, lymph nodes, bone marrow, skin and skeletal muscle were collected for preservation in 10% buffered formalin and RNAlater solution, according to procedures described in section 2.2.2. The formalin-fixed tissues were transported to Bangkok in ambient temperature in accordance with legal guidelines covering the transport of formalin-fixed

tissue, for tissue processing and histology slide production. The RNAlater-fixed tissues were initially stored at 4˚C for one day (in the fridge) and then transferred to –20˚C (freezer) for storage until use.

6.2.2 Bangkok autopsy series

Case selection

This autopsy study included non-randomised routine autopsies at the Pathology and Forensic Departments of King Chulalongkorn Memorial Hospital, Bangkok, Thailand. The ethical permission for autopsy and the use of tissue collection was approved by the Institutional Review Board of the Faculty of Medicine, Chulalongkorn University. Only cases with written permission to conduct an autopsy and to retain tissue samples for research, given by the next-of-kin, were recruited into this series. Detailed medical records of cases dying after admission to hospital were collected (n=1); however, most cases were forensic cases who died outside the hospital (n=9). Time of death, time of initial refrigeration, refrigeration duration and the time of autopsy were recorded. In cases where the time of death was not certain, the time of death was estimated from post-mortem changes and circumstances of the death. All candidates for the study were tested for hepatitis B, hepatitis C and HIV infections using post-mortem serum through commercially available rapid tests (SD Bioline Rapid Test for HBsAg, anti-HCV and anti-HIV 1&2, Standard Diagnostic Inc., Korea). Only cases with negative results for all three markers were recruited into the study.

The body was kept refrigerated at 4˚C for variable periods of time from the receipt of the body until the autopsy. The autopsy was performed using standard techniques. All internal organs were removed and dissected in the usual fashion and completely examined. All macroscopic findings at autopsy were recorded in a standardised form. The brain was removed and dissected. A gross neuropathological examination was completed on each brain. Four specific areas of the brain were collected from each case, including the primary motor cortex (dorsal part of precentral gyrus),

anterior nucleus of thalamus, medulla oblongata and posterior lobe of cerebellar hemisphere. Samples from the lungs, liver, spleen and kidneys were also collected.

Tissue handling and storage

At autopsies, tissues from predefined areas of the brain, kidney, lung, liver and spleen were collected. For each fresh specimen, a single tissue fragment was subdivided into four small aliquots. Replicate aliquots were immediately triaged into four storage conditions: 1) snap freezing in LN then storage at –70˚C; 2) immersion in RNAlater at 4˚C for 24 hours then storage at –70˚C (RNAlater A); 3) immersion in RNAlater at room temperature (around 27–35˚C in Bangkok) for 24 hours then storage at –20˚C (RNAlater B); and 4) 10% formalin at room temperature for several days then embedded in paraffin block. Tissues immersed in RNAlater or snap frozen in LN were cut into 5 mm squares, in order to ensure the quick and complete immersion of RNAlater solution or immediate freezing process of LN to avoid ice crystal artefacts. Tissues immersed in 10% formalin were cut into a 20x20x5 mm dimension for later paraffin embedding and histopathological examination.

This experimental design allowed the comparison of the quality of RNA from the same tissue fragment with three different tissue-preservation techniques (LN, RNAlater A and RNAlater B). Only brain tissues were studied in the comparison of tissue-preservation techniques. In total, there were 90 samples from three areas of the brains of 10 cases with three different preservation techniques to be analysed.

RNA isolation and analysis

Samples of brain tissue were homogenised by a handheld rotor-stator homogeniser (PRO200, PRO Scientific, USA) in the RLT buffer provided by RNeasy Lipid Tissue Mini Kit (Qiagen, UK). Total RNA was isolated according to the manufacturer's instructions. RNA purity was assessed by Nanodrop-1000 (Thermo Scientific, USA) using the A260/A280 ratio and A260/A230 ratio (A260 = absorbance at 260 nm, A280 = absorbance at 280 nm, A230 = absorb-

ance at 230 nm). The digital-format electropherogram of RNA was generated by Agilent 2100 Bioanalyzer (Agilent Technologies, USA) with RNA 6000 Nano-LabChip, according to the manufacturer's protocol. The RIN was calculated using an algorithm based on several features in the electropherogram, including pre-region, 5S-region, fast-region, 18S-fragment, inter-region, 28S-fraction, precursor-region and post region 7 (automated calculation from Agilent's software).

Statistical analysis

Analyses were performed using Stata/SE 9.2 (StataCorp LP, Texas, USA), with a *P*-value of less than 0.05 being taken as statistically significant. Data were summarised with median and interquartile values, and non-parametric tests including the Kruskal-Wallis, Mann-Whitney U test, and Wilcoxon matched-paired signed-ranks test were used to compare between groups where appropriate.

6.3 Results

6.3.1 Paediatric fatal malaria and control cases in MEMA

Infection rates for malaria amongst admissions with fever were relatively high. Since May 2010, a total of 1,223 paediatric patients admitted to the acute paediatrics unit with fever were screened with RDT, of whom 585 (48%) tested positive for *P. falciparum* malaria. However, reported death rates from paediatric malaria in this series were relatively low according to the hospital reporting figures. For example, according to Beira Hospital's record during the seven months between August 2011 and February 2012, the paediatric malaria death rate was only 3.5% (21 deaths from 599 admitted with malaria) compared to 5.3% in adults (71 deaths from 1,343 admitted with malaria). This death rate seems low compared to other studies, and suggested an ascertainment problem in the hospital, clinical misdiagnosis and inaccurate certification.

Since May 2010, 27/585 RDT+ve cases died (mortality rate overall 4.6%) and had consent for autopsy requested, of whom up to the start of the molecular study I had successfully recruited

three cases (autopsy acceptance rate 11%). We also performed full autopsy on three fatal paediatric cases whose causes of death were not related to malarial infection. These three non-malaria deaths were used as controls for further molecular pathology studies. Clinical and pathological findings of cases in MEMA are summarised in Table 6-1. Figures 6-1 and 6-2 show photomicrographs of some of the pathological findings in these cases.

The three malaria cases showed a varying pathological picture typical of the snapshot effect caused by examining individual cases dying at different stages in the disease. MAL1 died shortly after developing coma, although there was little sequestration of PRBC in brain capillaries, with some brain oedema and evidence of haemorrhages in the brainstem (6.1A). MAL2 and MAL3 also showed low levels of PRBC sequestration (6.1B), compatible with the clinical absence of coma, but some evidence of previous parasitisation including pigment deposition and pigmented leukocytes within brain capillaries, some of which were filled by a mixed population of leukocytes (6.1C). MAL3 showed few perivascular haemorrhages (6.1D) but occasional Dürck's granulomas, surrounded by an early astroglial response and with a central fibrin-platelet thrombus in the vessel (6.1E). Other features of malaria pathology previously described were also noted including brain oedema (6.1F) around vessels, in the parenchyma or in white matter tracts, and foci of axonal injury (6.1G).

The three control case available for use by the time this study was done included children dying of pneumonia, meningitis and a brain tumour. CON1 showed acute pneumonia as the cause of death (Fig 6.2A) along with marked steatosis and hepatocyte necrosis in the liver (6.2B), which raised the possibility of Reyes syndrome or hepatotoxicity due to ingestion of a herbal remedy. CON2 showed acute pyogenic meningitis (6.2C and D), and CON3 a brain tumour (pilocytic astrocytoma) arising from the cerebellum and invading the brainstem (6.2E and F), which had presented with intractable fitting prompting a clinical diagnosis of possible CM. None of these cases had a positive RCT test or evidence of PRBC on post-mortem blood film or histologically.

Table 6-1. Summary of malaria and control autopsy cases in MEMA

Case	Age	Sex	Clinical diagnosis	Malaria test	Hours to death	Hours to PM	WHO 2000 clinical criteria for severe Malaria	Major autopsy findings	Notes
CON1	17 m	F	Dehydrated, GI infection	-ve RDT, -ve BS	8	11	-	Pneumonia	Liver pallor and steatosis. Mild gastric erosions. Abdominal lymphaednopathy. Consolidation lungs
CON2	6 m	M	Unknown	-ve RDT	Brought in dead	24	-	Pyogenic meningitis	Softened brain and liver steatosis
CON3	4 y	F	Unknown	-ve RDT	2	45	-	Cerebellar pilocytic astrocytoma	Untreatable fits, thought to be CM, suffered cardiac arrest. Pulmonary oedema, Large brainstem tumour and compression of brainstem with mild cerebral oedema 1380g
MAL1	10 y	M	Malaria, +/- Pneumonia	+ve RDT, +ve BS, PC=106132/ul	4.5	20	Coma, ARF, Anaemia	Brain swelling, brainstem haemorrhages, AKI, pulmonary oedema, no pneumonia	Acute presentation with respiratory distress, anuria, lapsed into coma (BCS 1) and died
MAL2	19 m	M	Malaria	+ve RDT (weak)	1	14	Anaemia, Convulsions, Dyspneoa	Several meningeal punctate haemorrhages, slight brain swelling.	Fever for 10 days prior to admission. Bilateral old pleural adhesions.
MAL3	2 y	M	Malaria	+ve RDT, +ve BS	11	66	Anaemia, Dyspneoa	Generalised congested lungs, Pigmented liver & spleen, Mild brain swelling	Admitted aemaeic with some abdominal distension, diagnosed SMA, given quinine, Pen & Gent, Cardiac arrest and died despite attempts at CPR

F = female, M = male, m = month, y = year, RDT = malaria rapid diagnostic test, BS = malaria blood smear, PC = parasite count, TB = tuberculosis, BSC = Blantyre Coma Scale, GI = gastrointestinal, SMA = severe malarial anaemia, Pen & Gen = penicillin and gentamicin

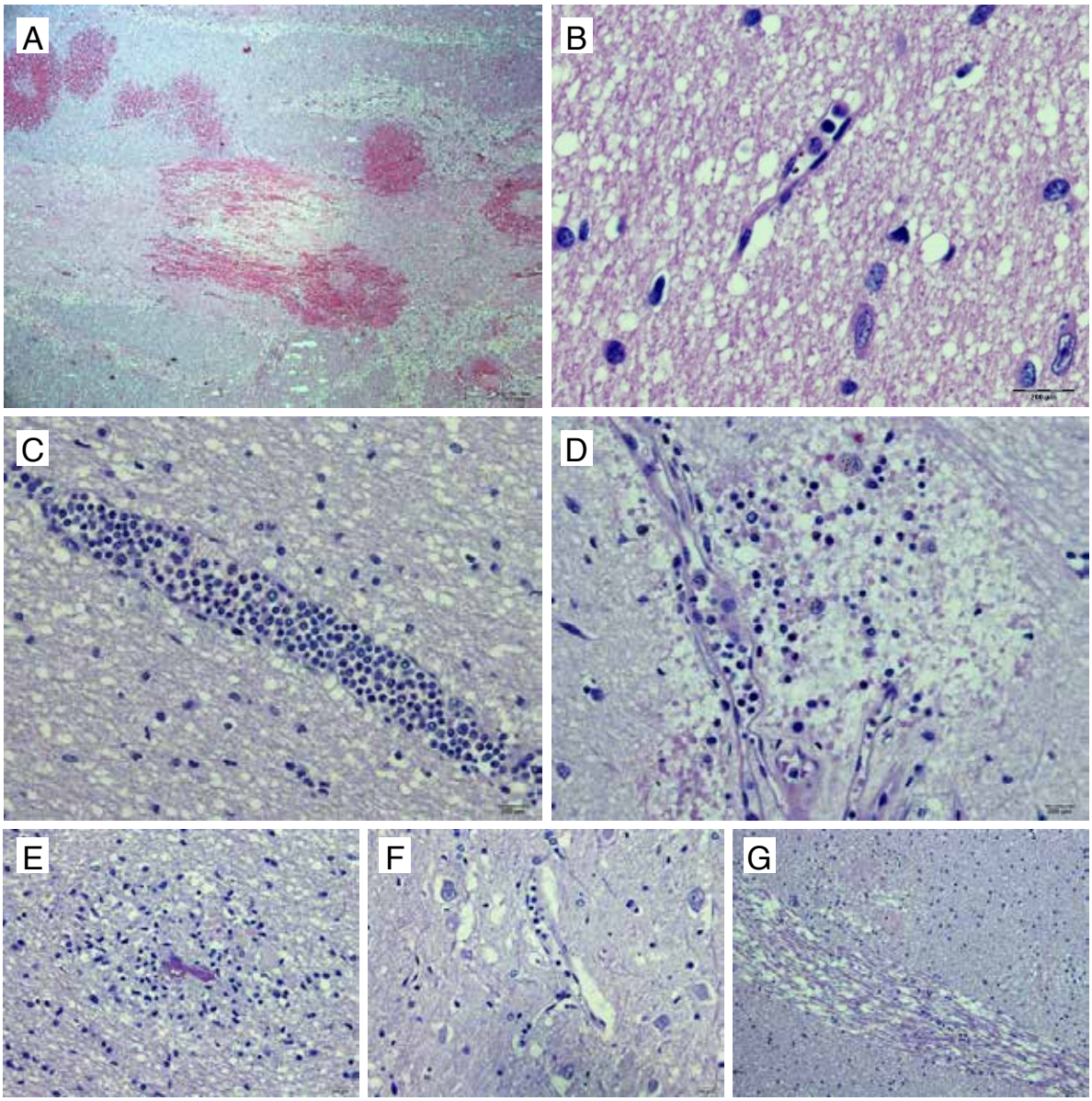

Figure 6-1. Representative histological findings from MEMA malaria cases

Various histological findings were found in the brain of the 3 malaria cases including (A) punctate and ring haemorrhage, (B) low level of PRBC sequestration, (C) malarial pigments and pigmented leukocytes deposition, (D) perivascular haemorrhages, (E) Dürck's granuloma surrounded by an early astroglial response and with a central fibrin-platelet thrombus in the vessel, (F) perivascular oedema and (G) axonal injury. (A = 40x; B, C, D, E, F = 400x; G = 200x: original magnification).

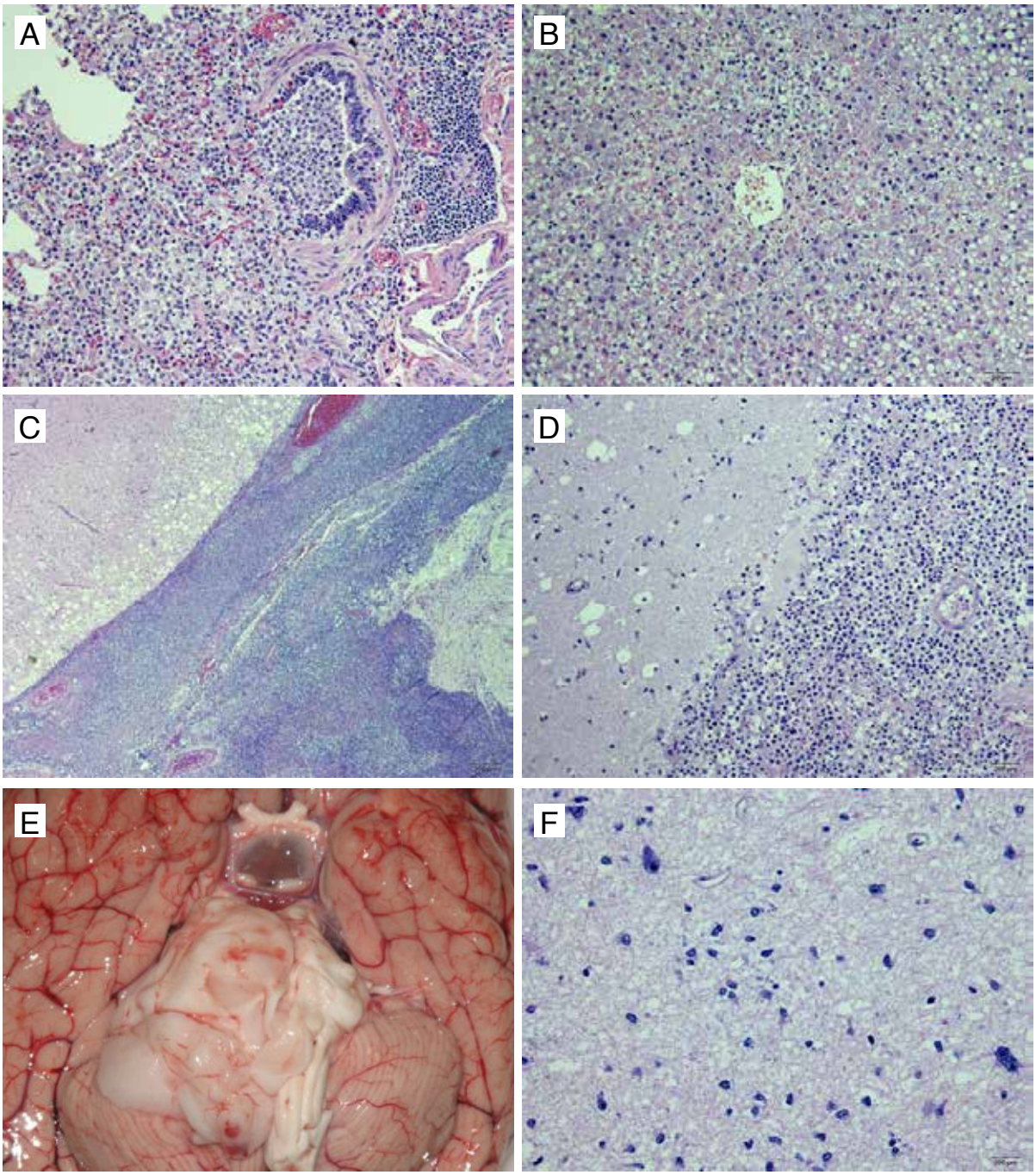

Figures 6-2. Representative histological findings from MEMA control cases

The figure shows various main pathological findings from the heterogeneous group of MEMA control cases. CON1 had (A) acute pneumonia and (B) severe hepatic steatosis and liver necrosis. CON2 had (C, D) acute pyogenic meningitis. CON3 had (E, F) pilocytic astrocytoma arising from the cerebellum and invading the brainstem. (A, B, D = 200x; C = 40x; F = 400x: original magnification).

6.3.2 Bangkok autopsy series and the comparison of different tissue-preservation techniques

Post-mortem characteristics

A clinical summary of cases recruited (n=10) into this autopsy series is presented in Table 6-2. Autopsy was conducted within 24 hours in every case (median = 10 hours, range 4 – 19). Nine out of 10 were forensic cases with acute unexpected onset of death. Eight cases did not have any brain pathology in histological examination. One case had mild congestion and diffuse atherosclerosis (CU1). The other (CU2) was a hospital case, who underwent intensive treatments and a prolonged agonal phase and this was the only case with brain pathology (granulomatous amoebic encephalitis). Clinical and pathological findings of cases in Bangkok autopsy series are summarised in Table 6-2.

RNA sample purity

The A260/A280 ratio and A260/A230 ratio were used to assess the sample purity. Generally, the A260/A280 ratio of ~2.0 is accepted as "pure" for RNA, and the A260/A230 is commonly in the range of 2.0–2.2, which is often a little higher than A260/A280. If the ratios are much lower than expected, it would indicate the presence of contaminants.

Overall, RNA samples extracted from this series of autopsy were of high purity, regardless of the differences in preservation techniques or the areas of the brain (A260/A280 median = 2.08, IQR = 2.06–2.09; A260/A230 median = 2.14, IQR = 1.94–2.24). There was a significant difference in A260/A280 and A260/A230 ratios between different areas of the brain (P =0.048, P =0.017, respectively). The medulla had slightly lower RNA purity than the other areas, according to both ratios. However, the preservation techniques did not affect the A260/A280 and A260/A230 ratios (P =0.696, P =0.755, respectively) (Table 6-3).

Table 6-2. Summary of autopsy cases in Bangkok series

Case	Age	Sex	Race	Hours to PM	Average RIN	Cause of death	Brain pathology	Additioinal clinical history
CU1	68	M	Thai	5	7.33	AMI?	Congestion, diffuse atherosclerosis	N/A
CU2	19	F	Thai	17	3.44	GAE, SLE	GAE	Hx of SLE with lupus nephritis, ARDS, ARF, liver infarction
CU3	57	M	Japanese	10	4.37	AMI	Normal	Hx of asthma, heavy smoker
CU4	45	M	Caucasian	12	5.68	AMI?	Normal	N/A
CU5	54	M	Thai	11	5.83	Hypovolemic shock due to a stab wound	Normal	N/A
CU6	18	F	Thai	10	N/A	Inconclusive	Normal	N/A
CU7	38	M	Thai	19	5.2	Electrocution	Normal	-
CU8	52	M	Thai	10	6.17	Dissiminated CA liver	Normal	Hx of CA liver, HT
CU9	52	M	Thai	4	4.36	AMI	Normal	-
CU10	25	M	Burmese	9	6.53	Electrocution	Normal	N/A

F= female, M = male, PM = postmortem examination, N/A = not available, AMI = acute myocardial infarction, GAE = granulomatous ameobic encephalitis, SLE = systemic lupus erythematosus, ? = suspected, Hx = history, ARDS = acute respiratory distress syndrome, ARF = acute renal failure, CA = cancer

RIN

Overall, RNA samples extracted from this series of autopsy were of medium quality, according to RIN measured and calculated by Anglent 2100 Bioanalyzer (median = 5.7, IQR = 4.2 – 6.4). The RIN significantly differ between the areas of the brain (P = 0.024) and the thalamus was likely to have a lower RIN than the other areas. However, the preservation techniques did not affect the RIN (P = 0.301) (Table 6-3).

It is noteworthy that, when considering each case, the thalamus did not have the lowest RIN in every case and the patterns of RIN across different areas of the brain varied from case to case (data not shown). For example, the pattern of RIN in one case might be cortex > thalamus > medulla, but in another case the pattern might be medulla > cortex > thalamus.

Table 6-3. Summary of RNA sample quality as measured by RIN and purity ratios (A260/A280 and A260/A230)

		A260/A280	A260/A230	RIN
Overall		2.08 (2.06-2.09)	2.14 (1.94-2.24)	5.7 (4.2-6.4)
Preservation technique	LN	2.08 (2.06-2.08)	2.11 (1.85-2.16)	5.35 (3.8-6.3)
	RNAlater A	2.08 (2.06-2.09)	2.17 (1.97-2.24)	6 (4.9-7)
	RNAlater B	2.08 (2.06-2.09)	2.19 (1.99-2.24)	5.35 (4-6.4)
	P-value*	0.696	0.755	0.301
Area of the brain	Cortex	2.08 (2.08-2.1)	2.15 (1.94-2.25)	6.15 (5-7.3)
	Thalamus	2.08 (2.06-2.09)	2.21 (2.1-2.27)	4.45 (3.9-6)
	Medulla	2.07 (2.06-2.08)	2.06 (1.83-2.2)	6 (4.7-6.4)
	P-value*	0.048	0.017	0.024

*Kruskall-Wallis, Data presented as median (IRQ)

Post-mortem interval between death and autopsy (PMI)

There were significantly negative correlations between PMI and A260/A230 ratio (Spearman's rho = -0.262, P =0.012), and RIN (Spearman's rho = -0.375, P =0.002). No correlation with A260/A280 was found. Interestingly, even with the shortest post-mortem delay, the brain of case

CU9 (four-hour PMI) had relatively low averaged RIN (4.36), whilst the brain from case CU1 (five-hour PMI) had the highest averaged RIN (7.33). The examples of electropherogram of some samples from CU1 and CU9 were presented in Figure 6-3.

RNA yield

RNA extraction from the brain samples in this autopsy series using RNeasy Lipid Tissue Mini Kit (Qiagen, UK) yielded high amounts of total RNA (median 851 ng/ml, IQR = 709 – 1093 ng/ml, total 60 ml). As expected, RNA extraction quantity was significantly correlated with the amount of starting material (Spearman's rho = 0.454, P <0.0001). However, there were unexpected significant correlations between the RNA yield and A260/A280 ratio, A260/A230 ratio and RIN (Spearman's rho = 0.321, 0.223, 0.264; P =0.002, 0.034, 0.033, respectively).

6.4 Discussion

This project started from a desire to utilise advances in molecular pathology to gain a better understanding of the pathophysiology of severe malaria. All techniques in molecular pathology require well-preserved nucleic acids and proteins to work following extraction from tissues, which is not compatible with FFPE preservation and processing, such as is routinely and conveniently used in post-mortem tissue collection and routine histology. Thus, MEMA was designed with one specimen-collection method being small tissue samples taken into RNAlater, for subsequent molecular pathological studies including the integrated analysis of miRNA and mRNA expression profiling in the brain of fatal malaria as will be shown in Chapter 7.

The most common method of preserving tissues intended for RNA analysis is snap freezing, either in the liquid phase or vapour phase of LN. However, this requires trained technicians, specialised equipment and access to LN, which were not available in Beira. In addition, power supply fluctuations make the −70˚C freezer unreliable for tissue storage after snap freezing. In

order to circumvent these limitations, an alternative way to preserve tissue 'on site' has to be found, ideally using a method which would ensure stability at fridge or even room temperature.

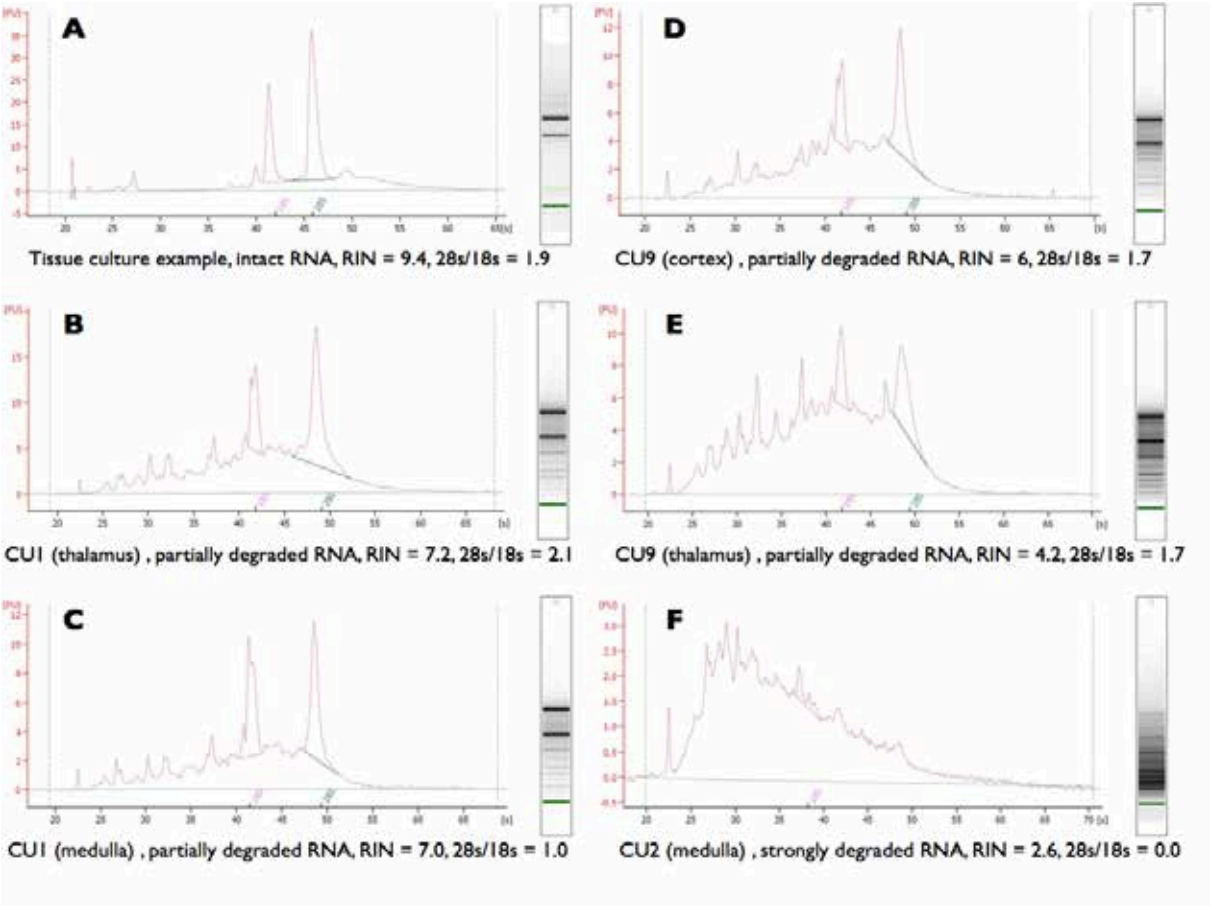

Figure 6-3. Digital gel-electrophoresis-like image and electropherograms of six representative RNA samples
(A) High-quality RNA sample from tissue culture. (B – C) RNA samples from case CU1 which had PMI of five hours. These two samples had good quality of RNA according to RIN values; however, rRNA ratios of these samples were dramatically different. Sample C with rRNA ratio of 1.0 would have been traditionally considered as a poor quality RNA sample. This evidence proved that the ratio of ribosomal bands does not reliably represent RNA degradation because this ratio takes only degradation of rRNA into account. (D-E) RNA from case CU9 with four-hour PMI. This case was a good example of the existence of unpredictable and unexplainable confounds affecting RNA quality. Even with the similar pre- and post-mortem conditions as case CU1, this case (CU9) had much poorer RNA quality than case CU1. Moreover, the RIN value of thalamus was considerably lower than that of cortex of the same brain with the same preservation technique. (F) This RNA sample from case CU2 showed highly degraded RNA. This case had prolonged agonal status.

There is an increasing number of studies that use commercially available RNA stabilising reagents as an alternative to snap freezing for collection of human tissue. RNAlater (Ambion), which is compatible with most RNA isolation protocols and downstream application including RT-PCR and microarrays, is most widely tested and used. This reagent eliminates the need to immediately process or snap freeze the tissue because tissue stored in this solution at room temperature for one week gives comparable RNA yield and quality to snap freezing tissue. Tissue in RNAlater can also be stored at –20°C or –80°C for long-term preservation after allowing thorough penetration of the solution into the tissue at room temperature or 4°C. Therefore, submerging tissue in RNAlater seemed to be a better solution for tissue collection in MEMA instead of LN.

Data from the Bangkok series showed that storage of fresh human brain tissues in RNAlater at room temperature of a tropical country (27–35°C) for 24 hours before storing in a normal domestic freezer at –20°C did not decrease the quality of RNA, compared to snap freezing in LN which required much more specialised procedures and equipment. This finding led us to use RNAlater for tissue preservative in Mozambique, because the ambient room temperature is much higher in tropical countries than temperate countries where most publications on RNAlater originate. This finding enabled me to design a specimen-collection protocol that was practical for conducting research in a resource-limited place as in Mozambique and later transporting the specimens to a well-equipped central laboratory in Oxford for subsequent molecular biology techniques.

Post-mortem interval was still one of the key factors determining tissue quality. It was significantly negatively correlated with the RIN and A260/A280 ratio in the optimisation study. This finding suggested that the autopsy and tissue collection should be conducted as soon as possible after death to minimise RNA degradation. However, tissue quality was not only affected by post-mortem factors. Pre-mortem agonal factors were contributing factors affecting tissue quality. This was supported by the finding that the two cases with the shortest post-mortem delay (CU9 and CU1) had a significant difference in RNA degradation. CU9 (four-hour PMI) had averaged RIN

of 4.36, while CU1 (five-hour PMI) had averaged RIN of 7.33. In addition, the case with the lowest RIN in this autopsy series is CU2, who had prolonged agonal status before death. These indicated that patient course pre-mortem was an important source of variation of the tissue quality.

Data also showed that all tested perseveration techniques were compatible with the RNA isolation kit by Qiagen and they all yielded a high quantity of high-purity RNA. This assured us that post-mortem tissue in RNAlater was compatible with the RNA isolation kit designed for fresh frozen tissue and the quantity and quality of RNA were not affected by different preservation techniques. Previous studies of other neurological diseases had shown that RNA could be successfully isolated and used for molecular pathology techniques, despite doubts from scientists (rather than pathologists) as to the value of tissues taken at autopsy (Tan et al. 2009; Mitsios et al. 2007; Tatro et al. 2010).

In conclusion, the main cause of variability in post-mortem tissue quality for subsequent RNA extraction was the tissue source (e.g. clinical history of an individual patient). Some factors could not be explained such as the variability of quality in tissue from a different area of the same brain or different patient with the same agonal and post-mortem intervals. Post-mortem factors, especially PMI, inevitably contribute to RNA degradation, but can be controlled by a well-designed study. Other factors clearly cannot – they appear dependent on the patient, who – if they have had a prolonged agonal course – may have RNA degradation. Tissue in RNAlater had a similar RNA quality to that of fresh frozen tissue and was compatible with the similar RNA isolation kit. The use of RNAlater as an RNA preservative at normal ambient temperature opens the opportunity for human tissue collection in resource-limited settings for subsequent molecular-based studies.

Chapter 7

Integrated Analysis of miRNA and mRNA Expression Profiling in the Brain of Fatal Human Malaria Cases

7.1 Introduction

This chapter presents the results of the first large-scale profiling of mRNA and miRNA expression in the human brain from fatal cases of falciparum malaria. The aims were to validate the use of post-mortem human tissue in molecular pathological studies of human malaria and identify new biological pathways potentially associated with the pathogenesis of severe malaria.

Genome-wide screening of mRNA and miRNA transcript expression profiling was performed on 18 brain samples from three malaria and three control deaths in the MEMA autopsy study (three matched areas of the brain in each case), using microarray technology. Significant differences in mRNA and miRNA expression patterns were identified between the brains of malaria and non-malaria deaths. An integrated analysis of the miRNA and mRNA expression profiles was conducted using bioinformatics software, in order to examine the likely interactions between miRNA and mRNA differentially expressed in the same brain specimen. This technique, using *in silico* algorithms, identified putative mRNA targets of dysregulated miRNAs whose expression correlated with the inverse expression of the predicted mRNA targets. The biological significance of these dysregulated molecules was examined using Ingenuity Pathway Analysis, which uncovered a wide range of biological mechanisms associated with severe malaria pathophysiology, and

allowed comparison with families and pathways of gene expression previously studied in other diseases.

7.2 Material and methods

7.2.1 Malaria and non-malaria cases

A total of six cases was included from the MEMA autopsy study as detailed in Chapter 6. Three of these were fatal malaria cases and the other three were deaths without malarial infection. The clinical diagnosis of these children was made by clinical history, physical examination and laboratory results. The confirmation of malaria diagnosis was made by blood smears and malaria RDT Paracheck-Pf®. The cause of death was reviewed and confirmed by full autopsy. Detailed information on the six cases was summarised in Table 6.1.

7.2.2 Brain specimens

The brain specimens were collected at autopsy, using a sterile technique cutting tissue on a petri dish on top of a cooled metal table pre-treated with 70% ethanol and the RNAzap solution, to remove environmental RNases. The tissue was immediately preserved in RNAlater solution, as previously described in section 2.2, cooled at 4°C for 24 hours, then transferred to a –20°C freezer. It was transported to Oxford at ambient temperature followed by –20°C storage until use. Total RNA including mRNA and miRNA were isolated as described in section 2.6. The quality of the isolated RNA samples was assessed by Nanodrop and Bioanalyzer 2100 as described in section 2.7 prior to microarray experiments. Three areas of the brain including the cortex, thalamus and medulla were preserved from each individual (total n = 18 brain samples) and included in the microarray study.

7.2.3 miRNA expression profiling

The miRNA profiles of the brain specimens from malaria (n = 9) and non-malaria (control, n = 9) were generated using Affymetrix GeneChip miRNA Array version 2, which provides complete coverage of human miRNA listed on the Sanger miRBase database release 15 (April 2010). The microarray hybridisation, scanning and data processing were done according to the manufacturer's protocol, as described in section 2.8.

7.2.4 Whole-genome expression profiling

The mRNA profile of the same brain specimens as used in the analysis of the miRNA profile was generated using Illumina Human-12 V4 BeadChip, which provides genome-wide transcriptional coverage of the 47,231 transcripts listed in the NCBI Human RefSeq Release 38 (November 2009) and the legacy UniGene database. The laboratory procedures associated with the Illumina microarray platform (including array hybridisation and scanning) were carried out in collaboration with the High-Throughput Genomics groups at the WTCHG, Oxford University, and the data processing and analysis were performed by the author, as described in section 2.9. The data processing pipeline for gene expression analysis is summarised in Figure 2-2.

7.2.5 Pathway analysis

The pathophysiology of CM is complex and multi-faceted, and thus information can be lost when responses of the host to malaria parasites are examined in a reductionist fashion, i.e. one or a few genes at a time. Genomic approaches using whole-genome microarray technology have emerged as a very useful tool to examine the responses of the system as a whole at the transcriptional level. However, this generates a large dataset which represents a challenge to attempts at analysis and extrapolation to biologically meaningful results. To facilitate the analysis of the gene microarray data, *in silico* genomics network analyses have been proposed (reviewed in Nam and S. Y. Kim

2008), and Ingenuity Pathways Analysis (IPA) (Ingenuity® Systems, www.ingenuity.com) is one of the widely used software packages.

IPA is a web-based pathway analysis tool for subsequent bioinformatics analysis to microarray data interpretation, which creates a series of analyses termed network, functional and canonical pathway analyses. IPA groups differentially expressed genes (DEGs) into known functions, pathways and networks based primarily on other published studies. The Ingenuity Pathways Knowledge Base (IPKB), which is the database behind the IPA software, is a manually curated database that is built on published, peer-reviewed scientific literature, and continuously updated.

In this chapter, IPA Spring Release 2012 was used to identify the biological and molecular networks underlying changes in brain samples from malaria, compared to controls, by mapping gene expression data into biologically relevant pathways and networks based on their functional annotation and known molecular interactions.

Approach used in IPA

The following analyses were run on the dataset of DEGs generated from microarray analysis.

Functional analysis of an entire dataset. The functional analysis identified the biological functions that were most significant to the dataset. DEGs from malaria patients (fold-change cutoff of 1.5) that were associated with biological functions and/or diseases in Ingenuity's Knowledge Base were considered for the analysis. The right-tailed Fisher's exact test was used to calculate a *P*-value, determining the probability that each biological function and/or disease assigned to that dataset is due to chance alone. In IPA, biological processes and disease or toxicological functions are also referred to collectively as functions.

Canonical pathway analysis of an entire data set. Canonical pathway analysis identified canonical pathways from the IPA library that were most significant to the dataset. DEGs from the dataset that met the fold-change cutoff of 1.5 and were associated with a canonical pathway in IPKB were

considered for analysis. The significance of the association between genes from the dataset and the canonical pathway (in the IPKB) was measured in two ways as described in the IPA documentation: 1) a ratio was calculated of the number of genes from the dataset that map to a given pathway divided by the total number of genes making up the canonical pathway; and 2) Fisher's exact test was used to calculate a *P*-value determining the probability that the association between the genes in the dataset and the canonical pathway is explained by chance alone.

Network analysis. DEGs successfully imported and mapped into IPA are called Network Eligible Molecules, which were overlaid onto a global molecular network developed from information contained in Ingenuity's Knowledge Base. Networks of Network Eligible Molecules were then algorithmically generated based on their connectivity. The generated networks were then ranked by the network score in order of their degree of significance. The score took into account the number of Network Eligible Molecules in the network and its size, as well as the total number of Network Eligible Molecules analysed and the total number of the molecules in the IPKB that could potentially be included in networks. The score was based on hypergeometric distribution and was the negative exponent of the right-tailed Fisher's exact test result. The IPA network generation algorithm is summarised in Calvano et al. (2005).

Network graphical representation. A network or pathway is a graphical representation of the relationships between molecules. Molecules are represented as nodes and the biological relationship between two nodes is represented by a line, which represents an association supported by at least one reference from the literature, textbook, or canonical information stored in the IPKB. The intensity of the node colour indicates the degree of up- (red) or down- (green) regulation. Nodes are displayed using various shapes that represent the functional class of the gene product.

In IPA, canonical pathways are distinct from gene networks in several ways. Networks are generated *de novo* based on the input data and do not have directionality. Canonical pathways are

generated prior to data input by IPA (e.g. are based on existing studies in IPKD) such as 'JAK family kinase' or 'IL-6 signalling') and have directionality.

7.3 Results

7.3.1 Overview of the mRNA expression data generated in 18 brain samples

The genome-wide mRNA profile of the brains from malaria samples (n = 9) and non-malaria samples (control, n = 9) were generated using Illumina HumanHT-12 V4 BeadChip array. These 18 brain samples were from six individuals (three malaria cases vs. three control cases), whose brains were sampled from the three matched areas of the cortex, medulla and thalamus. Expression of 43,225 mRNA transcripts was detectable in at least one sample, either in malaria or non-malaria samples by our analysis pipeline.

Unsupervised cluster analysis

Unsupervised cluster analysis of complete mRNA transcripts in all samples was conducted using several hierarchical clustering algorithms available in GeneSpring GX version 11.5. All the algorithms used revealed heterogeneity of the mRNA expression patterns in the brain samples which could not be clustered according to malarial infection status or the areas of the brain. Figure 7-1 shows the unsupervised cluster analysis using a Euclidean distance measure and centroid linkage rule. This heatmap contrasts with the results of the miRNA clustering analysis for the kidney (Chapter 5), which did show clustering of malaria cases compared to controls. The lack of a clear association between patterns of gene expression in malaria is due to the low statistical power imposed on the analysis by the relatively limited number of cases.

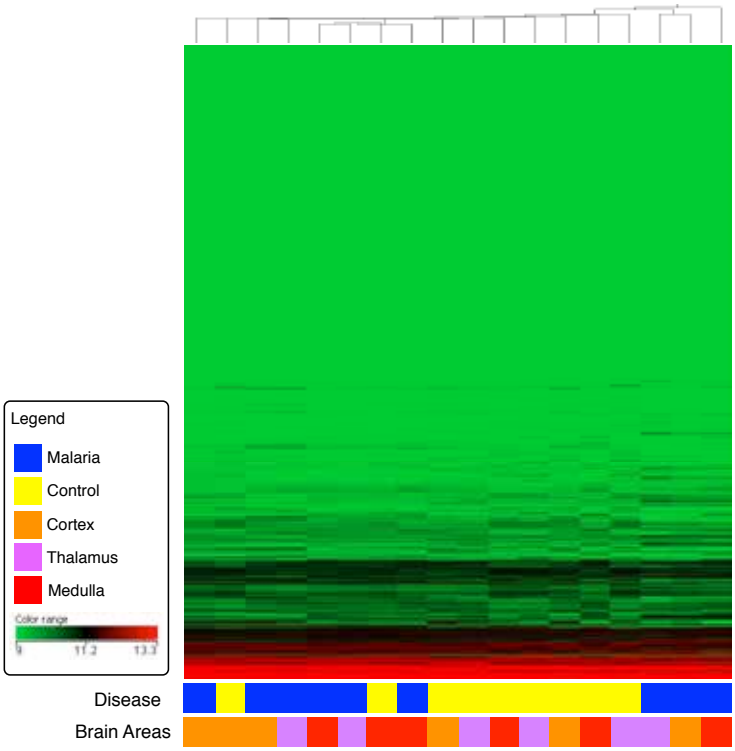

Figure 7-1. Unsupervised hierarchical cluster analysis of total mRNA expression data from the brain of malaria and control samples

The heatmap shows the whole-genome expression values of more than 47,000 well-characterised genes and splice variants, which cannot be clustered according to malaria infection status or the areas of the brain. Heatmap colour represents relative mRNA expression as indicated in the colour key.

Differential expression analysis of mRNA transcripts in malaria vs control cases

Initially, genes were filtered for statistical significance using Benjamini and Hochberg's FDR with an FDR-adjusted *P*-value (q-value) cutoff of 0.05 and fold-change cutoff of 0.05. However, at this statistical stringency, only 22 DEGs were found, which is too low for generating meaningful pathway analysis. Thus, the statistical stringency was adjusted to use a raw *P*-value to rank genes by likelihood of differential expression with a cutoff of 0.05 and fold-change cutoff of 0.05, which gave 223 DEGs. Table 7-1 shows the numbers of DEGs at different statistical stringency. Of 223 mRNA transcripts, 172 were up- regulated and 51 were down-regulated in malaria compared to control cases. Table 7-2 and Table 7-3 show the top 10 up-regulated and down-regulated genes in severe malaria compared to control cases, respectively. The list of DEGs was then used for IPA. A complete list of the 223 DEGs is presented in Appendix C, Table C-1 and C-2.

Table 7-1. The number of DEGs at various levels of statistical stringency

Probeset Counts for Different Cutoffs												
Fold Change Cutoff	1	1.1	1.2	1.5	2	2.5	3	3.5	4	4.5	5	10
q≤0.001 (FDR)	0	0	0	0	0	0	0	0	0	0	0	0
q≤0.01 (FDR)	5	5	4	3	0	0	0	0	0	0	0	0
q≤0.05 (FDR)	113	106	90	22	5	2	1	1	1	1	0	0
q≤0.1 (FDR)	415	380	284	54	11	5	3	2	2	2	1	0
q≤1 (FDR)	30310	6842	2777	319	49	18	9	6	3	2	1	0
p≤0.001	389	360	269	53	11	5	3	2	2	2	1	0
p≤0.01	1585	1285	850	133	25	12	6	4	2	2	1	0
p≤0.05	4278	2937	1669	223	41	17	9	6	3	2	1	0
p≤0.1	6588	3996	2073	266	44	17	9	6	3	2	1	0
p≤1	30310	6842	2777	319	49	18	9	6	3	2	1	0

7.3.2 Pathway analysis on DEGs associated with Malaria

The DEGs associated with severe malaria were uploaded into IPA along with the gene identifiers and corresponding fold-change values. 220 DEGs were successfully mapped to their corresponding gene objects in IPKB, while the current version of IPKB could not map the other three DEGs, i.e. LOC728643, HLA-H and LOC644936. The following analyses were run on this dataset.

Functional analysis: Overall

IPA functional analysis has three primary categories of functions: 1) Disease and Disorder; 2) Molecular and Cellular Functions; and 3) Physiological System Development and Function. There are currently 85 high-level (Level-1) functional categories classified under these three primary categories. Functions in IPA are categorised into several levels. The lower-level functions are classified within the higher-level functional categories. The lowest level function in IPA, named "specific-level function", contains a population of associated molecules (e.g. mRNA transcripts) according to IPKB. The lower-level function and specific-level function might be classified within multiple high-level functional categories. The high-level (Level-1) functions will be written in *italic* in this section for easy recognition.

Table 7-2. List of the top-10 up-regulated genes in malaria

Gene symbol	Entrez gene name	Fold change	*P*-value	Summary of gene function
HBA1/HBA2	Haemoglobin, alpha 1	5.037	0.0006	Haemoglobin alpha chain is involved in oxygen transport and deletions lead to thallasaemia. Also plays a role in erythrocyte development; hydrogen peroxide catabolic process; positive regulation of cell death; and regulation of neuronal cell death due to hypoxia
FCGBP	Fc fragment of IgG binding protein	4.529	0.0001	Mucin-like protein expressed in colon and placenta, with roles in immune protection and inflammation. Implicated in ulcerative colitis
HAMP	Hepcidin antimicrobial peptide	4.335	0.0143	Cellular iron ion homeostasis; defence response to pathogens; immune responses, acute phase response protein
S100A8	S100 calcium binding protein A8	3.879	0.0107	Myeloid cell-related calcium-binding protein, found in cytoplasm of a variety of cells. TLR-4 signalling agonis implicated in CNS ischaemia/hypoperfusion injury. Acute inflammatory response protein; induces chemotaxis
CCL2 / MCP-1	Chemokine (C-C motif) ligand2 = Monocyte Chemotactic Protein-1	3.528	0.0096	A chemokine-causing leukocyte localisation, adhesion and chemotaxis in response to cytokine-mediated activation of endothelium; modulates immune and inflammatory responses; positive regulation of NOS and synaptic transmission; Signal transduction in Angiogenesis and Apoptosis for molecules like TGFb and VEGF
SPP1 / OPN	Osteopontin = secreted phosphoprotein 1	3.525	0.0014	A small soluble phosphoprotein involved in biomineral tissue development, cell matrix adhesion, vitamin D responses and bone ossification. Also expressed by CNS cells and has a role in axonal response to injury and demyelination
S100A9	S100 calcium binding protein A9	3.362	0.0006	Intercellular EF-hand motif calcium-binding protein, actin cytoskeleton reorganization; cell-cell signalling; leukocyte chemotaxis and inflammatory responses. Can associate and self-assemble protein complexes with S100A8. Implicated in a number of disease processes
ANGPTL4	angiopoietin-like protein 4	2.918	0.0175	Soluble, hypoxic inducible angiopoietin-like molecule which induces vascular permeability, stimulates angiogenesis. Involved in the regulation of cellular lipid metabolic process and response to starvation. Decreases apoptosis and increases angiogenesis
SNAP25	synaptosomal-associated protein, 25kDA	2.889	0.0030	A SNARE protein involved in axonogenesis; calcium ion-dependent neurotransmitter secretion and uptake including glutamate and NMDA; endosome transport; energy reserve metabolic processes; potassium ion transmembrane transport; regulation of synapse assembly; Polmorphisms implicated in adult type ADHD
HILPDA, HIG2	hypoxia inducible lipid droplet-associated, Hypoxia inducible gene-2	2.853	0.0013	Hypoxia induced protein first identified in renal cell carcinoma cell lines. Regulation of cell proliferation through Wnt-1/Beta catenin signalling in epithelial tumours; promoter of lipid storage

The genes are sorted in order of degrees of fold-change.

Table 7-3. List of the top-10 down-regulated genes in malaria

Gene symbol	Entrez gene name	Fold change	*P*-value	Summary of gene function
PENK	Preproenkephalin	-3	0.042	A preprotein opioid neurotransmitter expressed in various neuronal subsets, involved in sensory perception of pain, satiety and behaviour. Decreased expression shown in HIV encephalitis, excitiotoxic injury and dependence syndromes. Involved in synaptic plasticity and remodelling.
IFI6	Interferon alpha-inducible protein 6-16	-2.668	0.000	Mitochondrial protein, induced by interferon, stabilises mitochondrial function and opposes apoptosis; implicated in innate immune responses to infections.
NNAT	Neuronatin	-2.646	0.023	Involved in neuronal differentiation, synaptic plasticity and brain development. Modulates dendritic calcium levels; calcium-dependent regulation of insulin secretion in pancreatic islet cells. Astrocye expression of NNAT reduced in HIV infection
IGFBP3	Insulin-like growth factor binding protein 3	-2.234	0.036	Induced by insulin-like growth factor receptor signalling pathway and hypoxia. Suppresses cell proliferation and protein phosphorylation via MAP kinase signalling cascade. Induces apoptotic process; regulation of cell growth and glucose related metabolic processes. Linked to hypocretin-expressing neurons in narcolepsy
LAMP5	Lysosomal-associated membrane protein family, member 5	-2.158	0.018	LAMP proteins are involved in phagocytosis, cellular responses to intracellular pathogens and have been implicated in chaperone-mediatied neuronal autophagy after hypoxic stress.
ISG15	ISG15 ubiquitin-like modifier	-2.149	0.002	Forms a complex with ubiquitin-like pathway and conjugates to target proteins, suppressing type I interferon and IFN-mediated signalling pathways, implicated in innate immune responses to chronic infections like HCV. In the CNS, cerebral protein ISGylation is neuroprotective following focal ischaemia
DLL3	Delta-like 3	-1.893	0.001	DLL3 is a ligand for the Notch signaling pathway;which is involved in a number of cell differentiation and development processes - somatigenesis, including skeletal and CNS development, angiogenesis, astrocyte differentiation and neurogenesis.
ALB	Albumin	-1.774	0.042	A serum protein involved in transport of a large number of proteins and metabolism. De novo synthesis of albumin in ischaemic neurons occurs via stimulation by hepatocyte nuclear factor-1a/p300 pathway in ischaemia
IFI27	Interferon, alpha-inducible protein 27	-1.768	0.001	Type I interferon-mediated signaling pathway, induced by IFN, related to important immune pathways such as antigen presentation, inflammation, apoptosis and response to viral infections. Activates apoptosis. Upregulated in brain in Venezuelan equine encephalitis viral infection
CD24	CD24A molecule	-1.754	0.001	A GPI-linked sialoglycoprotein expressed by many B cells and mature granulocytes involved in B cell activation, adhesion and migration; induction of apoptosis, positive regulation of MAP and protein tyrosine kinase activity; regulation of Wnt receptor signaling pathway. Expressed in brain and plays a role in diverse processes including adaptive immunity, inflammation, autoimmune diseases and cancer

The genes are sorted in order of degrees of fold-change.

Overall, using IPA to analyse the entire list of DEGs associated with severe malaria uncovered a wide number of significant biological functions, mainly associated with activation of immune- and inflammatory-related functions as well as overall inhibition of activities related to cell death.

Figure 7-2 shows significantly over-represented Level-1 functional categories based on *P*-value and the three primary categories. The functional analysis can also be visualised by a hierarchal heatmap of Downstream Effect Analysis, which predicts the effect of gene expression changes in our dataset on biological functions (Figure 7-3).

Functional analysis: Diseases and disorders

The current version of IPKB contains no database for molecular pathways in malaria disease. Therefore, associations with malaria in the Diseases and Disorders category would not appear in this IPA analysis. The most significant Level-1 function in this primary category was *Neurological Disease* and IPA predicted that it contained two decreased specific-level functions (progressive motor neuropathy and neuropathy), and that it contained increased demyelination. In *Inflammatory Response*, IPA predicted increased activities in inflammation, immune response, accumulation of myeloid cells, migration of phagocytes, chemotaxis of leukocytes, phagocytes and myeloid cells, recruitment and cell movement of phagocytes and monocytes.

Functional analysis: Molecular and cellular functions

The detailed inspection of the functional analysis results in this primary category revealed that there are a wide range of specific-level functions predicted to be significantly increased in malaria. These molecular and cellular activities (Level-1 functional categories are presented in parenthesis) included production of reactive oxygen species (in *Free Radical Scavenging*); recruitment of phagocytes, leukocytes and myeloid cells, adhesion of immune cells, response of blood cells and activation of neuroglia (in *Cell-to-Cell Signalling and Interaction*); migration, chemotaxis and recruitment of leukocytes, phagocytes and myeloid cells, homing of cells and blood cells, infiltration of leukocytes, and migration of cells, myeloid cells, phagocytes and granulocytes (in *Cellular*

Movement); accumulation of lipid (in *Lipid Metabolism*); quantity of metal and calcium, and accumulation of lipid (in *Molecular transport*).

In *Cell Death* (Level-1 function), although it contained significantly increased cell survival and apoptosis of hippocampal neurons, most of the specific functions in *Cell Death* were decreased (but not to a statistically significant level), including cell death of muscle cells, epithelial cells, connective tissue cells, T lymphocytes and leukocytes, activation-induced cell death and fragmentation of DNA. These results indicated an overall decrease in transcriptional activities leading to cell death. In *Cellular Function and Maintenance*, cellular homeostasis was significantly increased but assembly of microtubules and polymerisation of microtubules were decreased.

Functional analysis: Physiological system development and function

In this category, similar specific-level functions associated with the immune system that were predicted to increase in the other categories were also found. These specific-level functions include adhesion, chemotaxis, migration and infiltration of immune cells, including leukocytes, phagocytes, granulocytes, monocytes and myeloid cells (in *Hematological System Development and Function,* and *Immune Cell Trafficking*); and activation of neuroglia (in *Nervous System Development and Function*). However, decreased activity in relation to a specific-level function labelled as quantity of IgG (in *Humoral Immune Response*) was predicted.

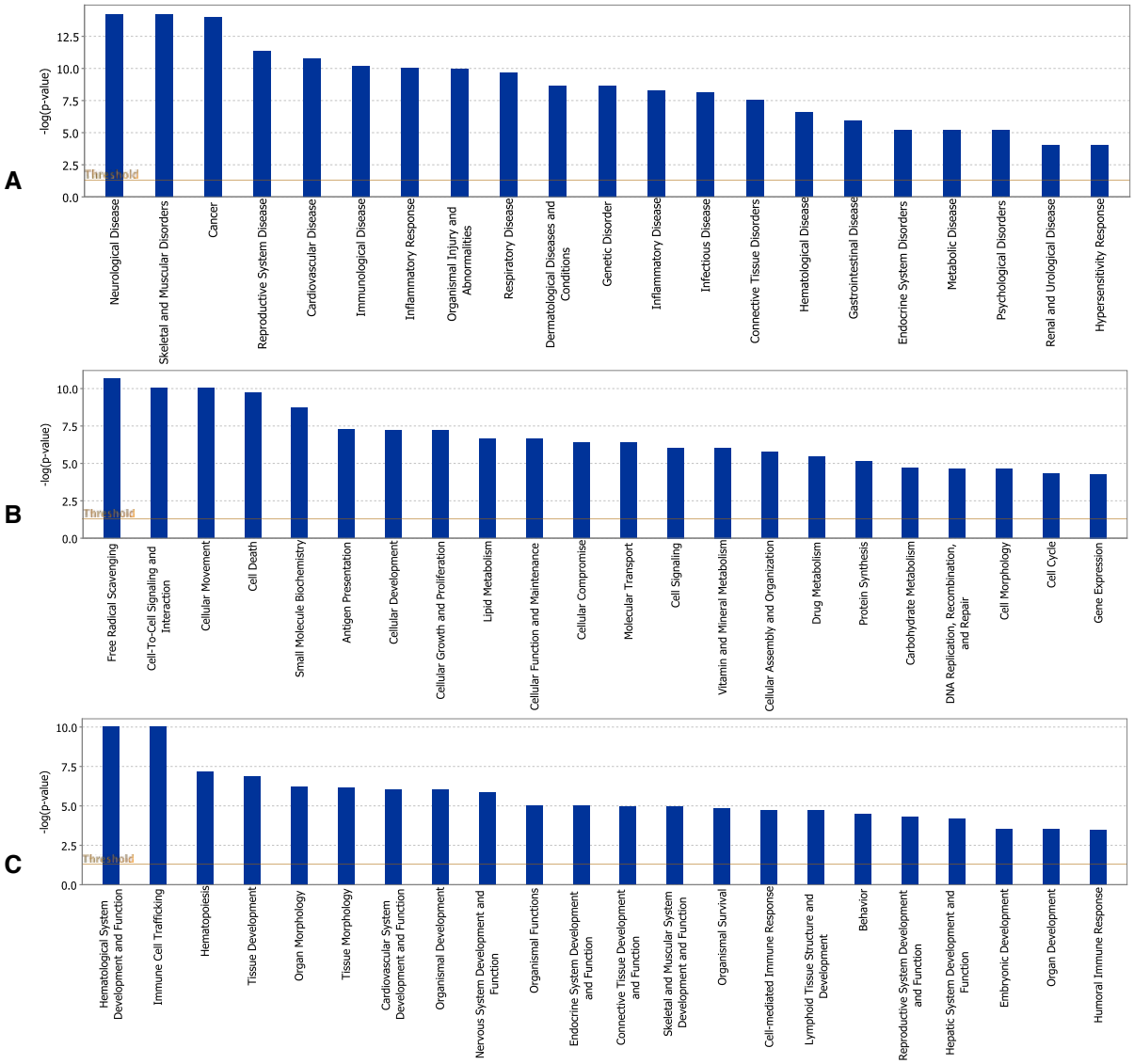

Figure 7-2. Functional analysis from IPA of the entire DEGs associated with malaria

This figure displays the most significant Level-1 biological functions that are over-represented in the dataset based on –log(p-value) (the higher the bar graph, the more significant p-value) and primary categories of functions: (A) Diseases and Disorders, (B) Molecular and Cellular Functions, (C) Physiological System Development and Function. The straight orange line indicates a *P*-value threshold of 0.05 (-log 1.3).

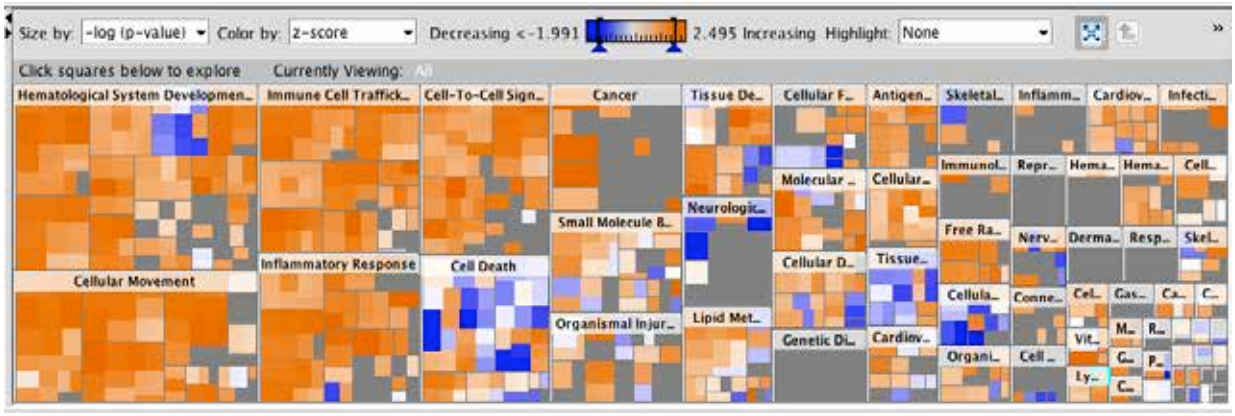

Figure 7-3. Hierarchical heatmap of the downstream effect analysis

The squares in the heatmap represent biological functions in IPA, which are categorised into three hierarchical levels: Level-1 (high-level function) e.g. *Cell Death, Cellular Movement* and *Cancer*; Level-2 (mid-level function); Level 3 (specific-level function) e.g. Free Radical Scavenging. The size of the squares reflects the –log(p-value) associated with the particular specific function. The colour of the squares reflects the direction of changes for the specific function based on z-score (Orange = positive z-score = increased function, blue = negative z-score = decreased function).

Canonical pathways

The top canonical signalling and metabolic pathways from DGEs associated with malaria are shown in Table 7-4. Detailed diagrams of selected pathways are shown in figures 7-4 and 7-5. As for the functional analysis, most canonical pathways detected via IPA analysis were related to immune or inflammatory functions. Most of the IPA canonical pathways significantly affected were signalling pathways (n = 76), while a few were metabolic pathways (n = 7).

Among the signalling pathways, the data revealed that children dying from malaria had numerous dysregulated genes associated with several mechanisms in immune and inflammatory responses, including the signalling pathways that regulate the acute-phase response of the immune system (e.g. JAK family kinases, IL-6 and IL-17A, glucocorticoid). However, other up-regulated signalling pathways were previously characterised as involved in chronic inflammation in other settings (e.g. Atherosclerosis, Type I diabetes mellitus and hepatic fibrosis). Other signalling pathways up-regulated in malaria indicate a cytokine storm phenomenon (e.g. Hypercyto-

kinemia), allergic response (e.g. IL-17F and IL-22), immune responses (e.g. dendritic cell maturation, HMBG1, production of NO and reactive oxygen species in macrophages, OX40, activation of IRF), and pathways which bridge between innate and adaptive immunity (e.g. IL-12).

Some significantly enriched pathways were directly associated with the central nervous system such as HMGB1 signalling (neurite outgrowth), Huntington disease signalling (neuronal death) and reelin signalling in neurons. Two significant pathways were associated with the calcium metabolism (VDR/RXR and LXR/RXR).

Relatively few metabolic pathways were found to be significantly changed in this analysis. The top five are the propanoate metabolism, nicotinate and nicotinamide metabolism, pyruvate metabolism, glycolysis/gluconeogenesis, and inositol phosphate metabolism.

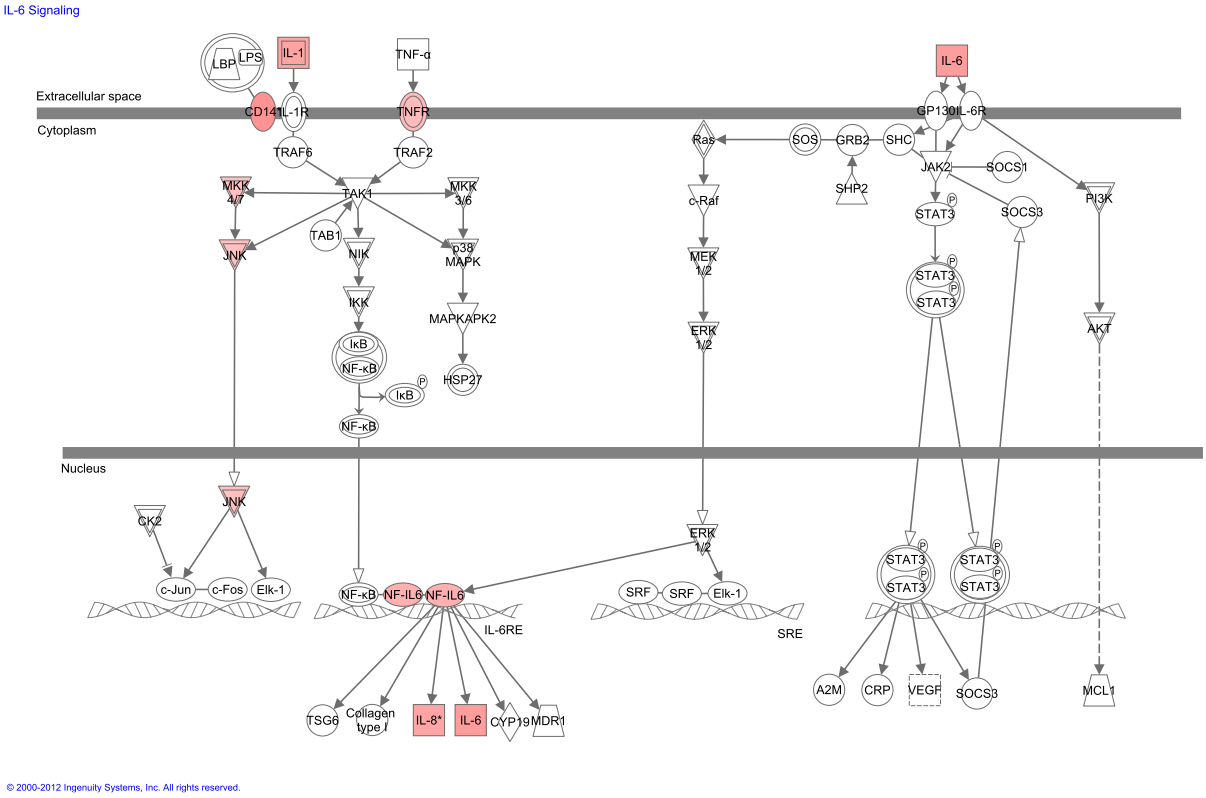

Figure 7-4. Canonical pathway showing changes in the IL-6 signalling pathway among 223 DEGs associated with malaria

Red denotes up-regulation and green denotes down-regulation of the gene.

Table 7-4. Top signalling and metabolic canonical pathways from IPA among the 223 DEGs associated with malaria

Ingenuity canonical Pathways	-log(p-value)	Ratio	Gene	Up/Down	Functions (from IPA)
Signalling pathways					
Atherosclerosis Signalling	5.2	0.070	129	8/1	Chronic inflammation pathway resulting from interaction between inflammatory cells, plasma lipoproteins and extracellular matrix of the arterial wall
IL-6 Signalling	4.31	0.065	124	8/0	Regulator of acute-phase responses and a lymphocyte stimulatory factor
LXR/RXR Activation	4.18	0.059	136	6/2	Involved in the regulation of lipid metabolism and inflammation
Dendritic Cell Maturation	4.15	0.049	185	7/2	Dendritic cells are key antige- presenting cells and important initiators of immune responses.
HGF Signalling	3.9	0.067	105	7/0	Stimulates cell proliferation, differentiation, motility and invasiveness
IL-17 Signalling	3.81	0.068	74	3/2	Promotes expansion and recruitment of innate immune cells, and stimulates production of beta-defensins and other anti-microbial peptides
Role of JAK family kinases in IL-6-type Cytokine Signalling	3.79	0.148	27	3/1	Acute-phase Inflammatory response
Communication between Innate and Adaptive Immune Cells	3.25	0.055	109	4/2	Cross talk between the innate and adaptive immune systems namely via soluble factors (chemokines and cytokines) and cell-to-cell communication.
Huntington's Disease Signalling	3.12	0.038	236	8/1	Late-onset neurodegenerative disorder characterized by a selective neuronal cell death in cortex and striatum
IL-12 Signalling and Production in Macrophages	3.12	0.045	155	5/2	IL-12 serves as a bridge between innate and adaptive immunity
Production of Nitric Oxide and Reactive Oxygen Species in Macrophages	3.04	0.038	210	6/2	Important pathways of extra and intracellular infection control
IL-10 Signalling	3	0.064	78	5/0	Limit and terminate the inflammatory response
Hypercytokinemia/hyperchemokinemia in the Pathogenesis of Influenza	2.83	0.091	44	4/0	This phenomenon is referred to as a 'cytokine storm'
Reelin Signalling in Neurons	2.71	0.061	82	3/2	In the hippocampus, reelin regulates the growth and/or distribution of afferent entorhinal and commissural axons.
IL-22 Signalling	2.62	0.080	25	2/1	A novel cytokine belonging to the IL-10 family, suggesting its involvement in the generation of inflammatory and allergic responses.
Metabolic pathways					
Propanoate Metabolism	2.44	0.033	122	4/0	-
Nicotinate and Nicotinamide Metabolism	2.29	0.037	135	5/0	-
Pyruvate Metabolism	2.19	0.030	135	4/0	-
Glycolysis/Gluconeogenesis	1.78	0.031	130	4/0	-
Inositol Phosphate Metabolism	1.55	0.026	194	5/0	-

The –log(p-value) denotes the significance of the enrichment of a pathway within the DEGs dataset. The larger the –log(p-value), the less likely that association is random and the more significant the association. Also shown are the Ratio (the number of DEGs associated with the pathway/total number of genes known to be associated with the pathway), Gene (the total number of genes known to be associated with the pathway), and Up/Down (the number of up- and down- regulated DEGs in the pathway).

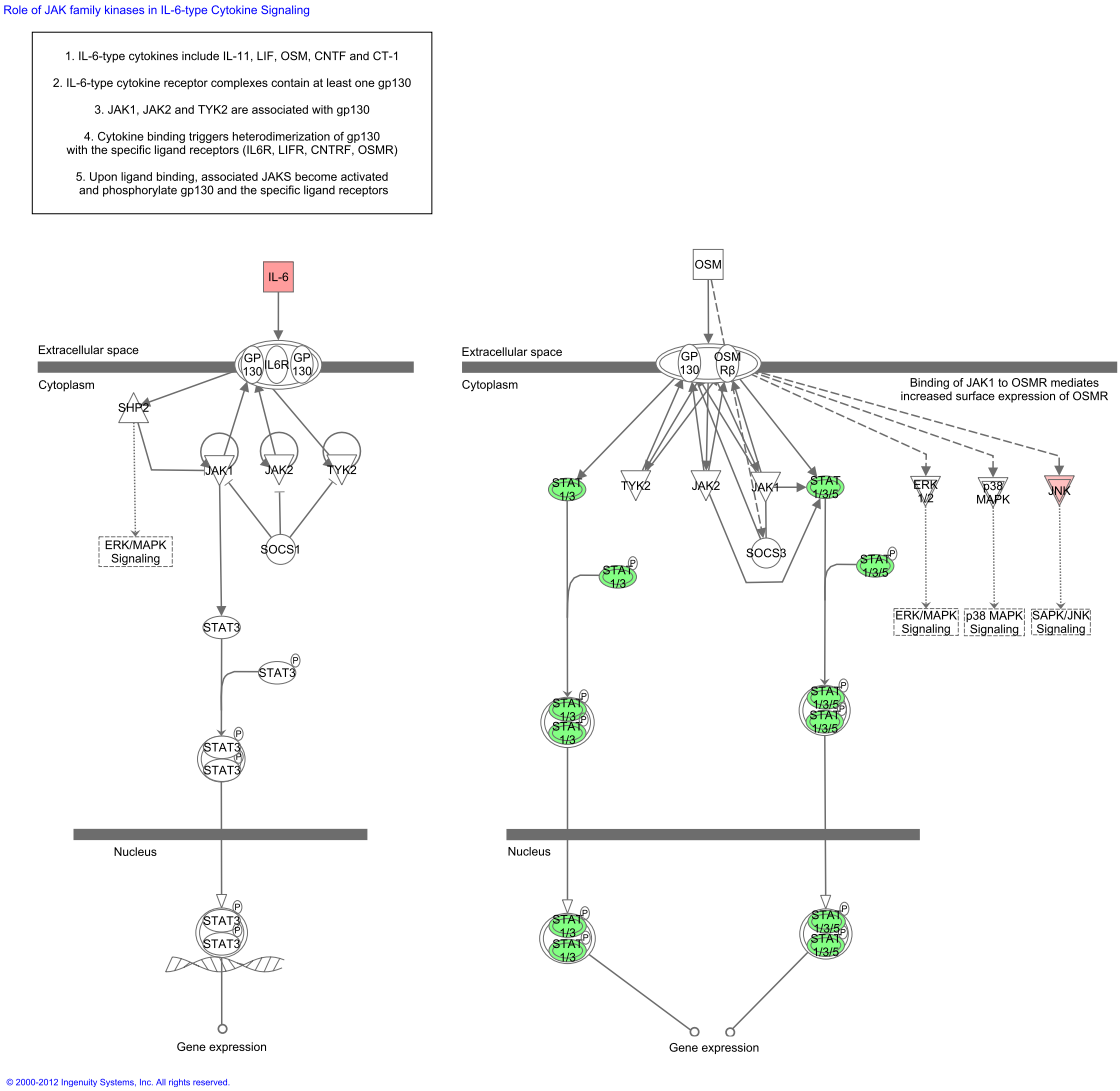

Figure 7-5. Canonical pathway showing changes in the role of JAK family kinases in IL-6- type cytokine signalling pathway, among 223 DEGs associated with malaria

Red denotes up-regulation and green denotes down-regulation of the gene.

Network analysis

A total of 16 significantly enriched networks associated with malaria were identified within IPA analyses using DEGs from the whole-genome microarray experiment (Appendix C, Table C-3). The top five networks were merged to form a single network representing the potential major interactions of transcriptional molecules underlying host response to malarial infection in the human brain (Figure 7-6). These networks included a total of 175 genes interconnected with 84 DEGs involved in network functions, including Neurological Disease, Cell-To-Cell Signalling

and Interaction, Inflammatory Response, Cell Cycle, Lipid Metabolism, Humoral and Cell-mediated Immune Responses, and Protein Synthesis. Examples of three of these networks are shown in figures 7-7 to 7-9

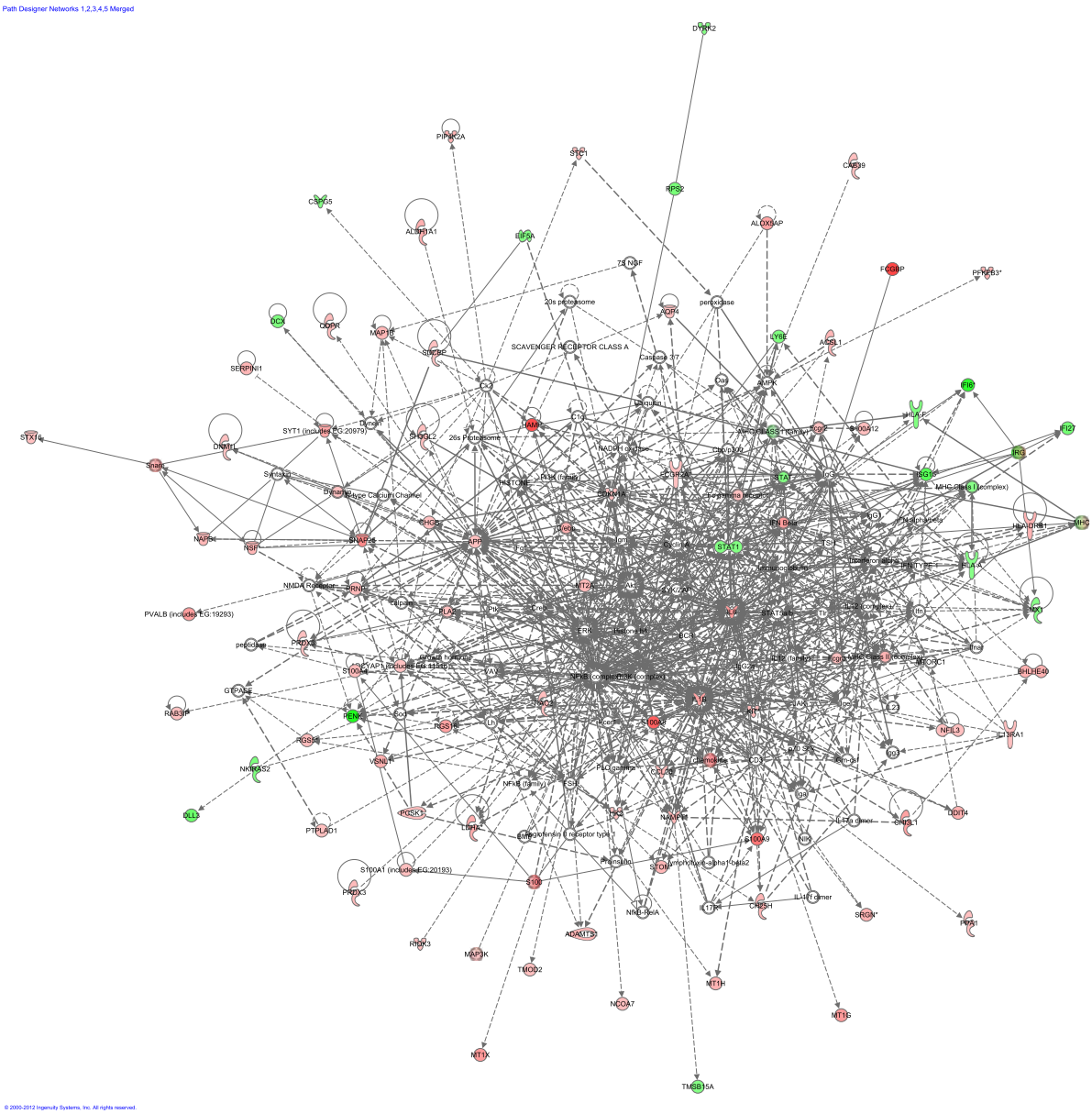

Figure 7-6. An overall gene network representation of mRNA changes and their relationship with potential biological processes in malaria cases

The network was generated from merging the top-five networks from IPA analyses, consisting of a total of 173 genes interconnected with 86 genes dysregulated in malaria cases compared to controls. Genes are represented as nodes and a biological relationship between two nodes is represented as a line (solid line = direct relationship and dashed line = indirect relationship). The arrows indicate directionality of the interaction (e.g. A acts on B). Red denotes up-regulation and green denotes down-regulation of the gene.

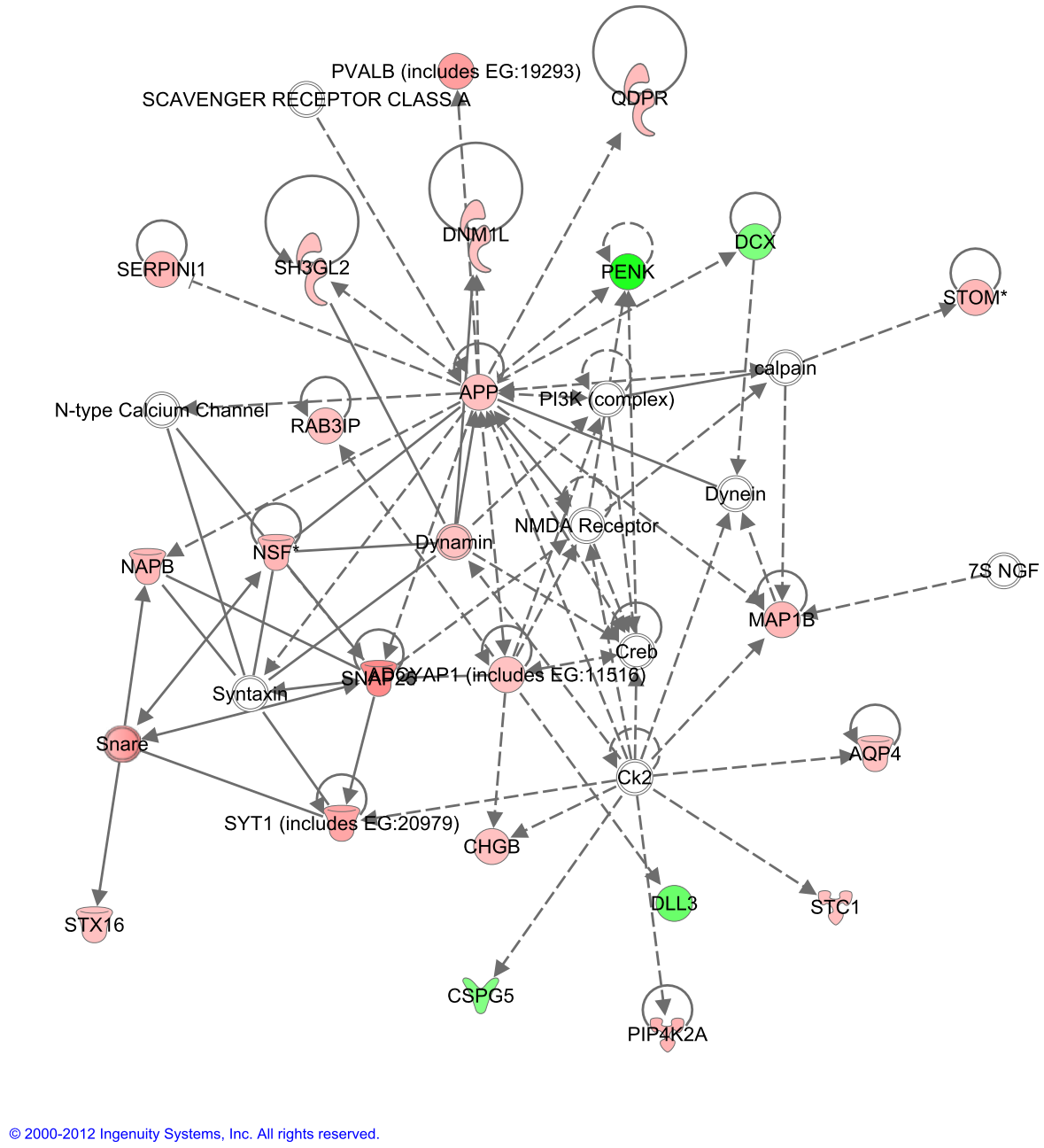

Figure 7-7. The representative gene network 1 derived from IPA network analysis of the DEGs in malaria cases
This network shows significant increases in the APP gene. β-APP protein is known to be increased in the brain in severe malaria, as a marker of axonal injury. Other up-regulated transcripts in this pathway code for the proteins SNAP35 and SNARE, which regulate neuronal transmission at synapses. Another member of this network is the Aquaporin gene AQP4, which controls water transport in endothelial cells and neurons/microglia. PENK, a precursor of the opioid neurotransmitter proenkephalin is down-regulated in this network.

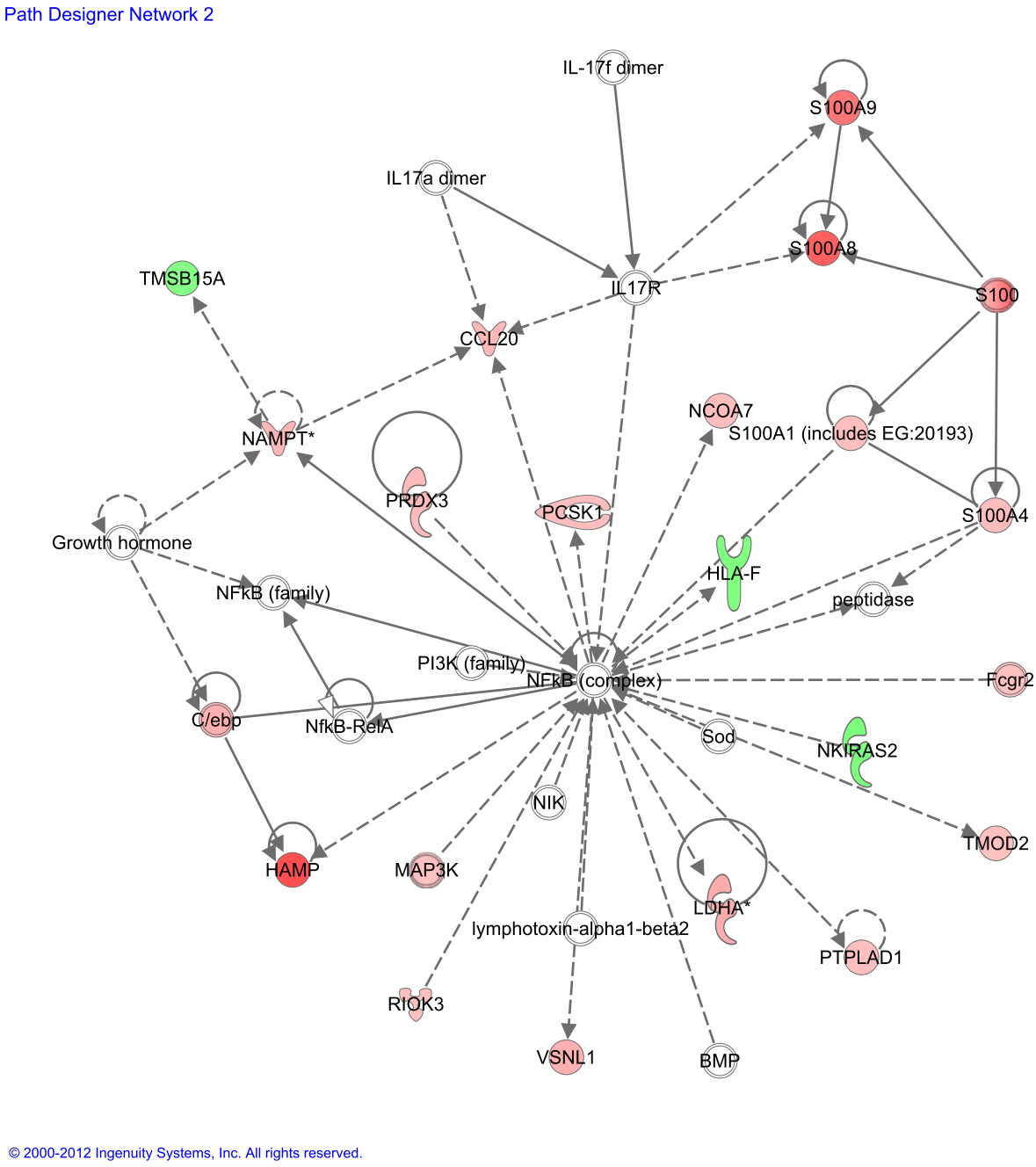

Figure 7-8. The representative gene network 2 derived from IPA network analysis of the DEGs in malaria cases
This network shows marked up-regulation of the gene coding for HAMP, a hypoxic inducible lipid raft-associated protein. Transcripts for S100 proteins are also significantly up-regulated. Several intracellular signalling pathways including MAP-kinase and PCSK are increased but no overall change in transcript for NF-κB was found.

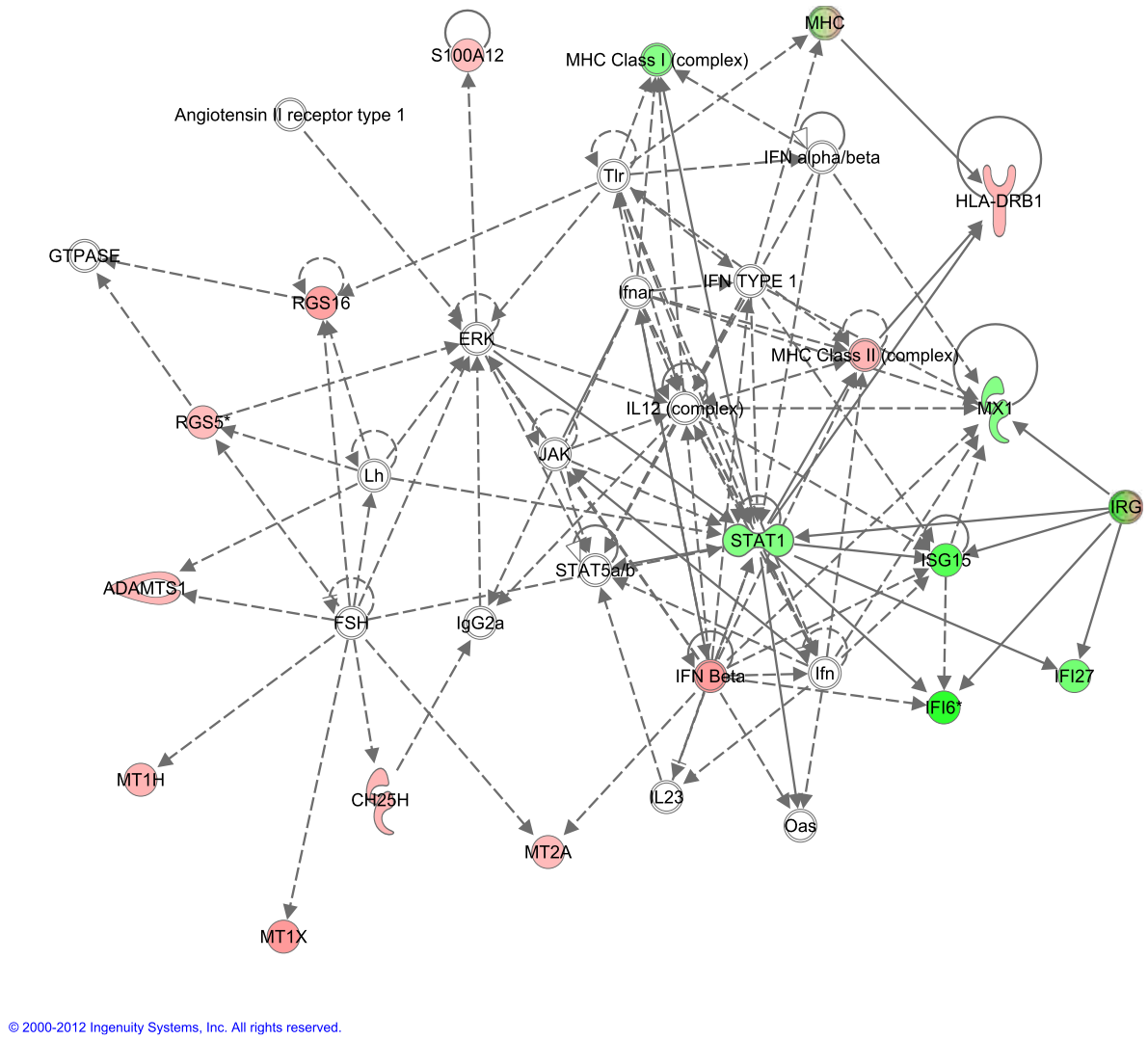

Figure 7-9. The representative gene network 5 derived from IPA network analysis of the DEGs in malaria cases
This network shows results including cytokine and other transcripts. This confirmed the known association of increased ADAMTS expression in the brain in malaria. INF-β transcript expression was increased whilst IFN-γ was decreased, despite this being an important effector molecule in the murine model of CM. Several interferon-inducible effector molecules were also down-regulated, including IFI6 and IFI27.

7.3.3 Overview of the miRNA expression data generated in 18 brain samples

All miRNA samples used in this miRNA microarray analysis were extracted from the same piece of the brain tissue used for the above whole-genome mRNA Illumina microarray. The expressions of 729 human mature miRNAs were determined to be detectable in at least one sample, either in malaria or non-malaria brains, by our analysis pipeline (on the basis of "detected above background" in Affymetrix miRNA QC Tool software).

A total of 625 miRNAs were present in at least one malaria sample and 699 miRNAs were present in at least one control sample. The Venn diagram in Figure 7-10A shows that 30 miRNAs were present only in the malaria group but not in the control and that 104 miRNAs were present only in controls but absent in malaria. Most of the miRNAs (595 miRNAs) were detectable in at least one sample in both groups.

A total of 200 miRNAs were present in all nine malaria samples and 260 miRNAs were present in all nine control samples. The Venn diagram generated from these lists (Figure 7-10B) shows that 24 miRNAs were present in the malaria group only but absent in the control group, and that 84 miRNAs were present in the control group only but absent in the malaria group. 176 miRNAs were detectable in all samples in both clinical groups.

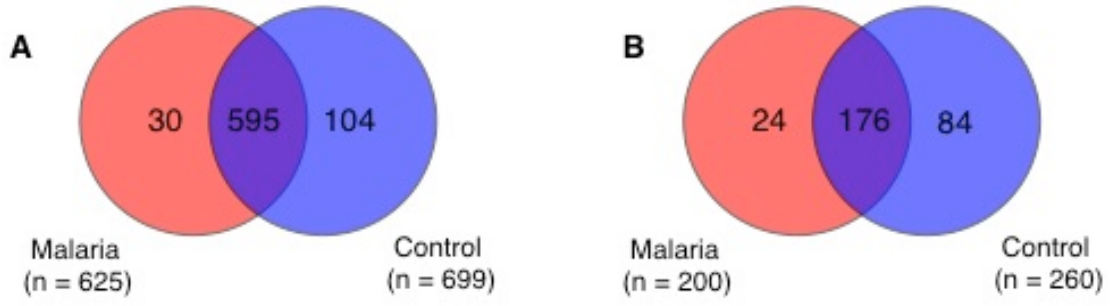

Figure 7-10. Venn diagram of miRNAs present in (A) at least one sample in either clinical group, (B) in 100% of the samples in either clinical group

Unsupervised cluster analysis

The heterogeneity in the miRNA transcription profile of the brain was identified using unsupervised cluster analysis. Several hierarchical clustering algorithms available in GeneSpring GX version 11.5 were performed and demonstrated that there was neither a distinct miRNA expression pattern in malaria-infected brain compared to the control nor in different areas of the brain. Figure 7-11 shows the unsupervised cluster analysis using a Euclidean distance measure and average linkage rule.

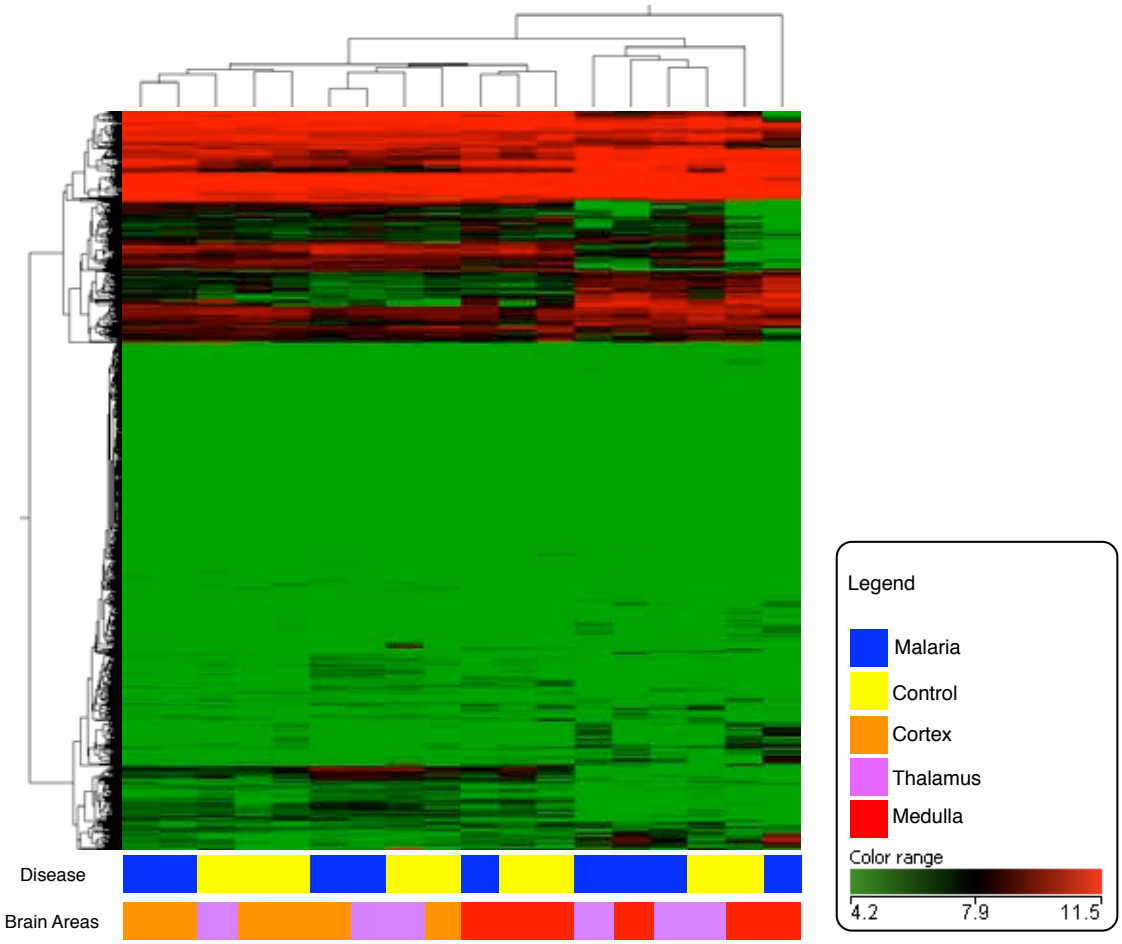

Figure 7-11. Unsupervised hierarchical cluster analysis of miRNA expression from malaria and control samples
The heatmap shows the expression of complete human mature miRNAs (miRBase release 15.0, n = 1,105). Heatmap colour represents relative miRNA expression as indicated in the colour key. The X axis shows a lack of association between specific miRNA gene signature and either clinical group or brain area.

Differential expression analysis of malaria vs. control

In an effort to identify a miRNA expression in the brain that was specific to malaria-infected cases, differential expression analysis was performed using the t-test in GeneSpring GX 11.5. Initially, miRNAs were filtered for statistical significance using Benjamini and Hochberg's FDR with an FDR-adjusted *P*-value cutoff of 0.05. This statistical stringency gave no miRNAs that were differentially expressed between malaria and control groups. Reducing the statistical stringency to an unadjusted *P*-value from a t-test with a cutoff of 0.05 and fold-change cutoff of 1.5 gave a total of 54 differentially expressed miRNAs in malaria compared to controls. Of these 54 differentially expressed miRNAs, 32 were up- and 22 were down- regulated (Appendix C, Table C-4 and C-5).

7.3.4 miRNA and mRNA expression data integration

Identification of putative mRNA targets of miRNAs

The first step to integration of mRNA and miRNA expression data was the identification of putative mRNA targets of miRNAs using the miRNA Target Filter function in Ingenuity IPA. The mRNA targets of differentially expressed miRNAs in malaria (n = 54, *P*-value cutoff of 0.05 and fold-change cutoff of 1.5) were retrieved from four databases: TarBase, miRecords, TargetScan and Ingenuity Expert Findings. Using the 54 dysregulated miRNAs, the target-prediction algorithms generated 10,523 putative mRNA targets (setting the prediction stringency at a combination of moderate predictive, high predictive and experimentally observed – e.g. already published in other studies).

Filtering mRNA targets using DEGs

The results of the mRNA target prediction in the earlier step were then filtered by matching putative mRNA targets (from target prediction) with the DEGs specifically associated with malaria (n = 223), which represented the real dysregulated mRNA genes from the same tissue as the miRNA transcripts. This step used corresponding mRNA expression data to identify miRNAs

that target the mRNAs under the same experimental conditions. 131 mRNAs from 223 DEGs were identified as targets of the miRNAs differentially expressed in malaria.

Expression pairing

Because miRNA has post-transcriptional regulatory effects (translational blockage or transcript degradation), it was sensible to consider the directions of miRNA and mRNA expression in data integration process. At this step, miRNA-mRNA expression pairing was applied to identify cases where the miRNA and mRNA expression was changing in opposite directions (miRNA up with mRNA down, miRNA down with mRNA up). Thus, only miRNA and mRNAs that had opposite directions of changes could pass through the filter, generating a list of 24 miRNAs targeting 87 mRNAs (Table 7-5).

7.3.5 Pathway analysis from IPA on integrated miRNA and mRNA expression data

To investigate the functional significance of the putative mRNA targets of differentially expressed miRNAs, the negatively correlated mRNA targets (n = 87) of both up- and down-regulated miRNAs were analysed using IPA.

Functional analysis

Functional analysis using IPA on the 87 mRNA targets of dysregulated miRNAs gave a list of over-represented biological functions similar to the results using the entire list of DEGs associated with malaria. A wide number of biological functions were enriched, mainly associated with activation of immune-related and inflammatory-related functions, as well as inhibition of activities related to cell death. Figure 7-12 shows the significant over-represented Level-1 functional categories based on *P*-value and primary categories.

Canonical pathways

The top canonical signalling and metabolic pathways from the 87 mRNA targets of dysregulated miRNAs are reported in Table 7-6. Most of the enriched pathways associated with this dataset were the same pathways as found when analysing the entre list of DEGs associated with malaria. Interestingly, there were 13 signalling pathways and two metabolic pathways that were not present in the analysis using the entire list of DEGs as previously shown in Table 7-4.

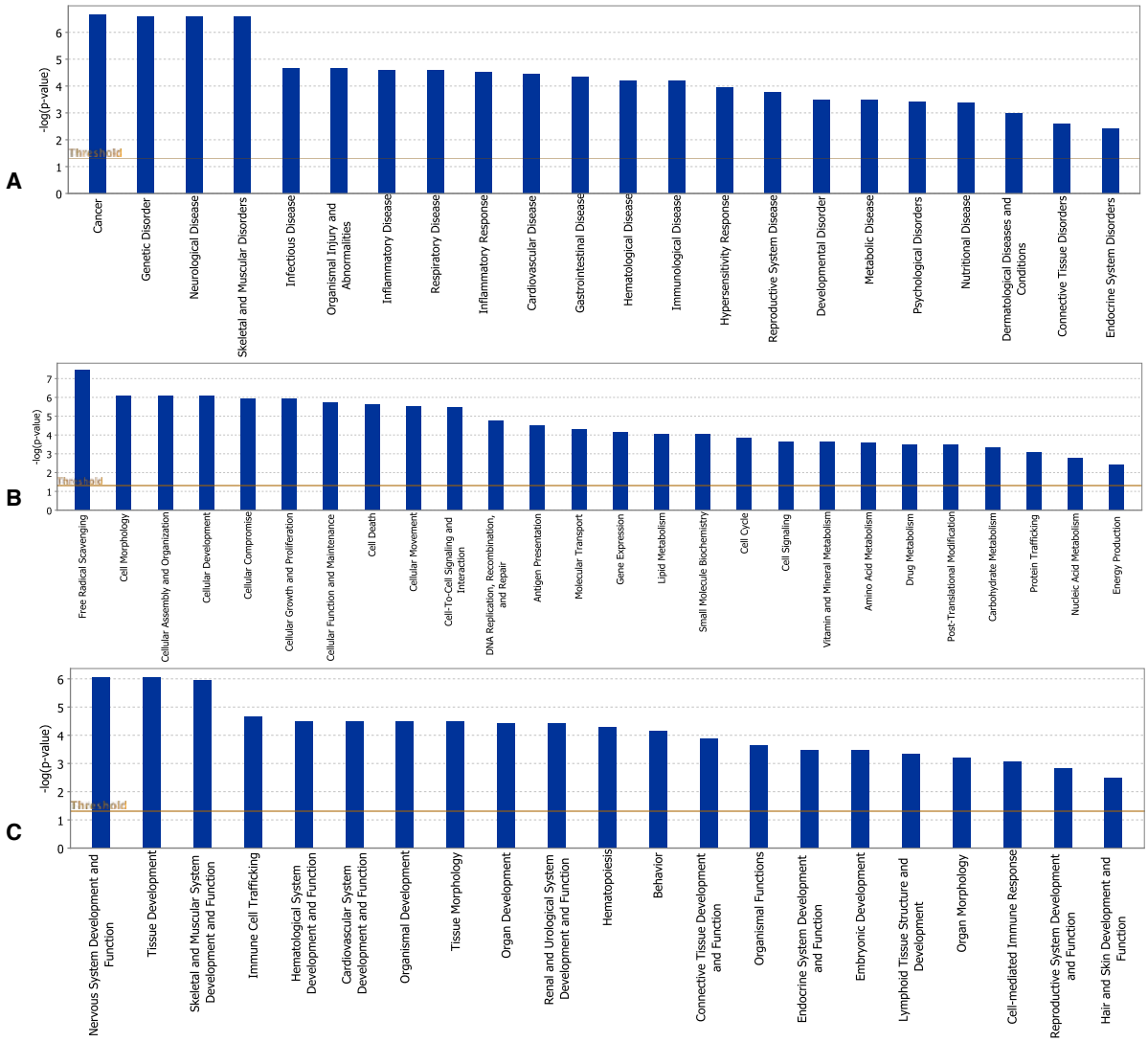

Figure 7-12. Functional analysis from IPA of the 87 negatively correlated mRNA targets of both up- and down-regulated miRNAs in malaria

This figure shows the most significant biological functions that are over-represented in the dataset based on –log(p-value) (the higher the bar graph, the more significant the *P*-value) and primary categories of functions: (A) Diseases and Disorders, (B) Molecular and Cellular Functions, (C) Physiological System Development and Function. The straight orange line indicates a *P*-value threshold of 0.05 (-log 1.3).

Table 7-5. miRNA transcripts changing in malaria cases

Up-regulated miRNA	No. of targeted mRNAs	Down-regulated target mRNA predicted by IPA
miR-1184	4	CSMD2, IGFBP3, SOX11, UPK3BL
miR-1260a/miR-1260b	1	DCX
miR-1281	1	KLHL35
miR-1299	4	CD24, GBP4, LPPR2, STAT1
miR-146b-3p/miR-1231-3p	2	CSMD2, DCK
miR-28-3p/miR-28*	1	DYRK2
miR-29b-3p/miR-29b/miR-29c-3p (includes others)	4	C17orf70, DCX, NKIRAS2, SPATA2L
miR-382-5p/miR-382	3	DCX, DYRK2, LPPR2
miR-498	5	CD24, CSPG5, MARCH4, RPL13A, SOX11
miR-557/miR-507	3	IRF2BPL, LYPD1, NKIRAS2
miR-939	5	CSMD2, DCX, H1FX, LAMP5, NKIRAS2
miR-940	1	IRF2BPL
Down-regulated miRNA	**No. of targeted mRNAs**	**Up-regulated target mRNA predicted by IPA**
miR-101-3p/miR-101a/miR-101b-3p (includes others)	11	ADCYAP1, APP, BTBD3, DDIT4, DNM1L, G3BP2, MAP4, NECAB1, SASH1, SGK1, STC1
miR-1246	9	HIGD1A, NAMPT, NCOA7, PIP4K2A, RGS5, SH3GL2, STC1, WAC, WASF3
miR-1291	2	IL1B, SLC16A3
miR-17-5p/miR-20b-5p/miR-93-5p (includes others)	22	APP, AQP4, C2CD2, CDKN1A, EFR3A, F3, IL8, LPIN1, MAP3K8, MPZL2, PFKFB3, PIP4K2A, PRNP, SASH1, SH3BGRL2, SLC11A1, STC1, STOM, SYNM, TRIM37, WAC, WASF3
miR-18b-5p/miR-18a-5p/miR-18a (includes others)	13	ADCYAP1, BAALC, CAB39, CDKN1A, EFR3A, F3, GLS, KIT, PCSK1, SCG3, SH3BGRL2, SYNM, WASF3
miR-324-5p	7	ADCYAP1, AQP9, LPIN1, NAPB, PRNP, SH3BGRL2, SYNM
miR-34c-5p/miR-449a/miR-449c-5p (includes others)	9	ACSL1, C2CD2, INA, KIT, LDHA, PFKFB3, SH3BGRL2, STC1, SYT1
miR-4712-5p/miR-770-5p	10	AQP4, CAB39, DNM1L, LPIN1, MAP2K4, NAMPT, NECAB1, RAC2, RCAN2, STC1
miR-576-3p	11	ADAMTS1, BTBD3, CAB39, MAP1B, MAP2K4, MPZL2, PCSK1, QDPR, RCAN2, SGK1, WASF3
miR-654-5p/miR-541-3p	1	STC1
miR-891a	2	BHLHE40, PTPLAD1
miR-92a-3p/miR-92a/miR-363-3p (includes others)	21	ADM, AQP4, CD93, CDKN1A, DDIT4, EFR3A, EPDR1, G3BP2, ITM2B, LPIN1, MAP1B, MAP2K4, MPZL2, NEFM, NSF, SGK1, SLC2A3, STOM, SYT1, UGP2, VSNL1

miR-29b-3p/miR-29b/miR-29c-3p (includes others) = hsa-miR-102, hsa-miR-29a, hsa-miR-29a-3p, hsa-miR-29b, hsa-miR-29b-3p, hsa-miR-29c, hsa-miR-29c-3p; miR-17-5p/miR-20b-5p/miR-93-5p (includes others) = hsa-miR-106a, hsa-miR-106a-5p, hsa-miR-106b, hsa-miR-106b-5p, hsa-miR-17, hsa-miR-17-5p, hsa-miR-20, hsa-miR-20a, hsa-miR-20a-5p, hsa-miR-20b, hsa-miR-20b-5p, hsa-miR-519d, hsa-miR-526b*, hsa-miR-526b-3p, hsa-miR-93, hsa-miR-93-5p; miR-18b-5p/miR-18a-5p/miR-18a (includes others) = hsa-miR-18, hsa-miR-18a, hsa-miR-18a-5p, hsa-miR-18b, hsa-miR-18b-5p, hsa-miR-4735-3p; miR-34c-5p/miR-449a/miR-449c-5p (includes others) = hsa-mir-172, hsa-miR-34a, hsa-miR-34a-5p, hsa-miR-34c, hsa-miR-34c-5p, hsa-miR-449, hsa-miR-449a, hsa-miR-449b, hsa-miR-449b-5p; miR-92a-3p/miR-92a/miR-363-3p (includes others) = hsa-miR-25, hsa-miR-25-3p, hsa-miR-32, hsa-miR-32-5p, hsa-miR-363, hsa-miR-363-3p, hsa-miR-367, hsa-miR-367-3p, HSA-MIR-92, hsa-miR-92a, hsa-miR-92a-3p, hsa-miR-92b, hsa-miR-92b-3p, hsa-miR-92b MM2

List of 24 dysregulated miRNAs and their 87 putative dysregulated mRNA targets, identified from IPA miRNA target filter. Only negative associations/interactions of expression between each mRNA with the 24 miRNAs were identified.

Table 7-6. List of the top signalling and metabolic canonical pathways from IPA among the 87 negatively correlated mRNA targets of dysregulated miRNAs

Ingenuity canonical Pathways	-log(p-value)	Ratio	Gene	Up/ Down	Functions (from IPA)
Signalling pathways					
Glucocorticoid Receptor Signalling	2.80	0.0204	294	5/1	Regulate immune, metabolic, cardiovascular and behavioral functions.
Role of BRCA1 in DNA Damage Response	2.52	0.0462	65	1/2	-
IL-22 Signalling	2.23	0.0800	25	1/1	A novel cytokine belonging to the IL-10 family, suggesting involvement in inflammatory and allergic responses.
Role of JAK family kinases in IL-6-type Cytokine Signalling	2.20	0.0741	27	1/1	Acute-phase Inflammatory response
Reelin Signalling in Neurons	2.19	0.0366	82	2/1	In the hippocampus, reelin regulates the growth and/or distribution of afferent entorhinal and commissural axons.
p38 MAPK Signalling	1.84	0.0283	106	2/1	Response to stress by activated p38 MAPKs culminates in enhanced transcriptional activity, protein synthesis and cell death.
Docosahexaenoic Acid (DHA) Signalling	1.82	0.0408	49	2/0	DHA plays an important role in neuronal survival by modulating Phosphatidylserine levels and by stimulating Neuroprotectin-D1 (NPD1) synthesis.
Role of IL-17F in Allergic Inflammatory Airway Diseases	1.74	0.0435	46	2/0	IL-17F is an inflammatory cytokine, especially important in the pathogenesis of allergic airway inflammation
Atherosclerosis Signalling	1.74	0.0233	129	3/0	Chronic inflammation resulting from interaction between inflammatory cells, plasma lipoproteins and extracellular matrix of the arterial wall
IL-6 Signalling	1.74	0.0242	124	3/0	Regulator of acute-phase responses and a lymphocyte stimulatory factor
Role of Hypercytokinemia/hyperchemokinemia in the Pathogenesis of Influenza	1.72	0.0455	44	2/0	This phenomenon is referred to as a 'cytokine storm'
EGF Signalling	1.69	0.0385	52	1/1	The epidermal growth factor (EGF) family is a group of structurally related proteins that regulate cell proliferation, migration and differentiation, via tyrosine kinase receptors on target cells.
CD27 Signalling in Lymphocytes	1.60	0.0351	57	2/0	CD27 is a member of the Tumor Necrosis Factor Receptor (TNFR) superfamily, play a very important role in cell growth and differentiation, as well as apoptosis or programmed cell death.
IL-12 Signalling and Production in Macrophages	1.58	0.0194	155	2/1	IL-12 serves as a bridge between innate and adaptive immunity
TREM1 Signalling	1.56	0.0303	66	2/0	TREM1 activation is involved in diverse aspects of innate and adaptive immune response.
Role of Cytokines in Mediating Communication between Immune Cells	1.54	0.0364	55	2/0	Innate and adaptive responses are two main branches of the immune system.
ATM Signalling	1.51	0.0339	59	2/0	Ataxia Telangiectasia Mutated Protein (ATM) is a key regulator of multiple signalling cascades which respond to DNA strand breaks. These responses involve the activation of Chks, DNA repair and apoptosis.
B Cell Receptor Signalling	1.49	0.0192	156	3/0	the development, survival and activation of B lymphocytes.
Metabolic pathways					
Nicotinate and Nicotinamide Metabolism	2.88	0.0296	135	4/0	-
Inositol Phosphate Metabolism	2.22	0.0206	194	4/0	-
D-glutamine and D-glutamate Metabolism	1.72	0.0385	26	1/0	-
Propanoate Metabolism	1.53	0.0164	122	2/0	-
Nucleotide Sugars Metabolism	1.42	0.0154	65	1/0	-

Highlighted in grey are pathways that are not present in the IPA analysis on the 223 DEGs (Table 7-4). –log(p-value) denotes the significance of the enrichment of a pathway within the DEGs dataset. The larger the –log(p-value), the less likely that the association is random and the more significant the association. Also shown are the Ratio (the number of DEGs associated with the pathway/the total number of genes known to be associated with the pathway), Gene (the total number of genes known to be associated with the pathway), and Up/Down (the number of up- and down- regulated DEGs in the pathway.

Network analysis

Using the 87 negatively correlated mRNA targets of dysregulated miRNAs, a total of 10 significant networks were identified within IPA analysis (data not shown). Taking the same approach as when analysing the DEGs associated with malaria, the top five networks were merged to evaluate relationships between individual mRNA targets. These networks included a total of 175 molecules interconnected with 63 negatively correlated mRNA targets of dysregulated miRNAs, which were involved in network functions including Cellular Assembly and Organisation, Cellular Function and Maintenance, Neurological Disease Cell Death Cell-To-Cell Signalling and Interaction, Nucleic Acid Metabolism, Cellular Development, Cellular Growth and Proliferation, and Cell Death.

An example of such a network generated by cross referencing miRNA data to potential target mRNAs is shown in Figure 7-13. This confirms the up-regulation of transcripts such as APP and AQP4, which had previously been significantly raised in the mRNA data alone, and the lack of change in mRNA for TNF.

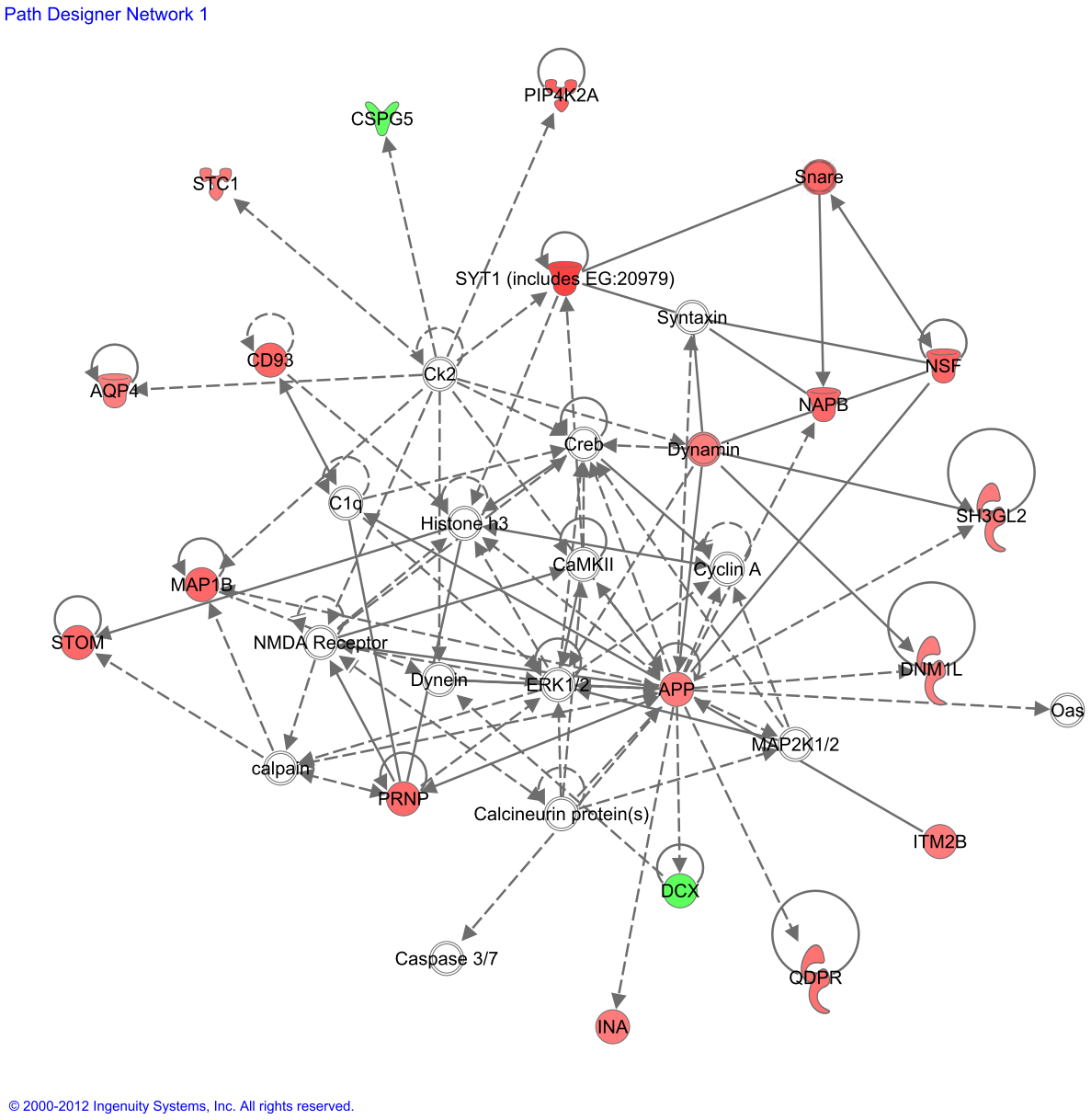

Figure 7-13. Network derived from mapping changes in miRNA levels onto the mRNA transcripts of DEGs in malaria cases

This confirmed the increase in genes such as APP and AQP4.

7.4 Discussion

This is the first study to simultaneously examine human responses to malaria parasite infection at the transcriptional and post-transcriptional levels in the human brain. The findings confirm that this approach is possible in post-mortem tissues, and offers extended knowledge on the molecular mechanisms of the pathogenesis of human malaria.

As with any experimental method, using human tissue to study gene expression changes in malarial infection has its own limitations. I had initially hoped to recruit more patients through the MEMA study so larger groups of patients could be compared, so as to improve the statistical power of the bioinformatics analysis. Another advantage of larger clinical groups is that the questions which can be asked of the results are wider. For instance, with a larger group of malaria patients, clinical groups dying with or without coma could be used to compare gene expression profiles not only between malaria cases and controls but also between malaria cases with or without coma. However, the recruitment rate for the MEMA study was low and, as a consequence, by the time I started the array work for this part of my thesis I was limited to including six cases. It was therefore necessary to use rather low statistical stringency to identify the differentially expressed mRNAs and miRNAs ($P < 0.05$, fold-change cutoff = 1.5, no FDR control), which increases the probability of false positive results. In fact, it is generally advisable that any microarray results for an individual gene should be subsequently validated by other independent techniques including the use of additional microarrays, qRT-PCR and Northern blots, to prevent false positive results.

In order to improve statistical power to detect any differences in malaria cases, the number of biological replicates was increased by using three brain samples from each individual (area matched), improving the total number of brain samples from six to 18 different pieces (nine malaria vs. nine control). This experimental design did improve the statistical power and was perfectly appropriate to answer the question "what genes are differentially expressed in the brain

between malaria and non-malaria-associated deaths in Mozambican children?" However, this experimental design was not appropriate to investigate other interesting questions in malaria research such as "what genes are involved in the genesis of coma in CM?" or "are there differences in gene profiles from different areas of the brain after malarial infection?"

IPA was used to translate the large dataset generated from the genome-wide mRNA and miRNA microarrays to more biologically interpretable findings. Some findings chime with the previous knowledge on the pathogenesis of severe malaria and some are novel and will be interesting to explore further.

The lists of differentially expressed genes (such as the 'top-ten' most up- and down-regulated genes) included transcripts for molecules which, empirically at least, were relevant to malaria pathophysiology as we understand it currently. These included genes which were induced by hypoxia, acute-phase and inflammatory mediators such as chemokines and interferon-inducible genes. Others were unexpected, and suggested interesting potential pathways which could be involved in the genesis or response to malarial infection in the brain, such as the haemoglobin A chain, proteins involved in synaptic transmission and neuropeptides.

There is a risk of imposing preconceived ideas about pathophysiology on such a list, but several transcripts which were up-regulated, such as APP, were reassuring as its protein β-APP had previously been shown to increase in the brain in fatal malaria (and not just CM cases) (Medana, Day, et al. 2002). A predominance of genes which, on pathway analysis, were involved in immune or inflammatory stimuli again raises the issue of the degree to which inflammatory host responses occur in the brain in fatal malaria. This is a controversial area both because cellular immune responses vary pathologically and because the murine model of disease certainly shows a preponderance of immune/inflammatory responses. This has also been shown in paediatric African cases, although our understanding of the pathological correlation of inflammation in the brain is poor, and extends beyond the simple appearance of intravascular leukocyte collections. Therefore, the

increased expression of molecules such as CCL2 (also known as MCP-1, monocyte chemotactic protein-1) would be expected given the reported increase in monocyte/macrophage recruitment to the brain in paediatric malaria, and the histological findings of dense lymphocytic/monocytic infiltrates in some vessels in the malaria cases (e.g. MAL3, Figure 6.1C). However, MCP-1 is also expressed by neurons as well as ECs in the brain, and has been shown in an animal model to be involved in hypoxic preconditioning (Stowe et al. 2012). Hence, the mRNA transcripts detected here may in part reflect neuronal responses.

The most up-regulated gene found in this study was the haemoglobin alpha chain (HBA1). This study examined expression of mRNA transcripts in the brain, so this represents production of HBA1 mRNA by brain cells, rather than relating to systemic responses such as increased synthesis in the bone marrow due to anaemia. Haemoglobin proteins are synthesised and expressed in neurones, where they form an intracellular oxygen storage mechanism in these metabolically active, oxygen-consuming cells (Schelshorn et al. 2009), although oxygen transport from the blood into cells in the brain is not well understood. Neuroglobin is another heme-containing molecule expressed in neurons (and some glial cells), and has potential roles in oxygen homeostasis, scavenging of reactive oxygen species or sustaining energy metabolism (Hankeln et al. 2004). A study of neuroglobin expression in the brain in CM showed no specific changes in CM versus NCM patients (Medana et al. unpublished data). The up-regulation of HBA1 is therefore interesting in that it may represent an adaptive response to neurons in a hypoxic state during malaria, to try and ensure oxygen delivery to neurons. However, this needs to be confirmed by examining the cellular specificity of its expression and levels of protein expression in the brain during malaria. The results indicated up-regulation of several proteins involved in hypoxic pathways, such as the hypoxia-inducible lipid-droplet associated protein (HIG2) and angiopoietin like molecule 4 (ANGPTL4).

Interestingly, several interferon gamma-inducible proteins were down-regulated. Levels of TNF and IFN-γ transcripts were unchanged, despite their apparent importance in mediating inflammatory changes in the brain in the murine model. The interferon-inducible genes IFI6 and IFI27 were down-regulated, and both of these have been implicated in the response of cells to viral infections.

One drawback of using microarray techniques to examine differential gene expression is that the results depend on comparison with a control group. Our control group of non-malaria deaths included several cases of infection (due to pneumonia and meningitis), which would render the patient septic. It may therefore be that cytokine mediated pathways in the brain of these patients were raised, which would decrease the sensitivity of detecting specific changes in malaria brains. A better comparison would be using controls who died of sudden unexpected death such as trauma, without infection, where the baseline gene expression would be expected to be as 'normal' as possible.

Proteins involved in calcium homeostasis and signalling such as S100A8/A9 were up-regulated, as was osteopontin/SSP-1, which has been implicated in repair of demyelination and axonal injury responses (C. Zhao et al. 2008). Several other transcripts showing significant changes are associated with synaptic functioning or neurotransmission, such as SNAP-25, NNAT and PENK. Clearly, this may be a reflection of damage to CNS cells and non-specific injury responses, but it raises the possibility that specific changes to synaptic pathways and neurotransmission could be occurring, which might be a link to processes such as consciousness, coma and seizure activity during coma.

Overall, the transcription profiling indicated that, specifically in malaria cases versus controls, there was an excess of hypoxic activation, immune and inflammatory response genes and signalling pathways, and a decrease in gene families accelerating cell death responses.

Analysis of the miRNA transcripts dysregulated in malaria cases was used for two main purposes. Firstly, I attempted to see whether a 'signature' of malaria could be determined using unsupervised clustering analysis, similar to that which was done successfully in the previous study of miRNA in the kidney (Chapter 5). However, again due to the low number of cases, no specific association between malaria and a miRNA signature could be found. However, the changes in miRNA did allow confirmation of significant changes in targeted mRNA transcripts, giving the study a degree of internal confirmation that changes to these transcripts were real, rather than false positive results.

Not all of the gene families suggested by the analysis of differentially expressed mRNA transcripts were shown to be correlated with complementary miRNA transcripts generated from the brain in the same case. Also, some pathways of known miRNA regulation that might be expected to change in malaria showed no obvious changes. Interestingly, the miRNA-210, which is known to be involved in hypoxic gene regulation (X. Huang et al. 2010) showed no changes in malaria cases in our study. However, using IPA I confirmed that miRNAs targeting genes such as the major cytokines TNF or INF-γ did not change, but there was evidence of changes to miRNAs affecting genes of interest such as APP, ADAMST13, signalling pathways and synaptic function, which could be relevant to the pathophysiology of severe malaria.

Further analysis of a larger sample size is required to improve the power of the study, decrease potential false positive findings and confirm the changes in individual transcripts. However, the genomics approach described in this chapter can also be extended to other tissues linked to organ-specific complications of malaria such as lung or renal disease.

Chapter 8

Discussion

8.1 Overview

Despite over a century of research, malaria remains one of the world's major health burdens, especially in developing countries, due to its toll of mortality and morbidity, the lack of an effective vaccine and the difficulties of diagnosis and treatment. CM is the most common and severest complication of malaria; in spite of human pathology and animal model studies, understanding of CM pathophysiology remains limited. Moreover, other severe clinical syndromes such as MARF and lung injury have not been well studied. Different approaches have been used to study the pathology and pathophysiology of severe malaria, but currently one of the most utilised, the murine *P. berghei*-ANKA model, is controversial because different authors disagree on how representative the murine model is of human disease. A better understanding of the pathophysiological mechanisms of malaria remains key to designing newer weapons to fight against this deadly disease, including mosquito control measures, vaccination, and drug treatments.

Most studies of malarial pathophysiology look at one molecule or pathway, whether through *in vitro* approaches using EC co-culture with PRBC, animal models or human tissues. As well as using these 'traditional' approaches to examine aspects of the role of the Ang-Tie-2 pathway in my thesis, the other major aim was to try a different approach using the more recent developments in molecular pathology. This strategy allowed the examination of the whole transcriptomic dataset from the malaria-infected human tissue, to suggest new molecules and pathways which may potentially be involved in the pathogenesis of malaria. I therefore had to access newer cases of

malaria and controls via an autopsy study in Mozambique to determine if they would provide sufficiently high-quality mRNA and miRNA for use in subsequent transcriptomic analyses

8.2 The Ang-Tie-2 receptor pathway in Malaria

Ang-Tie-2 is one pathway potentially linking EC activation in the brain (and attendant BBB leakage, sequestration and immune activation). Ang-2 and Ang-2/Ang-1 ratios are now well established as a biomarker for severe malaria and, in some series, CM, as well as fatal outcome.

It is clear that widespread EC activation occurs systemically and in the brain during a malaria episode, and that this activation may be in part due to the direct contact of PRBC sequestered in the microvasculature and in part due to the systemic effects of severe malaria. If this causes functional changes in EC, such as increased leakiness or adhesion molecule expression, or induction of apoptosis, then preventing this might interfere with processes contributing to poor outcome in malaria (adjunctive vascular or neuroprotective therapy).

The therapeutic use of angiopoietins has been investigated in experimental murine models of brain ischemia, where Ang-1 inhibits the BBB breakdown, stimulates the recruitment of neuroblasts and promotes behavioural recovery (Ohab et al. 2006). Other treatment strategies aim to increase bioactive NO availability in the EC, which is a major inhibitor of Ang-2 and is reduced in severe malaria (Yeo et al. 2007). Kain's group is planning a randomised controlled trial using inhaled NO as an adjunctive therapy to reduce morbidity and mortality of severe malaria in Ugandan children, although it is questionable whether this will reach the brain microcirculation in a bioactive form (Hawkes et al. 2011).

However, the tissue-specific expression and specificity in a target organ such as the brain had not been studied in human fatal malaria cases, so one of the aims of the work in my thesis was to examine expression in the brain to see if there was a link between coma and Ang-Tie-2 expression in CM versus NCM, and then model this process along with PRBC sequestration and hypoxia *in*

vitro. In this thesis, the plasma concentrations of Ang-2 and the Ang-2/Ang-1 ratio were also confirmed as independent predictors of death in severe *falciparum* malaria, in Southeast Asian patients.

Patterns of immunostaining of Ang-1, Ang-2 and Tie-2 in malaria cases were altered in fatal severe malaria compared to controls, but not different in CM compared to NCM. Activation of the Ang-Tie-2 pathway in severe malaria was correlated to acidosis, a number of severity criteria and fatal outcome, but not a specific event in the brain during CM.

The lack of significant differences in the patterns or extent of staining of any of these constituents between CM and NCM cases is consistent with recent data using systemic measures of activation of the Ang-Tie-2 pathway, where elevated plasma levels of Ang-2 were no higher in CM than in non-cerebral severe malaria (Conroy et al. 2009). Taken together, results do not support elevated Ang-2 as a predictive biomarker for CM, as previously proposed (Lovegrove et al. 2009). Indeed, in the current study, circulating Ang-2 was elevated less in those with CM as the only manifestation than in those with other severe malaria criteria, and was shown to be related to an incremental increase in the severity

There are potential problems with this study which necessarily limit the interpretation of the results. As with other post-mortem studies, the issues of post-mortem artefacts may alter immunohistochemical staining patterns and increase background staining due to diffusion of proteins. This necessitated the use of control cases with similar post-mortem and tissue-collecting processes and storage conditions to the malaria cases.

The absence of increased Ang-2 expression in brain ECs in fatal malaria cases, despite elevated plasma concentrations of Ang-2, was unexpected. One possible explanation is that exocytosis of cerebral endothelial WPB products was already complete at the time of death, with inadequate re-synthesis. Alternatively, WPB exocytosis and Ang-2 release may occur predominantly in the

extra-cerebral systemic circulation in both CM and NCM. Alternatively, a post-mortem artefact could have degraded protein expression so IHC may not work. With regard to this, as a confirmation of changes to the Ang-Tie-2 proteins in kidney following the miRNA study, I attempted to extract proteins from FFPE tissues to use in Western blotting, but was unable to do so. Hence, there may be a degree of false negative staining on IHC.

Each death in an autopsy series gives a 'snapshot' effect of pathology in an individual case with varying treatment, time to death and clinical complications of disease, which differ between cases. Inferring a single unifying pattern of pathology with a temporal sequence from a group of such cases may therefore be difficult. Severe malaria in Vietnamese adults is a multi-organ process with a high prevalence of renal, liver, respiratory and metabolic dysfunction as well as anaemia and CM. Despite this, and the relatively limited case numbers in each group, it was reassuring that the data on the plasma and CSF levels of Ang-1, Ang-2 and Tie-2 were in keeping with previously published series on these mediators in severe and fatal malaria (Yeo et al. 2008; Lovegrove et al. 2009; Conroy et al. 2009; Conroy et al. 2010; Erdman et al. 2011). This lends weight to the findings that, despite the significant increases in the Ang-2 and Ang2/Ang-1 ratio in severe malaria, there was no evidence that this was a process which was specifically up-regulated in the brain in cerebral versus non-CM cases.

The effects of Ang-1, Ang-2 and Tie-2 signalling on neurons and glial cells as opposed to ECs has not yet been as well studied. It was notable that expressions of Ang-1, Ang-2 and Tie-2 were increased in neurons and glial cells in fatal CM and NCM. Recent studies indicate that Tie-2 signal transduction might have neuroprotective and mitogenic effects on neuronal cells. Ang-1-Tie-2 signalling promotes neural outgrowth from dorsal root ganglion cells (Kosacka et al. 2005), supports neuronal differentiation in neural progenitor cells (Bai, Cui, et al. 2009), alters dendrite organisation (Ward et al. 2005) and protects against apoptosis of neurons (Bai, Meng, et al. 2009; Valable 2003). Interestingly, the Ang-1 effect on neurons is not exclusively limited to Tie-2-

receptor dependence. Ang-1 can induce neurite outgrowth via a β1-integrin receptor on neurons (Chen et al. 2009). Studies have also found a positive effect of Ang-2 on neurogenesis and migration of neuroblasts (X. S. Liu et al. 2009). For these reasons, it is therefore possible that increased expression of both Ang-1 and Ang-2 in neuronal cells are adaptive, neuroprotective responses in both cerebral and NCM.

As well as its independent association with fatal outcome, Ang-2 was associated with a number of organ complications, metabolic acidosis, and ARF, both in this study and as previously shown by Yeo et al. (2008). In contrast, the other major WPB product which increased in severe malaria, VWF, is not associated with either lactate/metabolic acidosis or fatal outcome in severe malaria (Erdman et al. 2011; Phiri et al. 2011). Taken together, these findings suggest a pathogenic role for Ang-2 in the pathways leading to death in both CM and NCM. Ang-2-related amplification of endothelial activation, injury and microvascular sequestration may thus play a key role in impairment of microvascular perfusion in severe malaria. Given the association of plasma Ang-2 level with ARF in this and other series and the relationship with metabolic acidosis in the multivariate analysis, further studies should examine the role of the Ang-Tie pathway in regulating blood flow and microvascular pathology in the kidney in adult severe malaria patients.

8.3 The *in vitro* co-culture model of HBEC and PRBC

The Ang-Tie-2 pathway does not act in isolation in the malaria-infected brain. It is part of a complex signalling interplay with other pathways and molecules related to endothelial activation, angiogenesis, inflammation, hypoxia and BBB leakage. It is well established that PRBC sequestration and normal RBC congestion are significantly linked to pre-mortem coma in severe malaria patients (Pongponratn et al. 2003; Ponsford et al. 2012). It seems obvious that these two processes should alter the metabolic microenvironment within the brain vessels and cause some degree of hypoxia at the surrounding brain parenchyma. Of these changes, glucose utilisation and oxygen

supply are crucial for normal neuronal function, and changes in either or both may affect global metabolic functioning in the brain and present as clinical changes in consciousness or fitting.

Functional neuroimaging techniques such as positron emission tomography and functional magnetic resonance imaging (fMRI) have been used to study the brain activity *in vivo* by measuring the glucose and oxygen utilisation and blood flow at specific regions of the brain (Gusnard et al. 2001). Using these newer neuroimaging technologies, the simian model of CM has been shown to suffer a widespread metabolic dysfunction during coma (Kawai and Sugiyama 2010).

Although hypoxia seems to be an important factor contributing to the functional changes in the brain of CM, results from studies examining hypoxic markers such as HIF-1α, VEGF and DEC using IHC on the human post-mortem brain tissue have been inconclusive (Medana et al. 2010). This is probably because they are necessarily short-lived and under tight molecular control, resulting in their highly labile property. Thus, IHC is not the best approach to examine the 'fingerprint' of hypoxia in CM.

In this thesis, I demonstrated that the effects of the complex interrelationship between Ang-Tie-2 pathways, hypoxia and PRBC sequestration on the BBB integrity could be studied using an *in vitro* models of BBB. The leakiness of the BBB could be monitored non-invasively in real time using the ECIS system, and endothelial activation could be confirmed by measuring its soluble markers using multiplex ELISA. Whole transcriptomic alteration of the HBEC cultures was to be examined using microarrays. However, apart from the TEER experiments using the ECIS system, the planned subsequent analyses were not possible due the misidentification and cross-contamination of the cell line used in this project.

Although these experiments were unsuccessful, the questions remain highly relevant in the CM pathogenesis and this work will be repeated using commercial HBEC lines and other EC models

including tri-culture with astrocytes, in order to examine the effects of other BBB structures in modulating responses seen in PRBC–HBEC co-culture models.

8.4 The miRNA expression profiling in the malaria-infected kidney

MARF is relatively common in severe *falciparum* malaria in Southeast Asian adults, but it is reported to be rare in African children. This manifestation of severe malaria is important because it can cause mortality if not recognised and managed appropriately. The mainstays of treatment consist of appropriate antimalarial drug therapy, fluid management and dialysis. Clinical recognition would be aided by a biomarker of renal injury and early recognition of patients who may need treatment. There is a need to investigate why people get ARF/AKI in malaria, why this happens in adults more than paediatric cases, and also how to prevent or treat this in adults. Understanding the pathophysiology of MARF would help, and it has not been well studied. Tubular injury has been reported, and there are some reports of glomerular injury, but histology indicates both ATN and immune cell localisation (Das 2008; Ehrich and Eke 2007; Nguansangiam et al. 2007).

I used molecular pathology techniques to examine miRNA expression profiles in the archival FFPE kidney of fatal malaria patients with MARF and NARF and fatal non-malaria controls. However, because of a lack of fresh tissue, a complete transcriptome analysis on the same tissue was not possible for parallel comparison. This lack of a transcriptome makes it more difficult to interpret miRNA in isolation from mRNA, although data from murine studies and data from mRNA target-prediction algorithms give clues as to the genes being influenced.

Although there were differences between control and malaria cases, within the malaria cases the cluster analysis did not differentiate between MARF and NARF on the basis of the miRNA signature – mainly due to the low numbers of cases available. However, future work will be aimed at gathering more MARF cases (potentially using post-mortem biopsy material) to repeat and

extend these results, compare them with a mRNA transcriptome and use the results to study cellular and molecular pathology within the kidney during malarial infection.

The profile of miRNAs changing in malaria cases imply that targeted mRNAs include groups of genes controlling apoptosis and programmed cell death. One area where this would seem relevant is tubular epithelial cell injury. This may be being induced by PRBC sequestration, immune cell localisation in the interstitium or circulating mediators as part of systemic infection. However, tubular epithelial cell apoptosis is not seen commonly in autopsy histology studies. Assuming that potential factors causing renal injury in malaria include shock, hypoperfusion, anaemia, sequestration causing hypoxia and leukocyte infiltration, it was interesting to compare miRNA signatures with those already defined in other diseases such as Hypoxic/Ischaemic injury (El-Assaad et al. 2011). Our miRNA signature included three of the nine miRNA shown in this study, but only one was similarly increased, so I conclude that the signature is different, implying that AKI in MARF is not the same as that caused by hypoxia/ischaemic injury. However, that study was based in mice.

Because of my interest in the Ang-Tie2 pathway and its potential role in MARF, I specifically used a series of *in vitro* luciferase experiments to look at the influence of changes to miRNA targeting Ang-1, Ang-2 and Tie-2 genes. This study revealed for the first time that two miRNAs including miR-204 and miR-486-5p, which were significantly down-regulated in kidneys from malaria cases, could bind to and suppressed the expression of Ang-1 and Tie-2 genes, respectively. This finding still requires further follow-up studies to examine the effect of these miRNAs on the suppression of the expression of Ang-1 and Tie-2 *in vivo*.

8.5 The integrated analysis of miRNA and mRNA expression profiling of the malaria-infected brain

The work done in this thesis presents for the first time complete mRNA and miRNA expression profiles from the brain tissue of fatal human malaria cases. I have also generated similar data on other organs but these have not yet been fully analysed. Using the example of the brain data it is likely that these analyses should await inclusion of more cases to make them clearer and more significant.

This project was a technically challenging enterprise in terms of the logistics, expense and time for data analysis. It has generated a wealth of data, but as with all genomic approaches the challenge is how to put this data in a proper clinical context and interpret it with sufficient care. The first step in this process is to interrogate the dataset with clear, simple questions. At the outset I hoped to ask "which genes are differentially expressed in the brain between CM and NCM?" However, the low numbers of recruited cases and lack of CM cases and proper NCM controls meant that I can really only ask "which genes are differentially expressed in the brain between malaria and non-malaria-associated death?" In the future, when a larger number of cases from the more homogenous clinically-defined group is available (e.g. comparing fatal malaria cases with and without coma, and fatal non-malaria cases with and without coma), the gene expression signature specifically associated with CM could potentially be generated.

The data presented are based on the cases that were available at the time of data analysis, and therefore specifically this is not a study of the gene expression profile in the brain between CM versus NCM. The small sampling group also means it was necessary to reduce the stringency of the statistical analysis, which will increase the risk that some of the detected mRNA changes may be false positives and would drop out later in analyses with larger numbers of cases. Moreover, the small sample size causes the study to be quite underpowered in terms of detecting genes with the more subtle changes.

In this study, a microarray-based technique was used rather than whole-genome sequencing. The sequencing is more expensive (but may become less so with newer sequencing techniques), more time consuming and technically more difficult, as well as being more difficult to interpret with bioinformatics. However, it offers the benefit of discovering potential new transcripts that have not previously been recognised (annotated). Arrays use previously annotated gene probes, and may miss novel transcripts associated with malaria.

Generating transcriptome data is very useful for the greater understanding of malaria pathogenesis, but this approach comes with some caveats. Firstly, the data does not account for post-translational events. For example, a protein could be markedly changed in malaria and have an important function, but its activity might be controlled not by transcriptional control (level of mRNA or suppression/release by miRNA) but by subsequent enzymatic activity, activation by signal transduction or phosphorylation, control due to epigenetic factors like methylation, or changes in metabolism. So, a transcriptome may not say much about parasite-induced physical-mechanical factors like hypoxia, glucose, neurotransmitter or vasoactive mediator release. For instance, the levels of molecules that were pre-synthesised and stored in WPB such as VWF and Ang-2 may change without detectable transcriptional activation or suppression during malarial infection. This concept can also apply to soluble mediators such as NO, where its activity might influence malaria pathogenesis because of iNOS induction, but not gene transcription changes in the iNOS transcript itself.

Another caveat is that the data is not directly causal. Up- or down-regulation of a mRNA transcript in malaria does not mean that levels of the protein associated with the particular mRNA will change. Protein expression also depends on post-transcriptional and translational controls. Equally, miRNA can be predicted *in silico* as targeting a particular mRNA but this may not happen *in vitro* or *in vivo*, as was demonstrated by the data in Chapter 5, where in total only two out of 12 putative miRNA-mRNA interactions were validated by the luciferase assay.

Moreover, the gene expression profile could reflect other mechanical events such as tissue damage, attempts at neuro-protection and adjustment to metabolic changes, rather than being specific to malarial infection. In other words, the gene expression profile could reflect non-specific responses to disease rather than being directly implied in causing malaria-associated pathology or coma. This is just the same as association with a marker in IHC or animal studies, where the level of an individual cytokine may change in malaria (but not be specific), but patterns of multiple genes or proteins may be more significant. Comparison with published (and archived) data in other diseases should help address this potential problem.

A potential problem with bioinformatics analysis as performed here is that the pathway analysis methods make assumptions by looking at groups of genes, which might lead to some associations being biased toward established knowledge in databases, but might miss something potentially important that has not been incorporated in such databases previously. The pathway analysis software uses a reference library generated from previous publications, which are often from different types of diseases occurring preferentially in the Western population like cancer or chronic conditions rather than acute infectious diseases. This is shown by the fact that there is no publically available gene set (or miRNA set) database containing a well-established pathway of malaria pathogenesis, although there are a lot of available pathways involved in various types of cancer or chronic conditions such as diabetes, atherosclerosis and allergy. All pathway analysis software packages including IPA and GSEA, as used in this thesis, rely on gene set databases of biological pathways (reference library) to compare with the gene expression data generated by the microarray experiment and generate a statistical prediction about which pathways (gene sets) are over-represented in the given gene expression data (Nam and S. Y. Kim 2008). This is why some groups of the DEGs in malaria did map onto pathways generated from other diseases such as "neurological" disease or "cardiovascular" disease in IPA. So, referencing results back to a 'library'

to compare and judge significance would lack specificity if the library does not have the 'right book' in it.

The gene expression data generated in this study have been analysed in different ways. The first level of analysis is unsupervised cluster analysis, which makes no assumptions about any individual or groups of gene, but only tries to examine the whole transcriptomic profile to see if there are differences in the gene expression signatures between clinical groups (e.g. malaria vs. controls, or MARF vs. NARF). This has been very successful at distinguishing the transcriptome of a cancer from normal tissue or sub-classifying cancers (as seen in Lawrie et al. 2007) and is so good in fact that it is now being used as a basis for suggesting different clinical groups based on transcriptomic signature, both for mRNA and miRNA.

Another type of analysis is differential expression analysis. This allowed me to determine the genes changing most highly in malaria compared to control cases, for instance the top-ten most up- and down-regulated genes as shown in Chapter 7. Of these there were some interesting hits, which make empirical sense (like MCP-1, which could attract monocytes to the brain) or are novel but clearly interesting (like hypoxic inducible proteins or precursors for neurotransmitters like PENK). However, this also reflects the natural tendency to 'superimpose' on the results our own prejudices or ideas about pathophysiology. Nevertheless, they can also act as a springboard for new directions in understanding pathogenesis in malaria.

Perhaps most interesting are the genes such as haemoglobin alpha 1 (HBA1). Why is this mRNA increased in the brain? Is the protein being translated and if so in what cell? What is it doing in the brain; is it expressed? Does it have an unknown function, like perhaps a neuroglobin analogue allowing hypoxic sensing by neurons? This data generates many questions and issues surrounding what to do with the results.

Given an interesting potential candidate DEG, the first priority is to validate the result and further investigate its potential role in malaria. To confirm that this is a real finding rather than by chance, the mRNA expression must be examined using either Northern blots (which require a lot of extracted RNA) or the qRT-PCR technique, which has become a technique of choice for microarray result validation as discussed and carried out in Chapter 5. Less noise interferes with the result in PCR because only one transcript is being examined in one reaction (unlike on a microarray where tens of thousands of transcripts are being examined simultaneously). If a mRNA increases or decreases (as it has done on array or sequencing platforms) in an qRT-PCR experiment, then this makes it much more likely to be a real result from the array.

The next step would be to examine the translation of a mRNA transcript to a protein by looking at the protein expression using Western blot or IHC in tissues from same clinical groups like CM versus NCM versus controls (ideally the same tissues used to generate mRNA expression profile on the microarray). Similarly, the protein can be examined in a relevant model (if one exists) such as the murine or simian models. If there is a gene knockout in a murine model this might allow a study of the effects of a particular protein on the disease course. Proteomics approaches either on clinical samples, *in vivo* animal models or in *vitro* cell culture may also allow for the mapping of changes in corresponding proteins to mRNAs and miRNAs transcripts. Depending on the nature of the protein coded for by the mRNA, it may also be possible to examine its expression using an *in vitro* model. For example, changes to adhesion molecules or chemokines occurring in the cerebral microvasculature during malarial infection can be modelled using the co-culture system of HBEC and PRBC.

In summary, this study is proof of principal, and results should not be over-interpreted because the clinical groups are small and not homogeneous. The malaria deaths showed low levels of PRBC sequestration, variable time to death and clinical syndromes of severe malaria. The control cases were also heterogeneous, including cases dying of pneumonia, meningitis and a brain

tumour. Despite all the potential problems mentioned above, several features suggest that the results contain genuine changes specific to malaria. The miRNA expression data were used as an internal control. A DEG was viewed as being more significant if the corresponding miRNA – which was predicted to target the particular mRNA transcript (the DEG) – was also differentially expressed in the opposite direction. Thus, it was reassuring because in this series one of the genes most highly up-regulated in the brain in malaria was APP, and the internal controls of miRNA mapping to the APP were correspondingly down-regulated. There is previous evidence from IHC that axonal injury, measured using βAPP protein expression, is significantly increased in the brain in malaria (Dorovini-Zis et al. 2011; Medana, Day, et al. 2002). Hence, this links a theoretical change at miRNA and mRNA level to protein expression and a putative (histologically confirmed) pathological process.

Overall, the genomic data presented in this thesis have proved that molecular pathological approaches can be successfully applied to the study of malaria even in quite a challenging environment. They can be applied to post-mortem material, which is more difficult to deal with than living tissue but an absolute requirement of such studies in neurological diseases. Similar approaches have been used in diseases such as dementia (Glanzer et al. 2004) and multiple sclerosis (Lock et al. 2002) and specifically neurological infectious diseases like HIV (Tatro et al. 2010) and West Nile Virus (Munoz-Erazo et al. 2012). Therefore, although arguably suboptimal (like any other method using autopsy material), these studies can be done. The dataset is large and complex but comparable to other available studies. This study helps to establish mRNA and miRNA expression profiles specific to malarial infection in humans. However, this is the first transcriptome study using malaria-infected human brain tissue, so general conclusions should be drawn with care.

The data need expansion with more cases and available comparisons exist with:

1. Other neurological diseases including infectious disease in CNS in humans;

2. Animal models (only the murine, not the more relevant simian model); and

3. *In vitro* data (HUVEC and HBEC transcriptomes are available).

Thus, if a DEG or a pathway is up-regulated in other diseases like HIV, it is more likely to represent a pattern of reaction (response) than it is a specific malaria-induced pathological change – e.g. be a causal pathway in CM pathogenesis. This reflects the need to look at patterns or mechanisms through changes in whole populations of genes, rather than concentrate too much on the role of individual genes in a complex disease such as malaria.

Overall comparison of our gene set to the published murine data shows some important differences, such as the potential role for cytokines in the genesis of the neurological syndrome. However, there were changes to both immune response and inflammatory gene sets, which may reflect a genuine difference in the pathology seen in African paediatric cases, where cellular immune localisation in the brain is more notable histologically than in Southeast Asian adults. Underlying this issue, however, is our poor understanding of what 'inflammation' – in terms of its role and definition – is in the brain.

Comparison of the present gene set with publications on EC transcriptomes also shows some important differences. First, the range of genes studied here is not endothelial specific because other cellular compartments are also examined, including neurons, microglial and astroglial cells. Transcriptome data of 'pure EC' (Chakravorty et al. 2007; Tripathi et al. 2009) in *in vitro* co-culture models with PRBC have indicated increases in inflammatory and signalling pathways and marked increases in signals for cellular apoptosis. The transcriptome data of the brain tissue in this thesis showed some similar pro-inflammatory changes, but key central mediators such as TNF, IFN-γ and the NF-κB signalling axis were not increased. Similarly, the apoptotic pathways were not induced but transcripts involved in these seemed generally suppressed. This may reflect the

influence of modification of such processes in one cell set (such as HBEC) *in vivo* by other components of the BBB such as astrocytes, which are not present in the *in vitro* models.

A number of up-regulated genes in the malaria-infected brain also had putative roles in the responses to hypoxia, suppression of cell death and some neurotransmitter/synaptic protein pathways. This raises interesting questions about how far genomic approaches to post-mortem material can take us in understanding the interaction between metabolism in the brain, and its effect on neurotransmitter release as part of processes causing coma and fitting in malaria. This requires further investigation.

8.6 Future work

The results presented in this thesis suggest a number of subsequent experiments which will be necessary to continue my work. The study of the role of the Ang-Tie-2 pathways may be extended to their role in the kidney and lungs using both fresh tissues from further adult cases, both for IHC, Western blotting and qRT-PCR validation. I also wish to repeat the *in vitro* co-culture experiments with an authentic primary HBEC line to study the interactions of hypoxia, the Ang-Tie-2 pathway and PRBC sequestration on the BBB integrity. In particular, given the transcriptome data, it would be interesting to examine putative EC-specific transcripts identified in microarray experiments using HBEC, such as the induction and expression of MCP-1 and aquaporin 4 and 9, to determine whether these play a role in the functional effects of PRBC binding by influencing host leukocyte recruitment, permeability and oedema formation.

IHC on existing FFPE brain tissue could also be used to study the expression of MCP-1 and chemokine receptors, to study whether ECs' release of MCP-1 in brain microvessels correlates with leukocyte co-localisation. Another area which the transcriptome data suggests is the roles of oxygen transporter molecules within the brain, and particularly neurons. An immunohistochemical screening of HBA1 and neuroglobin expression in the brain is required in order to determine

whether these proteins are up-regulated in neurons or astroglial cells during CM, or specific to CM versus NCM cases.

My work has begun to allow analysis of human malaria in terms of organ-specific gene signatures, and this genomic approach requires more cases, with clearly defined clinical syndromes of malaria, as well as appropriate controls. This would enable us to examine specific gene signatures of coma in CM, or relate gene expression profiles to established pathological correlates like PRBC sequestration or axonal injury in the brain. In addition, the results from other organs can be analysed in a similar fashion – although this requires extensive work and resources.

The results show that there are acute processes occurring in the brain which are malaria specific, such as induction of a hypoxic microenvironment, suppression of programmed cell death, and immune modulation, which are difficult to examine using standard post-mortem pathological methods. The next step in examining malaria-infected human tissues would therefore be to generate a 'metabolome' of the metabolic processes happening in the brain during life in CM. This has been attempted in humans on organotypic brain slice cultures, and to some extent in the brain from the murine CM model (Rae et al. 2004). It will be important to compare these results with data arising from the ongoing fMRI trial in Malawi, and simian models of CM. Alternatively, some data may be available by examining neurotransmitters or their metabolites levels using ELISA or proteomics techniques, which have been used to study glutamate metabolism (Miranda et al. 2010) and the kynurenic acid pathway (Medana, Hien, et al. 2002) in CSF from malaria patients.

Finally, the field needs new ways of linking physio-mechanical events in the brain (such as sequestration and congestion) to molecular events influencing brain function to cause coma. My results demonstrate our lack of understanding of immune and inflammatory responses in the brain in human malaria. These differ in the murine model, African paediatric and Southeast Asian adult cases, which has caused controversy. However, it seems clear that immune response through

astroglial activation (e.g. parenchymal responses rather than leukocyte localisation in vessels) is occurring during fatal malaria, and the study of the pathways which bring this about will be important. This may provide a link between the presence of the parasite in PRBC, host leukocyte responses in the vasculature, and parenchymal responses. The key findings of EC activation, increased BBB permeability, neuronal dysfunction, tissue hypoxia and axonal injury may be linked through signalling pathways to specific synaptic and neurotransmitter dysfunction, providing a mechanism whereby fitting and loss of consciousness can result. Through this approach I would hope to find potential pathways towards adjuvant neuroprotective therapy in human fatal malaria.

8.7 Conclusions

In this thesis I have shown the following new data:

- Serum levels of Ang-2 and the Ang-2/Ang-1 ratio are related to fatal outcome in severe malaria in Vietnamese adults.
- Ang-2 levels are related to disease severity (number of severe disease criteria and acidosis) but are not an independent biomarker for CM in this group.
- Expression of Ang-1, Ang-2 and Tie-2 in the brain in malaria is different from controls, but does not distinguish CM from NCM deaths.
- Molecular pathology techniques can be applied to human tissues from malaria patients successfully to investigate pathogenesis.
- RNAlater preservation allows successful extraction and processing of mRNA and miRNA for transcriptomic analysis from post-mortem brain tissue.
- miRNA expression profile of adult kidneys with malaria is significantly different from that of control, and has a unique gene signature.

- Luciferase reporter assay *in vitro* confirmed that two miRNAs, including miR-204 and miR-486-5p, identified as down-regulated in malaria kidney, bound to and suppressed mRNA expression of Ang-1 and Tie-2, respectively.
- Several miRNA are expressed in MARF target genes of the Ang-Tie-2 pathway, as confirmed by luciferase reporter assays *in vitro*.
- mRNA and miRNA transcriptomes from the brain of fatal malaria and control cases allowed delineation of differentially expressed genes in malaria cases.
- Families of genes showing differential expression in malaria included up-regulation of transcripts involved in inflammation and immune response, immune cell trafficking and signalling, cell homeostasis and metabolism, and down-regulation of cell death programmes.
- Individual genes of interest such as hypoxia-induced proteins, neurotransmitter precursors and proteins involved in synaptic stabilisation were up-regulated.

References

Abbott, N.J., Rönnbäck, L. and Hansson, E. (2006). Astrocyte-endothelial interactions at the blood-brain barrier. *Nature Reviews Neuroscience*, 7(1), pp.41–53.

Adjuik, M. et al. (2004). Artesunate combinations for treatment of malaria: meta-analysis. *Lancet*, 363(9402), pp.9–17.

Aikawa, M. (1988). Morphological changes in erythrocytes induced by malarial parasites. *Biology of The Cell*, 64(2), pp.173–181.

Aikawa, M. et al. (1992). A primate model for human cerebral malaria: Plasmodium coatneyi-infected rhesus monkeys. *The American Journal of Tropical Medicine and Hygiene*, 46(4), pp.391–397.

Allison, D.B. et al. (2006). Microarray data analysis: from disarray to consolidation and consensus. *Nature Reviews Genetics*, 7(1), pp.55–65.

Amani, V. et al. (2000). Involvement of IFN-gamma receptor-medicated signaling in pathology and anti-malarial immunity induced by Plasmodium berghei infection. *European Journal of Immunology*, 30(6), pp.1646–1655.

American Type Culture Collection (ATCC) Standards Development Organization Workgroup ASN-0002. (2010). Cell line misidentification: the beginning of the end. *Nature Reviews Cancer,* 10(6), pp.441–448.

André, F.E. (2003). Vaccinology: past achievements, present roadblocks and future promises. *Vaccine*, 21(7-8), pp.593–595.

Anstey, N.M. et al. (2009). The pathophysiology of vivax malaria. *Trends in Parasitology*, 25(5), pp.220–227.

Auburn, S. et al. (2008). Association of the GNAS locus with severe malaria. *Human Genetics*, 124(5), pp.499–506.

Awandare, G.A. et al. (2007). Role of monocyte-acquired haemozoin in suppression of macrophage migration inhibitory factor in children with severe malarial anemia. *Infection and Immunity*, 75(1), pp.201–210.

Bai, Y., Meng, Z., et al. (2009). An Ang1-Tie2-PI3K axis in neural progenitor cells initiates survival responses against oxygen and glucose deprivation. *Neuroscience*, 160(2), pp.371–381.

Bai, Y., Cui, M., et al. (2009). Ectopic expression of angiopoietin-1 promotes neuronal differentiation in neural progenitor cells through the Akt pathway. *Biochemical and Biophysical Research Communications*, 378(2), pp.296–301.

Balbuena, P. et al. (2010). Comparison of Two Blood-Brain Barrier In Vitro Systems: Cytotoxicity and Transfer Assessments of Malathion/Oxon and Lead Acetate. *Toxicological Sciences*, 114(2), pp.260–271.

Barbier, M. et al. (2008). Family-based association of a low producing lymphotoxin-alpha allele with reduced Plasmodium falciparum parasitemia. *Microbes and infection / Institut Pasteur*, 10(6), pp.673–679.

Barsoum, R.S. (2000). Malarial acute renal failure. *Journal of the American Society of Nephrology : JASN*, 11(11), pp.2147–2154.

Bartel, D.P. (2009). MicroRNAs: target recognition and regulatory functions. *Cell*, 136(2), pp.215–233.

Beare, N.A.V. et al. (2006). Malarial retinopathy: a newly established diagnostic sign in severe malaria. *The American Journal of Tropical Medicine and Hygiene*, 75(5), pp.790–797.

Beeson, J.G. et al. (2000). Adhesion of Plasmodium falciparum-infected erythrocytes to hyaluronic acid in placental malaria. *Nature Medicine*, 6(1), pp.86–90.

Benjamini, Y. and Hochberg, Y. (1995). Controlling the false discovery rate: a practical and powerful approach to multiple testing. *Journal of the Royal Statistical Society. Series B (Methodological)*, 57(1), pp.289–300.

Berendt, A.R. et al. (1989). Intercellular adhesion molecule-1 is an endothelial cell adhesion receptor for Plasmodium falciparum. *Nature*, 341(6237), pp.57-9.

Berendt, A.R. et al. (1992). The binding site on ICAM-1 for Plasmodium falciparum-infected erythrocytes overlaps, but is distinct from, the LFA-1-binding site. *Cell*, 68(1), pp.71-81

Berkley, J.A. et al. (1999). Cerebral malaria versus bacterial meningitis in children with impaired consciousness. *An International Journal of Medicine*, 92(3), pp.151–157.

Bernas, M.J. et al. (2010). Establishment of primary cultures of human brain microvascular endothelial cells to provide an in vitro cellular model of the blood-brain barrier. *Nature Protocols*, 5(7), pp.1265–1272.

Bhamarapravati, N. et al. (1973). Glomerular changes in acute plasmodium falciparum infection. An immunopathologic study. *Archives of pathology*, 96(5), pp.289–293.

Boctor, F.N. and Dorion, R.P. (2008). Malaria and hereditary elliptocytosis. *American Journal of Hematology*, 83(9), pp.753–753.

Boonpucknavig, V. and Sitprija, V. (1979). Renal disease in acute Plasmodium falciparum infection in man. *Kidney International*, 16(1), pp.44–52.

Bridges, D.J. et al. (2010). Rapid activation of endothelial cells enables Plasmodium falciparum adhesion to platelet-decorated von Willebrand factor strings. *Blood*, 115(7), pp.1472–1474.

Brown, H. et al. (2001). Blood-brain barrier function in cerebral malaria in Malawian children. *The American Journal of Tropical Medicine and Hygiene*, 64(3-4), pp.207–213.

Bull, P.C. and Marsh, K. (2002). The role of antibodies to Plasmodium falciparum-infected-erythrocyte surface antigens in naturally acquired immunity to malaria. *Trends in Microbiology*, 10(2), pp.55–58.

Bull, P.C. et al. (1998). Parasite antigens on the infected red cell surface are targets for naturally acquired immunity to malaria. *Nature Medicine*, 4(3), pp.358–360.

Bushati, N and Cohen, S. M. (2007). microRNA functions. *Annual Review of Cell and Developmental Biology*, 23, pp.175-205

Calvano, S.E. et al. (2005). A network-based analysis of systemic inflammation in humans. *Nature*, 437(7061), pp.1032–1037.

Carter, J.A. et al. (2005). Developmental impairments following severe falciparum malaria in children. *Tropical Medicine International Health*, 10(1), pp.3–10.

Carter, R. and Mendis, K.N. (2002). Evolutionary and Historical Aspects of the Burden of Malaria. *Clinical Microbiology Reviews*, 15(4), pp.564–594.

Chakravorty, S.J. et al. (2007). Altered phenotype and gene transcription in endothelial cells, induced by Plasmodium falciparum-infected red blood cells: Pathogenic or protective? *International Journal for Parasitology*, 37(8-9), pp.975–987.

Chandrasekaran, K. et al. (2012). Role of microRNAs in kidney homeostasis and disease. *Kidney International*, 81(7), pp.617–627.

Chen, X. et al. (2009). Angiopoietin-1 induces neurite outgrowth of PC12 cells in a Tie2-independent, beta1-integrin-dependent manner. *Neuroscience Research*, 64(4), pp.348–354.

Chittiboina, P. et al. (2012). Angiopoietins as promising biomarkers and potential therapeutic targets in brain injury. *Pathophysiology*, in press.

Chong, A.Y. et al. (2004). Plasma angiopoietin-1, angiopoietin-2, and angiopoietin receptor tie-2 levels in congestive heart failure☆. *Journal of the American College of Cardiology*, 43(3), pp.423–428.

Chookajorn, T., Ponsuwanna, P. and Cui, L. (2008). Mutually exclusive var gene expression in the malaria parasite: multiple layers of regulation. *Trends in Parasitology*, 24(10), pp.455–461.

Clark, I.A. et al. (2006). Human malarial disease: a consequence of inflammatory cytokine release. *Malaria Journal*, 5, p.85.

Cockburn, I.A. et al. (2004). A human complement receptor 1 polymorphism that reduces Plasmodium falciparum rosetting confers protection against severe malaria. *Proceedings of the National Academy of Sciences of the United States of America*, 101(1), pp.272–277.

Conroy, A.L. et al. (2009). Whole blood angiopoietin-1 and -2 levels discriminate cerebral and severe (non-cerebral) malaria from uncomplicated malaria. *Malaria Journal*, 8, p.295.

Conroy, A.L. et al. (2010). Endothelium-based biomarkers are associated with cerebral malaria in Malawian children: a retrospective case-control study. *PLoS ONE*, 5(12), p.e15291.

Cowman, A.F. and Crabb, B.S. (2006). Invasion of red blood cells by malaria parasites. *Cell*, 124(4), pp.755–766.

Cox, F.E. (2010). History of the discovery of the malaria parasites and their vectors. *Parasites and Vectors*, 3(1), p.5.

Cox-Singh, J. et al. (2008). Plasmodium knowlesi malaria in humans is widely distributed and potentially life threatening. *Clinical Infectious Diseases*, 46(2), pp.165–171.

Cox-Singh, J. et al. (2010). Severe malaria - a case of fatal Plasmodium knowlesi infection with post-mortem findings: a case report. *Malaria Journal*, 9(1), p.10.

Craig, A.G. et al. (2012). The Role of Animal Models for Research on Severe Malaria. *PLoS Pathogens*, 8(2), p.e1002401.

Crawley, J. et al. (1996). Seizures and status epilepticus in childhood cerebral malaria.*: An International Journal of Medicine*, 89(8), pp.591–597.

Das, B.S. (2008). Renal failure in malaria. *Journal of Vector Borne Diseases*, 45(2), pp.83–97.

David, S. et al. (2010). Circulating angiopoietin-2 levels increase with progress of chronic kidney disease. *Nephrology Dialysis Transplantation*, 25(8), pp.2571–2579.

Davis, S. et al. (1996). Isolation of angiopoietin-1, a ligand for the TIE2 receptor, by secretion-trap expression cloning. *Cell,* 87(7), pp.1161-1169.

Day, N.P.J. et al. (1999). The prognostic and pathophysiologic role of pro- and antiinflammatory cytokines in severe malaria. *The Journal of Infectious Diseases*, 180(4), pp.1288–1297.

Day, N.P.J. et al. (2000). The pathophysiologic and prognostic significance of acidosis in severe adult malaria. *Critical Care Medicine*, 28(6), pp.1833–1840.

de Mast, Q. et al. (2007). Thrombocytopenia and release of activated von Willebrand Factor during early Plasmodium falciparum malaria. *The Journal of Infectious Diseases*, 196(4), pp.622–628.

de Mast, Q. et al. (2009). ADAMTS13 deficiency with elevated levels of ultra-large and active von Willebrand factor in P. falciparum and P. vivax malaria. *The American Journal of Tropical Medicine and Hygiene*, 80(3), pp.492–498.

Deininger, M.H. et al. (2003). Angiogenic proteins in brains of patients who died with cerebral malaria. *Journal of Neuroimmunology*, 142(1-2), pp.101–111.

Dejana, E. (2004). Endothelial cell-cell junctions: happy together. *Nature Reviews Molecular Cell Biology*, 5(4), pp.261-270

Delahaye, N.F. et al. (2007). Gene expression analysis reveals early changes in several molecular pathways in cerebral malaria-susceptible mice versus cerebral malaria-resistant mice. *BMC Genomics*, 8, p.452.

Deli, M. A. et al. (2005). Permeability Studies on In Vitro Blood–Brain Barrier Models: Physiology, Pathology, and Pharmacology. *Cellular and Molecular Neurobiology,* 25(1), pp.59-127.

Desai, M. et al. (2007). Epidemiology and burden of malaria in pregnancy. *The Lancet Infectious Diseases*, 7(2), pp.93–104.

Dhangadamajhi, G. et al. (2009). The CCTTT pentanucleotide microsatellite in iNOS promoter influences the clinical outcome in P. falciparum infection. *Parasitology Research*, 104(6), pp.1315–1320.

Dijkstra, J.R. et al. (2012). MicroRNA expression in formalin-fixed paraffin embedded tissue using real time quantitative PCR: the strengths and pitfalls. *Journal of Cellular and Molecular Medicine*, 16(4), pp.683–690.

Dirks, W.G., MacLeod, R.A. and Drexler, H.G. (1999). ECV304 (endothelial) is really T24 (bladder carcinoma): cell line cross- contamination at source. *In Vitro Cellular Developmental Biology - Animal*, 35(10), pp.558–559.

Dondorp, A.M. et al. (2000). Abnormal blood flow and red blood cell deformability in severe malaria. *Parasitology Today*, 16(6), pp.228–232.

Dondorp, A.M., Desakorn, V., et al. (2005). Estimation of the total parasite biomass in acute falciparum malaria from plasma PfHRP2. *PLoS Medicine*, 2(8), p.e204.

Dondorp, A.M., Nosten, F., et al. (2005). Artesunate versus quinine for treatment of severe falciparum malaria: a randomised trial. *Lancet*, 366(9487), pp.717–725.

Dondorp, A.M. et al. (2009). Artemisinin resistance in Plasmodium falciparum malaria. *The New England Journal of Medicine*, 361(5), pp.455–467.

Dondorp, A.M. et al. (2010). Artesunate versus quinine in the treatment of severe falciparum malaria in African children (AQUAMAT): an open-label, randomised trial. *Lancet*, 376(9753), pp.1647–1657.

Dondrup, M. et al. (2009). An evaluation framework for statistical tests on microarray data. *Journal of Biotechnology*, 140(1-2), pp.18–26.

Doolan, D.L., Dobaño, C. and Baird, J.K. (2009). Acquired Immunity to Malaria. *Clinical Microbiology Reviews*, 22(1), pp.13–36.

Dorovini-Zis, K. et al. (2011). The Neuropathology of Fatal Cerebral Malaria in Malawian Children. *The American Journal of Pathology*, 178(5), pp.2146–2158.

Drexler, H.G. et al. (2002). Bladder carcinoma cell line ECV304 is not a model system for endothelial cells. *In Vitro Cellular Developmental Biology - Animal*, 38(4), pp.185–186.

Drexler, H.G. et al. (2003). False leukemia–lymphoma cell lines: an update on over 500 cell lines. *Leukemia*, 17(2), pp.416–426.

Du, P., Kibbe, W.A. and Lin, S.M. (2008). lumi: a pipeline for processing Illumina microarray. *Bioinformatics*, 24(13), pp.1547–1548.

Durand, P.M. and Coetzer, T.L. (2008). Pyruvate kinase deficiency protects against malaria in humans. *Haematologica*, 93(6), pp.939–940.

Ehrhardt, S. et al. (2005). High levels of circulating cardiac proteins indicate cardiac impairment in African children with severe Plasmodium falciparum malaria. *Microbes and Infection*, 7(11-12), pp.1204–1210.

Ehrich, J.H.H. and Eke, F.U. (2007). Malaria-induced renal damage: facts and myths. *Pediatric Nephrology*, 22(5), pp.626–637.

Eiam-Ong, S. and Sitprija, V. (1998). Falciparum malaria and the kidney: a model of inflammation. *American Journal of Kidney Diseases*, 32(3), pp.361–375.

Eiam-Ong, S. (2003). Malarial nephropathy. *Seminars in nephrology*, 23(1), pp.21–33.

El-Assaad, F. et al. (2011). Differential microRNA expression in experimental cerebral and noncerebral malaria. *Infection and Immunity*, 79(6), pp.2379–2384.

Enevold, A. et al. (2008). Reduced risk of uncomplicated malaria episodes in children with alpha(+)-thalassemia in northeastern Tanzania. *The American Journal of Tropical Medicine and Hygiene*, 78(5), pp.714–720.

Erdman, L.K. et al. (2011). Combinations of Host Biomarkers Predict Mortality among Ugandan Children with Severe Malaria: A Retrospective Case-Control Study S. Pied, ed. *PLoS ONE*, 6(2), p.e17440.

Fernando, S.D. et al. (2003). The impact of repeated malaria attacks on the school performance of children. *The American Journal of Tropical Medicine and Hygiene*, 69(6), pp.582–588.

Ferrer, I. et al. (2008). Brain banks: benefits, limitations and cautions concerning the use of post-mortem brain tissue for molecular studies. *Cell and Tissue Banking*, 9(3), pp.181–194.

Fiedler, U. (2004). The Tie-2 ligand Angiopoietin-2 is stored in and rapidly released upon stimulation from endothelial cell Weibel-Palade bodies. *Blood*, 103(11), pp.4150–4156.

Fiedler, U. and Augustin, H. (2006). Angiopoietins: a link between angiogenesis and inflammation. *Trends in Immunology*, 27(12), pp.552–558.

Fiedler, U. et al. (2006). Angiopoietin-2 sensitizes endothelial cells to TNF-alpha and has a crucial role in the induction of inflammation. *Nature Medicine*, 12(2), pp.235–239.

Florens, L. et al. (2002). A proteomic view of the Plasmodium falciparum life cycle. *Nature*, 419(6906), pp.520–526.

Francischetti, I.M.B. (2008). Does activation of the blood coagulation cascade have a role in malaria pathogenesis? *Trends in Parasitology*, 24(6), pp.258–263.

Francischetti, I.M.B., Seydel, K.B. and Monteiro, R.Q. (2008). Blood coagulation, inflammation, and malaria. *Microcirculation (New York, NY : 1994)*, 15(2), pp.81–107.

Franke-Fayard, B. et al. (2005). Murine malaria parasite sequestration: CD36 is the major receptor, but cerebral pathology is unlinked to sequestration. *Proceedings of the National Academy of Sciences of the United States of America*, 102(32), pp.11468–11473.

Fried, M. and Duffy, P.E. (1996). Adherence of Plasmodium falciparum to chondroitin sulfate A in the human placenta. *Science*, 272(5267), pp.1502–1504.

Fry, A.E. et al. (2008). Common variation in the ABO glycosyltransferase is associated with susceptibility to severe Plasmodium falciparum malaria. *Human Molecular Genetics*, 17(4), pp.567–576.

Gale, N. W. et al. (2002). Angiopoietin-2 is required for postnatal angiogenesis and lymphatic patterning, and only the latter role is rescued by Angiopoietin-1. *Developmental Cell,* 3(3), pp.411-423.

García, F. et al. (1999). Endothelial cell activation in muscle biopsy samples is related to clinical severity in human cerebral malaria. *The Journal of Infectious Diseases*, 179(2), pp.475–483.

Gentleman, R.C. et al. (2004). Bioconductor: open software development for computational biology and bioinformatics. *Genome Biology*, 5(10), p.R80.

Genton, B. et al. (1995). Ovalocytosis and cerebral malaria. *Nature*, 378(6557), pp.564–565.

Glanzer, J.G., Haydon, P.G. and Eberwine, J.H. (2004). Expression profile analysis of neurodegenerative disease: advances in specificity and resolution. *Neurochemical research*, 29(6), pp.1161–1168.

Godfrey, T.E. et al. (2000). Quantitative mRNA expression analysis from formalin-fixed, paraffin-embedded tissues using 5' nuclease quantitative reverse transcription-polymerase chain reaction. *The Journal of Molecular Diagnostics*, 2(2), pp.84–91.

Godwin, J.G. et al. (2010). Identification of a microRNA signature of renal ischemia reperfusion injury. *Proceedings of the National Academy of Sciences of the United States of America*, 107(32), pp.14339–14344.

Good, M.F. and Doolan, D.L. (2007). Malaria's journey through the lymph node. *Nature Medicine*, 13(9), pp.1023–1024.

Grau, G.E.R. et al. (2003). Platelet accumulation in brain microvessels in fatal pediatric cerebral malaria. *The Journal of Infectious Diseases*, 187(3), pp.461–466.

Greenwood, B.M. et al. (2005). Malaria. *Lancet*, 365(9469), pp.1487–1498.

Greenwood, B.M. et al. (2008). Malaria: progress, perils, and prospects for eradication. *Journal of Clinical Investigation*, 118(4), pp.1266–1276.

Griffiths-Jones, S. et al. (2008). miRBase: tools for microRNA genomics. *Nucleic Acids Research*, 36(Database Issue), pp.D154–158.

Guerra, C.A., Snow, R.W. and Hay, S.I. (2006). Mapping the global extent of malaria in 2005. *Trends in Parasitology*, 22(8), pp.353–358.

Gunderson, K.L. et al. (2004). Decoding randomly ordered DNA arrays. *Genome Research*, 14(5), pp.870–877.

Gusnard, D.A., Raichle, M.E. and Raichle, M.E. (2001). Searching for a baseline: functional imaging and the resting human brain. *Nature Reviews Neuroscience*, 2(10), pp.685–694.

Guyatt, H.L. and Snow, R.W. (2001). The epidemiology and burden of Plasmodium falciparum-related anemia among pregnant women in sub-Saharan Africa. *The American Journal of Tropical Medicine and Hygiene*, 64(1-2 Suppl), pp.36–44.

Gwer, S., Newton, C.R.J.C. and Berkley, J.A. (2007). Over-diagnosis and co-morbidity of severe malaria in African children: a guide for clinicians. *The American Journal of Tropical Medicine and Hygiene*, 77(6 Suppl), pp.6–13.

Haldar, K. and Mohandas, N. (2007). Erythrocyte remodeling by malaria parasites. *Current Opinion in Hematology*, 14(3), pp.203–209.

Haldar, K. et al. (2007). Malaria: mechanisms of erythrocytic infection and pathological correlates of severe disease. *Annual Review of Pathology*, 2, pp.217–249.

Handunnetti, S.M. et al. (1992). Involvement of CD36 on erythrocytes as a rosetting receptor for Plasmodium falciparum-infected erythrocytes. *Blood*, 80(8), pp.2097–2104.

Hankeln, T. et al. (2004). The cellular and subcellular localization of neuroglobin and cytoglobin -- a clue to their function? *International Union of Biochemistry and Molecular Biology Life*, 56(11-12), pp.671–679.

Hatabu, T. et al. (2003). Binding of Plasmodium falciparum-infected erythrocytes to the membrane-bound form of Fractalkine/CX3CL1. *Proceedings of the National Academy of Sciences of the United States of America*, 100(26), pp.15942–15946.

Hatherell, K. et al. (2011). Development of a three-dimensional, all-human in vitro model of the blood-brain barrier using mono-, co-, and tri-cultivation Transwell models. *Journal of Neuroscience Methods*, 199(2), pp.223–229.

Hatzis, C. et al. (2011). Effects of tissue handling on RNA integrity and microarray measurements from resected breast cancers. *Journal of the National Cancer Institute*, 103(24), pp.1871–1883.

Hawkes, M. et al. (2011). Inhaled nitric oxide for the adjunctive therapy of severe malaria: Protocol for a randomized controlled trial. *Trials*, 12(1), p.176.

Hawkins, B.T. and Davis, T.P. (2005). The blood-brain barrier/neurovascular unit in health and disease. *Pharmacological Reviews*, 57(2), pp.173–185.

Hempel, C. et al. (2011). CNS hypoxia is more pronounced in murine cerebral than noncerebral malaria and is reversed by erythropoietin. *American Journal Of Pathology*, 179(4), pp.1939–1950.

Hien, T.T. et al. (1996). A controlled trial of artemether or quinine in Vietnamese adults with severe falciparum malaria. *The New England Journal of* Medicine, 335(2), pp.76–83.

Ho, J. et al. (2008). Podocyte-specific loss of functional microRNAs leads to rapid glomerular and tubular injury. *Journal of the American Society of Nephrology*, 19(11), pp.2069–2075.

Huang, X., Le, Q.-T. and Giaccia, A.J. (2010). MiR-210--micromanager of the hypoxia pathway. *Trends in Molecular Medicine*, 16(5), pp.230–237.

Huber, W. et al. (2002). Variance stabilization applied to microarray data calibration and to the quantification of differential expression. *Bioinformatics (Oxford, England)*, 18(suppl 1), pp.S96–S104.

Hynd, M.R. et al. (2003). Biochemical and molecular studies using human autopsy brain tissue. *Journal of neurochemistry*, 85(3), pp.543–562.

Idro, R. et al. (2005). Clinical manifestations of severe malaria in the highlands of southwestern Uganda. *The American Journal of Tropical Medicine and Hygiene*, 72(5), pp.561–567.

Idro, R. et al. (2010). Cerebral Malaria: Mechanisms of Brain Injury and Strategies for Improved Neurocognitive Outcome. *Pediatric Research*, 68(4), pp.267–274.

Jain, V. et al. (2011). Plasma levels of angiopoietin-1 and -2 predict cerebral malaria outcome in Central India. *Malaria Journal*, 10(1), p.383.

Jambou, R. et al. (2010). Plasmodium falciparum Adhesion on Human Brain Microvascular Endothelial Cells Involves Transmigration-Like Cup Formation and Induces Opening of Intercellular Junctions J. W. Kazura, ed. *PLoS Pathogens*, 6(7), p.e1001021.

Janes, J.H. et al. (2011). Investigating the Host Binding Signature on the Plasmodium falciparum PfEMP1 Protein Family K. Deitsch, ed. *PLoS Pathogens*, 7(5), p.e1002032.

Jiang, H. et al. (2008). Detection of genome-wide polymorphisms in the AT-rich Plasmodium falciparum genome using a high-density microarray. *BMC Genomics*, 9(1), p.398.

Jung, M. et al. (2010). Robust MicroRNA Stability in Degraded RNA Preparations from Human Tissue and Cell Samples. *Clinical Chemistry*, 56(6), pp.998–1006.

Kauffmann, A., Gentleman, R.C. and Huber, W. (2009). arrayQualityMetrics--a bioconductor package for quality assessment of microarray data. *Bioinformatics*, 25(3), pp.415–416.

Kawai, S., Kano, S. and Suzuki, M. (1995). Rosette formation by Plasmodium coatneyi-infected erythrocytes of the Japanese macaque (Macaca fuscata). *The American Journal of Tropical Medicine and Hygiene*, 53(3), pp.295–299.

Kawai, S. and Sugiyama, M. (2010). Imaging analysis of the brain in a primate model of cerebral malaria. *Acta Tropica*, 114(3), pp.152–156.

Kim, H. et al. (2011). Endothelial activation and dysregulation in malaria: a potential target for novel therapeutics. *Current Opinion in Hematology*, 18(3), pp.177–185.

Klopfleisch, R. and Weiss, A. (2011). Excavation of a buried treasure-DNA, mRNA, miRNA and protein analysis in formalin fixed, paraffin embedded tissues. *Histology and Histopathology,* 26(6), pp.797-810

Kosacka, J. et al. (2005). Angiopoietin-1 promotes neurite outgrowth from dorsal root ganglion cells positive for Tie-2 receptor. *Cell and Tissue Research*, 320(1), pp.11–19.

Krek, A. et al. (2005). Combinatorial microRNA target predictions. *Nature Genetics*, 37(5), pp.495–500.

Kretzschmar, H. (2009). Brain banking: opportunities, challenges and meaning for the future. *Nature Reviews Neuroscience*, 10(1), pp.70–78.

Krishnegowda, G. et al. (2005). Induction of proinflammatory responses in macrophages by the glycosylphosphatidylinositols of Plasmodium falciparum: cell signaling receptors, glycosylphosphatidylinositol (GPI) structural requirement, and regulation of GPI activity. *The Journal of biological chemistry*, 280(9), pp.8606–8616.

Kyes, S.A., Kraemer, S.M. and Smith, J.D. (2007). Antigenic Variation in Plasmodium falciparum: Gene Organization and Regulation of the var Multigene Family. *Eukaryotic Cell*, 6(9), pp.1511–1520.

Lamikanra, A.A. et al. (2009). Haemozoin (malarial pigment) directly promotes apoptosis of erythroid precursors. *PLoS ONE*, 4(12), p.e8446.

Larkin, D. et al. (2009). Severe Plasmodium falciparum Malaria Is Associated with Circulating Ultra-Large von Willebrand Multimers and ADAMTS13 Inhibition D. Baruch, ed. *PLoS pathogens*, 5(3), p.e1000349.

Lawrie, C.H. et al. (2007). MicroRNA expression distinguishes between germinal center B cell-like and activated B cell-like subtypes of diffuse large B cell lymphoma. *International Journal of Cancer*, 121(5), pp.1156–1161.

Lee, K.-S. et al. (2011). Plasmodium knowlesi: Reservoir Hosts and Tracking the Emergence in Humans and Macaques. *PLoS Pathogens*, 7(4), p.e1002015.

Leoratti, F.M.S. et al. (2008). Variants in the toll-like receptor signaling pathway and clinical outcomes of malaria. *The Journal of Infectious Diseases*, 198(5), pp.772–780.

Lewis, B.P., Burge, C.B. and Bartel, D.P. (2005). Conserved seed pairing, often flanked by adenosines, indicates that thousands of human genes are microRNA targets. *Cell*, 120(1), pp.15–20.

Li, J. et al. (2007). Comparison of miRNA expression patterns using total RNA extracted from matched samples of formalin-fixed paraffin-embedded (FFPE) cells and snap frozen cells. *BMC Biotechnology*, 7(1), p.36.

Li, J.J. et al. (2001). Thrombin induces the release of angiopoietin-1 from platelets. *Thrombosis and Haemostasis*, 85(2), pp.204–206.

Lim, L.P. et al. (2005). Microarray analysis shows that some microRNAs downregulate large numbers of target mRNAs. *Nature*, 433(7027), pp.769–773.

Lin, S.M. et al. (2008). Model-based variance-stabilizing transformation for Illumina microarray data. *Nucleic Acids Research*, 36(2), p.e11.

Lins, A.M. et al. (1998). Development and population study of an eight-locus short tandem repeat (STR) multiplex system. *Journal of Forensic Sciences*, 43(6), pp.1168–1180.

Liu, A. et al. (2009). MicroRNA Expression Profiling Outperforms mRNA Expression Profiling in Formalin-fixed Paraffin-embedded Tissues. *International Journal of Clinical and Experimental Pathology*, 2(6), pp.519–527.

Liu, W. et al. (2010). Origin of the human malaria parasite Plasmodium falciparum in gorillas. *Nature*, 467(7314), pp.420–425.

Liu, X.S. et al. (2009). Angiopoietin 2 mediates the differentiation and migration of neural progenitor cells in the subventricular zone after stroke. *Journal of Biological Chemistry*, 284(34), pp.22680–22689.

Lock, C. et al. (2002). Gene-microarray analysis of multiple sclerosis lesions yields new targets validated in autoimmune encephalomyelitis. *Nature Medicine*, 8(5), pp.500–508.

Lopez, J.A. (2010). Malignant malaria and microangiopathies: merging mechanisms. *Blood*, 115(7), pp.1317–1318.

Lovegrove, F.E. et al. (2007). Expression microarray analysis implicates apoptosis and interferon-responsive mechanisms in susceptibility to experimental cerebral malaria. *The American Journal of Pathology*, 171(6), pp.1894–1903.

Lovegrove, F.E. et al. (2008). Parasite Burden and CD36-Mediated Sequestration Are Determinants of Acute Lung Injury in an Experimental Malaria Model. *PLoS Pathogens*, 4(5), p.e1000068.

Lovegrove, F.E. et al. (2009). Serum angiopoietin-1 and -2 levels discriminate cerebral malaria from uncomplicated malaria and predict clinical outcome in African children. *PLoS ONE*, 4(3), p.e4912.

Lucas, J.Z. and Sherman, I.W. (1998). Plasmodium falciparum: thrombospondin mediates parasitized erythrocyte band 3-related adhesin binding. *Experimental Parasitology*, 89(1), pp.78–85.

Lucas, S.B. et al. (1996). Severe cerebral swelling is not observed in children dying with malaria. *Quarterly Journal of Medicine*, 89(5), pp.351–354.

Lukasz, A. et al. (2008). Circulating angiopoietin-1 and angiopoietin-2 in critically ill patients: development and clinical application of two new immunoassays. *Critical Care*, 12(4), p.R94.

Maitland, K. and Marsh, K. (2004). Pathophysiology of severe malaria in children. *Acta Tropica*, 90(2), pp.131–140.

Maitland, K. and Newton, C.R.J.C. (2005). Acidosis of severe falciparum malaria: heading for a shock? *Trends in Parasitology*, 21(1), pp.11–16.

Maitland, K. et al. (2011). Mortality after fluid bolus in African children with severe infection. *The New England Journal of Medicine*, 364(26), pp.2483–2495.

Maisonpierre, P.C. et al. (1997) Angiopoietin-2, a natural antagonist for Tie2 that disrupts in vivo angiogenesis. *Science,* 277(5322), pp.55–60.

Makinde, T. and Agrawal, D.K. (2008). Intra and extravascular transmembrane signalling of angiopoietin-1-Tie2 receptor in health and disease. *Journal of Cellular and Molecular Medicine*, 12(3), pp.810–828.

Mali, S. et al. (2012). Malaria surveillance - United States, 2010. *Morbidity and Mortality Weekly Report, Surveillance Summaries, CDC*, 61(2), pp.1–17.

Maneerat, Y. et al. (2000). Inducible nitric oxide synthase expression is increased in the brain in fatal cerebral malaria. *Histopathology*, 37(3), pp.269–277.

Mankhambo, L.A. et al. (2010). The role of angiogenic factors in predicting clinical outcome in severe bacterial infection in Malawian children. *Critical Care*, 14(3), p.R91.

MAQC Consortium et al. (2006). The MicroArray Quality Control (MAQC) project shows inter- and intraplatform reproducibility of gene expression measurements. *Nature Biotechnology*, 24(9), pp.1151–1161.

Maragkakis, M. et al. (2009). DIANA-microT web server: elucidating microRNA functions through target prediction. *Nucleic Acids Research*, 37(Web Server), pp.W273–W276.

Maubert, B. et al. (2000). Cytoadherence of Plasmodium falciparum-infected erythrocytes in the human placenta. *Parasite Immunology*, 22(4), pp.191–199.

Maude, R.J. et al. (2009). The spectrum of retinopathy in adults with Plasmodium falciparum malaria. *Transactions of the Royal Society of Tropical Medicine and Hygiene*, 103(7), p.665.

McGuire, W. et al. (1994). Variation in the TNF-alpha promoter region associated with susceptibility to cerebral malaria. *Nature*, 371(6497), pp.508–510.

McGuire, W. et al. (1999). Severe malarial anemia and cerebral malaria are associated with different tumor necrosis factor promoter alleles. *The Journal of Infectious Diseases*, 179(1), pp.287–290.

Medana, I.M., Chaudhri, G. and Chan-Ling, T. (2001). Central nervous system in cerebral malaria: "Innocent bystander" or active participant in the induction of immunopathology? *Immunology and Cell Biology,* 79, pp.101–120

Medana, I.M., Day, N.P.J., et al. (2002). Axonal injury in cerebral malaria. *The American Journal of Pathology*, 160(2), pp.655–666.

Medana, I.M., Hien, T.T., et al. (2002). The clinical significance of cerebrospinal fluid levels of kynurenine pathway metabolites and lactate in severe malaria. *The Journal of Infectious Diseases*, 185(5), pp.650–656.

Medana, I.M. and Turner, G.D.H. (2006). Human cerebral malaria and the blood-brain barrier. *International Journal for Parasitology*, 36(5), pp.555–568.

Medana, I.M. et al. (2010). Induction of the vascular endothelial growth factor pathway in the brain of adults with fatal falciparum malaria is a non-specific response to severe disease. *Histopathology*, 57(2), pp.282–294.

Medana, I.M. et al. (2011). Coma in fatal adult human malaria is not caused by cerebral oedema. *Malaria Journal*, 10(1), p.267.

Mehta et al. (2001). Severe acute renal failure in malaria. *Journal of Postgraduate Medicine*, 47(1), p.24.

Mexal, S. et al. (2006). Brain pH has a significant impact on human postmortem hippocampal gene expression profiles. *Brain Research*, 1106(1), pp.1–11.

Miller, L.H. et al. (2002). The pathogenic basis of malaria. *Nature*, 415(6872), pp.673–679.

Miranda, A.S. et al. (2010). Increased levels of glutamate in the central nervous system are associated with behavioral symptoms in experimental malaria. *Brazilian Journal of Medical and Biological Research*, 43(12), pp.1173–1177.

Miron, M. et al. (2006). A methodology for global validation of microarray experiments. *BMC Bioinformatics*, 7, p.333.

Mishra, S.K. and Das, B.S. (2008). Malaria and acute kidney injury. *Seminars in Nephrology*, 28(4), pp.395–408.

Mitsios, N. et al. (2007). A microarray study of gene and protein regulation in human and rat brain following middle cerebral artery occlusion. *BMC Neuroscience*, 8(1), p.93.

Miu, J., Hunt, N.H. and Ball, H.J. (2008). Predominance of interferon-related responses in the brain during murine malaria, as identified by microarray analysis. *Infection and Immunity*, 76(5), pp.1812–1824.

Mohan, A., Sharma, S.K. and Bollineni, S. (2008). Acute lung injury and acute respiratory distress syndrome in malaria. *Journal of Vector Borne Diseases*, 45(3), pp.179–193.

Mohanty, S. et al. (2003). Complications and mortality patterns due to Plasmodium falciparum malaria in hospitalized adults and children, Rourkela, Orissa, India. *Transactions of the Royal Society of Tropical Medicine and Hygiene*, 97(1), pp.69–70.

Molyneux, M.E. et al. (1993). Circulating plasma receptors for tumour necrosis factor in Malawian children with severe falciparum malaria. *Cytokine*, 5(6), pp.604–609.

Mu, J. et al. (2005). Recombination Hotspots and Population Structure in Plasmodium falciparum. *PLoS Biology*, 3(10), p.e335.

Muehlenbachs, A. et al. (2008). Natural selection of FLT1 alleles and their association with malaria resistance in utero. *Proceedings of the National Academy of Sciences of the United States of America*, 105(38), pp.14488–14491.

Munoz-Erazo, L. et al. (2012). Microarray analysis of gene expression in West Nile virus-infected human retinal pigment epithelium. *Molecular Vision*, 18, pp.730–743.

Murray, C.J.L. et al. (2012). Global malaria mortality between 1980 and 2010: a systematic analysis. *Lancet*, 379(9814), pp.413–431.

Mutabingwa, T.K. et al. (2005). Maternal Malaria and Gravidity Interact to Modify Infant Susceptibility to Malaria. *PLoS Medicine*, 2(12), p.e407.

Nag, S., Manias, J. and Stewart, D.J. (2009). Pathology and new players in the pathogenesis of brain edema. *Acta Neuropathologica*.

Nair, S. et al. (2008). Adaptive copy number evolution in malaria parasites. *PLoS Genetics*, 4(10), p.e1000243.

Nam, D. and Kim, S.Y. (2008). Gene-set approach for expression pattern analysis. *Briefings in Bioinformatics*, 9(3), pp.189–197.

Neill, A.L. and Hunt, N.H. (1992). Pathology of fatal and resolving Plasmodium berghei cerebral malaria in mice. *Parasitology*, 105 (Pt 2), pp.165–175.

Newbold, C.I. et al. (1999). Cytoadherence, pathogenesis and the infected red cell surface in Plasmodium falciparum. *International Journal for Parasitology*, 29(6), pp.927–937.

Newman, R.D. et al. (2004). Malaria-related deaths among US travelers, 1963–2001. *Annals of Internal Medicine*, 141(7), pp.547–555.

Nguansangiam, S. et al. (2007). A quantitative ultrastructural study of renal pathology in fatal Plasmodium falciparum malaria. *Tropical Medicine and International Health*, 12(9), pp.1037–1050.

Nguyen, T.H. et al. (1996). Post-malaria neurological syndrome. *The Lancet*, 348(9032), pp.917–921.

Noedl, H. et al. (2008). Evidence of artemisinin-resistant malaria in western Cambodia. *The New England Journal of Medicine*, 359(24), pp.2619–2620.

Nosten, F. et al. (1999). Effects of Plasmodium vivax malaria in pregnancy. *The Lancet*, 354(9178), pp.546–549.

Nuchnoi, P. et al. (2008). Significant association between TIM1 promoter polymorphisms and protection against cerebral malaria in Thailand. *Annals of Human Genetics*, 72(Pt 3), pp.327–336.

Nuchsongsin, F. et al. (2007). Effects of malaria heme products on red blood cell deformability. *The American Journal of Tropical Medicine and Hygiene*, 77(4), pp.617–622.

O'Donnell, A. et al. (2009). Interaction of malaria with a common form of severe thalassemia in an Asian population. *Proceedings of the National Academy of Sciences of the United States of America*, 106(44), pp.18716–18721.

Oakley, M.S. et al. (2008). Host Biomarkers and Biological Pathways That Are Associated with the Expression of Experimental Cerebral Malaria in Mice. *Infection and Immunity*, 76(10), pp.4518–4529.

Ockenhouse, C.F., Magowan, C. and Chulay, J.D. (1989). Activation of monocytes and platelets by monoclonal antibodies or malaria-infected erythrocytes binding to the CD36 surface receptor in vitro. *Journal of Clinical Investigation*, 84(2), p.468.

Ockenhouse, C.F., Betageri, R., et al. (1992). Plasmodium falciparum-infected erythrocytes bind ICAM-1 at a site distinct from LFA-1, Mac-1, and human rhinovirus. *Cell*, 68(1), pp.63–69.

Ockenhouse, C.F., Tegoshi, T., et al. (1992). Human vascular endothelial cell adhesion receptors for Plasmodium falciparum-infected erythrocytes: roles for endothelial leukocyte adhesion molecule 1 and vascular cell adhesion molecule 1. *The Journal of Experimental Medicine*, 176(4), pp.1183–1189.

Oh, H. et al. (1999). Hypoxia and vascular endothelial growth factor selectively up-regulate angiopoietin-2 in bovine microvascular endothelial cells. *The Journal of Biological Chemistry*, 274(22), pp.15732–15739.

Oh, S.S. et al. (1997). Erythrocyte membrane alterations in Plasmodium falciparum malaria sequestration. *Current Opinion in Hematology*, 4(2), pp.148–154.

Ohab, J.J. et al. (2006). A neurovascular niche for neurogenesis after stroke. *The Journal of Neuroscience*, 26(50), pp.13007–13016.

Ouma, C. et al. (2008). Haplotypes of IL-10 promoter variants are associated with susceptibility to severe malarial anemia and functional changes in IL-10 production. *Human genetics*, 124(5), pp.515–524.

Outlaw, D.C. and Ricklefs, R.E. (2011). Rerooting the evolutionary tree of malaria parasites. *Proceedings of the National Academy of Sciences*, 108(32), pp.13183–13187.

Park, Y. et al. (2008). Refractive index maps and membrane dynamics of human red blood cells parasitized by Plasmodium falciparum. *Proceedings of the National Academy of Sciences of the United States of America*, 105(37), pp.13730–13735.

Parroche, P. et al. (2007). Malaria haemozoin is immunologically inert but radically enhances innate responses by presenting malaria DNA to Toll-like receptor 9. *Proceedings of the National Academy of Sciences of the United States of America*, 104(6), p.1919.

Perkins, D.J. et al. (2011). Severe malarial anemia: innate immunity and pathogenesis. *International Journal of Biological Sciences*, 7(9), pp.1427–1442.

Peters, L. and Meister, G. (2007). Argonaute proteins: mediators of RNA silencing. *Molecular Cell*, 26(5), pp.611–623.

Peyron, F. et al. (1994). Soluble intercellular adhesion molecule-1 and E-selectin levels in plasma of falciparum malaria patients and their lack of correlation with levels of tumor necrosis factor alpha, interleukin 1 alpha (IL-1 alpha), and IL-10. *Clinical and Diagnostic Laboratory Immunology*, 1(6), pp.741–743.

Pfaff, D., Fiedler, U. and Augustin, H.G. (2006). Emerging roles of the Angiopoietin-Tie and the ephrin-Eph systems as regulators of cell trafficking. *Journal of Leukocyte Biology*, 80(4), pp.719–726.

Phiri, H.T. et al. (2011). Elevated Plasma Von Willebrand Factor and Propeptide Levels in Malawian Children with Malaria. *PLoS ONE*, 6(11), p.e25626.

Planche, T. and Krishna, S. (2006). Severe malaria: metabolic complications. *Current Molecular Medicine*, 6(2), pp.141–153.

Pober, J.S. and Sessa, W.C. (2007). Evolving functions of endothelial cells in inflammation. *Nature Reviews Immunology*, 7(10), pp.803–815.

Pongponratn, E. et al. (2003). An ultrastructural study of the brain in fatal Plasmodium falciparum malaria. *The American Journal of Tropical Medicine and Hygiene*, 69(4), pp.345–359.

Ponsford, M.J. et al. (2012). Sequestration and microvascular congestion are associated with coma in human cerebral malaria. *The Journal of Infectious Diseases*, 205(4), pp.663–671.

Price, R.N., Douglas, N.M. and Anstey, N.M. (2009). New developments in Plasmodium vivax malaria: severe disease and the rise of chloroquine resistance. *Current Opinion in Infectious Diseases*, 22(5), pp.430–435.

Prudêncio, M., Rodriguez, A. and Mota, M.M. (2006). The silent path to thousands of merozoites: the Plasmodium liver stage. *Nature Reviews Microbiology*, 4(11), pp.849–856.

Rae, C. et al. (2004). Brain gene expression, metabolism, and bioenergetics: interrelationships in murine models of cerebral and noncerebral malaria. *The Journal of the Federation of American Societies for Experimental Biology*, 18(3), pp.499–510.

Raghavendra, K. et al. (2011). Malaria vector control: from past to future. *Parasitology Research*, 108(4), pp.757–779.

Rajeevan, M.S. et al. (2001). Validation of array-based gene expression profiles by real-time (kinetic) RT-PCR. *The Journal of Molecular Diagnostics*, 3(1), pp.26–31.

Rathjen, T. et al. (2006). Analysis of short RNAs in the malaria parasite and its red blood cell host. *Federation of European Biochemical Societies Letters*, 580(22), pp.5185–5188.

Roberts, D.D. et al. (1985). Thrombospondin binds falciparum malaria parasitized erythrocytes and may mediate cytoadherence. *Nature*, 318(6041), pp.64–66.

Roberts, D.J. et al. (1992). Rapid switching to multiple antigenic and adhesive phenotypes in malaria. *Nature*, 357(6380), pp.689–692.

Rocke, D.M. and Durbin, B. (2001). A model for measurement error for gene expression arrays. *Journal of Computational Biology*, 8(6), pp.557–569.

Rogerson, S.J., Mwapasa, V. and Meshnick, S.R. (2007). Malaria in pregnancy: linking immunity and pathogenesis to prevention. *The American Journal of Tropical Medicine and Hygiene*, 77(6 Suppl), pp.14–22.

Roll Back Malaria. (2006). *Economic Costs of Malaria*. WHO, Geneva, Switzerland

Rondaij, M. et al. (2006). Dynamics and plasticity of Weibel-Palade bodies in endothelial cells. *Arteriosclerosis, Thrombosis, and Vascular Biology*, 26(5), pp.1002–1007.

Sachs, J. and Malaney, P. (2002). The economic and social burden of malaria. *Nature*, 415(6872), pp.680–685.

Sato, T. N. et al. (1995). Distinct roles of the receptor tyrosine kinases Tie-1 and Tie-2 in blood vessel formation. *Nature,* 376(6535), pp.70-74.

Schaecher, K. et al. (2005). Genome-wide expression profiling in malaria infection reveals transcriptional changes associated with lethal and nonlethal outcomes. *Infection and Immunity*, 73(9), pp.6091–6100.

Schelshorn, D.W. et al. (2009). Expression of hemoglobin in rodent neurons. *Journal of Cerebral Blood Flow and Metabolism*, 29(3), pp.585–595.

Schmid, R. et al. (2010). Comparison of normalization methods for Illumina BeadChip HumanHT-12 v3. *BMC Genomics*, 11(1), p.349.

Schnürch, H. and Risau, W. (1993). Expression of tie-2, a member of a novel family of receptor tyrosine kinases, in the endothelial cell lineage. *Development,* 119(3), pp.957-968.

Schofield, L. et al. (1996). Glycosylphosphatidylinositol toxin of Plasmodium up-regulates intercellular adhesion molecule-1, vascular cell adhesion molecule-1, and E-selectin expression in vascular endothelial cells and increases leukocyte and parasite cytoadherence via tyrosine kinase-dependent signal transduction. *Journal of Immunology*, 156(5), pp.1886–1896.

Schroeder, A. et al. (2006). The RIN: an RNA integrity number for assigning integrity values to RNA measurements. *BMC Molecular Biology*, 7, p.3.

Schumann, R.R. (2007). Malarial fever: Haemozoin is involved but Toll-free. *Proceedings of the National Academy of Sciences of the United States of America*, 104(6), p.1743.

Schwartz, L. et al. (2012). A review of malaria vaccine clinical projects based on the WHO rainbow table. *Malaria Journal*, 11(1), p.11.

Schwarz, N.G. et al. (2008). Placental Malaria Increases Malaria Risk in the First 30 Months of Life. *Clinical Infectious Diseases*, 47(8), pp.1017–1025.

Sepramaniam, S. et al. (2010). MicroRNA 320a functions as a novel endogenous modulator of aquaporins 1 and 4 as well as a potential therapeutic target in cerebral ischemia. *Journal of Biological Chemistry*, 285(38), pp.29223–29230.

Sethupathy, P., Corda, B. and Hatzigeorgiou, A.G. (2006). TarBase: A comprehensive database of experimentally supported animal microRNA targets. *RNA (New York, N.Y.)*, 12(2), pp.192–197.

Sexton, A. et al. (2004). Transcriptional profiling reveals suppressed erythropoiesis, up-regulated glycolysis, and interferon-associated responses in murine malaria. *The Journal of Infectious Diseases*, 189(7), pp.1245–1256.

Shapiro, M.D. et al. (2011). MicroRNA expression data reveals a signature of kidney damage following ischemia reperfusion injury. *PLoS ONE*, 6(8), p.e23011.

Sharma, Y.D. (1997). Knob proteins in falciparum malaria. *The Indian Journal of Medical Research*, 106, pp.53–62.

Sharma, Y.D. (1991). Knobs, knob proteins and cytoadherence in falciparum malaria. *The International Journal of Biochemistry*, 23(9), pp.775–789.

Shelby, J. et al. (2003). A microfluidic model for single-cell capillary obstruction by Plasmodium falciparum-infected erythrocytes. *Proceedings of the National Academy of Science of the United States of Americas*, 100(25), pp.14618–14622.

Siano, J.P. et al. (1998). Short report: Plasmodium falciparum: cytoadherence to alpha(v)beta3 on human microvascular endothelial cells. *The American Journal of Tropical Medicine and Hygiene*, 59(1), pp.77–79.

Silamut, K. and White, N.J. (1993). Relation of the stage of parasite development in the peripheral blood to prognosis in severe falciparum malaria. *Transactions of the Royal Society of Tropical Medicine and Hygiene*, 87(4), pp.436–443.

Smyth, G.K. (2004). Linear models and empirical bayes methods for assessing differential expression in microarray experiments. *Statistical Applications in Genetics and Molecular Biology*, 3(1), article 3.

Snow, R.W. et al. (2005). The global distribution of clinical episodes of Plasmodium falciparum malaria. *Nature*, 434(7030), pp.214–217.

Stan, A. et al. (2006). Human postmortem tissue: What quality markers matter? *Brain Research*, 1123(1), pp.1–11.

Stears, R.L., Getts, R.C. and Gullans, S.R. (2000). A novel, sensitive detection system for high-density microarrays using dendrimer technology. *Physiological Genomics*, 3(2), pp.93–99.

Stins, M.F., Gilles, F. and Kim, K.S. (1997). Selective expression of adhesion molecules on human brain microvascular endothelial cells. *Journal of Neuroimmunology*, 76(1-2), pp.81–90.

Stowe, A.M. et al. (2012). CCL2 upregulation triggers hypoxic preconditioning-induced protection from stroke. *Journal of Neuroinflammation*, 9, p.33.

Subramanian, A. et al. (2005). Gene set enrichment analysis: a knowledge-based approach for interpreting genome-wide expression profiles. *Proceedings of the National Academy of Sciences of the United States of America*, 102(43), pp.15545–15550.

Suri, C. et al. (1996). Requisite role of angiopoietin-1, a ligand for the TIE2 receptor, during embryonic angiogenesis. *Cell,* 87(7), pp.1171-1180.

Szafranska, A.E. et al. (2008). Accurate molecular characterization of formalin-fixed, paraffin-embedded tissues by microRNA expression profiling. *The Journal of Molecular Diagnostics*, 10(5), pp.415–423.

Takahasi, K. and Sawasaki, Y. (1992). Rare Spontaneously Transformed Human Endothelial-Cell Line Provides Useful Research Tool. *In Vitro Cellular Developmental Biology - Animal*, 28A(6), pp.380–382.

Tan, M.G. et al. (2009). Genome wide profiling of altered gene expression in the neocortex of Alzheimer's disease. *Journal of Neuroscience Research*, pp.1157-1169.

Tatro, E.T. et al. (2010). Evidence for Alteration of Gene Regulatory Networks through MicroRNAs of the HIV-infected brain: novel analysis of retrospective cases. *PLoS ONE*, 5(4), p.e10337.

Taylor, T.E. et al. (2004). Differentiating the pathologies of cerebral malaria by postmortem parasite counts. *Nature Medicine*, 10(2), pp.143–145.

Taylor, W.R.J. et al. (2008). Changes in the total leukocyte and platelet counts in Papuan and non Papuan adults from northeast Papua infected with acute Plasmodium vivax or uncomplicated Plasmodium falciparum malaria. *Malaria Journal*, 7, p.259.

Teeranaipong, P. et al. (2008). A functional single-nucleotide polymorphism in the CR1 promoter region contributes to protection against cerebral malaria. *The Journal of Infectious Diseases*, 198(12), pp.1880–1891.

Tomita, H. et al. (2004). Effect of agonal and postmortem factors on gene expression profile: quality control in microarray analyses of postmortem human brain. *Biological Psychiatry*, 55(4), pp.346–352.

Trager, W. and Jensen, J.B. (1976). Human malaria parasites in continuous culture. *Science*, 193(4254), pp.673–675.

Trager, W. and Jenson, J.B. (1978). Cultivation of malarial parasites. *Nature*, 273(5664), pp.621–622.

Trang, T.T.M. et al. (1992). Acute renal failure in patients with severe falciparum malaria. *Clinical Infectious Diseases*, 15(5), p.874.

Treutiger, C.J. et al. (1997). PECAM-1/CD31, an endothelial receptor for binding Plasmodium falciparum-infected erythrocytes. *Nature Medicine*, 3(12), pp.1405–1408.

Tripathi, A.K. et al. (2009). Plasmodium falciparum-infected erythrocytes induce NF-kappaB regulated inflammatory pathways in human cerebral endothelium. *Blood*, 114(19), pp.4243–4252.

Tripathi, A.K., Sullivan, D.J. and Stins, M.F. (2007). Plasmodium falciparum-infected erythrocytes decrease the integrity of human blood-brain barrier endothelial cell monolayers. *The Journal of Infectious Diseases*, 195(7), pp.942–950.

Tripathi, A.K., Sullivan, D.J. and Stins, M.F. (2006). Plasmodium falciparum-infected erythrocytes increase intercellular adhesion molecule 1 expression on brain endothelium through NF-kappaB. *Infection and Immunity*, 74(6), pp.3262–3270.

Turner, G.D.H. et al. (1998). Systemic endothelial activation occurs in both mild and severe malaria. Correlating dermal microvascular endothelial cell phenotype and soluble cell adhesion molecules with disease severity. *The American Journal of Pathology*, 152(6), pp.1477–1487.

Turner, G.D.H., Morrison, H. and Jones, M. (1994). An immunohistochemical study of the pathology of fatal malaria: evidence for widespread endothelial activation and a potential role for intercellular adhesion molecule. *The American Journal of Pathology*, 145, pp.1057-1069.

Valable, S. (2003). Angiopoietin-1-induced phosphatidyl-inositol 3-kinase activation prevents neuronal apoptosis. *The Journal of the Federation of American Societies for Experimental Biology*, 17(3), pp.443-445.

Van Gelder, R.N. et al. (1990). Amplified RNA synthesized from limited quantities of heterogeneous cDNA. *Proceedings of the National Academy of Sciences of the United States of America*, 87(5), pp.1663–1667.

Vandesompele, J. et al. (2002). Accurate normalization of real-time quantitative RT-PCR data by geometric averaging of multiple internal control genes. *Genome Biology*, 3(7), research0034.1 - research0034.11 (online).

Vaughan, A.M., Aly, A.S.I. and Kappe, S.H.I. (2008). Malaria Parasite Pre-Erythrocytic Stage Infection: Gliding and Hiding. *Cell Host and Microbe*, 4(3), pp.209–218.

Vijaykumar, M., Naik, R.S. and Gowda, D.C. (2001). Plasmodium falciparum glycosylphosphatidylinositol-induced TNF-alpha secretion by macrophages is mediated without membrane insertion or endocytosis. *The Journal of Biological Chemistry*, 276(10), pp.6909–6912.

Vogt, A.M. et al. (2003). Heparan sulfate on endothelial cells mediates the binding of Plasmodium falciparum-infected erythrocytes via the DBL1alpha domain of PfEMP1. *Blood*, 101(6), pp.2405–2411.

Volkman, S.K. et al. (2006). A genome-wide map of diversity in Plasmodium falciparum. *Nature Genetics*, 39(1), pp.113–119.

Waldman, S.A. and Terzic, A. (2008). MicroRNA signatures as diagnostic and therapeutic targets. *Clinical Chemistry*, 54(6), pp.943–944.

Wang, Xiaowei. (2008). miRDB: a microRNA target prediction and functional annotation database with a wiki interface. *RNA*, 14(6), pp.1012–1017.

Wang, Xu et al. (2009). Cellular microRNA expression correlates with susceptibility of monocytes/macrophages to HIV-1 infection. *Blood*, 113(3), pp.671–674.

Ward, N.L. et al. (2005). Vascular-specific growth factor angiopoietin 1 is involved in the organization of neuronal processes. *The Journal of Comparative Neurology*, 482(3), pp.244–256.

Wassmer, S.C. et al. (2008). Platelet-induced clumping of Plasmodium falciparum-infected erythrocytes from Malawian patients with cerebral malaria-possible modulation in vivo by thrombocytopenia. *The Journal of Infectious Diseases*, 197(1), pp.72–78.

Wassmer, S.C. et al. (2004). Platelets reorient Plasmodium falciparum-infected erythrocyte cytoadhesion to activated endothelial cells. *The Journal of Infectious Diseases*, 189(2), pp.180–189.

Weatherall, D.J. et al. (2002). Malaria and the red cell. *Hematology American Society of Hematology Education Program*, 2002, pp.35–57.

Weis, S. et al. (2007). Quality control for microarray analysis of human brain samples: The impact of postmortem factors, RNA characteristics, and histopathology. *Journal of Neuroscience Methods*, 165(2), pp.198–209.

White, N.J. (2008). Plasmodium knowlesi: The Fifth Human Malaria Parasite. *Clinical Infectious Diseases*, 46(2), pp.172–173.

White, N.J. et al. (2010). The murine cerebral malaria phenomenon. *Trends in Parasitology*, 26(1), pp.11–15.

White, V.A. et al. (2009). Retinal Pathology of Pediatric Cerebral Malaria in Malawi V. Moorthy, ed. *PLoS ONE*, 4(1), p.e4317.

World Health Organization (WHO). (2010). *Guidelines for the Treatment of Malaria*. WHO, Geneva, Switzerland.

World Health Organization (WHO). (1990). Severe and complicated malaria. *Transactions of the Royal Society of Tropical Medicine and Hygine*, 84(Supplement 2), pp.1–65.

World Health Organization (WHO). (2000a). Severe falciparum malaria. *Transactions of the Royal Society of Tropical Medicine and Hygine*, 94(Supplement 1), pp.1–90.

World Health Organization (WHO). (2000b). *The World Health Report 1999: Making a Difference.* WHO, Geneva, Switzerland.

World Health Organization (WHO). (2012). *World Malaria Report 2011*. WHO, Geneva, Switzerland

Xiao, F. et al. (2009). miRecords: an integrated resource for microRNA-target interactions. *Nucleic Acids Research*, 37(Database issue), pp.D105–110.

Xu, Y. (2001). Angiopoietin-1, Unlike Angiopoietin-2, Is Incorporated into the Extracellular Matrix via Its Linker Peptide Region. *Journal of Biological Chemistry*, 276(37), pp.34990–34998.

Xue, X. et al. (2008). No miRNA were found in Plasmodium and the ones identified in erythrocytes could not be correlated with infection. *Malaria Journal*, 7, p.47.

Yeo, T.W. et al. (2008). Angiopoietin-2 is associated with decreased endothelial nitric oxide and poor clinical outcome in severe falciparum malaria. *Proceedings of the National Academy of Sciences of the United States of America*, 105(44), pp.17097–17102.

Yeo, T.W. et al. (2007). Impaired nitric oxide bioavailability and L-arginine reversible endothelial dysfunction in adults with falciparum malaria. *Journal of Experimental Medicine*.

Zhao, C. et al. (2008). Osteopontin is extensively expressed by macrophages following CNS demyelination but has a redundant role in remyelination. *Neurobiology of disease*, 31(2), pp.209–217.

Zhao, M. et al. (2011). Assembly and initial characterization of a panel of 85 genomically validated cell lines from diverse head and neck tumor sites. *Clinical cancer research : an official journal of the American Association for Cancer Research*, 17(23), pp.7248–7264.

Zhu, J., Krishnegowda, G. and Gowda, D.C. (2005). Induction of proinflammatory responses in macrophages by the glycosylphosphatidylinositols of Plasmodium falciparum: the requirement of extracellular signal-regulated kinase, p38, c-Jun N-terminal kinase and NF-kappaB pathways for the expression of proinflammatory cytokines and nitric oxide. *The Journal of Biological Chemistry*, 280(9), pp.8617–8627.

Zinna, S., Vathsala, A. and Woo, K.T. (1999). A case series of falciparum malaria-induced acute renal failure. *Annals of the Academy of Medicine, Singapore*, 28(4), pp.578–582.

Appendix A

Recipes of buffers and culture media

Fixatives for tissue collection

10% Buffered formalin (pH 7.4)

900 ml distilled water	
100 ml Formaldehyde (final 4%)	Sigma (F15587)
4 g NaH_2PO_4	Sigma (S5011)
6.5 g Na_2HPO_4 (anhydrous)	Sigma (S5136)

Buffers for Immunohistochemistry

TBS

1000 ml distilled water	
6.1 g Trizma base	Sigma (T1503)
9 g NaCl	Sigma (S7653)
(Adjust pH to 8.4 by HCL)	Sigma (H1758)

Tris-EDTA (pH8)

1000 ml distilled water	
1.21 g Trizma base	Sigma (T1503)
0.37 g EDTA	Sigma (E9884)
(Adjust pH to 8 by HCl)	Sigma (H1758)

Media used in bacterial transformation and culture

LB agar plate with kanamycin

500 ml distilled water	VWR (DF0445-17)
20 g premix LB agar powder	Sigma (K1377)
50 mg kanamycin (final 100 μg/ml)	Sigma (K0254)

Media and buffer used in HEK293 culture

Supplemented culture medium

440 ml Minimum Essential Media (MEM) with GlutaMAX™	Gibco(41090-028)
50 ml heat-inactivated FBS (final 10%)	Gibco (10082-147)
5 ml sodium pyruvate MEM (final 1mM)	Invitrogen (11360-039)
5 ml MEM non-essential amino acids (final 0.1 mM)	Invitrogen (11140-050)

Non-supplemented culture medium

MEM with GlutaMAX™	Gibco(41090-028)

Media and buffers used in HBEC isolation, culture and characterisation

Isolation medium	
480 ml RPMI 1640	Gibco (21875-034)
10 ml heat-inactivated FBS (2%)	Gibco (10082-147)
5 ml Pen-Strep (1X) (penicillin 100 IU/ml and streptomycin 100 µg/ml)	Gibco (15140-122)
5 ml Fungizone® (1X) (amphotericin B 2.5 µg/ml)	Gibco (15290-026)
HBEC stock medium	
380 ml RPMI 1640	Gibco (21875-034)
50 ml heat-inactivated FBS (10%)	Gibco (10082-147)
50 ml NuSerum™ (10%)	BD Biosciences (355550)
5 ml sodium pyruvate MEM (1X) (1mM)	Invitrogen (11360-039)
5 ml MEM non-essential amino acids (1X) (0.1 mM)	Gibco (11140-050)
5 ml MEM vitamins (1X)	Gibco(11120-037)
5 ml Pen-Strep (1X)	Gibco (15140-122)
HBEC + E/H (ECGS and heparin)	
200 ml HBEC stock (as above)	
6 mg ECGS (Endothelial Cell Growth Supplement) (30 µg/ml)	BD Biosciences (356006)
16000 IU heparin (80 IU/ml)	Sigma (H3149)
PBS	
900 ml sterilised water	
100 ml BioReagent, 10X concentrated phosphate buffered saline	Sigma (P5493)
PBST	
990 ml PBS (as above)	
10 ml Triton X-100 (1%)	Sigma (T8532)
Blocking solution	
97.5 ml PBS (as above)	
5 ml Donkey serum (5%)	Abcam (ab7475)
2.5 ml Triton X-100 (2.5%)	Sigma (T8532)
Enzymatic digestion medium	
Isolation medium (as above)	
Collagenase dispase 0.5 mg/ml	Roche (10269638001)
DNase 0.2 ml/ml	Sigma (AMPD1)
HBSS	
900 ml sterilised water (distilled and deionised)	
100 ml HBSS, 10X	Gibco (14060-073)

Media used in malaria parasite culture

Malaria culture medium

500 ml RPMI 1640	Gibco (21875-034)
18.75 ml HEPES (37.5 mM)	Sigma (H0887)
5 ml 20% W/V glucose solution (0.2% W/V)	Sigma (49163)
3 ml 1M sodium hydroxide solution (1.5 mM)	Sigma (S2770)
1.25 ml gentamicin (25 μg/ml)	Sigma (G1272)
5 ml glutamine (20 μM)	Sigma (G7513)
5 ml hypoxanthine (1X)	Gibco (11067-030)

Complete malaria medium

460 ml malaria culture medium (as above)	
40 ml pooled human serum	(healthy blood donors)

Appendix B

Supplementary data for Chapter 5

Table B-1. List of 75 significantly up-regulated miRNAs in the kidney of malaria compared to control cases

Up-regulated miRNA	Fold change	Adjusted *P*
hsa-miR-1307	2.00500	0.02534
hsa-miR-1227	2.02300	0.03021
hsa-miR-34c-3p	2.02395	0.00018
hsa-miR-877	2.03417	0.01034
hsa-miR-768-5p	2.05188	0.01043
hsa-miR-668	2.05740	0.04969
hsa-miR-611	2.09376	0.02108
hsa-miR-920	2.09786	0.00121
hsa-miR-658	2.10005	0.04224
hsa-miR-1207-5p	2.11020	0.01892
hsa-miR-513a-5p	2.15267	0.01043
hsa-miR-25-star	2.16126	0.01930
hsa-miR-432	2.21856	0.00426
hsa-miR-423-5p	2.22994	0.00008
hsa-miR-593	2.24296	0.04055
hsa-let-7b-star	2.25057	0.01102
hsa-miR-1292	2.30502	0.02378
hsa-miR-1224-3p	2.31612	0.01344
hsa-miR-188-5p	2.33296	0.01646
hsa-miR-1228-star	2.36712	0.00093
hsa-miR-302c-star	2.38079	0.00032
hsa-miR-671-5p	2.38803	0.00836
hsa-let-7b	2.44538	0.02251
hsa-miR-1234	2.48863	0.01265
hsa-miR-1183	2.59973	0.02773
hsa-miR-663	2.60496	0.00265
hsa-miR-665	2.60562	0.02908
hsa-miR-92b-star	2.74994	0.00836
hsa-miR-1825	2.77442	0.00935
hsa-miR-1224-5p	2.78203	0.00705
hsa-let-7c	2.79836	0.02709
hsa-miR-623	2.83162	0.00672
hsa-miR-675	2.83234	0.00245
hsa-miR-1238	2.86307	0.01070
hsa-miR-637	2.87816	0.00875
hsa-miR-608	2.88665	0.00008
hsa-miR-23a-star	2.97911	0.03280
hsa-miR-498	3.01044	0.00049
hsa-miR-135a-star	3.04794	0.00030
hsa-miR-107	3.24722	0.01675
hsa-miR-150-star	3.26370	0.00698
hsa-miR-885-3p	3.48094	0.00180
hsa-miR-1182	3.58430	0.00295
hsa-miR-1225-5p	3.60879	0.00059
hsa-miR-191-star	3.61050	0.01070
hsa-miR-1202	3.66633	0.00059
hsa-miR-1275	3.71490	0.00006
hsa-miR-615-5p	3.76226	0.00123
hsa-miR-744	3.77320	0.00007
hsa-miR-557	3.82978	0.00188
hsa-miR-1228	3.96517	0.00123
hsa-miR-659	4.04621	0.00005
hsa-let-7g	4.13343	0.01488
hsa-miR-16	4.19380	0.03216
hsa-miR-760	4.27000	0.00038
hsa-miR-103	4.33630	0.02244
hsa-miR-940	4.38926	0.00235
hsa-miR-1281	4.45421	0.00093
hsa-miR-373-star	4.45884	0.00105
hsa-miR-939	4.52291	0.00024
hsa-let-7d	4.60909	0.00010
hsa-miR-106a	4.76339	0.01070
hsa-let-7f	4.82349	0.02193
hsa-miR-296-3p	4.82352	0.00001
hsa-miR-17	4.89359	0.01646
hsa-miR-1268	4.90388	0.00000
hsa-miR-20a	5.33574	0.01949
hsa-let-7i	5.56380	0.00078
hsa-miR-886-5p	5.66041	0.00006
hsa-let-7e	5.75188	0.00247
hsa-miR-371-5p	7.81706	0.00000
hsa-let-7a	8.36203	0.00093
hsa-miR-572	8.71257	0.00000
hsa-miR-1308	9.76120	0.00000
hsa-miR-509-3p	15.33136	0.00121

(FDR-adjusted $P < 0.05$ and fold-change cutoff = 2)

Table B-2. List of 82 significantly down-regulated miRNAs in the kidney of malaria compared to control cases

Down-regulated miRNA	Fold change	Adjusted *P*
hsa-miR-486-5p	-13.07143	0.00000
hsa-miR-151-3p	-12.81723	0.00000
hsa-miR-125b	-12.07673	0.00000
hsa-miR-1826	-11.24780	0.00001
hsa-miR-501-5p	-9.65268	0.00000
hsa-miR-193b	-9.16729	0.00000
hsa-miR-22	-6.23866	0.00005
hsa-miR-28-3p	-6.14089	0.00027
hsa-miR-19b	-6.01461	0.00002
hsa-miR-127-3p	-5.82931	0.00018
hsa-miR-145	-5.76655	0.00059
hsa-miR-99b	-5.70477	0.00001
hsa-miR-500	-5.66955	0.00076
hsa-miR-10b	-5.44571	0.00044
hsa-miR-30d	-5.40768	0.00008
hsa-miR-100	-4.92797	0.00006
hsa-miR-10a	-4.69872	0.00210
hsa-miR-125a-5p	-4.66798	0.00002
hsa-miR-576-3p	-4.65341	0.03075
hsa-miR-606	-4.44058	0.00685
hsa-miR-339-5p	-4.28807	0.00017
hsa-miR-422a	-4.06330	0.00006
hsa-miR-494	-4.02850	0.01675
hsa-miR-501-3p	-3.90317	0.00006
hsa-miR-181a	-3.78393	0.00196
hsa-miR-99a	-3.73887	0.00009
hsa-miR-191	-3.62189	0.01073
hsa-miR-122-star	-3.61775	0.00006
hsa-miR-32	-3.59083	0.02340
hsa-miR-423-3p	-3.56644	0.00149
hsa-miR-25	-3.49394	0.00472
hsa-miR-378-star	-3.44778	0.00010
hsa-miR-30e	-3.40003	0.00805
hsa-miR-143-star	-3.35343	0.00265
hsa-miR-923	-3.32741	0.03141
hsa-miR-548c-3p	-3.24891	0.00665
hsa-miR-26a-2-star	-3.07665	0.01688
hsa-miR-139-5p	-3.04839	0.00935
hsa-miR-451	-3.04279	0.03280
hsa-miR-129-3p	-3.03444	0.01693
hsa-miR-362-5p	-3.00904	0.01675
hsa-miR-202-star	-3.00324	0.03497
hsa-miR-96	-2.96065	0.00006
hsa-miR-155-star	-2.96013	0.04701
hsa-miR-204	-2.92771	0.00705
hsa-miR-1285	-2.89812	0.00836
hsa-miR-324-3p	-2.86291	0.00076
hsa-miR-187	-2.82270	0.01826
hsa-miR-181c	-2.78920	0.00355
hsa-miR-92a	-2.78186	0.00032
hsa-miR-192-star	-2.76107	0.00001
hsa-miR-345	-2.75832	0.00245
hsa-miR-542-3p	-2.69032	0.02108
hsa-miR-183-star	-2.68179	0.02106
hsa-miR-216a	-2.64317	0.01500
hsa-miR-23b-star	-2.64289	0.00875
hsa-miR-615-3p	-2.59746	0.00349
hsa-miR-340	-2.59110	0.00500
hsa-miR-424-star	-2.50616	0.01204
hsa-miR-331-3p	-2.48633	0.02773
hsa-miR-500-star	-2.47184	0.01173
hsa-miR-26b-star	-2.45725	0.01344
hsa-miR-339-3p	-2.43530	0.01693
hsa-miR-29c-star	-2.43300	0.00006
hsa-miR-139-3p	-2.39553	0.04055
hsa-miR-101	-2.38879	0.00515
hsa-miR-30a	-2.37015	0.00935
hsa-miR-769-5p	-2.34267	0.00123
hsa-miR-17-star	-2.27901	0.00911
hsa-miR-106b-star	-2.27773	0.02152
hsa-miR-448	-2.20258	0.01344
hsa-miR-182	-2.17994	0.03646
hsa-miR-874	-2.17225	0.02463
hsa-miR-214-star	-2.14635	0.00256
hsa-miR-92b	-2.14352	0.01110
hsa-miR-323-3p	-2.11888	0.02463
hsa-miR-378	-2.11874	0.03057
hsa-miR-502-3p	-2.11656	0.00228
hsa-miR-660	-2.11171	0.02427
hsa-miR-891b	-2.11012	0.01675
hsa-miR-548f	-2.08025	0.00001
hsa-miR-320d	-2.01278	0.03645

(FDR-adjusted $P < 0.05$ and fold-change cutoff = 2)

Table B-3. The list of differentially expressed miRNAs in malaria and the number of their experimentally proven mRNA targets

Up-regulated MicroRNA	No. of targeted mRNAs
let-7a/let-7f/let-7c (i.o.)	129
miR-103/miR-103a/miR-107	14
miR-16/miR-497/miR195 (i.o.)	176
miR20a/miR-106b/miR-17-5p (i.o.)	39
miR-292-5p/miR-290/miR-293* (i.o.)	21
miR-371b-5p/miR-616*/miR-373* (i.o.)	4
miR-509-3p (human)	1
miR-513a-5p	1
miR-615-5p/miR-615	1
miR-659	1
miR-675/miR-4466/miR-675-5p	1
Down-regulated MicroRNA	**No. of targeted mRNAs**
miR-100/miR-99a/miR-99b	6
miR-101/miR101a/miR-101b	7
miR-10a/miR-10b/miR-10a-5p	5
miR-125b-5p/miR-125a-5p/miR-125b (i.o.)	66
miR-127/miR-127-3p	4
miR-1285/miR-612/miR-3187-5p	1
miR-139-5p	1
miR-145	43
miR-181a/miR-181b/miR-181d (i.o.)	17
miR-182	4
miR-191	4
miR-193/miR-193b/miR-193a-3p	7
miR-19b/miR-19a	11
miR-211/miR-204	19
miR-216a	1
miR-22	4
miR-30c/miR-30a/miR-30d (i.o.)	98
miR-320d/miR-320b/miR-320c (i.o.)	4
miR-331-3p/miR-331	3
miR-339-5p/miR-3586-5p	4
miR-378*	2
miR-378d/miR-378/miR-422a (i.o.)	3
miR-424*	1
miR-451	4
miR-494	5
miR-92a/miR92b/miR-32 (i.o.)	13
miR-96/miR-1271	12

Abbreviations: i.o. = includes others in the same cluster

The associations between miRNAs and their targeted mRNAs in this list were experimentally confirmed in other studies (not by target prediction algorithms).

Appendix C

Supplementary data for Chapter 7

Table C-1. List of 172 significantly up-regulated mRNAs in the brain of malaria compared to control cases

Gene symbol	Fold change	*P*-value
HBA2	5.03719	0.00058
FCGBP	4.52949	0.00013
HAMP	4.33533	0.01430
S100A8	3.87876	0.01072
CCL2	3.52845	0.00959
SPP1	3.52491	0.00143
HBA1	3.49255	0.00060
S100A9	3.36235	0.01748
SPP1	3.16713	0.00297
ANGPTL4	2.91788	0.00134
SNAP25	2.88865	0.00050
C7orf68	2.85337	0.00389
CD14	2.65235	0.00424
HBA2	2.53863	0.00279
MT1X	2.48462	0.02404
MT1G	2.44454	0.00048
IL6	2.43989	0.00001
PVALB	2.39452	0.01056
NEFM	2.38746	0.02396
HBB	2.37650	0.00498
TM4SF1	2.32903	0.00009
RGS16	2.28828	0.02917
ZFP36	2.28229	0.01577
IL1B	2.26775	0.00000
CHI3L1	2.25746	0.00941
ALOX5AP	2.22709	0.03856
IL8	2.22155	0.04494
SYT1	2.19391	0.00334
C10orf10	2.18895	0.00336
CD14	2.16879	0.02775
SELE	2.06233	0.00028
LDHA	2.02984	0.00032
ADM	2.01806	0.01364
GTSF1	2.01427	0.00847
GLS	1.96079	0.00273
ALDH1A1	1.95952	0.01232
VSNL1	1.94894	0.01066
MYBPC1	1.93809	0.00364
CEBPB	1.91619	0.01636
BHLHE40	1.91014	0.00007
DDIT4	1.90624	0.00001
IL8	1.89538	0.02423
PIP4K2A	1.86942	0.02442
SRGN	1.86694	0.00370
MT1H	1.84606	0.00035
HLA-DRB1	1.83336	0.00848
LDHA	1.82934	0.00013
PFKFB3	1.80922	0.00618
ANGPTL4	1.80404	0.00001
CHI3L2	1.80303	0.01153
CH25H	1.80098	0.00502
RCAN2	1.79627	0.00956
NAMPT	1.79524	0.00699
MS4A6A	1.79294	0.00710
ACSL1	1.79094	0.01860
SRGN	1.78922	0.00368
NSF	1.78585	0.00015
CD93	1.77985	0.00233
SERPINI1	1.77957	0.01425
MS4A6A	1.77923	0.00083
LPIN1	1.76937	0.00004
NAPB	1.76382	0.00090
MAP1B	1.76001	0.01536
ADAMTS1	1.75661	0.00342
MT1A	1.75448	0.02927
BTBD3	1.75172	0.00252
STOM	1.74557	0.00599
TMEM176A	1.73699	0.00000
CCL20	1.73316	0.01446
ADORA3	1.73097	0.04319
PRNP	1.72068	0.00049
NECAB1	1.69921	0.00203
MT2A	1.68534	0.04038
MS4A6A	1.68297	0.01394
F3	1.68123	0.00226
PRDX3	1.67868	0.00000
EIF1AY	1.67495	0.04776
TNFRSF1B	1.67244	0.00972
MAPK10	1.66510	0.00003
MAP4	1.66461	0.00657
KIT	1.66182	0.02159
SH3BGRL2	1.65696	0.00960
NAMPT	1.65114	0.00426
RGS5	1.65028	0.01527
QDPR	1.64325	0.02333
BTBD3	1.64261	0.01402
LILRB3	1.64208	0.00048
PAMR1	1.64145	0.03901
UGP2	1.63773	0.00035
MYBPC1	1.63746	0.02661
S100A4	1.63312	0.00021
ETS2	1.63110	0.00004
MGST1	1.62882	0.02148
EPDR1	1.62400	0.01898
MGP	1.62142	0.04403
EFR3A	1.62028	0.00733
LOC728643	1.61364	0.00096
GCA	1.60970	0.00508
KIT	1.60781	0.04869
F3	1.60266	0.01396

(unadjusted $P < 0.05$ and fold-change cutoff = 1.5)

Table C-1 (*continued*). List of 172 significantly up -regulated mRNAs in the brain of malaria compared to control cases

Gene symbol	Fold change	*P*-value
TIPARP	1.59874	0.02607
PCSK1	1.59792	0.02341
ACP1	1.59710	0.00137
MYBPC1	1.59545	0.00028
SYNM	1.59431	0.01087
EPB41L3	1.59156	0.04795
S100A12	1.58937	0.04842
RAC2	1.58909	0.03144
NSF	1.58710	0.00721
AQP9	1.58464	0.00515
CACYBP	1.58278	0.00572
NCOA7	1.58128	0.00182
STMN2	1.57701	0.04175
CAB39	1.57682	0.00095
MPZL2	1.57669	0.00475
ANGPT2	1.57514	0.01770
GNG10	1.57475	0.00108
NSF	1.57261	0.00004
CTSH	1.56785	0.01725
IL13RA1	1.56551	0.01474
S100A1	1.56304	0.01116
PTPLAD1	1.56136	0.00018
AUH	1.56101	0.00012
STC1	1.56003	0.01990
SASH1	1.55746	0.02839
TMOD2	1.55457	0.02398
PPA1	1.55215	0.00720
CDKN1A	1.55184	0.02759
SGK1	1.55104	0.04576
MAP3K8	1.54986	0.00136
PRDX6	1.54603	0.00196
APP	1.54551	0.00257
UGP2	1.54389	0.00171
DTNA	1.54377	0.00787
WASF3	1.54309	0.00024
PRUNE2	1.54210	0.00589
SH3GL2	1.54186	0.00514
SLC11A1	1.54154	0.04353
TMEM14A	1.54124	0.00411
NFIL3	1.54029	0.01262
SLC2A3	1.53879	0.00021
CITED2	1.53830	0.02559
FCGR2A	1.53786	0.00544
BAALC	1.53643	0.02520
INA	1.53505	0.01925
RIOK3	1.53494	0.00237
ELOVL7	1.53477	0.00063
WAC	1.53467	0.00386
FCGR2A	1.53396	0.00311
G3BP2	1.53073	0.00021
SCG3	1.53008	0.04686
ITM2B	1.52903	0.00360
MAP3K6	1.52536	0.00031
CHGB	1.52354	0.04798
C20orf177	1.52061	0.00705
RGS5	1.51811	0.01765
RAB3IP	1.51630	0.00299
HIGD1A	1.51392	0.00020
MAP2K4	1.51353	0.01388
SDCBP	1.51236	0.00033
SLC16A3	1.51109	0.03361
DNM1L	1.51105	0.00472
PFKFB3	1.50987	0.00234
STOM	1.50736	0.00001
STX16	1.50729	0.00582
AQP4	1.50666	0.00801
C2CD2	1.50611	0.03819
DTNA	1.50574	0.00719
HK2	1.50347	0.00270
TRIM37	1.50340	0.00050
ADCYAP1	1.50209	0.03687
MDH1	1.50079	0.00083

(unadjusted $P < 0.05$ and fold-change cutoff = 1.5)

Table C-2. List of 51 significantly down -regulated mRNAs in the brain of malaria compared to control cases

Gene symbol	Fold change	*P*-value
PENK	-2.83566	0.04231
IFI6	-2.66790	0.00003
NNAT	-2.64554	0.02310
IGFBP3	-2.23366	0.03569
C20orf103	-2.15844	0.01819
ISG15	-2.14871	0.00153
IFI6	-2.00030	0.00148
IGFBP3	-1.98281	0.04167
DLL3	-1.89282	0.00142
LOC644936	-1.87752	0.00133
ALB	-1.77362	0.02711
IFI27	-1.76786	0.00022
CD24	-1.75420	0.04515
RPS2	-1.71660	0.00680
BCAN	-1.71484	0.00428
NKIRAS2	-1.65597	0.00004
CYB5R2	-1.65521	0.04041
SOX11	-1.65344	0.00139
MARCH4	-1.65314	0.01830
KLHL35	-1.64695	0.00053
DCX	-1.63163	0.03038
IRF2BPL	-1.62978	0.01259
H1FX	-1.62223	0.00088
UPK3BL	-1.62183	0.00000
PAFAH1B3	-1.61580	0.00253
COL20A1	-1.61500	0.01181
LY6E	-1.61028	0.00135
HLA-F	-1.60148	0.00203
LOC646836	-1.60045	0.00000
ARHGAP33	-1.59844	0.01739
PRIC285	-1.57807	0.00017
PLTP	-1.57336	0.04820
STAT1	-1.56574	0.04848
CSPG5	-1.55643	0.02471
TMSB15A	-1.55036	0.01997
LPPR2	-1.54525	0.01299
GBP4	-1.54209	0.04723
DAAM1	-1.53332	0.02028
MX1	-1.53310	0.03535
CSMD2	-1.53056	0.00986
HLA-H	-1.52980	0.00604
RPL13A	-1.52923	0.00259
DYRK2	-1.52699	0.01885
EIF5A	-1.52611	0.00074
HLA-A	-1.52446	0.00001
C17orf70	-1.52262	0.00723
KCNQ2	-1.51720	0.00162
LYPD1	-1.51075	0.00558
HBG2	-1.50566	0.03860
C20orf27	-1.50267	0.02758
SPATA2L	-1.50133	0.00743

(unadjusted $P < 0.05$ and fold-change cutoff = 1.5)

Table C-3. The list of 16 significantly enriched networks of genes associated with malaria, identified by IPA

ID	Molecules in network	Score	Focus molecule	Top functions
1	7S NGF, ADCYAP1 (includes EG:11516), APP, AQP4, calpain, CHGB, Ck2, Creb, CSPG5, DCX, DLL3, DNM1L, Dynamin, Dynein, MAP1B, N-type Calcium Channel, NAPB, NMDA Receptor, NSF, PENK, PI3K (complex), PIP4K2A, PVALB (includes EG:19293), QDPR, RAB3IP, SCAVENGER RECEPTOR CLASS A, SERPINI1, SH3GL2, SNAP25, Snare, STC1, STOM, STX16, Syntaxin, SYT1 (includes EG:20979)	41	23	Neurological Disease, Genetic Disorder, Psychological Disorders
2	BMP, C/ebp, CCL2, Fcgr2, Growth hormone, HAMP, HLA-F, IL-17f dimer, IL17a dimer, IL17R, LDHA, lymphotoxin-alpha1-beta2, MAP3K, NAMPT, NCOA7, NFkB (complex), NFkB (family), NfkB-RelA, NIK, NKIRAS2, PCSK1, peptidase, PI3K (family), PRDX3, PTPLAD1, RIOK3, S100, S100A4, S100A8, S100A9, S100A1 (includes EG:20193), Sod, TMOD2, TMSB15A, VSNL1	31	18	Cell-To-Cell Signaling and Interaction, Inflammatory Response, Cardiovascular Disease
3	20s proteasome, 26s Proteasome, ALDH1A1, AMPK, CAB39, Caspase 3/7, Cbp/p300, CD3, CDKN1A, chemokine, Cyclin A, DYRK2, FCGBP, HISTONE, Histone h4, HLA-A, Iga, IgG, Igm, IL6, IL12 (family), IL1B, Interferon alpha, MHC CLASS I (family), MT1G, PFKFB3, PPA1, PRNP, Proinsulin, Ptk, RAC2, RPS2, SRGN, STAT, Ubiquitin	24	15	Cell Cycle, Cell-To-Cell Signaling and Interaction, Lipid Metabolism
4	ACSL1, Akt, ALOX5AP, BCR, BHLHE40, C1q, CHI3L1, DDIT4, EIF5A, Fc gamma receptor, Fcer1, Fcgr3, FCGR2A, Fgf, Gm-csf, HK2, Ige, IgG1, Igg3, IL13RA1, Immunoglobulin, KIT, LY6E, MTORC1, NADPH oxidase, NFIL3, p70 S6k, peroxidase, PLA2, PLC gamma, PRDX6, SDCBP, SYK/ZAP, TSH, VAV	22	14	Humoral Immune Response, Protein Synthesis, Cell-mediated Immune Response
5	ADAMTS1, Angiotensin II receptor type 1, CH25H, ERK, FSH, GTPASE, HLA-DRB1, IFI6, IFI27, Ifn, IFN alpha/beta, IFN Beta, IFN TYPE 1, Ifnar, IgG2a, IL23, IL12 (complex), IRG, ISG15, JAK, Lh, MHC, MHC Class I (complex), MHC Class II (complex), MT1H, MT1X, MT2A, MX1, Oas, RGS5, RGS16, S100A12, STAT1, STAT5a/b, Tlr	22	14	Dermatological Diseases and Conditions, Immunological Disease, Inflammatory Disease
6	ADM, ALB, ALT, AQP9, CACYBP, Cebp, CEBPB (includes EG:1051), cyclooxygenase, ERK1/2, Fibrin, glutathione peroxidase, GOT, HBA1/HBA2, HBB, HBG2, hCG, HDL, hemoglobin, IGFBP3, Insulin, JINK1/2, MGP, N-cor, Nos, Nr1h, PEPCK, PLTP, Pro-inflammatory Cytokine, Rar, Rxr, SAA, SPP1 (includes EG:20750), TM4SF1, TMEM176A, VitaminD3-VDR-RXR	21	14	Organismal Injury and Abnormalities, Respiratory Disease, Genetic Disorder
7	AGTR1, C17orf70, C20orf27, CCL27, CD97, CSAD, ELOVL7, endocannabinoid, ENPP1, FANCB, G3BP2, H1FX, HRAS, IFI27, INA, LASP1, LPIN1, Mcpt1, MYL12B, NSDHL, PAFAH1B3, PLS3, PLTP, PPARA, PRIC285, RIN1, SASH1, SC5DL, SLC16A3, SREBF1, TERF2, TGFB1 (includes EG:21803), Tpm4, TYMP, UGDH	20	13	Cellular Development, Cellular Growth and Proliferation, Digestive System Development and Function

Table C-3 (*continued*). The list of 16 significantly enriched networks of genes associated with malaria, identified by IPA.

ID	Molecules in network	Score	Focus molecule	Top functions
8	14-3-3, alcohol group acceptor phosphotransferase, C8, Calcineurin protein(s), caspase, CCL2, CD14, Cytochrome c, DAAM1, E2f, F3, GCA, Hsp27, Hsp90, Ifn gamma, Jnk, MAP2K4, MAP2K1/2, MAP3K6, MAP3K8, MAPK10, Mek, MT1A, NFAT (complex), Nfat (family), NfkB1-RelA, Pak, Raf, RCAN2, SELE (includes EG:20339), Tnf, Tnf receptor, TNFRSF1B, trypsin, ZFP36	19	14	Hematological Disease, Infectious Disease, Organismal Injury and Abnormalities
9	ACP1 (includes EG:11431),Actin,Alp,Alpha catenin,ANGPTL4,Cdk,CITED2,Collagen type I,Collagen(s),Cyclin B,Cyclin E,DTNA,elastase,EPB41L3,ETS2,Focal adhesion kinase,Integrin,ITM2B,Laminin,MAP4,Mapk,MGST1,Mlc,Pdgf (complex),PDGF BB,PP2A,proprotein convertase,Rap1,Rock,SLC2A3,Sos,STMN2,SYNM,Tgf beta,WASF3	18	13	Cellular Assembly and Organization, Cellular Function and Maintenance, Genetic Disorder
10	ARHGAP33, BAALC, BCAN, C10orf10, CD48, CEP192, CHI3L2, COL13A1, COL16A1, COL17A1, COL20A1, COL25A1, COL6A1, COL6A2, collagen, CSMD2, CYLD, DMD, EGFR, FUT4, FYN, HEXA, MDH1, miR-7-5p/miR-7a-5p/miR-7a, MYBPC1, NEFM, PAMR1, PEPD, SEPP1, SPARCL1, SPATA2L, SRCIN1, TBXAS1, TNF, Wap	18	12	Dermatological Diseases and Conditions, Gastrointestinal Disease, Organismal Injury and Abnormalities
11	AUH, BCL2, BDNF, BNIP3, C14orf166, CCDC33, CCDC92, CTSH, EIF1AY, EIF5B, ELAVL4, EWSR1, FXR1, FXR2, IFT57, IL20, IL4 (includes EG:16189), LAMP5, LYPD1, MATK, MED7 (includes EG:171285), neuroprotectin D1, NNAT, PRUNE2, RALYL, SCG3, SH3BGRL2, STAT5A, TIPARP, TNFRSF4, TNFRSF17, TRIB2, TRIM37, UGP2, ZFPM1	18	12	Behavior, Cell-mediated Immune Response, Cellular Development
12	CALCRL, CD6, CD93, EFR3A, ELP2, GBP4, HBG2, Histone h3, HTATIP2, HTR7, IKK (complex), IRF2BPL, KISS1, LAX1, MAP3K6, MT1G, MTORC2, P38 MAPK, Rac, Ras, Ras homolog, RNA polymerase II, RPL13A, S1PR2, S1PR3, S1PR4, SGK1, SLC5A3, STOM, TCR, TIFA, TLR2/TLR4, TNFRSF1A, UPP1, Vegf	14	10	Cellular Compromise, Cell Morphology, Cellular Development
13	ALPL, CAPNS1, CCND2, CDK4/6, CDKN2D, CLEC3B, CTNNB1, CTSZ, CXADR, CYB5R2, CYB5R3, EPDR1, EZH2, FZD7, GNG10, HIGD1A, IGJ, Immunoglobulin, LILRB3, MARCH4, miR-26a-5p/miR-26b-5p, miR-302d-3p/miR-302a-3p/miR-291a-3p (includes others), MIR17HG, MPZL2, MYC, NDRG2, peptidase, PRKACB, RPL41, SLC11A1, STX2, TMEM14A, UBQLN4, WAC, XIST	13	10	Cancer, Hematological Disease, Cell Cycle
14	ADCY, ADORA3, ANGPT2, Ap1, Calmodulin, CaMKII, CD24, estrogen receptor, F Actin, Fibrinogen, G protein, G protein alphai, GLS, Gsk3, Hdac, HILPDA, HLA-DR, Hsp70, Ikb, IL1, IL8, KCNQ2, Ldh, LDL, LPPR2, Mmp, NECAB1, Notch, p85 (pik3r), Pka, Pkc(s), PLC, SOX11, SRC, Tubulin	13	10	Cardiovascular System Development and Function, Cellular Movement, Cellular Development
15	BTBD3, PLXNB3	2	1	
16	inosine, MS4A6A	2	1	Small Molecule Biochemistry, Gastrointestinal Disease, Hepatic System Disease

The networks are listed in order of their significance based on the IPA calculated network score, which is the negative exponent of the right-tailed Fisher's exact test result. Also shown is the Focus Molecules category, which indicates the number of network-eligible genes per network.

Table C-4. List of 32 significantly up-regulated miRNAs in the brain of malaria compared to control cases

Up-regulated miRNA	Fold change	*P*-value
hsa-miR-1299	8.38433	0.01419
hsa-miR-4286	7.50390	0.01577
hsa-miR-3187	6.87467	0.00607
hsa-miR-28-3p	6.25481	0.00273
hsa-miR-1184	6.14685	0.00303
hsa-miR-3188	5.92619	0.01920
hsa-miR-1280	5.36768	0.03417
hsa-miR-572	5.28427	0.00490
hsa-miR-1260	4.41176	0.02008
hsa-miR-4322	4.26530	0.01437
hsa-miR-498	4.19306	0.00832
hsa-miR-373-star	4.01006	0.00102
hsa-miR-939	3.89751	0.03814
hsa-miR-1825	3.87518	0.01192
hsa-miR-29a	3.62228	0.00951
hsa-miR-602	3.44777	0.02358
hsa-miR-1281	3.34222	0.01702
hsa-miR-1273d	2.96126	0.02283
hsa-miR-1909-star	2.88493	0.03429
hsa-miR-1228	2.78303	0.03325
hsa-miR-191-star	2.60469	0.00085
hsa-let-7f-1-star	2.52230	0.00119
hsa-miR-940	2.47175	0.03338
hsa-miR-1238	2.25930	0.04264
hsa-miR-382	2.23063	0.04229
hsa-miR-1237	2.07055	0.02782
hsa-miR-146b-3p	1.93119	0.01720
hsa-miR-500	1.86500	0.04769
hsa-let-7d-star	1.76671	0.02030
hsa-miR-557	1.70954	0.02941
hsa-miR-4323	1.52936	0.01194
hsa-miR-22	1.51947	0.04834

(unadjusted $P < 0.05$ and fold-change cutoff = 1.5)

Table C-5. List of 22 significantly down-regulated miRNAs in the brain of malaria compared to control cases

Down-regulated miRNA	Fold change	*P*-value
hsa-miR-34c-5p	-7.80489	0.02612
hsa-miR-1246	-6.18230	0.00357
hsa-miR-18a	-5.83293	0.02285
hsa-miR-1979	-4.18307	0.00623
hsa-miR-770-5p	-4.09647	0.04252
hsa-miR-505-star	-3.92401	0.03384
hsa-miR-4324	-3.22201	0.01975
hsa-miR-654-5p	-2.66088	0.02881
hsa-miR-891a	-2.64255	0.01277
hsa-miR-101	-2.63294	0.01778
hsa-miR-30b-star	-2.52894	0.03385
hsa-miR-135a-star	-2.41622	0.01256
hsa-miR-1291	-2.40532	0.00185
hsa-miR-92b	-2.12778	0.00124
hsa-miR-576-3p	-1.97455	0.04947
hsa-miR-324-5p	-1.85859	0.04254
hsa-miR-3177	-1.72468	0.02674
hsa-miR-18a-star	-1.70528	0.04236
hsa-miR-17	-1.70297	0.00046
hsa-miR-92a	-1.68346	0.02603
hsa-miR-106a	-1.54813	0.00089
hsa-miR-196a-star	-1.54651	0.03337

(unadjusted $P < 0.05$ and fold-change cutoff = 1.5)